



CATÓLICA

ESCOLA SUPERIOR DE BIOTECNOLOGIA

PORTO

DEVELOPMENT OF PEPTIDE-RICH EXTRACTS FROM YEAST BY- PRODUCTS FOR NUTRACEUTICAL APPLICATIONS

Thesis submitted to the *Universidade Católica Portuguesa* to attain
the degree of PhD in Biotechnology, with specialization in Food Science and Engineering

Ana Sofia da Silva Oliveira

June 2023



CATÓLICA
ESCOLA SUPERIOR DE BIOTECNOLOGIA

PORTO

**DEVELOPMENT OF PEPTIDE-RICH EXTRACTS FROM YEAST BY-
PRODUCTS FOR NUTRACEUTICAL APPLICATIONS**

Thesis submitted to the *Universidade Católica Portuguesa* to attain
the degree of PhD in Biotechnology, with specialization in Food Science and Engineering

Ana Sofia da Silva Oliveira

Supervision: **Ana Paula Taboada Costa Santos Carvalho, PhD**

Co-supervision: **Joana Odila Mendes de Sá Pereira, PhD**

Carlos Miguel Henriques Ferreira, PhD

June 2023

This work was co-financed by European Regional Development Fund (ERDF) through the Operational Program for Competitiveness and Internationalization (POCI) supported by the Amyris Bio Products Portugal, Unipessoal Lda and Escola Superior de Biotecnologia – Universidade Católica Portuguesa through Alchemy project ‘Capturing High Value from Industrial Fermentation Bio Products (POCI-01-0247-FEDER-027578)’. Thanks are also due to Universidade Católica Portuguesa and FCT/MCT for the financial support for the CBQF (project UIDB/50016/2020) research unit, through national funds and where applicable co-financed by the FEDER, within the PT2020 Partnership Agreement.



Resumo

Ao longo dos anos, a biologia sintética cresceu com o uso de leveduras geneticamente modificadas para produção de ingredientes sustentáveis. À semelhança da indústria cervejeira, é gerada uma quantidade considerável de levedura excendentária, que possui um valor nutricional notável como fonte proteica alternativa.

Considerando o aumento da população global e o consequente aumento da procura de proteína, a presente tese visa valorizar os péptidos de leveduras geneticamente modificadas, produzindo extratos ricos em péptidos quer da sua extração direta, quer a partir dos resíduos de extração de β -glucanas e mananas (componentes da parede celular das leveduras) numa abordagem de economia circular para a indústria nutracêutica.

Relativamente à extração de péptidos diretamente da levedura, foram usadas metodologias escaláveis e sustentáveis como a homogeneização a alta pressão, sonicação, hidrólise enzimática e autólise. Os extratos de leveduras geneticamente modificadas mostraram excelentes perfis nutricionais, semelhantes aos das estirpes não-modificadas. A autólise destacou-se como uma abordagem promissora, embora outras métricas de sustentabilidade ainda precisem ser estudadas para a implementação industrial desse processo.

Para aprofundar as propriedades biológicas dos péptidos do autolisado, testaram-se dois métodos de purificação: ultrafiltração e cromatografia por exclusão de tamanho. As frações resultantes exibiram diversos teores de proteína, distribuições de pesos moleculares e sequências de péptidos, apresentando uma elevada capacidade de inibição da enzima conversora da angiotensina, atividade antioxidante, e uma maior inibição da 3-hidroxi-3-metilglutaril-coenzima A (HMG-CoA) redutase do que o autolisado original, sugerindo a importância da purificação para produzir suplementos alimentares com efeito antiolesterolémico. Até onde sabemos, a inibição da HMG-CoA redutase associada a péptidos de levedura é aqui reportada pela primeira vez. Considerando o custo-benefício, a ultrafiltração parece ser o método mais adequado para a produção de extratos ricos em péptidos destinados ao mercado nutracêutico.

A ultrafiltração foi também aplicada aos sobrenadantes dos resíduos de extração de β -glucanas e mananas da levedura, maximizando a abordagem de economia circular para a produção de extratos ricos em péptidos. Estes extratos apresentaram um desempenho

nutricional e bioativo comparável aos obtidos diretamente da levedura, tornando-os excelentes ingredientes para o setor nutracêutico.

Considerando a composição dos aminoácidos nos extratos peptídicos, identificou-se potencial para formar complexos Fe-péptidos com a fração Gpep > 1 kDa (fração peptídica com peso molecular maior que 1 kDa proveniente dos resíduos de extração de β -glucanas) em condições anóxicas. Do desenho fatorial aplicado mostrou-se que as condições ótimas de reação ocorrem a pH 6,0 durante 30 min, sendo a complexação confirmada por análise química e estrutural.

Finalmente, os complexos foram submetidos à simulação *in vitro* da digestão gastrointestinal humana, e sua absorção foi analisada numa linha celular de adenocarcinoma do cólon humano, avaliando a absorção de Fe. Os resultados revelaram que os complexos se comportaram similarmente aos sais de Fe e bisglicinato de Fe comercial, indicando o seu potencial promissor para a suplementação dietética de Fe. Além disso, os péptidos dos complexos demonstraram atividade antioxidante, sugerindo a proteção do Fe contra a oxidação em diferentes ambientes gastrointestinais.

Em suma, esta tese promove a valorização de levedura excedentária geneticamente modificada, explorando tanto a biomassa diretamente, como os resíduos de extração de outros dos seus componentes. Isso resulta na produção de diversos extratos peptídicos que podem servir como fonte alternativa de alimento e/ou suplementos para controlo da anemia, bem como para outras áreas, tais como a cosmética, ou ingredientes na produção de microrganismos por fermentação.

Palavras-chave *Saccharomyces cerevisiae*, autólise, ultrafiltração, complexos Fe-péptidos, biodisponibilidade do Fe

Abstract

Over the years, synthetic biology has grown through the use of engineered yeasts for sustainable ingredients production. Similar to the brewing industry, a considerable amount of spent yeast has been generated, which holds a significant nutritional value as an alternative protein source.

Considering the increase of global population and the consequent rise in protein demand, this thesis aims to valorise peptides from engineered yeast by producing peptide-rich extracts. These extracts are derived either directly from yeast or from the waste residues of β -glucan and mannan extractions (yeast cell wall components), following a circular economy approach to be applied to nutraceutical industry.

For the direct extraction of peptides from yeast, scalable and sustainable methodologies such as high-pressure homogenization, sonication, enzymatic hydrolysis, and autolysis were employed. Engineered yeast extracts exhibited excellent nutritional profiles, similar to wild-type. Autolysis emerged as a promising approach, although additional sustainability metrics need to be studied for the industrial implementation of this process.

To further explore the biological properties of autolysate peptides, two purification methods were applied: ultrafiltration and size exclusion chromatography. The resulting fractions displayed diverse protein content, molecular weight distributions and peptide sequences, demonstrating high angiotensin-converting enzyme inhibition capacity, antioxidant activity, and greater inhibition of 3-hydroxy-3-methylglutaryl-coenzyme A (HMG-CoA) reductase than the original autolysate. This suggests the importance of purification in producing a cholesterol-reducing dietary supplement with these properties. To best of our knowledge, this thesis reports the first demonstration of yeast peptide-associated HMG-CoA reductase inhibition. Considering cost-effectiveness, ultrafiltration appears to be the most suitable method for producing peptide-rich extracts for the nutraceutical market.

Ultrafiltration was also applied to the supernatants of β -glucan and mannan extraction residues, maximizing the circular economy approach for peptide-rich extract production. These extracts exhibited similar nutritional and bioactive performance to those directly obtained from yeast, making them excellent ingredients for the nutraceutical sector.

Considering the amino acid composition within the peptide extracts, the production of Fe-peptide complexes was studied and the complexes produced with Gpep > 1 kDa fraction

(peptide fraction with molecular weight higher than 1 kDa derived from β -glucan extraction residues) under anoxic conditions were identified as the most adequate. From the applied factorial design, the reaction conditions were optimized (pH 6.0 for 30 min), and complexation was confirmed through chemical and structural analysis.

Finally, the complexes were subjected to an *in vitro* simulation of human gastrointestinal tract, and Fe absorption was analysed using a human colon adenocarcinoma cell line. The results revealed that the complexes behaved similarly to Fe salts and commercial Fe bisglycinate, indicating their promising potential for dietary Fe supplementation. Additionally, the peptides from the complexes demonstrated antioxidant activity, suggesting protection of Fe against oxidation in different gastrointestinal environments.

In summary, this thesis promotes the valorisation of spent engineered yeast, exploring the production of peptide extracts directly from biomass or from residues arising from other components extraction. Indeed, this production can represent an alternative food source and/or dietary supplements for managing anaemia, as well as providing peptide extracts for several other areas such as cosmetics or ingredients for microorganisms' fermentation.

Keywords *Saccharomyces cerevisiae*, autolysis, ultrafiltration, Fe-peptide complexes, Fe bioavailability

Acknowledgments

Ao refletir na forma de iniciar este capítulo, olho em redor do meu quarto e me fixo num mini-cartaz emoldurado na parede, que me lembra diariamente: *It's all about the journey*. E nessa frase, percebo claramente o resumo dos últimos anos. Aqui estão os desafios, as escolhas, os avanços e recuos, e a capacidade de seguir em frente. Aqui está uma imensa aprendizagem técnica, científica e pessoal. Aqui estão as instituições e grupos de investigação onde me senti acolhida desde o primeiro dia. Aqui estão os Professores, orientadores e mentores que partilharam comigo o seu conhecimento, me guiaram, apoiaram e motivaram a ir mais além. Aqui estão as minhas Pessoas, a minha família e amigos que me apoiam incondicionalmente, e outras maravilhosas que esta jornada me trouxe e que sei que ficam comigo para a vida. Aqui estão os colegas de laboratório com os *brainstorms*, onde surgem ideias incríveis e outras completamente disparatadas, com as conversas e risadas, mas também com os desabafos. Aqui entram os convívios, as cantorias, as danças e dezenas de bolos de aniversário. Tudo e todos têm um lugar e fazem parte deste percurso maravilhoso. E por tanto, só me resta agradecer:

Em primeiro lugar, agradeço às principais instituições envolvidas pela oportunidade que me deram em abraçar este percurso e onde me senti verdadeiramente acolhida como doutoranda:

À Escola Superior de Biotecnologia da Universidade Católica Portuguesa e à Amyris Bio Products Portugal por fornecerem todas as condições imprescindíveis para a sua realização, quer o conhecimento, financiamento, e também o ambiente fértil para a contínua geração de ideias;

E à Católica Porto Business School pela oportunidade de aprendizagem *out of the box*.

Não menos importante, agradeço ao Super Bock group pelo fornecimento de levedura excedentária e por se mostrar sempre disponível em se ajustar às nossas condições de ensaios para as respetivas recolhas.

Em segundo lugar, agradeço às Pessoas que acompanharam de perto esta jornada:

À Professora Manuela Pintado pelo otimismo e por ter sempre a palavra necessária no momento certo;

Aos meus orientadores, Ana Carvalho, Joana Odila e Carlos Ferreira (e à “orientadora de coração” Ana Margarida Pereira) por tantos *pepstorms*, por ouvirem as minhas ideias e preocupações, por me orientarem, ajudarem e sempre me motivarem;

À minha equipa *Yeaster Eggs* porque nada disto era possível sem eles e esta tese é também um bocadinho parte de todos;

Aos meus *Los Bomberos* pela verdadeira camaradagem, pelas partilhas de bons e outros mais desafiadores momentos, pela diversão e pela amizade que certamente permanecerá;

À *Confraria das Marmotas* e aos *Leves* pelas conversas, momentos de descontração e companheirismo que tornaram este percurso bem mais leve;

E a todos os restantes colegas de laboratório e amigos (e são tantos que me era impossível nomeá-los...) por toda a ajuda, convívios e carinho ao longo destes anos!

Por último, agradeço às minhas Pessoas:

Aos meus pais que são os principais responsáveis pelo que sou hoje e pela força e apoio incondicionais;

À minha Marlene, a mana de coração que está comigo em todos os momentos;

Às minhas *partners in crime*, Mary e Debs, pela motivação e apoio constantes, e alinharem sempre nas minhas loucuras;

Aos meus *Apanha-Bonés* (à Ritinha, ao Brandon, ao Jojo, à Bá e à Marie) que o trabalho me trouxe e que a amizade permanece até hoje;

Ao meu *Trio* (Marilu e Isabel) que partilhou tanto de tudo isto comigo;

Aos meus mentores que estiveram nesta jornada (à Joana, à Ana, à Ângela, à Vera e ao Ricardo) por me impulsionarem a evoluir todos os dias;

Aos meus colegas e amigos bailarinos que tive o prazer de partilhar salas de ensaio, pistas e palcos e que são essenciais na minha estrutura.

“A verdadeira sabedoria está em reconhecer que ainda temos muito a aprender.”

Table of contents

Table of contents	XI
List of tables	XIX
List of figures	XXI
List of supplementary material	XXV
Abbreviations	XXVII
Chapter 1	33
Introduction	33
1.1. Framework	35
1.2. Literature review	36
1.2.1. Microorganisms: an emerging source of protein and peptides	36
1.2.2. Spent yeast valorisation	38
1.2.2.1. Proteins & peptides	39
<i>Extraction</i>	41
Physical methods	42
Driven by pressure	43
Bead milling	43
High-pressure homogenization	44
Supercritical carbon dioxide	45
Driven by waves	45
Ultrasonication	45
Pulsed electric field	46
Chemical methods	53
Enzymatic methods	54
Autolysis	54

Enzymatic hydrolysis.....	55
<i>Isolation and purification</i>	59
Selective precipitation	59
Membrane filtration.....	60
Dialysis	62
Chromatography	62
Nucleic acids extraction.....	65
<i>Characterization</i>	66
Protein content.....	67
Amino acid determination	68
Molecular weight.....	72
Mass spectrometry	72
SDS-PAGE	72
Size-exclusion chromatography.....	74
<i>Bioactive properties</i>	76
Antihypertensive.....	76
Antioxidant	83
Antimicrobial.....	90
Other bioactivities	95
Applications to agri-food sector	96
1.2.2.2. To sum up.....	101
1.3. Scope & outline	103
1.4. Scientific output	106
Chapter 2	109
Peptides directly extracted from spent yeast	109
2.1. Peptide-rich extracts production	111
2.1.1. Introduction.....	111

2.1.2.	Materials and methods	112
2.1.2.1.	Yeast Strains.....	112
2.1.2.2.	Yeast pre-treatment	112
2.1.2.3.	Extraction methods.....	113
	<i>High-pressure homogenization</i>	113
	<i>Sonication</i>	113
	<i>Autolysis</i>	113
	<i>Enzymatic Hydrolysis</i>	114
	<i>Sustainable metrics</i>	114
2.1.2.4.	Yeast extract characterization	115
	<i>Protein</i>	115
	<i>Dry weight</i>	115
	<i>MW distribution</i>	115
	<i>Amino acids</i>	115
	<i>Neutral sugars</i>	116
	<i>Minerals</i>	116
	<i>Statistical analysis</i>	117
2.1.3.	Results and Discussion	117
2.1.3.1.	Peptide rich-extracts characterization	117
	<i>Protein content (% w/w)</i>	117
	<i>Molecular weight distribution</i>	119
2.1.3.2.	Extraction methodology evaluation	120
	<i>Protein recovery</i>	120
	<i>Sustainable metrics</i>	122
2.1.3.3.	Choice of peptide-rich extract for future purification process	123
2.1.4.	Conclusions.....	124
2.1.5.	Supplemental material	125

2.2.	Separation & purification	127
2.2.1.	Introduction.....	127
2.2.2.	Material and methods.....	129
2.2.2.1.	Peptide-rich autolysate “ESY1”	129
2.2.2.2.	Purification of bioactive peptides.....	129
	<i>Ultrafiltration</i>	129
	<i>Size-exclusion chromatography</i>	130
2.2.2.3.	Peptides chemical characterization	130
	<i>Protein determination</i>	130
	Dumas	130
	Bicinchoninic acid & dry weight.....	131
	<i>Molecular weight distribution</i>	131
	<i>Proteomics</i>	131
2.2.2.4.	Peptides bioactivity	132
	<i>Antimicrobial</i>	132
	<i>ACE inhibition assay</i>	133
	<i>Antioxidant</i>	133
	Scavenging activity using ABTS.....	133
	Oxygen radical absorbance capacity	134
	<i>HMG-CoA reductase inhibition assay</i>	134
2.2.2.5.	Statistical analysis	134
2.2.3.	Results and Discussion	135
2.2.3.1.	Protein content (% w/w).....	135
2.2.3.2.	Molecular weight distribution	137
2.2.3.3.	Proteomics analysis	139
2.2.3.4.	Bioactivities.....	140
	<i>Antimicrobial</i>	140

<i>Anticholesterolemic, antihypertensive and antioxidant activities</i>	142
2.2.4. Conclusion	145
2.2.5. Supplementary material	146
Chapter 3	149
Peptides from waste streams	149
3.1. Application for nutraceutical market	151
3.1.1. Introduction.....	151
3.1.2. Material and methods.....	152
3.1.2.1. Yeast strain.....	152
3.1.2.2. Peptide-rich extracts production.....	152
3.1.2.3. Peptide-rich extracts characterization	153
<i>Protein</i>	153
<i>Dry weight</i>	153
<i>Amino acids</i>	153
<i>Neutral sugars</i>	153
<i>Minerals</i>	154
<i>Molecular weight distribution</i>	154
<i>In vitro cytotoxicity assessment</i>	154
Caco-2 cell culture	154
Cytotoxicity assay.....	154
<i>Biological activities</i>	155
ACE inhibition assay	155
Antioxidant capacity.....	155
Scavenging activity using ABTS.....	155
Scavenging activity using DPPH [•]	155
Oxygen radical absorbance capacity.....	156
HMG-CoA reductase inhibition assay.....	156

3.1.2.4.	Statistical analysis	156
3.1.3.	Results and discussion	156
3.1.3.1.	Nutritional analysis	156
3.1.3.2.	Molecular weight profile	161
3.1.3.3.	<i>In vitro</i> cytotoxicity assessment	162
3.1.3.4.	Biological activity	164
	<i>Anti-cholesterolemic, antihypertensive and antioxidant activities</i>	164
3.1.4.	Conclusion	166
3.1.5.	Supplementary material	167
3.2.	Fe-peptide complexes	168
3.2.1.	Introduction.....	168
3.2.2.	Material and methods.....	170
3.2.2.1.	Peptide-rich fraction production.....	170
3.2.2.2.	Chemical characterization of peptide-rich fractions	171
	<i>Protein</i>	171
	<i>Dry weight</i>	171
3.2.2.3.	Fe-peptides complexation	171
	<i>Fraction initial screening - reaction without N₂</i>	171
	<i>Complex formation – anoxic conditions</i>	171
	Experimental setup	171
	Reaction protocol.....	172
	Factorial design and statistical analysis.....	173
	<i>Fe determination</i>	173
3.2.2.4.	Complex characterization.....	174
	<i>X-ray diffraction</i>	174
	<i>Intrinsic fluorescence</i>	174
	<i>Fourier-transform infrared spectroscopy</i>	174
	<i>Scanning Electron Microscopy</i>	174

<i>Particle size</i>	174
3.2.3. Results and Discussion	175
3.2.3.1. Protein content.....	175
3.2.3.2. Fraction complexation capacity screening	175
3.2.3.3. Complex formation conditions optimization.....	178
3.2.3.4. Complex characterization.....	182
<i>X-ray diffraction</i>	182
<i>Intrinsic fluorescence</i>	183
<i>FTIR spectroscopy</i>	184
<i>Scanning electron microscopy</i>	186
<i>Particle size</i>	188
3.2.4. Conclusion	188
3.2.5. Supplementary material	189
3.3. <i>In vitro</i> Fe bioavailability	190
3.3.1. Introduction.....	190
3.3.2. Material and methods.....	192
3.3.2.1. Production of peptide fraction.....	192
3.3.2.2. Synthesis of Fe-peptide complexes	192
3.3.2.3. <i>In vitro</i> simulation of human gastrointestinal tract	192
3.3.2.4. Fe uptake using a Caco-2 monolayer	193
<i>Cell culture</i>	193
<i>Cell viability</i>	193
<i>Fe uptake</i>	194
<i>Ferritin production</i>	195
3.3.2.5. Chemical characterization of GIT samples	195
<i>Protein content</i>	195
<i>Protein and peptides molecular weight</i>	195
<i>Fe determination</i>	196

3.3.2.6. Biological activity of GIT samples	196
<i>ACE inhibition assay</i>	196
<i>Antioxidant capacity</i>	196
Scavenging activity using ABTS	196
Scavenging activity using DPPH'	196
Oxygen radical absorbance capacity	197
<i>HMG-CoA reductase inhibition assay</i>	197
3.3.2.7. Statistical analysis	197
3.3.3. Results and Discussion	197
3.3.3.1. <i>In vitro</i> simulation of gastrointestinal tract	197
<i>Fe bioaccessible (%)</i>	197
<i>Protein profile</i>	199
3.3.3.2. Fe uptake study	201
<i>Cell viability</i>	201
<i>Fe uptake and ferritin production</i>	202
3.3.3.3. Biological activity of GIT samples	206
3.3.4. Conclusion	208
3.3.5. Supplementary material	208
Chapter 4	209
Final remarks	209
4.1. Conclusions	211
4.2. Future work	214
References	217

List of tables

Table 1. Physical extraction methods for protein release from <i>S. cerevisiae</i>	48
Table 2. Chemical extraction methods for protein release from <i>S. cerevisiae</i>	54
Table 3. Enzymatic extraction methods for protein release from <i>S. cerevisiae</i>	57
Table 4. EAA content in protein-rich <i>S. cerevisiae</i> extracts to be potentially used as food supplements.	71
Table 5. MW characterization methods for evaluation of protein from <i>S. cerevisiae</i>	75
Table 6. Antihypertensive activity of bioactive peptides from <i>S. cerevisiae</i>	79
Table 7. Antioxidant activity of bioactive peptides from <i>S. cerevisiae</i>	87
Table 8. Antimicrobial activity of bioactive peptides from <i>S. cerevisiae</i>	93
Table 9. Protein-rich extracts from commercially available yeast.	98
Table 10. Protein content (% w/w) of raw yeast and extracts obtained from each extraction process applied to the different yeast strains (CSY, ESY1 and ESY2).....	118
Table 11. Sustainable metrics (PMI, WI and EIS) of each extraction process applied to the different yeast strains (CSY, ESY1 and ESY2).	122
Table 12. Protein content (% w/w), sugars (% w/w) and minerals (ng/g extract) of peptide-rich extract obtained from autolysis of ESY1.	123
Table 13. EAA (mg/g protein) of peptide-rich extract obtained from autolysis of ESY1.	124
Table 14. Protein content (% w/w) of original ESY1 extract and fractions obtained from ultrafiltration (ESY1 >1 kDa and ESY1 < 1 kDa) and SEC (1 to 4).....	136
Table 15. Protein and peptides MW distribution in SEC fractions represented as percentage of chromatogram total area (% total area).	138
Table 16. Peptide sequences identified in original ESY1 extract, and fractions obtained from ultrafiltration (ESY1 > 1 kDa and ESY1 < 1 kDa) and SEC (1 to 4), together with their bioactivities reported in PBD.	139

Table 17. IC50 values (mg/mL) obtained in ACE-inhibition assay, ABTS ^{•+} and ORAC activities (μmol TE/g sample), and HMG-CoA reductase inhibition (%) of original ESY1 extract and fractions obtained from ultrafiltration (ESY1 > 1 kDa and ESY1 < 1 kDa) and SEC (1 to 4).	143
Table 18. Protein concentration (% w/w), sugars (% w/w) and minerals (ng/g extract) of peptide-rich extracts.	158
Table 19. EAA content (mg/g protein) of peptide-rich extracts.	160
Table 20. IC50 values (mg/mL) at ACE-inhibition assay, HMG-CoA reductase inhibition (%), and ABTS ^{•+} , ORAC and DPPH [•] (μmol TE/g extract) activities of peptide-rich extracts.	164
Table 21. Protein concentration (% w/w) of peptide-rich fractions.....	175
Table 22. Soluble Fe (% of initial) found for each condition tested in the experimental factorial design.	179
Table 23. Particle size distribution parameters of peptide fraction Gpep > 1 kDa and Gpep>1kDa-Fe complexes.	188
Table 24. Bioaccessible Fe concentration (mg/L) of GIT samples and successive dilutions performed for PrestoBlue [®] assay.....	193
Table 25. Final soluble Fe concentration (mg/L) in samples after <i>in vitro</i> GIT simulation and its percentage (%) in comparison with initial protocol concentration (200 mg/L).....	197
Table 26. Fe concentration (mg/L) on initial samples of Caco-2 exposure (GIT samples theoretically diluted for 50 μM in fresh medium).	202
Table 27. Antioxidant activity (ABTS ^{•+} , DPPH [•] and ORAC), expressed as μmol TE/g of protein, and inhibition percentage (%) of ACE and HMG-CoA reductase of GIT samples: blank, Gpep > 1 kDa and Gly.	207

List of figures

Figure 1. Schematic representation of protein valorisation from spent yeast, applying different extraction processes, followed by purification steps and extracts characterization. Adapted from the graphical abstract of Oliveira, Ferreira et al. (2022b).	39
Figure 2. Schematic longitudinal section of <i>S. cerevisiae</i> cell and their protein composition (cell structures and components are not in scale).	40
Figure 3. Classification of protein extraction methods from <i>S. cerevisiae</i> according to operation mode.	42
Figure 4. Schematic representation of spent yeast peptides valorisation, extracted by several methods, and their main bioactivities already reported in order to be applied at agri-food sector. Adapted from the graphical abstract of Oliveira et al. (2022a).	76
Figure 5. Main bioactivities and possible mechanisms reported for peptides from <i>S. cerevisiae</i>	96
Figure 6. Outline of the present thesis by general segments.	104
Figure 7. Detailed scheme of the thesis.	105
Figure 8. Schematic overview of <i>Section 2.1</i> , illustrating the extraction methods used for both engineered and wild-type yeast strains. Adapted from the graphical abstract of Oliveira, Odila Pereira et al. (2022).	111
Figure 9. Peptides MW distribution (%) in peptide-rich extracts obtained from each extraction process (Aut – autolysis, Hyd – enzymatic hydrolysis, Sonic – sonication) applied to the different yeast strains (CSY, ESY1 and ESY2). ND – not detected (below low detection limit).	119
Figure 10. Protein recovery (%) of each extraction process (Aut – autolysis, Hyd – enzymatic hydrolysis, Sonic – sonication) applied to the different yeast strains (CSY, ESY1 and ESY2).	121

Figure 11. Schematic overview of <i>Section 2.2</i> , outlining the purification techniques employed for autolysate ESY1, such as ultrafiltration and SEC. Adapted from the graphical abstract of article in preparation*	127
Figure 12. Diagram of ultrafiltration process for production of peptide-rich fractions with different MW: “ESY1 > 1 kDa” and “ESY1 < 1 kDa”.	130
Figure 13. Elution profile of the SEC purification of peptide-rich extract “ESY1”. Four different peptide fractions, corresponding to the four peaks observed, were collected (SEC 1 to 4).....	135
Figure 14. Growth curves for <i>E. coli</i> (A) and <i>S. aureus</i> (B) exposed to original ESY1 extract and fractions obtained from ultrafiltration (ESY1 > 1 kDa and ESY1 < 1 kDa; on the left) and SEC (1 to 4; on the right).....	141
Figure 15. Schematic overview of this <i>Section 3.1</i> , illustrating the process of generating peptide-rich extracts through 1 kDa ultrafiltration using β -glucans and mannans waste streams extraction from spent yeast. Adapted from the graphical abstract of Oliveira et al. (2022).	151
Figure 16. Diagram for ultrafiltration process of waste streams of β -glucans and mannans extraction processes from spent yeast to obtain peptide-rich extracts.....	153
Figure 17. FPLC profiles of the (A) Gpep and (B) Mpep original supernatants (non-treated waste streams).	157
Figure 18. Peptides MW distribution (%) in peptide-rich extracts under and above 1 kDa.	161
Figure 19. Caco-2 metabolic inhibition after 24 h-exposure to peptide-rich extracts (0.8-5 mg/mL) ($n=4$).....	163

Figure 20. Schematic overview of <i>Section 3.2</i> , showcasing the process of generating peptide-Fe complexes derived from spent yeast peptide-rich extracts. Adapted from the graphical abstract of submitted article*	168
Figure 21. Diagram for ultrafiltration of protein-rich supernatants from yeast β -glucan and mannan extraction processes to obtain peptide fractions.	170
Figure 22. A: Experimental design of the complexation reaction setup using N_2 , pH control and NaOH probe. B: Conditions of pH and time on the complexation reaction efficiency assays. ●: combination tested; ○: combination not tested.	172
Figure 23. A: Soluble Fe (% of initial) after complexation reaction with no N_2 atmosphere ($n=2$). B: Soluble Fe (% of initial) after complexation reaction with solution purge and N_2 atmosphere ($n=6$).	176
Figure 24. Soluble Fe in complexation reactions tested at experimental factorial design, as percentage of initially added, in function of pH (A) and in function of time (B) ($n=3$)...	180
Figure 25. Response surface depicting soluble Fe (as % of initial added) versus time and pH. Model obtained from applying multivariate regression to complexation data, according to formula described in the main text.	181
Figure 26. XRD patterns of Gpep > 1 kDa, Gpep>1kDa-Fe complex and Fe hydroxides (Fe(OH) _x) from 3° to 80°.....	182
Figure 27. Fluorescence emission spectra of Gpep > 1 kDa and Gpep>1kDa-Fe complexes ($n=3$). Excitation wavelength = 280 nm; emission wavelength = 300 to 400 nm.....	183
Figure 28. FTIR spectra of Gpep > 1 kDa, Gpep>1kDa-Fe complex and Fe hydroxides (Fe(OH) _x) in the region from 4000 to 550 cm^{-1} and identification of the main peaks observed.	185
Figure 29. SEM microscopic morphology of Gpep > 1 kDa freeze-dried samples (A) versus freeze-dried Fe-peptide complexes formed with Gpep > 1 kDa (B).	187

Figure 30. Schematic overview of *Section 3.3*, demonstrating the *in vitro* absorption performance of Fe-peptide complexes, Fe salt and benchmark. Adapted from the graphical abstract of submitted article* 190

Figure 31. Peptides MW distribution (%) in Fe-peptide complex before (left) and after (right) *in vitro* GIT simulation..... 200

Figure 32. Fe uptake by Caco-2 cells exposed to Fe-peptide complexes, Fe salt and benchmark. All samples were compared by Tukey’s test ($n=6$)..... 203

Figure 33. FER produced by Caco-2 cells exposed to Fe-peptide complexes, Fe salt and benchmark in relation to cells exposed to GIT control. All samples were compared by Tukey’s test ($n=6$). 204

List of supplementary material

Tables

Table S1. <i>P</i> -values of comparison of protein content (% w/w) between different yeast strains.....	125
Table S2. <i>P</i> -values of comparison of protein content (% w/w) between different extraction methodologies.....	125
Table S3. <i>P</i> -values of comparison of protein recovery (%) between different yeast strains.	126
Table S4. <i>P</i> -values of comparison of protein recovery (%) between different extraction methodologies.....	126
Table S5. <i>P</i> -values of comparison of protein content (% w/w) between ESY1 and fractions obtained from ultrafiltration and SEC.	146
Table S6. Peptides identification on original ESY1 and respective ultrafiltration (ESY1 > 1 kDa and ESY1 < 1 kDa) and SEC (1 to 4) fractions.	146
Table S7. <i>P</i> -values of comparison of HMG-CoA reductase and ACE inhibition assays, together with antioxidant activities (ABTS and ORAC), between ESY1 and fractions obtained from ultrafiltration and SEC.	147
Table S8. <i>P</i> -values of comparison of nutritional analysis between different Gpep and Mpep peptide-rich fractions: sugars (%) and minerals (ng/g extract).	167
Table S9. <i>P</i> -values of comparison of ACE inhibition (IC ₅₀ - mg/mL) and ORAC (μmol TE/g extract) assays between different Gpep and Mpep peptide-rich fractions.....	167
Table S10. <i>P</i> -values of comparison of antioxidant activity (ABTS ^{•+} and ORAC) and inhibition percentage (%) of ACE and HMG-CoA reductase between GIT samples: blank, Gpep > 1 kDa and Gly.....	208

Figures

Figure S1. Residual distribution of the fitted model versus the experimental data.....189

Abbreviations

A	ABTS	2,2'-Azinobis (3-ethyl-benzothiazoline-6- sulfonic acid) diammonium salt
	ABTS ⁺	2,2'-Azinobis (3-ethyl-benzothiazoline-6- sulphonate) radical cation
	ACE	Angiotensin-converting enzyme
	A _{control}	Absorbance of control
	Ala / A	Alanine
	ANOVA	Analysis of variance
	APD	Antimicrobial Peptide Database
	Arg / R	Arginine
	Asn / N	Asparagine
	AOAC	Association of Official Analytical Chemists
	A _{sample}	Absorbance of sample
	Asp / D	Aspartic acid
	ATP	Adenosine triphosphate
	ATR	Attenuated total reflectance
	AU	Anson Unit
	AUC	Area under curve
	Aut	Autolysis
B	BCA	Bicinchoninic acid
	BHUT	Barbell Horn Ultrasonic Technology
C	CAGR	Compound annual growth rate
	CAMP	Collection of Anti-Microbial Peptides
	CHP	Cyclo-His-Pro
	CSY	Control spent yeast
D	DBAASP	Database of Antimicrobial Activity and Structure of Peptides
	DEAE	Diethylaminoethyl
	DMEM	Dulbecco's Modified Eagle's Medium
	DMT1	Divalent metal transporter 1
	DNA	Deoxyribonucleic acid

DPP4	Dipeptidyl peptidase-4
DPPH [•]	2,2-Diphenyl-1-picrylhydrazyl
DRAMP	Data repository of antimicrobial peptides
DTT	Dithiothreitol
Dv10	10th percentile of the cumulative volume distribution
Dv50	50th percentile of the cumulative volume distribution
Dv90	90th percentile of the cumulative volume distribution
[DMAPA]FA	3-(Dimethylamino)-1-propylaminium formate
E EAA	Essential amino acids
EBA	Expanded bed adsorption
EDTA	Ethylenediaminetetraacetic acid
EFSA	European Food Safety Authority
EIS	Energy Intensity Score
ELISA	Enzyme-linked immunosorbent assay
ESI	Electrospray ionization
ESY1	Engineered strain yeast 1
ESY1 < 1 kDa	Permeate of ESY1 with MW under 1 kDa
ESY1 > 1 kDa	Retentate of ESY1 with MW above 1 kDa
ESY2	Engineered strain yeast 2
F FAO	Food and Agriculture Organization of the United Nations
F _{control}	Fluorescence of control
FDA	Food and Drug Administration
FER	Ferritin
FPLC	Fast protein liquid chromatography
F _{sample}	Fluorescence of sample
FTIR	Fourier-transform infrared
[Fe] _{2h}	Fe concentration of collected samples after 2 h exposure
[Fe] _i	Fe concentration in the initial samples
[FER] _p	FER produced amount
G 5'-GMP	Guanosine-5'-monophosphate
GABA	Amino acid γ -aminobutyric acid
GAPDH	Glyceraldehyde-3-phosphate dehydrogenase
GC-FID	Gas chromatography-flame ionization

GIT	Gastrointestinal tract
Gln / Q	Glutamine
Glu / E	Glutamic acid
Gly / G	Glycine
GMO	Genetically modified organisms
Gpep < 1 kDa	Peptide-rich extract from waste stream of β -glucans extraction with MW under 1 kDa
Gpep < 1 kDa DF	Diafiltrate permeate fraction from waste stream of β -glucans extraction with MW under 1 kDa
Gpep < 1 kDa FS	First ultrafiltration permeate fraction from waste stream of β -glucans extraction with MW under 1 kDa
Gpep > 1 kDa	Peptide-rich extract from waste stream of β -glucans extraction with MW above 1 kDa
GRAS	Generally Recognized as Safe
H His / H	Histidine
HMG-CoA	3-Hydroxy-3-methylglutaryl coenzyme A
HPH	High pressure homogenization
HPLC	High performance liquid chromatography
HPLC-UV/VIS	High-performance liquid chromatography coupled to ultraviolet and visible detector
HPMC	Hydroxypropyl methylcellulose
HVED	High-voltage electrical discharges
Hyd	Enzymatic hydrolysis
I IC50	Half maximal inhibitory concentration
ICP-OES	Inductively coupled plasma - optical emission spectrometry
IEC	Ion-exchange chromatography
Ile / I	Isoleucine
INFOGEST	International Network on Food Digestion and Health
IR	Infrared
ISO	International Organization for Standardization
L LAPU	Leucine aminopeptidase unit
LC	Liquid chromatography

	LC-ESI-qTOF/MS	Liquid chromatography coupled with electrospray-ionization quadrupole time-of-flight mass spectrometry
	Leu / L	Leucine
	LiAc	Lithium acetate
	LOD	Limit of detection
	Lys / K	Lysine
M	MALDI	Matrix-assisted laser desorption ionization
	Met / M	Methionine
	MH	Mueller Hinton
	MM	Molar mass
	Mpep < 1 kDa	Peptide-rich extract from waste stream of mannans extraction with MW under 1 kDa
	Mpep < 1 kDa DF	Diafiltrate permeate fraction from waste stream of mannans extraction with MW under 1 kDa
	Mpep < 1 kDa FS	First ultrafiltration permeate fraction from waste stream of mannans extraction with MW under 1 kDa
	Mpep > 1 kDa	Peptide-rich extract from waste stream of mannans extraction with MW above 1 kDa
	MS	Mass spectrometry
	MW	Molecular weight
N	NA	Not applicable
	NADPH	Nicotinamide adenine dinucleotide phosphate
	ND	Not detected
	NM	Not mentioned
O	OD	Optical density
	OPA	<i>o</i> -phthalaldehyde
	ORAC	Oxygen radical absorbance capacity
P	<i>p</i>	Probability value in statistical significance tests
	PBS	Phosphate-buffered saline
	PBD	Peptide bioactivity databases
	PEF	Pulsed electric field
	PepT1	Peptide transporter 1
	PET	Polyester

	Phe / F	Phenylalanine
	PMI	Process mass intensity
	Pro / P	Proline
	[Protein]	Cell well protein concentration
R	RAS	Rennin-angiotensin system
	RNA	Ribonucleic acid
	ROS	Reactive oxygen species
	RP-HPLC	Reversed-phase high-performance liquid chromatography
S	SCO ₂	Supercritical carbon dioxide
	SCP	Single cell protein
	SDPP	Spray dried porcine plasma
	SDS	Sodium dodecyl sulphate
	SDS-PAGE	Sodium dodecyl sulphate-polyacrylamide gel electrophoresis
	SEC	Size-exclusion chromatography
	SEC 1	First fraction of SEC of ESY1
	SEC 2	Second fraction of SEC of ESY1
	SEC 3	Third fraction of SEC of ESY1
	SEC 4	Fourth fraction of SEC of ESY1
	SEM	Scanning electron microscopy
	Ser / S	Serine
	SHR	Spontaneously hypertensive rats
	Sonic	Sonication
	SP	Sulphopropyl
	SPE	Solid-phase extraction
T	TE	Trolox equivalent
	Thr / T	Threonine
	TOF	Time-of-flight
	TPP	Three-phase partitioning
	Trp / W	Tryptophan
	TSA	Tryptic Soy Agar
	Tyr / Y	Tyrosine
U	U	Units

	UHR-QqTOF	Ultra-high-resolution quadrupole-quadrupole time of flight
	USA	United States of America
V	v/v	Volume <i>per</i> volume
	Val / V	Valine
	w/w	Weight <i>per</i> weight
W	WHO	World Health Organisation
	WI	Water intensity
	WKI	Wistar-Kyoto rats
X	XRD	X-ray diffraction

Chapter 1

Introduction

1.1. Framework

1.2. Literature review

1.3. Scope & outline

1.4. Scientific output

1.1. Framework*

Nowadays the world is facing the growing need to develop new strategies to provide resources, due to the global population growth and socio-demographic changes (Hayes, 2018). Regarding the global necessity for food, protein demand was estimated to be approximately 202 million tonnes when the world population was 7.3 billion (in 2017). Estimations using a population growth of 2.3 billion and similar protein consumption levels, resulted in an expected increase in protein demand for the next years in the range of 30% to 40% (Henchion et al., 2017).

To answer this problem, several competitive, sustainable and economically viable production processes have emerged in the last years, exploring different food sources (plants, animals, and microorganisms), in order to minimize planet resource depletion and environmental impact (Food and Agriculture Organization of the United Nations, 2018). Among those processes, fermentation technologies are able to produce a multiplicity of ingredients through the use of engineering or non-modified yeasts, using renewably sourced carbon from plants (Meadows et al., 2016; Nandy & Srivastava, 2018; Parapouli et al., 2020). However, similarly to what happens in brewing industry (Marson, de Castro, Belleville, et al., 2020), these large-scale fermentation processes generate significant amounts of spent yeast, expressing their treatment an additional and high cost for companies. Nevertheless, due to their nutritional value, namely the high protein content, bioactive ingredients, low cost and safety, spent yeast by-products have been investigated, primarily in dietary supplement market (Marson, de Castro, Belleville, et al., 2020; Mirzaei et al., 2021). Starting from this point, a deeper study on the production of peptide-rich products from spent yeast of fermentation processes, as well as their potential applications, may contribute to exploit new alternatives of food resources and health promoting dietary supplements.

* Oliveira, A. S., Ferreira, C., Pereira, J. O., Pintado, M. E., & Carvalho, A. P. (2022). Valorisation of protein-rich extracts from spent brewer's yeast (*Saccharomyces cerevisiae*): an overview. *Biomass Conversion and Biorefinery*, 1-23. <https://doi.org/10.1007/s13399-022-02636-5>. Ana P. Carvalho hereby authorizes the PhD student Ana Sofia Oliveira from CBQF/ESBUCP to include the following publication in her doctoral thesis entitled "Development of peptide-rich extracts from yeast by-products for nutraceutical applications" as a result of her activity: Valorisation of protein-rich extracts from spent brewer's yeast (*Saccharomyces cerevisiae*): an overview: Oliveira, A. S., Ferreira, C., Pereira, J. O., Pintado, M. E., & Carvalho, A. P..

1.2.1. Microorganisms: an emerging source of protein and peptides

Given the increase of worldwide protein demand, alternatives to non-animal protein have been widely emerged, with vegetal sources already representing 59% of global protein supply (141 453 675 ton), such as legumes, pseudocereals, seeds, almonds and nuts (Food Agricultural Organization of the United Nations, 2019; Sá et al., 2020).

However, other environmentally friendly choices, as edible insects and microorganisms, have also become important natural protein matrices since they have a high nutritional value, vitamins and minerals (Akhtar & Isman, 2018; Ritala et al., 2017). Indeed, microbial protein may represent more than 30% of crude protein in microorganism's biomass (microalgae, yeast and other fungi, and bacteria), being generally referred as "single cell protein" (SCP). High growth rates, the ability of some microorganisms to use single substrates, such as carbon dioxide or methane, the wide variety of microorganisms and the independence from seasonal factors when grown in bioreactors, make the extraction of microbial protein a potentially high efficient and sustainable scalable process (Nasseri et al., 2011; Ritala et al., 2017).

From the current microorganisms used for SCP production, yeast and fungi continue to dominate the traditional agri-food market with well-established processing methods (Ritala et al., 2017). In fact, the microbial protein products in market contain more than 30% of protein content, being higher than 65% for bacteria, 40-55% for yeasts, 35-55% for fungi and 30-40% from microalgal (Kuhad et al., 1997), providing a healthy balance of essential amino acids (EAA) and vitamins from B-complex group as well (Jones et al., 2020; Ritala et al., 2017).

* Oliveira, A. S., Ferreira, C., Pereira, J. O., Pintado, M. E., & Carvalho, A. P. (2022). Valorisation of protein-rich extracts from spent brewer's yeast (*Saccharomyces cerevisiae*): an overview. *Biomass Conversion and Biorefinery*, 1-23. <https://doi.org/10.1007/s13399-022-02636-5>. Ana P. Carvalho hereby authorizes the PhD student Ana Sofia Oliveira from CBQF/ESBUCP to include the following publication in her doctoral thesis entitled "Development of peptide-rich extracts from yeast by-products for nutraceutical applications" as a result of her activity: Valorisation of protein-rich extracts from spent brewer's yeast (*Saccharomyces cerevisiae*): an overview: Oliveira, A. S., Ferreira, C., Pereira, J. O., Pintado, M. E., & Carvalho, A. P..

† Oliveira, A. S., Ferreira, C., Pereira, J. O., Pintado, M. E., & Carvalho, A. P. (2022). Spent brewer's yeast (*Saccharomyces cerevisiae*) as a potential source of bioactive peptides: An overview. *International Journal of Biological Macromolecules*, 208, 1116–1126. <https://doi.org/10.1016/j.ijbiomac.2022.03.094>

Since the 19th century, yeast has been a commonly-used organism in the production of biomass for human consumption due to the high acceptability of fermented foods (Kuhad et al., 1997; Rudravaram et al., 2009). Apart from its acceptability and availability, the ability to grow at low pH (4.5 - 5.5), which reduces the need to work in strict aseptic conditions, is pointed as one of yeast advantages compared to other microorganisms employed for SCP production (Kuhad et al., 1997). Furthermore, they are rarely associated with the occurrence of gastroenteritis, intoxications or other infections related with food intake (Fleet, 2007), since they are capable to produce antimicrobial compounds, thus inactivating the growth of other microorganisms and providing a safe application in food area (Pereira et al., 2021). Currently, cheap wastes, such as carbohydrates materials (molasses, vinasse, wood hydrolysates, sulphite liquors, starch, lignin–cellulose, etc.), can be used as substrates to supply carbon and nitrogen for yeast growth in SCP production (Kurcz et al., 2018).

Yeast inactivated biomass has been suitable as SCP source at commercial scale because of their high nutritional quality. In 2018, many processed products were launched using yeast extract as a major ingredient, such as snacks, soups, sauces and seasonings (Bombe, 2019). In fact, the expected growth at a compound annual growth rate (CAGR) of 7.0% of the Global Specialty Yeast Market from 2019 to reach \$4.8 billion by 2025, is mainly attributed to increasing demand for processed foods which contain specialty yeast as a main ingredient (yeast extracts, autolysates and β -glucans) (Bombe, 2019). Low production costs, the larger size when compared with other microorganisms (easier to harvest) and the ability to grow at acidic pH, are other advantages pointed for the use of yeast as a food source. However, poor digestibility can be a constraint for protein extraction, because of yeast's complex and thick cell wall (Nasseri et al., 2011). Furthermore, the high nucleic acid content in yeast is still a problem in food industry, since their excess in diet has been related with uric acid increase, which can lead to diseases like gout (Jaeger et al., 2020). For this reason, the reduction of nucleic acid content in yeast products for use in food industry continues to be a challenge since it exceeds the limit dose for dietary supplements manufactured with yeast (Rakowska et al., 2017).

1.2.2. Spent yeast valorisation

Yeast market is currently led by *Saccharomyces cerevisiae* (*S. cerevisiae*) although there are thousands of yeast species (Bombe, 2019; Payen & Thompson, 2019). The growing launch of new products in beverage industry using yeast as ingredient is pointed as one of the major factors driving the growth of yeast market (Bombe, 2019). *S. cerevisiae* and *Saccharomyces pastorianus* (*S. pastorianus*) are the main two species of *Saccharomyces sensu stricto* species complex used for beer production (Stewart, 2016). Considering the annual world beer production of 1.82 billion hectolitres in 2020 (J. Conway, 2021) and 1.7 to 2.3 g of spent yeast per litre (Marson, de Castro, Belleville, et al., 2020), it was estimated the generation of 309,400 to 418,600 tonnes of brewer's spent yeast worldwide. For that reason, together with its recognition as "Generally Recognized as Safe" (GRAS) microorganism (Rakowska et al., 2017), spent brewer's yeast have been commercialized for years in yeast extracts but the increase of protein rate in the final product is still a challenge (Ritala et al., 2017).

On the other hand, new genetically modified strains of *S. cerevisiae* have been created by synthetic biology industry in order to produce tailored needs, such as farnesene (Meadows et al., 2016), propanol and butanol (Nandy & Srivastava, 2018), among others (Parapouli et al., 2020). Indeed, synthetic biology is progressively impacting a variety of spaces including biomanufacturing, food, agriculture, materials as well as healthcare (Tang et al., 2023), being estimated a CAGR of 19.0% until 2030 (Grand View Research, 2022). Although the global amount of spent yeast generated by this sector is not currently reported, its valorisation might be an integral practice in the circular economy approach since it adds value to materials that would otherwise be discarded, relieving pressure from virgin natural resources.

Figure 1 presents a comprehensive overview of the valorisation of spent yeast and the production of protein extracts derived from it. Several extraction processes, including physical, chemical and/or enzymatic techniques, can be employed, being followed by purification steps when necessary. The characterization of the extracts at different stages of the production process is crucial for evaluating their efficiency. Detailed descriptions of these procedures will be provided in the following sections.

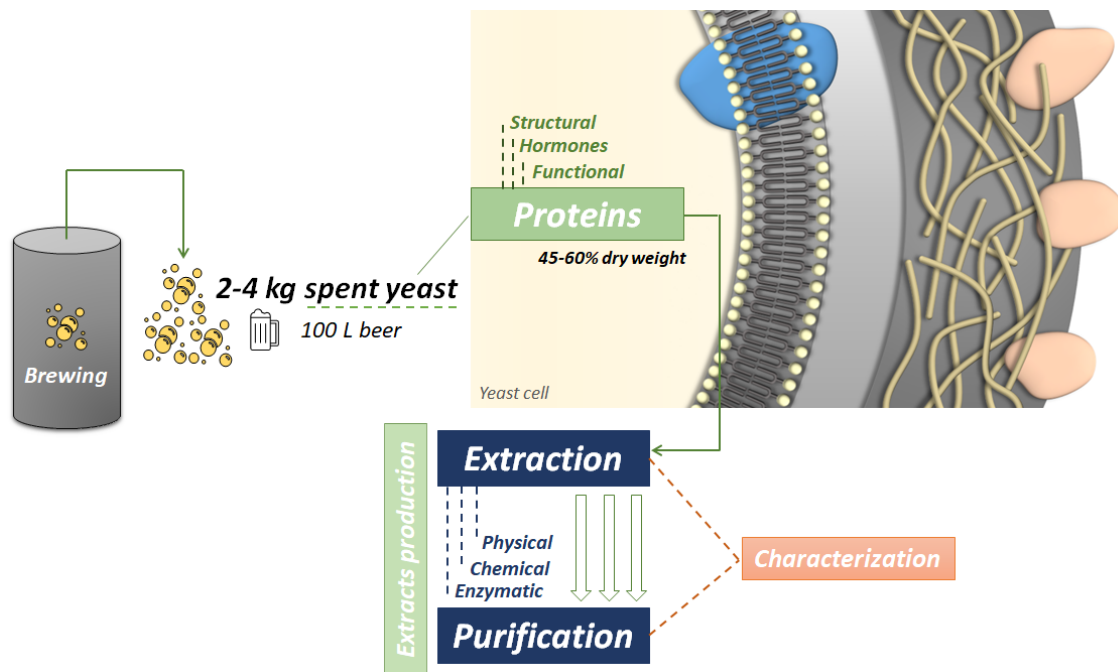


Figure 1. Schematic representation of protein valorisation from spent yeast, applying different extraction processes, followed by purification steps and extracts characterization. Adapted from the graphical abstract of Oliveira, Ferreira et al. (2022b).

1.2.2.1. Proteins & peptides

Proteins (structural, functional and hormones) are the main constituent of *S. cerevisiae*, representing 45-60% of dry weight (DW) basis, and including EAA in amounts similar to those recommended by Food and Agriculture Organization of the United Nations (FAO) and World Health Organisation (WHO) (Vieira et al., 2019). They are found in the yeast cell wall, plasma membrane and periplasm, as other cellular compounds (**Figure 2**). Other constituents are polysaccharides (25-35%) (mainly capsular and cell wall glucans, mannans and chitin), followed by glycoproteins (5 – 10%) which correspond to mannoproteins from cell wall and functional enzymes. Small amounts of nucleic acids (4-8%), lipids (4-7%) and polyphosphates (1-3%) are also present in yeast structure (Feldmann, 2012).

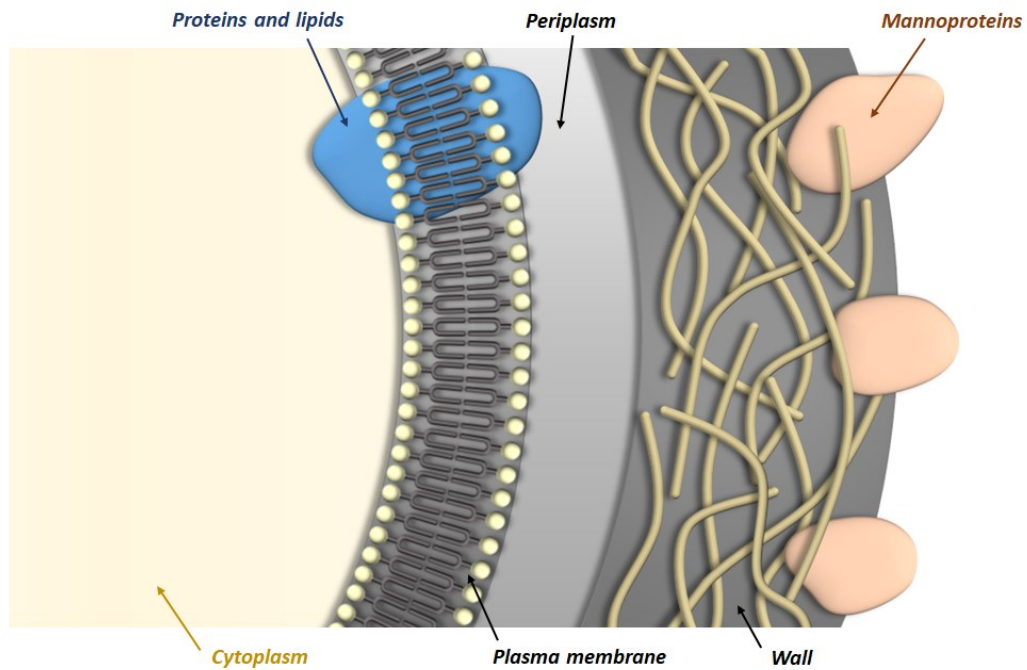


Figure 2. Schematic longitudinal section of *S. cerevisiae* cell and their protein composition (cell structures and components are not in scale).

In cell wall, most proteins are bound to polysaccharides, as mannoproteins. While mannoproteins may represent up to 40% of the DW of the cell wall, when isolated, proteins *per se* represent only a small fraction (13%) (Faustino et al., 2021; Klis et al., 2002). Other cell wall proteins can be linked to the β -1,6-glucan-chitin network as well, which provide elasticity and yet rigidity against cell disruption processes (Orlean, 2012; J. Wang et al., 2018). The thin semi-permeable lipid bilayer of plasma membrane is also formed by proteins in addition to lipids. These proteins play a vital role at controlling the permeability of the cell, in cell wall biosynthesis and overall protection. Secreted proteins that are unable to permeate the cell wall and the plasma membrane constitute the periplasm structure (D. Liu et al., 2016).

Peptides have been described as characteristic protein fragments that have a positive impact on body biological processes and may ultimately lead to health benefits. Indeed, they are involved in regulatory activities in humans, affecting particularly the digestive, immune, cardiovascular, and nervous systems when taken orally. Diverse food protein sources have demonstrated their presence, rising the interest of food market, since the gastrointestinal digestion of these food proteins contribute to their active production (Chauhan & Kanwar, 2019).

Spent yeast has been described as one of the recognized sources of bioactive peptides, where its proteins can be cleaved and freed from the cell envelope by physical, chemical

and enzymatic extraction processes applied, followed by isolation and purification steps, producing protein or peptide-rich extracts, depending on the molecules size (D. Liu et al., 2016). In fact, this production has become a highly relevant topic in last decades research due to the increasing interest in bioactive peptides for the nutraceutical and functional food markets since raw yeast biomass has a low bioactivity performance (M. Amorim et al., 2016; Podpora et al., 2015, 2016). Several biological activities of peptides have been reported over the years such as antioxidant (Mirzaei et al., 2019), antimicrobial (Gddoa Al-sahlany et al., 2020), anti-diabetic (Jung et al., 2011), anti-obesity (K. M. Kim et al., 2004), anticoagulant (Indumathi & Mehta, 2016), angiotensin-converting enzyme (ACE) inhibitors (M. Amorim, Marques, et al., 2019) and chelating effects (de la Hoz et al., 2014). Nowadays, they are also commercialized as food supplements or incorporated in some foods (Marson, de Castro, Belleville, et al., 2020; Okolie et al., 2019).

Extraction

In order to access *S. cerevisiae*'s protein, the extraction processing starts with cell disruption since most proteins are found within the cell. The choice of disruption method can significantly impact the yield and quality of the final product, as well as both fixed and variable costs on industrial processes (Jacob, Hutzler, et al., 2019; Jamshad & Darby, 2012). An efficient breakage of cell wall strength-providing components, namely mannoproteins and glucans, is necessary to effectively extract protein, since their release is determined by the functionality of the plasma membrane and the porosity of the yeast cell wall (Bzducha-Wróbel et al., 2014). Depending on the cell disruption method and subsequent purification and isolation processing steps, different amounts of proteins, peptides and free amino acids are found in the yeast extract product (Jacob, Hutzler, et al., 2019).

A way to classify the protein present in *S. cerevisiae* is according to their molecular weight (MW) since it is a relevant factor on the bioactivity of peptides (usually ranging from 3 to 20 amino acids) (M. Amorim, Marques, et al., 2019). Oligopeptides with 2000-3000 Da of MW usually represent the main group of total protein after yeast autolysis process, followed by di-, tri- and tetra-peptides (MW < 600 Da). Although only 2–5% of the total protein are oligo-peptides with a MW higher than 3000 Da (Rakowska et al., 2017), the ratio between di-, tri-, tetra, and oligo-peptides is strongly related with cell wall degradation during yeast lysis process (J. Wang et al., 2018).

The *S. cerevisiae* extraction methods for protein release described in literature can be classified, according to their main operation mode, in physical methods, either using pressure or waves, and chemical or enzymatic methods (autolysis and hydrolysis), supported by additional chemical substances or enzymes, respectively (**Figure 3**).

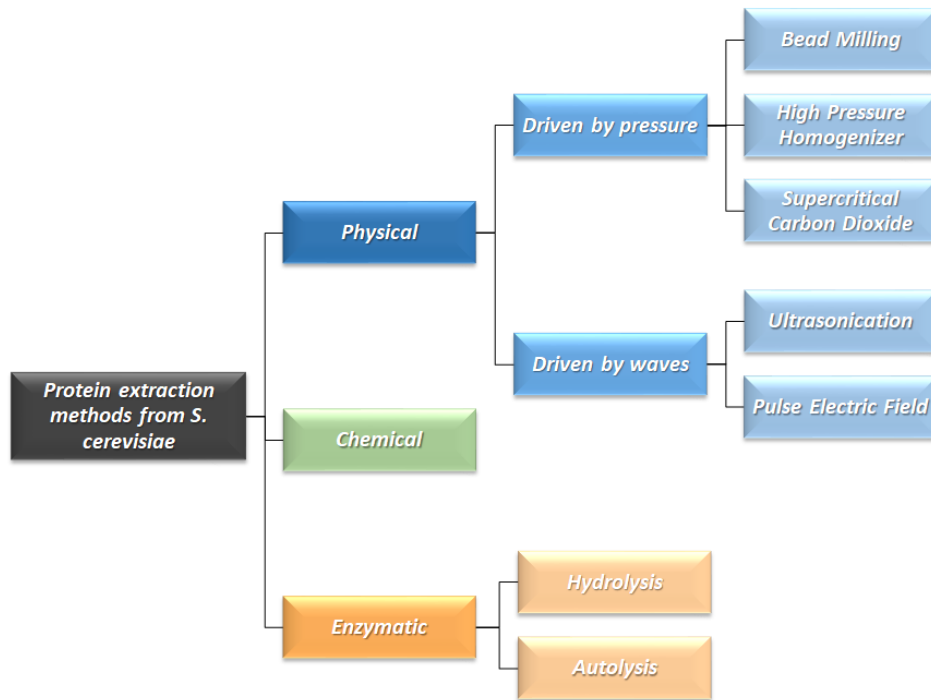


Figure 3. Classification of protein extraction methods from *S. cerevisiae* according to operation mode.

However, a combination of methods is also possible and often desirable. These treatments present a broad variation in their process conditions, which can be explored using the “One Factor At a Time” strategy, where one factor is changed and evaluated independently, or applying a factorial design in order to take all factors into account at the same time (Contreras et al., 2019). Over the years, many extraction processes have been developed attempting to achieve efficient and cost-effective release of proteins from their yeast cells.

Physical methods

Physical methods are described as non-specific and their extraction efficiency is highly dependent on the nature of the substrate of interest, the cell or tissue itself, like the extent of the cell's fragility (Ekpeni et al., 2015; Gaver & Huyghebaert, 1991). However,

there are some relevant scale-up and operation cost differences to be discussed at industry level processes.

Several studies using bead milling, high-pressure homogenization (HPH), ultrasonication, supercritical carbon dioxide (SCO₂) and pulsed electric field (PEF) have been described as physical extraction methods to release *S. cerevisiae*'s protein (**Table 1**).

In general, the former methods damage the yeast cell envelope with the breaking of cell wall due to stress produced by abrasion, pressure (with or without combination of temperature) or cavitation. On the other hand, PEF allows a permeabilization of yeast cell membrane that can be reversible or irreversible according to the electric parameters used. Temperature is not usually employed for protein extraction due to its irreversible effect on conformational modifications in protein structure (denaturation).

Driven by pressure

Bead milling

For decades, bead milling has allowed to achieve high recovery of intracellular compounds from yeast in a single-step operation with reasonable temperature control, easy to scale-up and low requirements in terms of sophisticated equipment or trained personnel (D. Liu et al., 2016; Middelberg, 1995). The various designs of bead mills are based on the principle of a cell suspension agitation with glass or zirconium beads performed in batch or in a continuous recycling mode where the yeast cell wall damage occurs by a mechanical disruption effect (Gaver & Huyghebaert, 1991). Currie, Dunnill and Lilly (1972) started to study the protein release from *S. cerevisiae* and established a first-order kinetics for disruption in a high-speed bead mill. Bead size, agitation, concentration of cell suspension, temperature, time and bead volume are the most studied variables, however, the authors seemed to disagree about the most significant factor to obtain the maximum of protein release (Currie et al., 1972; Gaver & Huyghebaert, 1991). In another study, Currie, Dunnill and Lilly (1972) concluded that temperature was not a determinant factor for protein release, whereas Gaver and Huyghebaert (1991) hypothesized the denaturation of certain proteins with temperature increase for a long disruption time (more than 7 passes). In fact, Gaver and Huyghebaert (1991) observed differences in excretion of two enzymes (glucose-6-phosphate dehydrogenase and

invertase) according to the number of disruption passes. This means that the full opening of the cell wall may not be a requirement to release cell wall-bounded molecules, such as invertase. Concentration of yeast suspension seemed to have no effect on disruption efficiency in this study (Gaver & Huyghebaert, 1991). Jacob, Striegel, et al. (2019) investigated three industrially applicable cell disruption methods for yeast extracts production and they found bead milling (321.56 mg/g), followed by ultrasonication (285.40 mg/g), as the method that released the highest protein content in comparison with autolysis (52.90 and 102.00 mg/g). Moreover, these extracts presented low degradation rates of polyphenols and glutathione, showing their potential in antioxidant and reduction properties. On the other hand, the free amino acids amount present in autolysis extracts (433.21 mg/g) was higher than the one found in mechanical methods (115.68 and 155.38 mg/g), raising questions about sub estimation of protein in these extracts, quantified by Bradford method. Hedenskog and Mogren (1973) showed that other processes could be coupled to bead milling for increased protein in the final extract, namely the selective alkaline precipitation of protein. Bead milling is frequently used for the extraction of specific cell wall components such as β -glucan (Bzducha-Wróbel et al., 2014).

High-pressure homogenization

HPH is based on forcing a cell suspension to pass at high pressure (several hundred bars) through a narrow gap called a homogenizing nozzle or a high-pressure valve (Koubaa et al., 2020). It is currently the most widely accepted disruption cell method by the biotechnology and pharmaceutical industries (Bystryak et al., 2015). Cells experience multiple actions of cavitation effect and high speed impact, disrupting through their interactions with valve and impact ring (D. Liu et al., 2016). Concerning its application for yeast protein extraction, Ekpeni et al. (2016) and Balasundaram and Harrison (2008) described that pressure plays an important role on protein extraction, since this variable induced alteration in yeast pH and viscosity related to the micronisation of the cell debris. However, Siddiqi, Titchener-Hooker and Shamlou (1997) observed that cell debris particle size distribution and the extent of the protein release were independent of the flow rate through the system (scale operation) or the design of HPH valve geometry. Most of the cells were disrupted by the end of fifth pass and, above that number, HPH caused a further degree of the debris formation (Siddiqi et al., 1997). Balasundaram and Harrison (2008) compared two cell disruption techniques where they discovered that HPH (1.7 mg/mL) allowed a higher protein release than hydrodynamic cavitation (0.1 mg/mL),

maintaining a low biomass concentration. In combination with HPH, Liu, Lebovka and Vorobiev (2013) coupled an electrical treatment to yeast suspension aiming to maximize the protein yield. It must be noticed that, by applying only PEF or high-voltage electrical discharges (HVED), a complete rupture of yeast cells was not observed (40 kV/cm, 500 pulses) (D. Liu, Lebovka, et al., 2013).

Supercritical carbon dioxide

A different physical method applied to disrupt and extract proteins from *S. cerevisiae* yeast cells is the use of SCO₂, which involves the application of SCO₂ followed by a sudden pressure drop. The expansion of SCO₂ within the cells forces cell wall breakage, releasing intracellular proteins (H. M. Lin et al., 1991, 1992). While using this technique, Lin et al. (1991) observed an efficient cell disruption at 1000 and 5000 psi of SCO₂ injection (15 h or 5 h, respectively) with simultaneous preservation of the protein functional properties, as indicated by enzymatic activities (alcohol dehydrogenase, invertase, glucose-6-phosphate dehydrogenase and fumarase). The addition of β -glucuronidase to the process decreased the extraction time (90 min at 5000 psi) since the combination of enzymatic hydrolysis with SCO₂ allowed the deactivation of the released enzymes, suggesting it may be used to reduce the cost of protein isolation (H. M. Lin et al., 1991).

Driven by waves

Ultrasonication

Ultrasound has also been extensively reported for extraction of proteins and peptides from yeast, facilitating higher yields and rates of extraction (Kadam et al., 2015). Ultrasound principally acts by generating bubble cavitation in the biological matrix through the conversion of sonic into mechanical energy, in the form of intense elastic shockwaves; cavitation is assumed to be the main mechanism of cell disruption (Kadam et al., 2015; D. Liu et al., 2016). Zhang et al. (2014) and Wu et al. (2015) suggested that ultrasound disruption mechanism starts with the breakdown of cell wall before continuing to the cell membrane, since a significant larger amount of polysaccharide was released at early stages of sonication. James, Coakley and Hughes (1972) established the kinetics of

protein release from an ultrasound batch and flow system, where a good agreement between the theoretical prediction and experimental results was observed. High acoustic power was pointed by several authors as the essential condition to increase protein release from *S. cerevisiae*, although this increment would not be feasible in terms of industrial energy consumption (Apar & Özbek, 2008; Iida et al., 2008; D. Liu, Zeng, et al., 2013; T. Wu et al., 2015). The increase of temperature, processed volumes or cell suspension concentration are other variables that can lead to a decrease in protein yield (Iida et al., 2008; D. Liu, Zeng, et al., 2013; T. Wu et al., 2015; L. Zhang et al., 2014). As in other physical disruption methods, protein could be denatured or suffer thermal coagulation due to temperature, duration of ultrasound treatment or even the sonicator type used (horn or bath) (Iida et al., 2008; D. Liu, Zeng, et al., 2013; L. Zhang et al., 2014). James, Coakley and Hughes (1972) suggested the use of a more efficient cooling system to minimize the activity loss of the released enzymes. The decrease of protein yield with high cell suspension concentration and high processed volume could be related with the decrease of number of cavitation bubbles available for each cell (L. Zhang et al., 2014). Agrawal and Pandit (2003) observed that soft alkaline conditions (pH 8) also allowed for higher protein release. At higher pH, however, a decrease in yield is found, likely due to proteases activity, which deactivate other enzymes or proteins.

Pulsed electric field

Electrical methods are those where yeast cells are treated with high intensity electric field pulses. One of them is PEF, which is based on the electro permeabilization phenomenon, where the applied electric field provokes an electroporation of yeast cell membrane, being this permeability reversible or irreversible according to the electric parameters used. Nevertheless, this treatment can cause leakage of cytoplasmic content, leading to cell breakdown (Ganeva et al., 2003). The variation of electric field strength, as well as the time of treatment, are the main factors responsible for the released protein yield obtained in the process, and need to be adjusted to the used cell suspension concentration (Ganeva et al., 2003; Ganeva & Galutzov, 1999; Ohshima et al., 1995). Ganeva, Galutzov and Teissié (2003) observed a electroextraction of proteins at 3.2 kV/cm (15 pulses, 2 ms, 6 Hz), in agreement with Ohshima, Sato and Saito (1995), which experienced an increase of protein release below 10 kV/cm with few cell deaths, suggesting that the disruption of cell membrane with PEF occurs without cell breakdown. Ganeva and Galutzov (1999) observed the release of cytoplasmic enzymes such as

glutathione reductase, 3-phosphoglycerate kinase and alcohol dehydrogenase, while the yeast cell wall remained intact. Other factors also considerably affect protein yield in PEF treatment, such as the cell growth phase, presence of monovalent ions in the medium, or the incubation of a reducing agent capable of break disulphide bonds, such as dithiothreitol (DTT) (Ganeva et al., 2003; Ganeva & Galutzov, 1999).

In conclusion, among the abovementioned physical methods for protein extraction in *S. cerevisiae*, ultrasonication seems to be quite effective, since it allows the recovery of periplasmic, membrane-bound and insoluble recombinant proteins (Agrawal & Pandit, 2003). However, due to operational and economical limitations of ultrasonication methods, such as amplitude and energy consumption, bead milling and HPH are widely favoured at industrial scale (Bystryak et al., 2015). On the other hand, bead milling and HPH have the downside of poor selectivity, with micronization of the cell debris which can substantially increase the costs of subsequent downstream operations of protein purification or isolation (L. Zhang et al., 2014). HPH and bead milling also require frequent and costly maintenance requirements since they easily get clogged (S. K. Kim, 2016). In order to overcome these methods limitations, Bystryak, Santockyte and Peshkovsky (2015) explored a pilot scale device of ultrasonic technology, namely Barbell Horn Ultrasonic Technology (BHUT), that achieved an productivity increase with respect to laboratory-scale results.

Table 1. Physical extraction methods for protein release from S. cerevisiae.

Physical methods		Cell suspension concentration	Quantification method	Maximum protein	Main conclusions	Reference
Driven by pressure	<i>Bead milling</i>	30%	Lowry	5.32 kg/h	Temperature was not a determinant factor for protein release. Bead size, agitation and yeast concentration had a considerable effect on total protein.	Currie et al. (1972)
		10%	Kjeldahl	60% of yield (DW)	Bead milling allowed the highest protein released compared to lyophilized, spray-dried or drum dried material. In these processes, no cell wall disruption or cell fragmentation could be observed.	Hedenskog & Mogren (1973)
		30%	Kjeldahl	80 mg/g yeast	A long disruption time and a high beads volume created a cumulative effect of the disruption forces which may cause denaturation of certain proteins. The yeast cell concentration seemed to have no effect on disruption efficiency.	Gaver & Huyghebaert (1991)
		7%	Bradford	321 mg/g yeast (DW)	Bead milling, followed by ultrasonication, increased the amount of protein in yeast extract produced in comparison with autolysis. However, the autolysis process allowed a higher release of free amino acids from yeast than mechanical methods.	Jacob, Striegel, et al. (2019)

Physical methods	Cell suspension concentration	Quantification method	Maximum protein	Main conclusions	Reference
<i>HPH</i>	NM	Bradford	96 mg/g yeast	The cell debris particle size distribution and the total protein release are independent of the scale of operation and HPH valve geometry.	Siddiqi et al. (1997)
	5%	Bradford	1.7 mg/mL yeast suspension	HPH showed the higher amount of protein release in relation to hydrodynamic cavitation. Alteration in the viscosity and pH of the disrupted cell suspension was obtained as a function of disruption intensity.	Balasundaram & Harrison (2008)
	5%	Bradford	50 µg/g dry yeast	The combination of electrical and HPH treatments allowed to obtain a good protein yield with low content of nucleic acids. Incomplete damage of yeast cells under PEF or HVED treatment.	Liu, Lebovka, et al.(2013)
<i>SCO₂</i>	30:70	Bradford	1.4 mg/mL yeast suspension	Protein yield showed an increment rate as the ratio yeast: buffer increases from 10:90 to 30:70. The pressure rise induced an alteration in yeast viscosity, influencing the protein release.	Ekpeni et al.(2016)
	NM	Lowry	33 mg/g wet yeast	High-pressure CO ₂ fluid could prevent the deactivation of the released enzymes. The use of lytic enzymes, as β-glucuronidase, decreased the extraction time which may reduce the cost of protein isolation.	Lin et al. (1991)

Physical methods		Cell suspension concentration	Quantification method	Maximum protein	Main conclusions	Reference
Driven by waves	<i>Ultrasonication</i>	20%	Lowry	9 mg/mL yeast suspension	Good agreement between the theoretical prediction of protein release and experimental results. A more efficient cooling system would be desirable to minimize the activity loss of the released enzymes.	James et al.(1972)
		2%	Lowry	1.27 mg/mL yeast suspension	At weak alkaline pH was observed the maximum of protein release under ultrasonication (11.62 W or 20% amplitude) for 60 min. Very alkaline media seemed to increase proteases or other enzymes activity which may deactivate other enzymes or proteins.	Agrawal & Pandit (2003)
		9%	Lowry	85 % of release	High acoustic power, duty cycle and the addition of glass beads to the process increase the protein release. No influence of different cell concentration. However, the increase of acoustic power is not feasible in terms of energy consumption.	Apar & Özbek (2008)
		1%	UV*/BCA	80 mg/g yeast	Maximal protein release was observed at high power conditions (80 W). The increase of cell concentration decreased the final protein level. Higher protein recovery using a 20 kHz-horn compared with 130 kHz-bath sonicator.	Iida et al.(2008)

Physical methods	Cell suspension concentration	Quantification method	Maximum protein	Main conclusions	Reference
	1%	Bradford	0.6 mg/mL yeast suspension	High acoustic power increased the protein release. However, the increase of sonication time may cause significant protein degradation due to high temperature.	Liu, Zeng, et al.(2013)
	10%	BCA	25% of release (DW)	Temperature showed to be the most important parameter to selective release of polysaccharide and protein. The increase of cell concentration, processed volumes and temperature decreased the final protein.	L. Zhang et al. (2014)
	20%	Bradford	16.6 mg/mL yeast suspension	The maximum protein released obtained in a pilot scale device of ultrasonic technology (BHUT) compared with conventional ultrasonication.	Bystryak et al. (2015)
	10%	BCA	92% of release (DW)	High acoustic intensity (24 and 39 W/cm ²) allowed the increase of protein release. The increase of cell concentration, processed volumes and temperature decreased the final protein.	Wu et al. (2015)
<i>PEF</i>	10 ⁸ - 10 ¹⁰ cells/mL	Lowry	40 µg/mL yeast suspension	Released protein increased with the electric field strength, increased rapidly in a region below 10 kV/cm. Protein can be released simultaneously with few cell deaths.	Ohshima et al. (1995)

Physical methods	Cell suspension concentration	Quantification method	Maximum protein	Main conclusions	Reference
	NM	Bradford	29% in final extract	Some cytoplasmic proteins were extracted with intact cell walls. The electro-induced protein release showed a strong dependence on the cell growth phase and the presence of monovalent ions in the medium. The pre-incubation with DTT provoked a faster and exponential protein efflux.	Ganeva & Galutzov (1999)
	4.5%	Commercial kit	85% in final extract	The parameter of field intensity is the core of this process and must be adjusted to the yeast concentration. A high protein yield required long extraction with DTT after PEF (> 4 h at 30 °C).	Ganeva et al. (2003)

NM - not mentioned, BCA - bicinchoninic acid kit. *Protein absorbance.

Chemical methods

Chemical treatments using chelating agents, detergents and solvents can lead to permeabilization or lysis of yeast cells, triggering the subsequent release of intracellular molecules. These procedures rely on the relative selective interaction of the chemicals with specific components of the membrane, allowing proteins to seep through the cell wall (Klimek-Ochab et al., 2011). In **Table 2**, the main chemical procedures for protein extraction from *S. cerevisiae* are listed.

Alkaline precipitation is one of the most used chemical procedures to extract *S. cerevisiae* protein, although the involved mechanism is not clear (Kushnirov, 2000; T. Zhang et al., 2011). Kushnirov (2000) hypothesized that under alkaline conditions (0.2 M NaOH) the O-chains of O-glycosylated proteins (covalently linked to other cell wall components, such as β -1,3-glucans), are cleaved off in a process called beta-elimination, which allow the release of O-glycosylated proteins. In order to increase the protein yield, Zhang et al. (2011) introduced a pre-treatment with lithium acetate (LiAc), described as an enhancer of cell wall permeabilization. Mukherjee (2020) tested several protein extraction methods already described in literature aiming to study *S. cerevisiae* at different growth phases. The modified protocol of Kushnirov (2000) with alkaline and sodium dodecyl sulphate (SDS) buffer treatment showed the maximum protein release at exponential and late stationary phase cells, in comparison with physical methods (glass beads, sonication or both) or individual SDS-buffer or alkaline treatment, displaying sharp and distinct bands in sodium dodecyl sulphate-polyacrylamide gel electrophoresis (SDS-PAGE). However, the loss of enzymatic activity may be a concern when applying this protocol (Mukherjee et al., 2020). Ionic liquids, namely 3-(dimethylamino)-1-propylaminium formate ([DMAPA]FA), were also tested for cell wall breakage, and the extracted target proteins maintained their properties unchanged (Ge et al., 2010).

Generally, the chemical approaches are followed by separation and purification techniques, such as SDS-PAGE (Ge et al., 2010; Kushnirov, 2000; Mukherjee et al., 2020; T. Zhang et al., 2011).

*Table 2. Chemical extraction methods for protein release from *S. cerevisiae*.*

Cell suspension concentration	Quantification method	Maximum protein release	Main conclusions	Reference
NM	NQ	NQ	Pre-treatment with 0.2 M NaOH, followed by 3 min of boiling in SDS-PAGE buffer, significantly increased the yield of extracted proteins.	Kushnirov (2000)
NM	NQ	NQ	[DMAPA]FA was the ionic liquid solution capable of the higher efficiency on protein extraction. Chemical properties of target proteins remained unchanged during the extraction process.	Ge et al. (2010)
NM	NQ	NQ	The combined pre-treatment with LiAc, followed by NaOH and SDS-PAGE buffer gave the best results in yeast whole protein extraction. Using LiAc or NaOH individually showed a lesser extent of protein extraction.	T. Zhang et al. (2011)
NM	Lowry	70 µg/g yeast	The modified method from (Kushnirov, 2000) revealed the maximum protein yield in comparison with physical (glass beads and sonication) and alkaline or SDS-buffer individual treatment.	Mukherjee et al. (2020)

NM - not mentioned, NQ – not quantified.

Enzymatic methods

Enzymatic methods for protein release involve attacking the mannoprotein complex and glucan backbone of the yeast cell by endogenous (autolysis) or exogenous lytic enzymes (D. Liu et al., 2016).

Autolysis

Autolysis is an endogenous process that represents the degradation of the cell components from inside out by action of yeast own enzymes. It occurs when the cell

growth cycle is completed and death phase is initiated (Takaloo et al., 2020). Intracellular enzymes are activated by appropriate process conditions, such as temperature, time and pH, which results in a partial degradation of the cell wall structures (Podpora et al., 2015). It was observed that a long autolysis time increase the amino acid content from 11.2% (2 h) to 77.5% (48 h), with a consequent decrease of peptide amounts and size, as they were decomposed into free amino acids (Podpora et al., 2015). The same observations were conducted by Jacob, Hutzler and Methner (2019), who concluded that a strong enzymatic degradation of protein takes place during the autolysis process; indeed, autolysis is biased to hydrolyse proteins to the greatest possible extent, in contrast with bead milling and ultrasound, thus obtaining an increase in free amino acids content and peptides with low MW (below 4 kDa). The precise control of autolysis extension leads to different fractions of free amino acids and peptides with distinct MW, which can be explored for the production of different protein-rich extracts in a single process (Podpora et al., 2015).

Enzymatic hydrolysis

If additional exogenous enzymes are added to the yeast, the process is named enzymatic hydrolysis. Hydrolysis is the most efficient method of solubilizing yeast, where proteolytic or cell wall lysis enzymes firstly hydrolyse the compounds in cell walls to promote cell lysis. These enzymes can also enhance the activities of endogenous enzymes, thereby accelerating the leakage of intracellular substances (Chae et al., 2001; Xie et al., 2017). The effect of enzymatic hydrolysis on proteins is mild, changing their MW, charge and exposure of hydrophobic groups and reactive amino acid side chains, but does not destroy them. The specificity of the enzymatic complex used determines which peptides are produced (Celus et al., 2007). The endopeptidases Alcalase[®], Corolase[®], Papain and Brauzyn[®], an aminopeptidase (Flavourzyme[®]) and other proteases (Protamex[®] and Promod[®]), as well as combinations thereof, are the enzymatic complexes most widely used for production of protein-rich extracts from *S. cerevisiae* (**Table 3**). Chae, Joo and In (2001) concluded that protein recovery is strongly dependent of the enzyme dosages, increasing with the hydrolysis length and being more responsive to Flavourzyme[®] than Protamex[®]. High solid concentrations of yeast cells (28%) also seemed to exert a positive influence in protein release (Xie et al., 2017). The maximum protein recovery reported was about 53–76%, regardless of the enzyme complex used or time treatment (Chae et al., 2001; Marson et al., 2022; Podpora et al., 2016; Xie et al.,

2017). In such conditions, the final profile of protein extracts presented a high percentage of low MW peptides (90% below 3 kDa) and free amino acid content, also independent of the protease that was used for hydrolysis (Chae et al., 2001; Marson et al., 2022; Podpora et al., 2016; Xie et al., 2017). The advantages of applying enzymes for protein extraction are mainly the gentle conditions employed and their specificity. However, the price of enzymatic complex may be a deterring factor on a large scale operation (Klimek-Ochab et al., 2011). Nevertheless, some patents have been issued for the production of yeast protein extracts for foodstuffs using hydrolytic enzymes (Ason, 2019; Hobson, 1991; Jolly, 1978; Kortes, 2020), with a final protein content about 60–80% (Ason, 2019; Hobson, 1991; Kortes, 2020). A yeast peptide hydrolysate for cosmetic industry was also patented by Farra (2015), where enzymatic hydrolysis was applied to degrade protein into peptides with low MW.

Among the abovementioned protein extraction methods, enzymatic hydrolysis is the most specific process; chemical methods are also relatively specific, although the violent experimental conditions and strong reagents may provoke alteration on final protein content or peptide and amino acid profile (L. Zhang et al., 2014). On the other hand, autolysis has the main advantage of only using yeast's own enzymes for the process, but the temperature and long-time treatment can lead to bacterial contamination on yeast suspension turning the final product unfeasible.

In general, process cost and selectivity are inversely related, although it must be in mind that a clean extract (i.e., without significant amounts of contaminants) will facilitate the downstream isolation and purification processes, thus decreasing the final cost of the overall process. Nevertheless, there are no general rules since the selection of the extraction method will be dictated by the final use of the protein extracts.

Table 3. Enzymatic extraction methods for protein release from *S. cerevisiae*.

Enzymatic methods	Cell suspension concentration	Quantification method	Maximum protein	Main conclusions	Reference
<i>Hydrolysis</i>	20%	Kjeldahl	53.6% recovery	Protein recovery was more responsive to Flavourzyme® than Protamex®, being strongly depended on the enzyme dosages and time treatment. After 12 h, Protamex® (0.6%) and Flavourzyme® (2%) exhibited the highest protein release. The optimized conditions produced yeast extract contained mostly low MW peptides and free amino acids.	Chae et al. (2001)
	NM	Kjeldahl	60% in final extract (w/w)	Papain was used to perform hydrolysis during 24 h (50-60 °C), resulting in a final extract with high content of free amino acids and only trace amounts of peptides (MW > 1740 Da).	Podpora et al. (2016)
	28%	Kjeldahl	67.7% recovery	High solid concentrations of yeast cells led to an increase of protein recovery. The hydrolysis degree was higher with Alcalase® (0.1%, 48 h, 55 °C) than Papain but the peptides MW were similar (< 3 kDa reached 90%). The addition of sodium chloride (1-3%) to cell suspension accelerated the hydrolysis process.	Xie et al. (2017)
	NM	Far-UV† (214 nm); Lowry	76% in final extract (w/w)	Brauzyn®, Protamex® and Alcalase® (2000 U/ g protein) hydrolysis at 50 °C during 2 h (pH 7.0) produced a yeast hydrolysate rich in peptides from 7000 to 1000 g/mol (43%) with a small amount of short peptides and amino acids (25% of 1000-100 g/mol). The sequential membrane filtration process applied to the hydrolysate increase protein purity regarding RNA and total sugars up to 1.7 and 2.7-fold, respectively.	Marson et al. (2022)
<i>Autolysis</i>	NM	HPLC-UV/VIS	324 mg/g in final extract (w/w)*	A longer autolysis (48 h) allowed a substantial increase of free amino acids content with the presence of peptides from 1000 to 2000 Da (about 10-20 amino acids). The precise control of autolysis time process led to obtain autolysates	Podpora et al. (2015)

			with varying free amino acid content and peptides of different MW tailored to the specific nutritional needs.	
NM	HPLC	350 mg/g final extract (w/w)*	The cleavage of protein (MW peptides < 4 kDa) and release of free amino acids was higher in autolysis (24 h, 50 °C) than bead milling or ultrasonication.	Jacob, Hutzler, et al. (2019)

NM - not mentioned, RNA - ribonucleic acid. * - sum of free amino acids, † - protein absorbance.

Isolation and purification

Following protein extraction from *S. cerevisiae* cells, purification and/or isolation steps are generally required to obtain protein isolates and concentrates. Depending on the physicochemical properties of proteins present and the final goal, different isolation and purification methods are applied to the “crude protein extract”. The aim of a purification process is not only the removal of unwanted contaminants, but also the concentration of the desired protein, preferably on a stable environment and in a form adequate for the intended application (Hedhammar et al., 2006). Cell debris with different size are contaminants resulting from the physical extraction, which can be easily removed by high-speed centrifugation, traditionally used for the primary recovery of soluble protein (D. Liu et al., 2010). On the other hand, chemical and enzymatic extraction methods create less contamination due to their selectivity, at the cost of lower protein recovery. As previously mentioned, such selectivity may have a positive impact on economic assessment of the large-scale process (Jacob, Hutzler, et al., 2019).

Several procedures hereby described and discussed for *S. cerevisiae* protein separation and purification were applied in order to isolate specific molecules and obtain a final product with the desired performance.

Selective precipitation

As previously described, alkaline precipitation is considered one of the chemical methods for protein extraction from *S. cerevisiae* (Kushnirov, 2000; Mukherjee et al., 2020; T. Zhang et al., 2011). In fact, protein precipitation is one of the most used methodologies to concentrate and purify yeast protein extract (Hedhammar et al., 2006; Mukherjee et al., 2020). Generally, this reaction is applied after disruption of yeast cell (Butylina et al., 2007; Caballero-Córdoba & Sgarbieri, 2000; Farra, 2015; Hedenskog & Mogren, 1973; Yamada & Sgarbieri, 2005) and can be followed by other purification processes such as dialysis and enzymatic hydrolysis, as patented by Farra (2015) for production of a cosmetic peptide hydrolysate. Simple alkaline precipitation was used by Hedenskog and Mogren (1973) and Butylina et al. (2007), with the latter performing acidic precipitation for nucleoprotein complexes production. On the other hand, *S. cerevisiae* protein concentrates were produced by Caballero-Córdoba and Sgarbieri (2000) using a salting out technique, with sodium perchlorate coupled to isoelectric

precipitation at pH close to 4. Protein phosphorylation with sodium trimetaphosphate at alkaline pH for modifying protein structure was explored by Yamada and Sgarbieri (2005) with the same intent. Organic solvents can also be used for protein precipitation as shown by Farra (2015), who proposed the use of a saline solution and an alcohol medium for protein precipitation. Since these yeast protein precipitations involved several steps and are difficult to scale-up, Akardere et al. (2010) developed a scalable three-phase partitioning (TPP) to purify a *S. cerevisiae* glycoprotein, namely invertase, in a single step, after sonication treatment. This technique combines salting out, use of organic solvents and precipitation pH techniques into one-step system where the crude protein extract is mixed with solid ammonium sulphate and t-butanol in order to obtain the desired proteins selectively partitioned and concentrated to one phase. Hydrophilicity and protein MW affected the partitioning process outcome (Akardere et al., 2010).

Membrane filtration

Membrane filtration is another alternative for separation of soluble intracellular proteins from cell lysates which allows filtrate recovery and cell debris removal with high selectivity and satisfactory efficiency both in cross-flow and dead-end systems and low energy consumption (D. Liu et al., 2010; Mohammad et al., 2012). In fact, this process is of great interest for increase of peptide fractions purity since it may promote the separation through sieving and charge-based mechanisms (Vollet Marson et al., 2020). Food processing industry has been using this technique over the last decades since peptides and proteins need a gentle product treatment (low temperatures and pH value close to neutrality) to maintain their structural and physicochemical characteristics since their bioactive properties depend on peptides and proteins sequence and structure (Marson, de Castro, Belleville, et al., 2020; Mohammad et al., 2012; Vollet Marson et al., 2020). Membrane selectivity and properties (material, structure and pore size), permeate flux (which is dependent on operating conditions such as temperature, pressure, process configuration, module characteristics, cleaning procedure) and feed characteristics (physicochemical of components, pH and concentration) are the main parameters that influence the separation performance (Vollet Marson et al., 2020). However, the membrane fouling control and their cleaning processes are still a challenge (Mohammad et al., 2012).

Membrane filtration has been reported for the isolation of *S. cerevisiae* bioactive peptides (Albergaria et al., 2010; Branco et al., 2014; Gddoa Al-sahlany et al., 2020; J. Kim et al., 2004; Mirzaei et al., 2015), specific proteins (D. H. Lee et al., 2007), nucleoprotein complexes (Butylina et al., 2007) and separation of yeast hydrolysates from sugars and ribonucleic acids (RNA) (Marson et al., 2022), being the intended application of separation an important aspect of process design (Vollet Marson et al., 2020). Many times, this technique was preceded by protein precipitation (Butylina et al., 2007), enzymatic hydrolysis (Albergaria et al., 2010; J. Kim et al., 2004; Marson et al., 2022; Mirzaei et al., 2015), autolysis (Mirzaei et al., 2015) and physical disruption methods, such as sonication (Mirzaei et al., 2015) or bead milling (D. H. Lee et al., 2007). Adsorption (Branco et al., 2014; Butylina et al., 2007) and chromatography [84,86-89] are other protein purification and fractionation methods used prior to membrane filtration. Ultrafiltration with 50 kDa (Marson et al., 2022), 15 kDa (Marson et al., 2022), 10 kDa (Albergaria et al., 2010; Branco et al., 2014; Gddoa Al-sahlany et al., 2020; Mirzaei et al., 2015), 8 kDa (Marson et al., 2022), 5 kDa (J. Kim et al., 2004; Mirzaei et al., 2015), 3 kDa (Mirzaei et al., 2015), 2 kDa (Albergaria et al., 2010; Branco et al., 2014; Gddoa Al-sahlany et al., 2020) and 1 kDa (D. H. Lee et al., 2007; Marson et al., 2022) cut-off membranes have been reported on yeast protein separation and concentration. In fact, several authors applied a sequential ultrafiltration process using a 10 kDa cut-off membrane followed by 2 kDa for production of antibacterial peptides (Albergaria et al., 2010; Branco et al., 2014; Gddoa Al-sahlany et al., 2020). Marson et al. (2022) applied two serial fractionation of 50, 8 and 1 kDa and 15, 8 and 1 kDa for separation of yeast hydrolysate from sugars and RNA, demonstrated that 15 kDa retained higher MW compounds, increasing performance of the next separation steps at 8 and 1 kDa. This fractionation was important for improvement of peptide purity of fractions from RNA and total sugars (1.7 and 2.7-fold, respectively). Potential antihypertensive and antioxidant peptides were also produced through ultrafiltration processes (J. Kim et al., 2004; Mirzaei et al., 2015) as well as β -secretase (D. H. Lee et al., 2007). Butylina et al. (2007) applied a cross-flow microfiltration system through track-etched membranes 0.3 μm to separate the high and low molecular mass fractions, concluding that the nucleoprotein complexes were retained by membrane and were found to activate repair pathways in oxidative stress cells of *S. cerevisiae*.

Dialysis

Dialysis is a conventional lab-scale technique to reduce or remove salt from protein extracts by osmotic phenomena using a semi-permeable membrane (Nehete et al., 2013). However, this procedure can take up several days, requires large volumes of water and can lead to low protein yields, since significant losses of low MW compounds can occur through the membrane system (Clark, 2001), turning this a non-scalable process for industries. Nevertheless, Farra (2015) patented a yeast peptide hydrolysate production process for cosmetic industry where a variant of the method includes a dialysis technique.

Chromatography

Chromatographic separation of protein mixtures has become one of the most effective and widely used techniques for purifying individual proteins. Depending on protein properties, such as size, charge, hydrophobicity, and bio specific interactions, different versions of liquid chromatography, with several types of stationary phases, are used for protein and peptide isolation from *S. cerevisiae*. As in the other brewer's yeast protein purification techniques, chromatographic methods are generally used after cell disruption methods (Agrawal & Pandit, 2003; Balasundaram & Harrison, 2008; Butylina et al., 2007; D. H. Lee et al., 2007) and/or fractions separation by ultrafiltration (Branco et al., 2014; Butylina et al., 2007; Gddoa Al-sahlany et al., 2020; J. Kim et al., 2004; D. H. Lee et al., 2007).

Size-exclusion chromatography (SEC), also known as gel-filtration chromatography, is one of the widely used chromatographic techniques for isolation of antimicrobial, antihypertensive and antidementia peptides from *S. cerevisiae*. SEC is a reference technique for the qualitative and quantitative analysis of protein aggregates in protein biotherapeutics because of its speed and reproducibility (Sui et al., 2018). It is based on the sieving properties of the stationary phase matrix, which is constituted by porous particles, with separation depending on protein's size and shape (Hedhammar et al., 2006). Preparative columns composed by gel matrices of dextran polymers and highly cross-linked agarose (Superdex) (Branco et al., 2014; Gddoa Al-sahlany et al., 2020) or epichlorohydrin (Sephadex) with different bead size are the most used in these studies. The surface of these supports contains predominantly hydroxyl groups and provides a good environment for hydrophilic proteins (Hedhammar et al., 2006). Gddoa Al-sahlany et al. (2020) obtained three different peptide fractions after employing gel filtration

chromatography using a purifying system (ÄKTA) with a Superdex column. As SEC allows to separate proteins according to their size, Butylina et al. (2007) used this method to estimate the molar mass (MM) distribution of yeast nucleoprotein complexes. The authors described the high MM fraction with tightly bound proteins in the first peak eluted since no dissociated protein molecules were detected.

Several studies described the application of ion-exchange chromatography (IEC) coupled with SEC in order to eliminate matrix contaminants or to concentrate the peptide fractions (Branco et al., 2014; Butylina et al., 2007; Dick et al., 1992). In fact, IEC is one of the most commonly used industrial chromatographic processes for purification of pharmaceutical proteins and peptides, since their mild conditions allows to maintain the native molecule structures and their resins have high binding capacities, offering a good and controllable selectivity (Grönberg, 2018). IEC is based on electrostatic interactions, being the protein separation accomplished by competition between proteins with different surface charges for oppositely charged groups on an ion exchanger adsorbent (Hedhammar et al., 2006). Protein binding to the stationary phase, as well as their desorption, can be modulated by changes in ionic strength and pH, through ionic competition or change in protein charge, respectively (Grönberg, 2018). Branco et al. (2014) pooled the most bioactive peptide fraction resulted from SEC separation at 2-10 kDa ultrafiltration process into two different strong cation and anion-exchange columns. A similar approach was used by Butylina et al. (2007) in order to remove protein from nucleoprotein complexes obtained after microfiltration (“retentate”). Although the aforementioned studies described combination of different chromatographic techniques, IEC has also been described as the unique chromatographic method for the separations of *S. cerevisiae* enzymes. Lothe et al. (1999) evaluated Amberlite™ XAD-16 and Indion NPA-1 resins performance to isolate α -glucosidase and invertase, trying to activate the adsorbent surface by ultrasound pre-treatment (“surface grafting”) in order to reduce the hydrophobicity and nonspecific adsorption of proteins. Nonspecific adsorption of proteins has considerably been reduced in grafting exchangers with an enhanced of adsorption enzymes selectively. Agrawal and Pandit (2003) also optimized the batch adsorption process by native and grafted XAD-16 for α -glucosidase isolation on *S. cerevisiae* cell extract. Based on principle of IEC, expanded bed adsorption (EBA) was also proposed as a preliminary purification technique to capture *S. cerevisiae* total soluble protein and α -glucosidase after HPH or hydrodynamic cavitation yeast treatment (Balasundaram & Harrison, 2008). This technique is capable to replace 3-4 unit

operations in a typical downstream process, since the unclarified yeast suspension (biomass and extracellular medium) can be directly applied to the adsorbent, eliminating the need for previous solid–liquid separation and concentration steps. A higher adsorption of α -glucosidase was observed in anionic Streamline[®] Diethylaminoethyl (DEAE) adsorbent than cationic Streamline[®] Sulphopropyl (SP), being the yeast disruption extent an influence of dynamic binding capacity. In fact, the increase of disruption cell degree allowed a high protein release and dynamic binding capacity for total protein and α -glucosidase. However, the cell debris resulted from strong disruption seemed to have a negative impact on α -glucosidase selective adsorption (Balasundaram & Harrison, 2008).

Reversed-phase high-performance liquid chromatography (RP-HPLC) has also been used after SEC fractionation for isolation of bioactive peptides from *S. cerevisiae* (J. Kim et al., 2004; D. H. Lee et al., 2007). RP-HPLC is a separation method based on hydrophobicity characteristics of the protein where the stationary phase, as well of hydrophobic nature, is based on silica gel or a synthetic polymer (Josic & Kovac, 2010). The strong hydrophobic interaction in RP-HPLC is almost enough to adsorb proteins in pure water (Hedhammar et al., 2006), although an acid (formic, acetic or trifluoroacetic acid) is generally added to the mobile phase to render the proteins and peptides positively charged and to reduce undesirable interactions with the stationary phase (Josic & Kovac, 2010). However, acids may cause the protein to denature. Pharmaceutically important globular proteins, peptides and small polypeptides are purified by RP-HPLC (Nehete et al., 2013). Nevertheless, the use of RP-HPLC is limited for large-scale processes since low mass yields and loss of biological activity of larger polypeptides can be found due to acidic buffering systems and hydrophobicity of silica columns (Nehete et al., 2013). The purification of several *S. cerevisiae* peptides, separation and concentration in preparative μ Bondapak C18 column (J. Kim et al., 2004; D. H. Lee et al., 2007) followed by analytical Protein & Peptide C18 column (J. Kim et al., 2004) was studied: Kim et al. (J. Kim et al., 2004) purified a novel decapeptide with antihypertensive properties through ultrafiltration, SEC and RP-HPLC separation with a yield of 3.5%. Lee et al. (2007) characterized a new antidementia peptide obtained by yeast bead milling disintegration, ultrafiltration, SEC and two RP-HPLC separation and concentration processes with a yield of 0.6%. In both uses of μ Bondapak C18 column, a linear gradient with 0.1% of trifluoroacetic acid in water was used as mobile phase (J. Kim et al., 2004; D. H. Lee et al., 2007).

Nucleic acids extraction

One of the challenges of using *S. cerevisiae* protein-rich extracts as food supplement for humans is the high content of nucleic acid, mainly RNA, since their high intake may result in health issues (Caballero-Córdoba & Sgarbieri, 2000). Several authors have already described processes of *S. cerevisiae* protein-rich extract production attending to obtain a low RNA content. However, the first proposed methods to reduce nucleic acid content from yeast protein involved strong chemical and enzymatic treatments which led to several harmful effects on the nutritional and functional qualities of the isolated protein. Potentially toxic compounds resulting from alkali treatment (J. K. Shetty & Kinsella, 1980a, 1980b), protein degradation by nucleic acid enzymatic hydrolysis (Lindblom, 1977) and the nutritional safety of proteins produced by their acid anhydride modification (J. K. Shetty & Kinsella, 1980a, 1980b; K. J. Shetty & Kinsella, 1979) were pointed.

On the other hand, chemical phosphorylation has been described for decades as one of the best RNA removal processes, since the addition of phosphorus oxychloride (Y. -T Huang & Kinsella, 1986; Kinsella & Damodaran, 1984) or sodium trimetaphosphate (Yamada & Sgarbieri, 2005) to the disrupted cell extract at alkaline pH caused dissociation of nucleoprotein complexes. Kinsella and Damodaran (1984) showed a maximum RNA reduction of 80% applying a minimum of phosphorus oxychloride/protein ratio. The proposed mechanism states that the net negative charges on the protein introduces a strong electrostatic repulsion within the nucleoprotein complexes. As the dissociated nucleic acids have an isoelectric pH around 1.5-2.0, they remain soluble during protein precipitation at pH 4.2 (Kinsella & Damodaran, 1984). Huang and Kinsella (1986) removed more than 85% of RNA by protein phosphorylation while no change in the amino acid composition of yeast proteins was observed. Despite modification of protein by phosphorylation may be more acceptable than other chemical methods with good percentages of RNA reduction, protein yield is pointed as one of the main issues since the reaction is depending on the pH of the protein precipitation (Y. -T Huang & Kinsella, 1986; Kinsella & Damodaran, 1984; Yamada & Sgarbieri, 2005). Yamada and Sgarbieri (2005) observe a 10.4% increase in RNA content in the final extract by tuning pH to 3.2 in order to raise the protein yield.

Adding a step of sodium perchlorate treatment to the disrupted cell extract is another method for RNA reduction, leading to its decrease from 7.04% (in biomass) for 2.26%

(in protein final extract) (Caballero-Córdoba & Sgarbieri, 2000). In fact, this reagent is used in experimental protocol for RNA determination in yeast extracts (Caballero-Córdoba & Sgarbieri, 2000; Yamada & Sgarbieri, 2005).

Liu, Lebovka and Vorobiev (2013) proposed a selective extraction of intracellular yeast components by electrical treatment (HVED and PEF) aiming to extract initially ionic and nucleic acid components and then proteins using HPH treatment, which can be useful for nucleic acid reduction in protein-rich extracts production. Besides, Chae, Joo and In (2001) used nuclease treatment to dissociate nucleotides from yeast protein previously hydrolysed in order to produce flavour ingredients, which can be potentially used for RNA reduction as well. After treatments using optimal combination of enzyme, enzyme dosages and treatment sequence, low MW peptides and free amino acids were obtained in final yeast extract with a yield of 3.67% of 5'-nucleotides content (Chae et al., 2001).

In another approach, some authors aim to produce protein-rich extracts with a high RNA content in order to be used as flavouring ingredients. Oliveira et al. (2011) optimized an autolysis process on spent yeast in order to obtain a RNA yield of 89% that results a yeast extract with 57.9% protein as well (55.2 °C, pH 5.1 with 9.8% NaCl for 24 h), being the heat treatment (60 °C, 15 min) prior to autolysis an essential step to increase the RNA content for 91.4%. Sombutyanchit et al. (2001) also studied a similar autolysis process of for disodium guanosine-5'-monophosphate (5'-GMP)-rich extracts production using yeast pre-heat treatment and 5'-phosphodiesterase. A yeast extract was produced with a 5'-GMP maximum of 0.93% (w/w).

Characterization

Characterization plays an important role throughout the entire process of protein-rich extracts production, since it helps to understand the chemical and biological potential of extracts, adapting the application to different sectors according to their performance. Furthermore, characterization techniques are able to evaluate the efficiency of protein extraction and the subsequent purification and isolation processes. Regarding protein analysis, protein and amino acids determination and MW evaluation are the main parameters assessed. Since *S. cerevisiae* protein extracts are mainly used as food supplement (Caballero-Córdoba & Sgarbieri, 2000; Podpora et al., 2015, 2016; Yamada & Sgarbieri, 2005) with potential low MW bioactive peptides (Albergaria et al., 2010;

Branco et al., 2014; Gddoa Al-sahlany et al., 2020; J. Kim et al., 2004; D. H. Lee et al., 2007), these parameters are the most relevant to monitor. Besides these, total sugars, lipids and fibre, fatty acids, ashes and RNA content are other nutritional and toxicological analysis included in evaluation of protein yeast extract composition (Caballero-Córdoba & Sgarbieri, 2000; Yamada & Sgarbieri, 2005).

Protein content

The quantification of protein is a routine procedure in many research laboratories, since it is required to calculate and monitor the protein yield after various enrichment or purification processes, as well as to optimize and standardize downstream experiments (Goetz et al., 2004). As listed in previous tables, several methods have been used for protein determination in *S. cerevisiae* extracts. Overall, most methods overestimate protein content since they use indirect readings, which may suffer interference from other chemical substances. Furthermore, it is described that the reported protein content depends on the protocol used for determination and from the initial matrix, making a direct comparison between studies difficult (Mæhre et al., 2018). A direct and precise protein determination is obtained when the amino acid residues are quantified (*Section "Amino acid determination"*).

Regarding indirect protein determination methods used in *S. cerevisiae* extracts, the Kjeldahl method has been applied by different authors (Chae et al., 2001; Gaver & Huyghebaert, 1991; Hedenskog & Mogren, 1973; Jacob, Striegel, et al., 2019; Podpora et al., 2016; Xie et al., 2017). In this method, the protein content is determined by the measurement of total nitrogen, which is multiplied by a conversion factor based on amino acid characterization of samples (spectrum, number of amino groups and MW) (Association of Official Analysis Chemists, 2005; Jacob, Striegel, et al., 2019). The main disadvantage of this method is the detection of other nitrogen containing non-protein compounds, such as nucleic acids, which can result in protein overestimation, besides the problem of unknown samples, where conversion factor cannot be accurately calculated (Jacob, Hutzler, et al., 2019). Due to its speed and simplicity, many authors have used spectrophotometric assays such as the Bradford, Lowry and bicinchoninic acid (BCA) protocols. The Bradford protocol is not capable of detecting low MW peptides or amino acids (Jacob, Hutzler, et al., 2019). On the other hand, Lowry and BCA assays are based on the identification of peptide bonds by protein-cooper chelation between Folin-

Ciocalteu reagent and the ring structure on aromatic amino acids (Lowry et al., 1951; Smith et al., 1985). The main advantage of BCA is that can be included in the copper solution to allow a one-step procedure, being stable at alkaline conditions. However, some single amino acids, such as cysteine (Cys), tyrosine (Tyr) and tryptophan (Trp) will also produce colour and can interfere in BCA results (Smith et al., 1985). Several examples of protein determination in yeast extracts performed by Lowry and BCA are present in **Table 1** and **Table 2**. Both of these methods respond more uniformly to different proteins than the Bradford protocol (Jacob, Hutzler, et al., 2019).

Amino acid determination

A constant amount of amino acids needs to be maintained for ensuring a balanced level of nitrogen in human cells. The human body is responsible for synthesise some of proteinogenic amino acids, namely the non-essential, while others have to be absorbed via protein dietary intake (EAA) (Jacob, Hutzler, et al., 2019). Since spent brewer's yeast has been described as a potential source of EAA, its protein-rich extracts are widely used for food supplementation (Puligundla et al., 2020), and thus amino acid determination is one of the most important characterization analysis to be performed. The determination of amino acid content is generally preceded by acid hydrolysis, in order to cleave peptide bonds (Caballero-Córdoba & Sgarbieri, 2000; Jacob, Hutzler, et al., 2019; Jacob, Striegel, et al., 2019; Podpora et al., 2015, 2016; Yamada & Sgarbieri, 2005). Specific amino acid analysers with post column ninhydrin reaction (Caballero-Córdoba & Sgarbieri, 2000; Yamada & Sgarbieri, 2005) and HPLC-UV/VIS with dansyl chloride derivatization (Podpora et al., 2015, 2016) were used for amino acid quantification. On the other hand, Trp is determined in the alkaline hydrolysate (Caballero-Córdoba & Sgarbieri, 2000; Podpora et al., 2015, 2016; Yamada & Sgarbieri, 2005) by HPLC-fluorescence detection (Podpora et al., 2015, 2016) or amino acid analyser equipment (Caballero-Córdoba & Sgarbieri, 2000; Yamada & Sgarbieri, 2005). In fact, yeasts themselves contain different types of proteases and peptidases responsible for the breakdown of the proteins into small peptides and then further into free amino acid (Rai et al., 2019).

Furthermore, many extraction processes on *S. cerevisiae* are also capable of breaking the protein into free amino acid, depending on cell disruption method and subsequent processing steps (**Table 4**). Jacob, Hutzler, et al. (2019) observed that the amino acid profile of yeast extract was dependent upon the disruption methods applied; autolysis (24

h, 50 °C) allowed for the higher amount of amino acid release, followed by sonotrode and bead milling (307, 155 and 115 mg protein/g yeast extract, respectively). In another study, the same authors confirmed this conclusion, since they observed a free amino content of 433.21 mg/g in autolysates in comparison with mechanical methods (115.68 and 155.38 mg/g) (Jacob, Striegel, et al., 2019) . In relation to EAA content, with the exception of glutamic acid (Glu), no differences were observed between the different disruption methods (Jacob, Hutzler, et al., 2019). Podpora and Swiderski (2015) also observed an increase of free amino acids during autolysis process from 11.2% to 77.5% (2 h from 48 h). In agreement, when performing enzymatic hydrolysis (Papain during 24 h; 50-60 °C), Podpora et al. (2016) also observed the breakdown of protein into free amino acids, establishing yeast extract as valuable source of EAA, such as isoleucine (Ile), lysine (Lys), valine (Val), threonine (Thr) and phenylalanine (Phe) + Tyr. High concentrations of Glu in the final extracts (3.84% and 2.07%) were also observed, leading to strong flavour-enhancing properties. Overall, the total EAA obtained by Podpora and Swiderski (2015), Podpora et al. (2016) and Jacob, Hutzler and Methner (2019) were above the FAO/WHO protein reference (**Table 4**) (World Health Organization, 2007) which turns yeast extracts an valuable components of several products from the group of functional foods and dietary supplements.

EAA profile of protein-rich *S. cerevisiae* extracts to be potentially used as food supplements are presented in **Table 4**. For phosphorylated yeast protein concentrates, sulphur amino acids were described as the limiting factor to the nutritive value of yeast protein (Caballero-Córdoba & Sgarbieri, 2000; Yamada & Sgarbieri, 2005). Caballero-Córdoba and Sgarbieri (2000) obtained an EAA level of 87.2% in protein concentrate based on available Lys (limiting amino acid) and comparable with the FAO/WHO reference standard. However, no pattern is clear: while Caballero-Córdoba and Sgarbieri (2000) observed a loss of Lys bioavailability in protein concentrate in comparison with yeast biomass, possibly explained by the reaction of the sodium perchlorate with the protein or by protein fractionation and/or precipitation with Lys loss, Yamada and Sgarbieri (2005) have observed a slightly increase of all EAA in protein concentrate which suggest higher degradation of amino acids in yeast biomass due to acid hydrolysis or selective precipitation of proteins in the protein concentrate. Yamada and Sgarbieri (2005) obtained a high content of Lys and Trp in the protein yeast concentrate, becoming a good candidate to enrich cereal proteins.

Regarding the amino acid sequencing of bioactive peptides, it is usually performed by mass spectrometry (MS). This technique has been proven as a robust and reliable tool for identification of amino acid sequence and protein post-translational modifications in proteomics (Kaltashov et al., 2020). Branco et al. (2014) identified two main antimicrobial peptides with the amino acid residues VSWYDNEYGYSTR and ISWYDNEYGYSAR in extracted fractions, and Kim et al. (2004) observed an amino acid sequence of YDGGVFRVYT for an antihypertensive peptide. Using protein sequencer equipment, Lee et al. (2007) also obtained the amino acid identification of a purified antidementia peptide (GPLGPIGS).

Table 4. EAA content in protein-rich *S. cerevisiae* extracts to be potentially used as food supplements.

Extraction and purification ^a	EAA (mg/g protein)										Total EAA (mg/g)	Reference
	<i>Thr</i>	<i>Met</i> + <i>Cys</i>	<i>Val</i>	<i>Ile</i>	<i>Leu</i>	<i>Leu</i> + <i>Nva</i>	<i>Tyr</i> + <i>Phe</i>	<i>Lys</i>	<i>His</i>	<i>Trp</i>		
Bead milling followed by sodium perchlorate treatment and protein precipitation at isoelectric pH	40.7	23.0	59.1	50.9	86.2	NQ	87.9	87.8	27.7	13.9	NM	Caballero-Córdoba & Sgarbieri (2000)
Bead milling followed by protein phosphorylation at alkaline pH	50.0	23.0	60.0	51.0	85.0	NQ	92.0	92.0	24.0	18.0	NM	Yamada & Sgarbieri (2005)
Autolysis (48 h, 47 °C)	61.3	23.8	69.7	23.7	NQ	65.1	90.6	47.2	NE	11.9	303	Podpora et al. (2015)
Enzymatic hydrolysis - Papain (24 h, 50-60 °C)	38.0	24	50.0	41.0	60.0	NQ	72.0	60.0	NE	11.0	356	Podpora et al. (2016)
Autolysis (24 h, 50 °C)	46.9	46.8	55.9	42.7	76.3	NQ	48.8	66.1	25.5	NQ	409	Jacob, Hutzler, et al. (2019)
FAO/WHO reference	11.0	20.0	15.0	15.0	21.0	NM	21.0	18.0	15.0	15.0	136	World Health Organization (2007)

^aMost efficient method for amino acids release. NQ – Not quantified; NM – Not mentioned; Met – Methionine; Leu – Leucine; Nva – Norleucine; His – Histidine.

Molecular weight

The determination of protein MW is a routine procedure in many research laboratories since it allows to identify specific proteins, oligomers and monomers (Goetz et al., 2004). In the characterization of *S. cerevisiae* protein, it has been described for the identification of invertase and peptides with antimicrobial, antidementia or antihypertensive properties (**Table 5**). Furthermore, MW analysis has also been described for the evaluation of protein extraction extent from brewer's yeast and characterization of yeast extracts produced for functional food (**Table 5**).

Mass spectrometry

MS has been used for characterization of the higher order structure of protein therapeutics as early as mid-1990s. Electrospray ionization (ESI) and matrix-assisted laser desorption ionization (MALDI) are complementary MS ionization techniques that allow MW determination of large biomolecules based on mass and charge (m/z) ratio. ESI-MS produces multiple charged ions with a mass range up to m/z 3000 with a mass limitation around 100 kDa, which allow a correct determination of protein MW (Goetz et al., 2004). As seen in **Table 5**, the MW of different bioactive peptides from *S. cerevisiae* was determined by ESI-MS.

MALDI in combination with time-of-flight (TOF) mass analyser has also been reported for protein MW characterization of *S. cerevisiae* extracts (**Table 5**).

This technique is highly sensitive, enabling the identification of unknown proteins at very low concentrations (Goetz et al., 2004). In comparison with ESI, MALDI generates ions with low charge states (≤ 3) which limits the identification of proteins with high MW (Ryan et al., 2019). Podpora and Swiderski (2015) produced yeast autolysates for food supplements with 74-96% of 1000-2000 Da peptides (about 10-20 amino acid residues) while Podpora et al. (2016) obtained yeast extracts contain large amounts of free amino acids and only trace amounts of peptides (1740 Da).

SDS-PAGE

Although protein MW characterization techniques are developing at a fast pace, the current standard method is still denaturing SDS-PAGE, which includes a number of laborious and time-consuming manual steps (Goetz et al., 2004). This technique separates

proteins according to their size as they are forced through a gel by an electrical current (Nehete et al., 2013). Generally, proteins are denatured by binding to SDS anionic detergent, where the amount of bound SDS is proportional to their size. The treatment with reducing agents as 2-mercaptoethanol or dithiothreitol is usually necessary to reduce protein disulphide bridges before the proteins adopt the random-coil configuration necessary for separation by size. Sizing accuracy depends on other protein characteristics since particular proteins are not truly migrating according to their MW, as is the case of glycosylated proteins (Goetz et al., 2004). As can be seen in **Table 5**, SDS-PAGE has been described for peptides and protein size evaluation in *S. cerevisiae*. Gddoa Al-sahlany et al. (2020) obtained a single band in SDS-PAGE that corresponded to a purified antibacterial peptide with approximately 9770 Da which might match the antibacterial activity produced by *S. cerevisiae*. Albergaria et al. (2010) obtained three small bands in SDS-PAGE (6.0, 4.5 and 4.0 kDa) produced by *S. cerevisiae* during alcoholic fermentation which might correspond to antimicrobial compounds that are active against some non-*Saccharomyces* wine-related strains. Estimating MW from specific proteins by SDS-PAGE, Akardere et al. (2010) obtained an invertase with 52 kDa by TPP extraction since MW of invertases vary according to their source and the applied method. *S. cerevisiae* provides internal and external invertase with MW from 50 to 300 kDa (Akardere et al., 2010).

In addition to estimate MW of specific peptides or proteins, SDS-PAGE has also been reported as a characterization technique to evaluate the extent of protein extraction in *S. cerevisiae* using different methods. In fact, most of the chemical approaches to extract protein from brewer's yeast, listed at **Table 2**, are followed by MW evaluation. Kushnirov (2000) used SDS-PAGE to optimize the introduction of a mild alkali treatment in yeast protein extraction protocol where the maximum extraction was obtained at 5 min. After 2 min, the reaction was almost complete except for proteins exceeding 100 kDa (Kushnirov, 2000). Zhang et al. (2011) evaluate the extent of yeast protein extraction with LiAc, followed by NaOH and SDS-PAGE buffer treatment using SDS-PAGE technique. Mukherjee et al. (2020) also used SDS-PAGE to evaluate protein pattern of different approaches to extract protein from *S. cerevisiae* at different growth phases. The hot-SDS method showed a better size distribution of protein bands with a good yield of proteins with MW higher than 80 kDa. The alkali pre-treatment allowed an apparent complete spectrum of proteins across a range of MW and the modified alkali pre-treatment (Kushnirov, 2000) resulted in maximum yield with sharp and distinct bands in SDS-

PAGE. However, loss of enzymatic activity may be of concern using these alkali protocols.

Some physical approaches for *S. cerevisiae* protein extraction have also used SDS-PAGE. Geneva et al. (2003) applied an electrical treatment to yeast crude extracts and supernatants obtaining the most of the bands above 29 kDa. Shynkaryk et al. (2009) compared protein patterns for untreated and PEF, HVED and HPH treated yeast suspensions. The more powerful physical cell disintegration allowed an effective extraction of high MW proteins. Electric treatments (PEF and HVED) can produce effective electroporation and accelerate release of the low MW components, but it was not sufficient for release of high MW intracellular components.

Using the principle of electrophoresis, commercial kits coupled to protein analyser equipment have recently been used for protein size fractionation. Protein 80 kit was used by Jacob, Hutzler, et al. (2019) in order to compare the protein profiles of different industrial methods to produce yeast extracts. Autolysis yeast extract only presented protein below 4 kDa in opposition to physical methods (cell mill and sonotrode) that yielded the most protein in the range from 3.5 to 63 kDa.

Size-exclusion chromatography

As described at *Section “Chromatography”*, SEC is a chromatographic technique that allow to separate and isolate proteins based on their size and shape. One of the most widely SEC techniques used for protein MW characterization is the fast protein liquid chromatography (FPLC). For that reason, this technique has also been used for protein MW estimation of nucleoprotein complexes (Butylina et al., 2007) and hydrolysates (Xie et al., 2017) from *S. cerevisiae*. They are determined by calibrating SEC column retention times or elution volumes with an appropriate series of macromolecular standards, as FPLC, or by employing molecular mass sensitive detection methods such as viscosimetry or light scattering (Goetz et al., 2004). Butylina et al. (2007) estimated MW distribution of yeast nucleoprotein complexes obtained three different fractions: firstly, a tightly bound proteins fraction; secondly, a 200–6 kg/mol nucleic acids fraction and the last only included single nucleotides (MM below 6 kg/mol). Xie et al. (2017) evaluate the MW distribution of hydrolysates acquired after 24 h of enzymatic hydrolysis at different solid concentrations and observed almost identical MW distribution in the Papain and Alcalase[®] hydrolysates with MW peptides below 3 kDa reaching 90%. However, Papain,

at high solid concentrations, produced hydrolysates with high fractions of low MW peptides (below 1 kDa) while Alcalase[®] fractions at different solid concentration were almost identical. Also, Marson et al. (2022) observed that 2 h of enzymatic hydrolysis with proteases cocktail (Brauzyne[®], Protamex[®] and Alcalase[®]) (pH 7.0, 50 °C) cleaved the yeast original protein into peptides from 7000 to 1000 g/mol (43%) and 1000-100 g/mol (25%) since non-treated yeast presented higher molecules with MW above 7000 g/mol.

Table 5. MW characterization methods for evaluation of protein from *S. cerevisiae*.

Methods	Extract characterization	Extraction and purification	Size (kDa)	Reference
<i>LC-ESI-MS</i>	ACE inhibitory peptide	Enzymatic hydrolysis (pepsin, trypsin, protease; 12 h) followed by 5 kDa ultrafiltration and SEC and RP-HPLC purification	1.18	J. Kim et al. (2004)
	Antidementia β -secretase inhibitor peptide	Bead milling followed by 1 kDa ultrafiltration and SEC and RP-HPLC purification	0.697	Lee et al. (2007)
	Antimicrobial peptides	10 and 2 kDa ultrafiltration followed by SEC and IEC purification	1.64 and 1.62	Branco et al. (2014)
<i>Maldi-TOF</i>	Yeast autolysates	Autolysis (2-48 h; 47 °C)	1.00-2.00	Podpora et al. (2015)
	Yeast extracts	Enzymatic hydrolysis (Papain; 24 h; 50-60 °C)	0.703-1.74	Podpora et al. (2016)
<i>SDS-PAGE</i>	Peptide fraction	Enzymatic hydrolysis (trypsin, alkaline protease mixture; 72 h; 37 °C) followed by 10 kDa and 2 kDa ultrafiltration	6.00, 4.50 and 4.00	Albergaria et al. (2010)
	Invertase	Sonication followed by TPP with ammonium sulfate and t-butanol	52	Akardere et al. (2010)
	Antimicrobial peptide	10 kDa and 2 kDa ultrafiltration followed by SEC purification	9.77	Gddoa Al-sahlany et al. (2020)

Bioactive properties

As abovementioned, several different biological activities have been reported for proteins and peptides extracted from spent brewer's yeast. **Figure 4** shows an overall representation of spent yeast valorisation highlighting its bioactive peptides and their potential in terms of antihypertensive, antioxidant, and antimicrobial activities. Each activity has its own mechanism of action and, while some peptide or protein extract have been described with one particular activity, one peptide can have more than one activity within its structure. On the following sections, the most commonly found activities will be discussed.

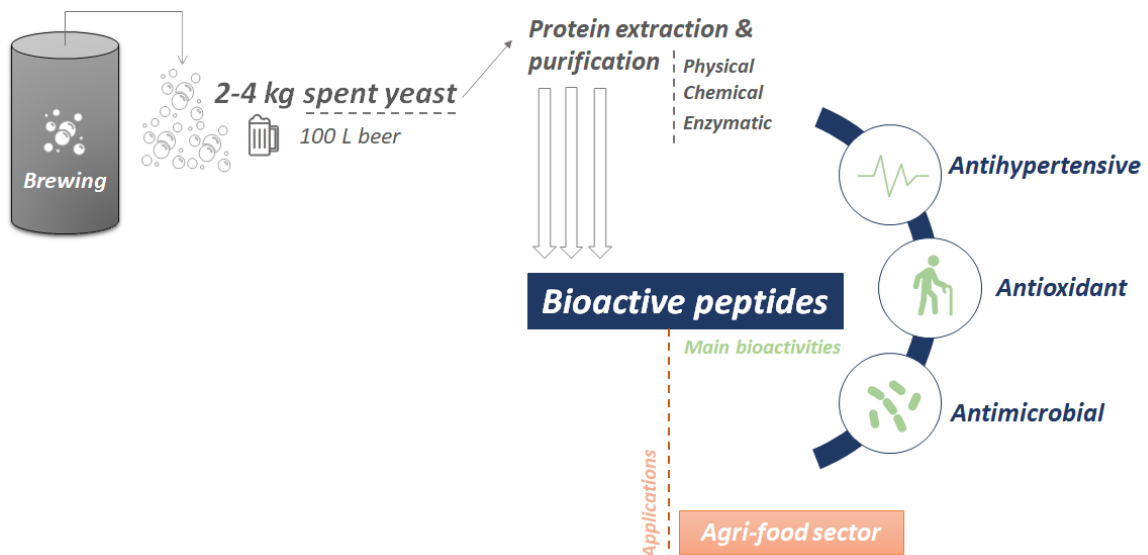


Figure 4. Schematic representation of spent yeast peptides valorisation, extracted by several methods, and their main bioactivities already reported in order to be applied at agri-food sector. Adapted from the graphical abstract of Oliveira et al. (2022a).

Antihypertensive

Hypertension represents one of the major risks for cardiovascular diseases in the developed world (Mirzaei et al., 2015). It is well established that blood pressure is regulated by the ACE and by the kinin-kallicrein system (Kohama et al., 1990). In fact, the rennin-angiotensin system (RAS) is physiologically responsible for the control of blood pressure, where ACE plays the conversion of angiotensin I to the potent vasopressor angiotensin II, releasing aldosterone and increasing of sodium plasma concentration (J. Kim et al., 2004).

Bioactive peptides from spent brewer's yeast have been described as an alternative for several ACE inhibitory drugs, such as captopril and enalapril (M. Amorim, Marques,

et al., 2019; M. Amorim, Pinheiro, et al., 2019). Some authors suggested a structure–activity relationship between the peptide and ACE inhibition, since their binding might be influenced by the hydrophobic amino acid nature of C-terminal tripeptide sequence of the substrate (peptides with 2-20 amino acids residues) that can interact with the subsites S1, S19, and S29 at the ACE active site (Mirzaei et al., 2018). However, several discovered peptides with ACE-inhibitory activities do not fit in with this model, exposing the weakness of this assumption, since it was only based on amino acids sequence (Ni, Li, Liu, et al., 2012). For this reason, the relationship of antihypertensive activity with yeast peptide structure and sequence is yet to be confirmed (Amorim et al., 2019).

In **Table 6**, several peptides extracted from *S. cerevisiae* are described as ACE activity inhibitors. In order to produce antihypertensive yeast hydrolysates with high protein, Huang et al. (Y. Huang et al., 2020) optimized the hydrolysis conditions with a crude enzyme containing protease and β -glucanase activities produced by *Bacillus subtilis* (*B. subtilis*) fermentation. They obtained a peptide rich hydrolysate with 67.3% of peptides in a range of 460 to 2145 Da, being 91.2% of these smaller than 1500 Da. The extract exhibited a strong ACE-inhibitory activity with the half maximal inhibitory concentration (IC₅₀) value of 26.13 μ g/mL, decreasing the blood pressure *in vivo* after single oral administration (100 mg/kg in spontaneously hypertensive rats (SHR)) and exhibiting a more persistent anti-hypertensive effect than captopril in long-term administration at 1200 mg/kg. Like some previous studies, the authors suggested a theoretical structure-function relation of peptides since they detected 428 of peptides with hydrophobic amino acid at N-end and 79 including Trp, Tyr and Pro at C-end. Kohama et al. (1990) extracted three decapeptides from yeast glyceraldehyde-3-phosphate dehydrogenase (GAPDH) with IC₅₀ values between 0.4 and 18 μ M, where the decapeptide PANLPWGSSNV contained the sequence homologous to vertebrate ACE inhibitors. The two other ACE-inhibitory decapeptides corresponded to different forms of yeast GAPDH with quite different sequences. Also Kim et al. (2004) obtained an ACE inhibitory decapeptide (1178 Da; YDGGVFRVYT) from *S. cerevisiae* enzymatic hydrolysis which presented a stronger antihypertensive activity (IC₅₀: 0.07 mg) than that of *Ganoderma frondosa* (*G. frondosa*; IC₅₀: 0.10 mg), but was slightly lower than that of the commercial antihypertensive drug captopril. However, the decapeptide was still considered a good candidate for antihypertensive drugs and functional foods, since it did not induce the side effects usually associated with captopril, such as coughs and allergies. On the other hand, Kim et al. (2004) when applying it, at a dosage of 1 mg decapeptide/kg, to SHR, observed

a decreased of blood pressure, similar to the captopril, at the end of 2 h, and without allergic reactions or coughing. Kanauchi et al. (2005) observed a similar decrease in blood pressure in the same *in vivo* model by administration of yeast peptide hydrolysate (0.4% in diet) and two peptide fractions of alanine (Ala):Phe and glycine (Gly):Phe (8 mg/rat). In fact, the obtained decrease for the two fractions corresponding to 62% of captopril positive control effect (5 mg/rat) and an *in vitro* ACE-IC₅₀ of 3.0 and 3.4 μmol/L was observed for Ala:Phe and Gly:Phe, respectively. In order to understand the ACE inhibition mechanism, Ni et al. (2012) studied a docking simulation of hexapeptide ACE-inhibitor based on its sequence to find reference molecules for drug design that target ACE. The authors showed binding interactions between N-terminal Thr1, Thr3, and glutamine (Gln) 4 residues of hexapeptide (TPTQQS) and the residues on the lid structure of ACE leading to enzyme inhibition in a non-competitive way by dislocation of the Zn ion from the active site (C-terminal serine (Ser) 6) which is critical for ACE catalysis.

Table 6. Antihypertensive activity of bioactive peptides from *S. cerevisiae*.

Extraction and purification method	Extract characterization	Activity	Reference
Enzymatic hydrolysis of yeast powder (enzyme/substrate ratio of 7000 U/g, 55 °C, 5 h) followed by spray drying	-Yeast hydrolysate (67.3% peptides)	ACE inhibitory activity: - IC50 value of 26.13 µg/mL.	Huang et al. (2020)
GAPDH EDTA-extraction followed by acid hydrolysis and SEC and RP-HPLC purification	Three GAPHD decapeptides (GHKIATFQER, GKKIATYQER, PANLPWGSSNV)	ACE inhibitory activity: -IC50 values of 0.4, 2 and 18 µM, respectively.	Kohama et al. (1990)
Enzymatic hydrolysis (pepsin, trypsin, protease; 12 h) followed by 5 kDa ultrafiltration and SEC and RP-HPLC purification	Decapeptide (1178 Da; YDGGVFRVYT)	ACE inhibitory activity: - IC50 value (0.07 mg) was slightly lower than commercial antihypertensive drug (17.9 nM).	Kim et al. (2004)
		<i>In vivo</i> : - Decreased of blood pressure in SHR (1 mg/kg dosage) with similar effects to positive control at the end of 2 h.	

Extraction and purification method	Extract characterization	Activity	Reference
Alkaline enzymatic hydrolysis (alcalase®; 12 h; 50 °C) followed by IEC, SEC and RP-HPLC purification	<ul style="list-style-type: none"> - Yeast peptide extract - Two peptide fractions: <ul style="list-style-type: none"> - Ala:Phe (1:1) - Gly:Phe (1:1 ~ 1:2) 	<p>ACE inhibitory activity:</p> <ul style="list-style-type: none"> - IC50 value of 3.0 and 3.4 μmol/L for Ala:Phe and Gly:Phe fractions, respectively. <p><i>In vivo:</i></p> <ul style="list-style-type: none"> - Decreased of blood pressure in SHR by administration of yeast extract (0.4% in diet) and two peptide fractions (8 mg/rat) in comparison with non-treated animals. - The effect of two peptide fractions estimated to be 62% of the activity of the captopril group (5 mg/rat). 	Kanauchi et al. (2005)
NM	Hexapeptide (TPTQQS)	ACE inhibition in a non-competitive manner by displacement of the Zn ion from the active site.	Ni et al. (2012)

Extraction and purification method	Extract characterization	Activity	Reference
Sonication-trypsin hydrolysis followed by 10, 5 and 3 kDa ultrafiltration and SEC and RP-HPLC purification	<ul style="list-style-type: none"> - Yeast protein hydrolysates - Peptide fraction (< 3 kDa) - Decapeptide (1057.45 Da; YGKPVAVPAR) 	<p>ACE inhibitory activity:</p> <ul style="list-style-type: none"> - Trypsin hydrolysate had the highest activity in antihypertensive assays (IC₅₀ = 0.84 ± 0.01 mg/mL) in comparison with sonication-chymotrypsin hydrolysates and autolysates. - Peptide fraction (< 3 kDa) exhibited the strongest ACE inhibitory (IC₅₀ = 0.32 mg/mL) activities in comparison with high MW peptide fractions. - Purified decapeptide increased the antihypertensive (IC₅₀: 0.42 ± 0.02 mg/mL) activity. 	Mirzaei et al.(2015)
10 kDa ultrafiltration followed by enzymatic hydrolysis (4% proteases) and 3 kDa nanofiltration	<p>-Four peptide hydrolysed fractions:</p> <ul style="list-style-type: none"> - Retentate > 3 kDa - Retentate < 3 kDa - Permeate > 3 kDa - Permeate < 3 kDa 	<p>ACE inhibitory activity:</p> <ul style="list-style-type: none"> -Retentate fractions showed low IC₅₀ (84.2 to 158 µg/mL) than retentates (198 to 259 µg/mL). -Fractions < 3 kDa were the main responsible for ACE-inhibitory activity since they showed IC₅₀ values of 84.2 and 198 µg/mL compared with peptides > 3 kDa (158 and 259 µg/mL) (retentate and permeate, respectively). <p><i>In vivo:</i></p> <ul style="list-style-type: none"> - Retentate < 3 kDa decreased systolic, diastolic and mean blood pressure in SHR (300 mg/kg) with similar effects to captopril (50 mg/kg) after 2 h administration, being this effect maintained throughout 24 h. 	Amorim, Marques et al. (2019)

Extraction and purification method	Extract characterization	Activity	Reference
Incubation of yeast powder with water (1:15) (pH 7.7, 60 °C, 30 min) followed by enzymatic hydrolysis (3.5% w/v, 6 h), ethanol precipitation (2 h, 4 °C) and 5 kDa filtration	<ul style="list-style-type: none"> -Yeast protein hydrolysates -Yeast peptide < 5 kDa 	<p>ACE inhibitory activity:</p> <ul style="list-style-type: none"> -Both samples showed high ACE activity with about 80% of enzyme inhibition -Ultrafiltration process increased the ACE inhibitory activity from IC₅₀ of 55.39 mg/mL for protein hydrolysate and 29.32 mg/mL for peptide < 5 kDa. 	Hu et al. (2014)

NM – Not mentioned; EDTA – Ethylenediaminetetraacetic acid, WKY – Wistar-Kyoto rats.

Antioxidant

Antioxidant ingredients those capable of inhibit oxidation reactions. By doing so, they protect cells against oxidative stress caused by reactive oxygen species (ROS) and nitrogen species, which are capable of damaging important cell components such as proteins, lipids and deoxyribonucleic acid (DNA), ultimately preventing the occurrence of several diseases. Many *S. cerevisiae* peptides have been reported by their antioxidant properties as described in **Table 7**.

Podpora and Swiderski (2015) and Podpora et al. (2016) observed high antioxidant activity on protein *S. cerevisiae* extracts produced from autolysis (32.73 mmol Trolox equivalent (TE) /100 mL) and enzymatic hydrolysis (506.9 mmol TE/100 mg), with the increase of 2,2'-azinobis(3-ethyl-benzothiazoline-6-sulphonate) radical cation (ABTS⁺) scavenging activity with the autolysis duration. However, the authors related these results with the presence of phenolic compounds (Podpora et al., 2015).

Selenium-rich extracts from brewer's yeast are currently used for animal and human Se supplementation. Given the known oxidative stress protection properties of Se, Guo et al. (2020) studied the effect of combining bioactive peptides with Se. All tested yeast protein hydrolysates presented strong ABTS⁺ scavenging activity, with scavenging rates from 70.2% to 85.4%. However, the Se-rich peptide fractions with MW < 1 kDa showed the highest antioxidant activity (85.4 ± 0.6%) compared with Se-rich peptides with MW < 3 kDa or higher yeast peptide fractions. Therefore, free radical scavenging activities seemed to be strongly influenced by MW. Furthermore, lipid peroxidation was also inhibited by all peptide fractions, with the Se-rich fraction presenting a significantly higher effect (maximum of 40% in liposome system and 70% in linoleic acid system). For this reason, the authors have suggested the use of Se and yeast peptides in a synergetic manner for lipid peroxidation prevention. Furthermore, Se-rich yeast peptide fraction showed excellent antioxidant activity *in vivo* (oral administration for 30 days: peptide dose of 150 mg/kg body weight/day and Se dose: 100 µg/kg body weight/day) by significantly decreased the level of malonaldehyde in liver and serum. From the abovementioned results, it can be postulated that Se-rich yeast peptides may be a great and promising functional food additive, given the reported antioxidative damage protection properties.

Together with antioxidant properties, several studies have also been reported for *S. cerevisiae* peptides as antihypertensive and antidiabetic ingredients. In fact, the incidence

of hypertension, aging and other diseases such as diabetes, cancer and neurodegenerative disturbances has been also related with antioxidant activity (M. Amorim, Marques, et al., 2019). For that reason, the combination of ACE inhibition, antioxidant activity and/or antidiabetic activity in one single product could be very useful for the control of these chronic diseases. Mirzaei et al. (2015) prepared different fractions of *S. cerevisiae* protein hydrolysates and purified a decapeptide (YGKPVAVPAR; 1057.45 Da) that could potentially replace the current antioxidant and antihypertensive agents of chemical origin. The trypsin hydrolysate had the highest activity in 2,2-diphenyl-1-picrylhydrazyl (DPPH[•]) scavenging ($179.2 \pm 4.8 \mu\text{M TE/mg protein}$), ABTS^{•+} scavenging ($4653 \pm 50 \mu\text{M TE/mg protein}$) and antihypertensive assays ($\text{IC}_{50} = 0.84 \pm 0.01 \text{ mg/mL}$) in comparison with sonication-chymotrypsin hydrolysates and autolysates (Mirzaei et al., 2015). As described above, the authors hypothesized a structure–activity relationship due to the total content of hydrophobic amino acids in the trypsin hydrolysate since some previous studies described these features among potent antioxidant and ACE inhibitors protein hydrolysates with DPPH[•] and ABTS^{•+} scavenging activities. However, there is no scientific evidence proving this relationship. The peptide fraction with MW under 3 kDa of trypsin hydrolysates exhibited the strongest DPPH[•] ($489.12 \pm 0.001 \mu\text{M TE/mg protein}$), ABTS^{•+} ($7718.30 \pm 57 \mu\text{M TE/mg protein}$) scavenging and ACE inhibitory ($\text{IC}_{50} = 0.32 \text{ mg/mL}$) activities in comparison with high MW fractions. In fact, small peptides are more efficient antioxidants and ACE inhibitors than macro peptides or proteins because of their higher accessibility to the oxidant/antioxidant test system, and better binding to the ACE active site. From the purification of this fraction resulted the decapeptide that was identified to be highly potent ABTS^{•+} scavenging ($26.25 \mu\text{M TE}/\mu\text{g protein}$) and ACE-inhibitory peptide ($\text{IC}_{50}: 0.42 \pm 0.02 \text{ mg/mL}$).

Amorim, Marques et al. (2019) also produced four peptide fractions from spent brewer's yeast (retentate > and < 3 kDa; permeate > and < 3 kDa) by 10 kDa ultrafiltration followed by enzymatic hydrolysis and 3 kDa nanofiltration that showed strong antihypertensive and antioxidant activities. The authors observed an inhibition of ACE activity *in vitro* with retentates showing the lowest IC₅₀ values fractions (84.2 to 158 $\mu\text{g/mL}$) compared with permeates (198 to 259 $\mu\text{g/mL}$). For this reason, the authors chose the retentate peptide fractions to study their effect in hypertension on SHR in a short-term oral exposure. The retentate < 3 kDa decreased systolic, diastolic and mean blood pressure in SHR (300 mg/kg) with similar effects to captopril (50 mg/kg) after 2 h administration, being this effect maintained throughout 24 h. Likewise, this fraction showed the highest

protective effect against peroxy radicals (7.25 μM TE/mg sample), followed by permeate < 3 kDa (5.50 μM TE/mg sample) following the same tendency of ACE inhibition. After MALDI-TOF/TOF analysis, tri and tetrapeptides were identified in this fraction (507 to 582 Da) with hydrophobic amino acid residues (SPQW, PWW and RYW) which can suggest again the binding affinity of peptide to ACE, but the structure-activity relationship was not confirmed yet. Besides, antioxidant activity can also be related with amino acids sequence of peptides (Tyr, Trp, Phe and the imidazole group of histidine (His)) which are able to quench the free radicals through a direct electron transfer mechanism, while the proline (Pro) pyrrolidine ring can interact with secondary structure of peptides, increasing its flexibility. It can also quench oxygen singlets thanks to its low ionization potential.

Also Hu et al. (2014) performed an 5 kDa filtration preceded by enzymatic hydrolysis and ethanol precipitation for production of hydrolysates from yeast powder, revealing that ultrafiltration process is an important step in order to enrich bioactivity of yeast peptides. Yeast peptides hydrolysate and peptide fraction < 5 kDa allowed a strong ACE inhibition (about 80%) with IC₅₀ values of 55.39 $\mu\text{g}/\text{mL}$ and 29.32 $\mu\text{g}/\text{mL}$, respectively, confirming an increase of ACE-inhibitory activity using ultrafiltration process, being the fraction < 5 kDa mainly constituted by 1 kDa oligopeptides (80.4%). The same increase of activity in 5 kDa fraction was observed in superoxide anion scavenging and α -glucosidase inhibitory activities (IC₅₀ values of 2.60 mg/mL and 10.62 mg/mL, respectively). On the other hand, no differences were found in DPPH^{*} scavenging activity probably related with the lack of polypeptide specificity for this assay. The authors also performed a stability study of the potential extracts, observing a good heat and pH stability and high resistant effect against gastrointestinal proteases in peptides < 5 kDa.

On a more simple approach, San Martin et al. (2021) produced yeast hydrolysates produced by enzymatic means with a protein extraction yield between 13.7% to 29.7%, which exhibit antioxidant activity, which range from 0.65 to 1.65 g of TE, by 2,2'-azino-bis(3-ethylbenzothiazoline-6-sulfonic acid) (ABTS) method. Due to this data, and to the fact that these hydrolysates also exhibit antimicrobial activity against *Aeromonas salmonicida* (*A. salmonicida*), *Bacillus cereus* (*B. cereus*), *B. subtilis* and *Salmonella enterica* (*S. enterica*), lead the authors to conclude that this hydrolysates have great potential for functional food ingredients (San Martin et al., 2021).

Concerning the therapy of metabolic disorders, Jung et al. (2011) produced a yeast hydrolysed rich in Cyclo-His-Pro (CHP) since the supplementation of this dipeptide

combined with Zn improved insulin sensitivity and glucose clearance. The extract prepared with Flavourzyme[®] showed the highest level of CHP (674 µg/g, 64.9% protein) and strong scavenging activity in DPPH[•] and ABTS^{•+} assays (IC₅₀ values of 1.9 and 0.9 mg/mL, respectively). Besides, the authors observed a significant decrease in glucose level of mice hyperglycemic models treated with yeast hydrolysate (100 mg/kg) compared with control at 30, 60, 90, and 120 min. Together, these results demonstrate the possibility to use a CHP-rich yeast extract as an antioxidative and/or antidiabetic ingredient in functional foods but further studies need to be performed to understand the role of CHP in antioxidant and antidiabetic mechanism.

Table 7. Antioxidant activity of bioactive peptides from *S. cerevisiae*.

Extraction and purification method	Extract characterization	Activity	Reference
Autolysis (20 h; 47 °C)	Yeast autolysates (1000-2000 Da; 16.06 g free amino acids/100 g)	- Increased with the duration of the autolysis process, where the 20 h-autolysate showed the highest activity in ABTS ^{•+} (32.73 mMol TE/100 mL).	Podpora and Swiderski (2015)
Enzymatic hydrolysis (papain; 24 h; 50-60 °C)	Yeast extracts (703-1740 Da; 60% protein)	- High activity in ABTS ^{•+} assay with concentrations ranging from 461.5 mmol TE/100 mg to 506.9 mmol TE/100 mg. - Se-rich peptides fraction (MW < 1 kDa) with the highest activity in ABTS ^{•+} (85.4 ± 0.6%) compared with Se-rich peptides (MW < 3 kDa) or normal peptide fractions.	Podpora et al. (2016)
Enzymatic alkaline hydrolysis (protease; 8 h; 60 °C) followed by 3 and 1 kDa ultrafiltration	- Eight peptide fractions from normal and Se-rich brewer's yeast (< 3 kDa and 1 kDa)	- Inhibitory effect of Se-rich peptide fractions in lipid peroxidation was significantly higher than normal yeast peptide fractions, suggesting a synergistic effect between Se and yeast peptides. - Decrease of malonaldehyde level in liver and serum of mice after oral treatment with Se-rich yeast peptide fraction (peptide dose of 150 mg/kg body weight/day and Se dose: 100 µg/kg body weight/day during 30 days).	Guo et al. (2020)
Sonication-trypsin hydrolysis followed by 10, 5 and 3 kDa ultrafiltration and SEC and RP-HPLC purification	- Yeast protein hydrolysates - Peptide fraction (< 3 kDa) - Decapeptide (1057.45 Da; YGKPVAVPAR)	- Trypsin hydrolysate had the highest activity in DPPH [•] (179.2 ± 4.8 µM TE/mg protein) and ABTS ^{•+} (4653 ± 50 µM TE/mg protein) in comparison with sonication-chymotrypsin hydrolysates and autolysates.	Mirzaei et al. (2015)

Extraction and purification method	Extract characterization	Activity	Reference
10 kDa ultrafiltration followed by enzymatic hydrolysis (4% proteases) and 3 kDa nanofiltration	-Four peptide hydrolysed fractions: - Retentate > 3 kDa - Retentate < 3 kDa - Permeate > 3 kDa - Permeate < 3 kDa	- Peptide fraction (< 3 kDa) exhibited the strongest DPPH [*] ($489.12 \pm 0.001 \mu\text{M TE/mg}$ protein) and ABTS ⁺⁺ ($7718.30 \pm 57 \mu\text{M TE/mg}$ protein) activities in comparison with high MW peptide fractions. - Purified decapeptide increased the ABTS ⁺⁺ ($26.25 \mu\text{M TE}/\mu\text{g}$ protein) activity. - Retentate fraction < 3 kDa with the highest antioxidant activity ($7.25 \mu\text{M TE/ mg}$ sample), followed by permeate < 3 kDa ($5.50 \mu\text{M TE/ mg}$ sample) in ORAC assay.	Amorim, Marques et al. (2019)
Incubation of yeast powder with water (1:15) (pH 7.7, 60 °C, 30 min) followed by enzymatic hydrolysis (3.5% w/v, 6 h), ethanol precipitation (2 h, 4 °C) and 5 kDa filtration	-Yeast protein hydrolysates -Yeast peptide < 5 kDa	-The ultrafiltration process enhanced the superoxide scavenging activity from IC ₅₀ of 3.98 mg/mL for protein hydrolysate and 2.60 mg/mL for peptide < 5 kDa. -Both extracts showed good DPPH [*] scavenging activity but no differences were observed between extracts.	Hu et al. (2014)
Enzymatic hydrolysis (48 h; enzymes:yeast of 1/100; 50 °C) followed by acid treatment and	-Yeast hydrolysate with high content of CHP (64.9% protein)	- Strong scavenging activity in DPPH [*] and ABTS ⁺⁺ assays (IC ₅₀ values of 1.9 and 0.9 mg/mL, respectively).	Jung et al. (2011)

Extraction and purification method	Extract characterization	Activity	Reference
a combined ultrafiltration and activated carbon treatment			
Enzymatic hydrolysis (up to 8 h, enzyme:substrate ratio up to 0.12, and up to 55 °C).	-Yeast protein hydrolysates	<ul style="list-style-type: none"> - Antioxidant capacity from 0.65 to 1.65 g TE. - Antimicrobial activity versus <i>A. salmonicida</i>, <i>B. cereus</i>, <i>B. subtilis</i> and <i>S. enterica</i>. 	San Martin et al. (2021)

ORAC – Oxygen radical absorbance capacity

Antimicrobial

In recent past we have witnessed an increase in the number of antibiotic resistant pathogens, with multiple antimicrobial classes becoming ineffective to combat infections in medical and agricultural fields (S. Sharma et al., 2011). In order to address this problem, antimicrobial peptides have been produced, isolated and purified from different sources, such as microorganisms, invertebrates and other species (Gddoa Al-sahlany et al., 2020). Antimicrobial peptides are small oligopeptides, usually with a MW under 10 kDa, and encoded within the sequences of native protein precursors with a net positive charge and an amphipathic structure (Gddoa Al-sahlany et al., 2020; Sánchez & Vázquez, 2017). They are involved in the growth inhibition and killing of several microorganisms such as bacteria and fungi (Sánchez & Vázquez, 2017). Their properties, such as amphipathicity, amino acid composition, cationic charge and size, are key factors in the attachment and infusion into pathogen membrane bilayers, allowing the formation of pores by 'barrel-stave', 'carpet' or 'toroidal-pore' mechanisms. However, it has been speculated that these mechanisms are not the sole reason for the antimicrobial properties of these peptides: the cytoplasmic membrane septum formation can be altered by translocated peptides, and other effects have been described such as the inhibition of cell-wall synthesis, nucleic-acid and protein synthesis or of enzymatic activity in general (Brogden, 2005).

Many studies have reported the production of antimicrobial peptides from spent *S. cerevisiae* (**Table 8**). Enzymatic hydrolysis or cell physical disruption technique, followed by ultrafiltration and SEC or IEC purification were the methods mostly used for antimicrobial peptides production (Albergaria et al., 2010; Branco et al., 2014, 2017; Caldeira et al., 2019; Comitini et al., 2005; Dick et al., 1992).

The malolactic fermentation is essential for certain types of wine, having a strong impact in their final performance, mainly in sensorial aspects such as decreasing acidity (Lonvaud-Funel, 2000). However, it has been described that yeast can produce antibacterial factors that can be responsible for the non-occurrence of malolactic fermentation (Dick et al., 1992). In fact, Dick, Molan and Eschenbruch (1992) showed that two cationic proteins isolated by cation exchange chromatography from *S. cerevisiae* strongly inhibited the lactic acid bacteria which are in charge of malolactic fermentation in wine. Comitini et al. (2005) analysed the interactions between *Oenococcus oeni* (*O.*

oeni), the dominant specie of lactic acid bacteria, and different yeasts in order to understand the mechanisms underlying the basis of the yeast–bacteria interactions in wine. They found that *S. cerevisiae* compounds of proteinaceous nature (MW < 10 kDa) inhibited the growth of different strains of *O. oeni* in a dose-dependent way, being related to yeast metabolic activity rather than to a competition for nutritional requirements. The proteinaceous factors of yeast can be explored on the inhibition of lactic bacteria, which offers new prospects for malolactic fermentation and its management. Beyond the inhibition of lactic acid bacteria, Albergaria et al. (2010) observed antimicrobial activity of *S. cerevisiae* secreted peptides with a MW between 2 and 10 kDa against *Hanseniaspora guilliermondii* (*H. guilliermondii*), a non-*Saccharomyces* yeast that contributes to increase the sensory complexity of wines. Conversely, a growth inhibitory effect versus *Kluyveromyces marxianus* (*K. marxianus*), *Kluyveromyces thermotolerans* (*K. thermotolerans*), *Torulaspora delbrueckii* (*T. delbrueckii*) and *H. guilliermondii* and a fungicidal effect versus *K. marxianus* was found in the same study, which suggests the use of bioactive peptides as a way to prevent wine spoilage caused by yeasts.

In their work, Branco et al. (2014) have shown the antimicrobial potential of a 2-10 kDa peptide fraction, testing it against a large range of wine related yeasts. Two peptides have resulted from the purification of this fraction with 1.638 and 1.622 kDa (VSWYDNEYGYSTR and ISWYDNEYGYSAR, respectively). These correspond to fragments from the *S. cerevisiae* GAPDH isoenzymes, namely GAPDH2/3 and GAPDH1. The authors denominated the GAPDH-derived peptides fraction as “Saccharomycin”, a natural biocide with fungicidal effect against several wine-related non-*Saccharomyces* yeasts during alcoholic fermentation (Branco et al., 2017; Caldeira et al., 2019). It was also found that “Saccharomycin” antimicrobial activity was significantly higher when compared to synthetic analogues while being dependent on a conjugated action of GAPDH2/3 and GAPDH1 (ideally at ration 4:1) for maximum antimicrobial action (2017). Furthermore, in contrast to synthetics alternatives, “Saccharomycin” is active under acidic conditions, suggesting molecular adaptations, likely involving the formation of aggregates of a number of peptide units in order to maintaining their solubility and bioactivity. When studying the death mechanism induced by GAPDH-derived peptides, these molecules were chemically synthesized, and it was observed their internalization by cell membrane permeabilization. These peptides were able to enter the cytoplasm of sensitive yeast cells (*H. guilliermondii* and *Dekkera bruxellensis* (*D. bruxellensis*)) by crossing the cell membrane.

In addition to production of antimicrobial peptides by *S. cerevisiae* related to fermentation processes, Gddoa Al-sahlany et al. (2020) isolated an antimicrobial peptide from *S. cerevisiae* culture medium suitable for use in sterilization and thermal processes in food production. After 24 h incubation, the peptide inhibits from 2 to 2.3 log units of gram-negative (*Escherichia coli* (*E. coli*) and *Klebsiella aerogenes* (*K. aerogenes*)) and 1.5 to 1.8 log units of gram-positive (*B. subtilis* and *Staphylococcus aureus* (*S. aureus*)) bacteria, respectively. The authors found that the mode of action fundamentally depends on the electrostatic interaction between peptides and bacteria cells membrane, since peptides were adsorbed by bacterial cell membrane leading to its complete damage. In order to establish a relation between MW and inhibition of bacteria, the authors also analysed the fraction from 3–10 kDa ultrafiltration where they observed smaller peptides with antibacterial biological activity as well.

Table 8. Antimicrobial activity of bioactive peptides from *S. cerevisiae*.

Extraction and purification method	Extract characterization	Activity	Reference
French press followed by SEC, cation IEC purification and 500 Da ultrafiltration	Two cationic proteins - Small protein with high isoelectric point - Lysozyme-like	Antimicrobial activity: - Strong inhibitory action against lactic acid bacteria.	Dick, Molan and Eschenbruch (1992)
10 kDa Ultrafiltration and dialysis (16 h, 4 °C)	<i>S. cerevisiae</i> compounds from proteinaceous nature (< 10 kDa)	Antimicrobial activity: - Strong inhibition growth and malic acid degradation of malolactic bacteria.	Comitini et al. (2005)
Enzymatic hydrolysis (trypsin, alkaline protease mixture; 72 h; 37 °C) followed by 10 kDa and 2 kDa ultrafiltration	2–10 kDa Peptide fraction (4.0, 4.5 and 6.0 kDa)	- Antimicrobial properties against <i>H. guilliermondii</i> . - Fungistatic effect against <i>K. marxianus</i> , <i>K. thermotolerans</i> , <i>T. delbrueckii</i> and <i>H. guilliermondii</i> . - Fungicidal effect against <i>K. marxianus</i> .	Albergaria et al. (2010)
10 and 2 kDa Ultrafiltration followed by SEC and IEC purification	- 2–10 kDa Peptide fraction - Fragments of the <i>S. cerevisiae</i> GAPDH isoenzymes: GAPDH2/3 and GAPDH1; 1.638 and 1.622 kDa; VSWYDNEYGYSTR and ISWYDNEYGYSAR)	Antimicrobial activity against a wide variety of wine-related yeasts and bacteria related with GAPDH activity.	Branco et al. (2014)
10 and 2 kDa Ultrafiltration followed by SEC purification	- 2–10 kDa Peptide fraction - “Saccharomycin”	- <i>S. cerevisiae</i> secretes several GAPDH-derived peptides with antimicrobial activity during alcoholic fermentation, namely a natural biocide “saccharomycin”.	Branco et al. (2017) Caldeira et al. (2019)

Extraction and purification method	Extract characterization	Activity	Reference
10 kDa and 2 kDa ultrafiltration followed by SEC purification	Peptide (9770 Da; thermostable at 50-90 °C for 30 min; tolerated a pH range of 5-7 at 4 °C and 25 °C for 24 h)	<p>- “Saccharomycin” exhibited a fungicidal effect against several wine-related non-<i>Saccharomyces</i> yeasts.</p> <p>- Antimicrobial activity of GAPDH-derived peptides was significantly higher than synthetic analogues.</p> <p>- The death of sensitive yeast cells (<i>H. guilliermondii</i> and <i>D. bruxellensis</i>) is related to the peptides capacity of cell penetration membrane.</p> <p>Antimicrobial activity:</p> <p>- Inhibition of 2 to 2.3 and 1.5 to 1.8 log units of gram-negative (<i>E. coli</i> and <i>K. aerogenes</i>) and gram-positive (<i>B. subtilis</i> and <i>S. aureus</i>) bacteria during 24 h of incubation, respectively.</p>	Gddoa Al-sahlany et al. (2020)

Other bioactivities

In addition to antihypertensive, antioxidant, antidiabetic and antimicrobial bioactivities, widely described for *S. cerevisiae* peptides, other bioactivities related to treatment and prevention of chronic diseases have also been studied.

Hoz et al. (2014) demonstrated the Fe-binding capacity of peptide hydrolysates from sugarcane yeast (*S. cerevisiae*) (MW < 5 kDa) which enhanced Fe bioavailability. The authors observed Fe stability during *in vitro* digestion by evaluation of Fe dialyzability (amount of soluble and stable Fe until intestinal digestion) after the production of Fe-peptide chelates, concluding that yeast peptide extracts were a promising Fe-delivery component to produce supplements targeted for anti-anemic market.

On the other hand, Amorim et al. (2016) observed the protection of gastric mucosa of rats against ulcerative lesions when treated with peptide hydrolysates from spent brewer's yeast. The peptide fraction under 3 kDa was able to reduce gastric injuries at the effective dose of 816 mg/kg, being pointed out a relation between a prostaglandin-mediated mechanism and the cytoprotective effect observed. However, this mechanism seems to be nonspecific. Furthermore, a cytotoxic effect against leukemia cells (K-562) was also revealed with the inhibition of more than 50% in concentration values (IC₅₀) of 2.5 µg/mL for this peptide fraction (25 µg/mL for fraction above 3 kDa). The authors suggested that the minerals also present in the extract may be the responsible for inhibition of tumor cells proliferation.

Recently, Jacob, Hutzler, et al. (2019) also hypothesized the potential use of yeast autolysates for stimulating immune cells and preventing diabetes due to the high amount of amino acid γ -aminobutyric acid (GABA) (10 mg protein/g yeast extract), since it acts as a strong secretagogue of insulin from the pancreas (Dhakal et al., 2012).

Figure 5 presents an overview of the abovementioned potential bioactive properties.

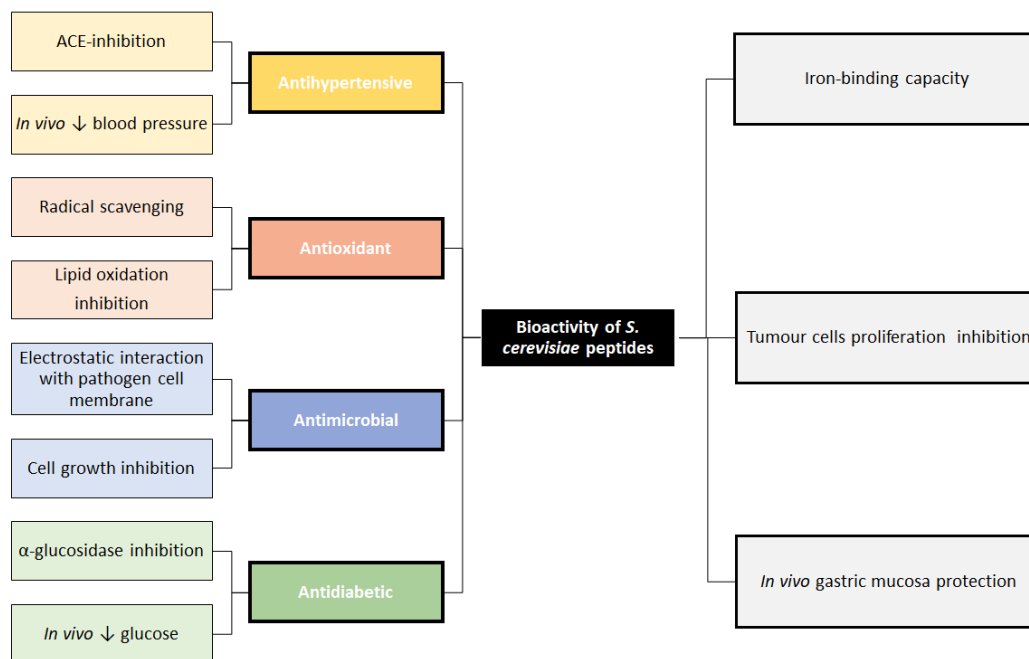


Figure 5. Main bioactivities and possible mechanisms reported for peptides from *S. cerevisiae*.

Applications to agri-food sector

Beyond the use of yeast peptides as bioactive ingredients for specifically targeted applications, some studies exploited the benefits of yeast protein extracts introduction in the food market and winemaking industry (Caballero-Córdoba & Sgarbieri, 2000; Gaspar et al., 2019). Caballero-Córdoba and Sgarbieri (2000) evaluated the nutritional and toxicological performance of yeast protein concentrates (extracted with sodium perchlorate) as single source of dietary protein. In fact, the authors observed an *in vivo* poor nutritional performance, since the food intake and growth rate were lower than that of the group fed by yeast biomass. Nevertheless, these results can be explained by a decrease in amino acid bioavailability such as Lys and methionine (Met), and/or the presence of residual sodium perchlorate (from extraction process) in the diet, which led to some evidenced liver toxicity. On the other hand, a yeast protein extract, with 50% > 15 kDa, was proposed as an effective alternative as a fining agent in red wine clarification and stabilization by Gaspar et al (2019). This alternative to traditional agents is health risk free, enhance phenolic compound extraction, promotes a significant brilliance and turbidity decrease, as well as colour improvement, when compared with reference traditional compounds such as albumin, bentonite or casein.

Yeast protein-rich extracts have also been used as human dietary supplements, flavour enhancers and animal feed. **Table 9** lists some of the protein-rich products currently on the market derived from yeast obtained from different extraction processes (hydrolysis and autolysis) and/or spray-dried. Beyond the high protein content described on the product information, these extracts are also rich in amino acids and bioactive peptides, among others, which are responsible for some of the bioactive properties observed. In fact, with the exception of being used as protein sources, several of the remaining applications of these extracts (e.g. flavour enhancement) are dependent on the smaller molecules present (amino acids), and the choice of commercializing the whole protein extract is usually mainly economic. Since the source of those commercial products is not usually provided in the label, it is difficult to ascertain which ones come from spent yeast; however, such labelling could even be a positive differentiation parameter, due to the growing consumer awareness and valorisation on sustainability issues and circular economy.

Table 9. Protein-rich extracts from commercially available yeast.

Company	Product	Composition	Use and function
DSM	LEVABON®	Rumen E ¹ Spray-dried autolyzed <i>S. cerevisiae</i> , rich in bioactive ingredients and nutrients such as nucleotides, EAA, peptides, cell wall carbohydrates and B-vitamins.	<ul style="list-style-type: none"> - Feeding of dairy cows during the lactation and close-up period. Also suitable for calves and beef cattle - Improves milk and meat production - Improves feed efficiency and organic matter digestibility - Creates a better rumen environment
		Aquagrow E ² Spray-dried and autolyzed <i>S. cerevisiae</i> , rich in bioactive ingredients and nutrients such as EAA, peptides, cell wall carbohydrates, nucleotides and B-vitamins.	<ul style="list-style-type: none"> - Aquaculture feeds - Contributes to immunity development - Improves animals 'stress resistance - Maintains intestinal integrity
Angel Yeast and Co., Ltd.	GroPro ³	Swine Provides young animal digestible proteins in the form of free amino acids/peptides and functional nucleic acids.	<ul style="list-style-type: none"> - Replaces SDPP in creep feed. - Promotes growth in weaned pigs
		Poultry Provides young animal digestible proteins in the form of free amino acids/peptides and functional nucleic acids.	<ul style="list-style-type: none"> - Feed ingredient - Promotes growth and reduces mortality in broilers - Improves laying rate and egg quality
		Aqua Provides young animal digestible proteins in the form of free amino acids/peptides and functional nucleic acids.	<ul style="list-style-type: none"> - Feed ingredient - Promotes growth and improves palatability
		Rumen High quality of nucleic acid, small peptide, amino acid, polysaccharides and other bioactives.	<ul style="list-style-type: none"> - Feed ingredient - Creates a better rumen environment

¹ <https://www.biomin.net/index.php?id=97&L=7>

² <https://www.biomin.net/index.php?id=98&L=3>

³ <https://en.angelyeast.com/products/animal-nutrition/gropro.html>

Company	Product	Composition	Use and function
			<ul style="list-style-type: none"> - Improves feed digestibility - Increases milk yield - Feed ingredient - Enhances palatability of pets' food - Promotes growth and development of young pets by improving digestion - Promotes the absorption of trace elements thus brighten the coats
	Pet	Rich in flavouring attractants such as peptides, amino acids and nucleic acids.	
	Fubon ⁴	Spent brewer's yeast extract with high efficient microprotein (about 40%) and B-vitamins.	<ul style="list-style-type: none"> - Improve animal feed quality and growth performance
	AJITOP ⁵	Yeast extract rich in natural glutamate and other amino acids, peptides, and nucleotides.	<ul style="list-style-type: none"> - Adds strong savoury taste - Provides the authentic taste of food materials
Kohjin Life Sciences Co., Ltd.	AROMILD ⁶	Yeast extract product with high level of natural nucleotides and strong umami.	<ul style="list-style-type: none"> - Adds savoury taste - Balances taste - Enriches middle taste
	AJIREX ⁷	Yeast extract product rich in peptides: balanced mix of amino acids, peptides, and nucleotides.	<ul style="list-style-type: none"> - Intensifies tastes of other ingredients - Provides saltiness
	AROMAWAY ⁸	Yeast product for body boost and flavour integration.	<ul style="list-style-type: none"> - Boosts body - Intensifies flavour of meat extracts

⁴ <https://en.angelyeast.com/products/animal-nutrition.html>

⁵ <https://www.kohjinls.com/en/business/foodmaterial/ajitop/>

⁶ <https://www.kohjinls.com/en/business/foodmaterial/aromild/>

⁷ <https://www.kohjinls.com/en/business/foodmaterial/ajitop/>

⁸ <https://www.kohjinls.com/en/business/foodmaterial/aromaway/>

Company	Product	Composition	Use and function
	NUCLEAMINE™ ⁹	Yeast extract containing 35% nucleotides and polyamines.	<ul style="list-style-type: none"> - Additive for infant milk formulas - Dietary supplement for anti-aging and skin beauty
Alltech	NuPro® ¹⁰	Yeast extract rich in nucleotides, Glu, amino acids, peptides and inositol (45% of crude protein).	<ul style="list-style-type: none"> - Increases feed intake and animal performance (beef cattle, dairy cows, poultry, pigs, aqua, pet and equine) due to improvement of palatability - Contains components that improve cell repair and growth

SDPP – Spray dried porcine plasma

⁹ <https://www.kohjinls.com/en/business/healthfoodmaterial/nucleamine/>

¹⁰ <https://www.alltech.com/nupro>

1.2.2.2. To sum up

Several strategies have been developed for spent yeast valorisation in a circular economy concept, due to the large amounts of spent yeast produced annually (for instance, brewing industry alone produces about 309,400 to 418,600 tonnes per year). Furthermore, its nutritional composition, with more than 50% of protein, as well as being an inexpensive source of bioactive ingredients, are pointed out as some of the reasons for the yeast valorisation growing market.

Although *S. cerevisiae* has been commercialized for years as yeast extracts, the production of protein-rich extracts is still a challenging affair due to the need for an increased protein content in the final product. With that objective, different protein extraction processes have been optimized to facilitate efficient and cost-effective release of proteins and peptides from yeast cells. Among the abovementioned methods, ultrasonication seems to be quite effective, although limited by operational and economical constraints, thus leading the way to bead milling and HPH as favoured physical extraction processes at industrial scale. However, since they both present the downside of poor selectivity, enzymatic hydrolysis may be preferred when specificity is the key parameter. Chemical methods are also relatively specific, although the experimental conditions may provoke alteration on final protein content or peptide and amino acid profile. Finally, autolysis has the main advantage of only using yeast's own enzymes for the process, but the temperature and long-time treatment can lead to bacterial contamination on yeast suspension, turning the final product unfeasible. In conclusion, process cost and selectivity are inversely related, although it must be kept in mind that a clean extract will decrease the downstream isolation and purification costs. Nevertheless, the selection of the extraction method will be dictated by the final use of the protein extract, as well as the coupled separation and purification procedures. Likewise, many of these separation and purification procedures are difficult to scale-up due to economic constraints, such as chromatography, or can lead to low protein yields, such as with the case of dialysis. On the other hand, membrane filtration has been widely used since is considered a gentle process, being quite fast and relatively economical, which makes it a potential tool to protein-rich extracts production.

Currently, one of the main challenges related to protein extraction from spent yeast remains in establishing a scalable, low cost, efficient and reproducible process in order to produce large amounts of bioactive peptides due to their growing interest for nutraceutical

sector. They are mainly characterized by antihypertensive, antioxidant and antimicrobial properties, although other studied bioactivities are being added to the portfolio. Several authors suggested yeast peptides as dietary supplements for treatment and prevention of chronic diseases, since they have a strong ACE inhibition activity, thus becoming an alternative for several ACE inhibitory drugs (such as captopril) in hypertension treatment, with the added bonus of having lower or no side effects. The protection of gastric mucosa is also pointed out as a health benefit since yeast peptides were able to reduce gastric injuries *in vivo* by prostaglandin-mediated mechanism. Furthermore, the high Fe-binding capacity of yeast peptides also makes them a promising Fe-delivery and anti-anaemic source to produce supplements with Fe-peptide chelates. Recently, some authors hypothesized their use for preventing diabetes, due to the high amount of GABA detected in yeast extracts.

Several yeast protein-rich extracts are already on the market, being used as human dietary supplements, flavour enhancers and animal feed, although info about their source is usually not provided. The labelling of the source as a sustainable one could be a promotion factor for the product, due to the increasing environmental awareness and concern from general consumers.

1.3. Scope & outline

The well-established synthetic biology company Amyris Inc., an American company that produces several ingredients such as farnesene, artemisinin and rebaudioside M by yeast fermentation, concomitantly generating (at least) 2,200 tons of spent yeast *per year*, which represents 20% of their produced waste, and corresponds to their second fermentation by-product by volume. Focusing on the importance of spent yeast valorisation, the main goal of the present thesis was the valorisation of peptides from yeast by-products provided from Amyris Inc., exploring their sustainable and economic extraction, in order to obtain peptide-rich extracts with bioactive properties for application in the nutraceutical market.

For this purpose, the present study started with the production of peptide-rich extracts following two different strategies: i) peptides directly extracted from spent yeast, and ii) peptides obtained from waste streams of β -glucan and mannan extraction processes (yeast cell wall components), in a circular economy approach.

For the first approach, a range of extraction methodologies were applied on spent yeast, prioritizing then the use of most sustainable process for purification. The objective was to assess significant bioactive properties relevant to the food/nutraceutical sector, such as antihypertensive, anticholesterolemic, antioxidant and antimicrobial activities. In the second route, in addition to evaluate the abovementioned bioactivities following the production of peptide-rich extracts, the focus shifted to assessing the capacity of peptides to chelate Fe and the optimization of the production of spent yeast Fe-peptide complexes was performed. Finally, in order to understand the potential application of complexes as dietary supplement, an *in vitro* Fe bioavailability study was conducted alongside a benchmark. Chemical characterization of peptide-rich extracts and Fe-peptide complexes was carried out throughout the study, with focus on the protein amount, MW peptides distribution and amino acids content.

To sum up, the present thesis is divided into three main general segments (**Figure 6**). The first starts with the thesis overview, comprising thesis contextualization, literature review of spent yeast peptides and its scientific output (**Chapter 1**), followed by the production of peptide-rich extracts and, their purification and potential nutraceutical applications (**Chapter 2 and 3**), being concluded with an integrated analysis of all the studies undertaken and future work (**Chapter 4**).

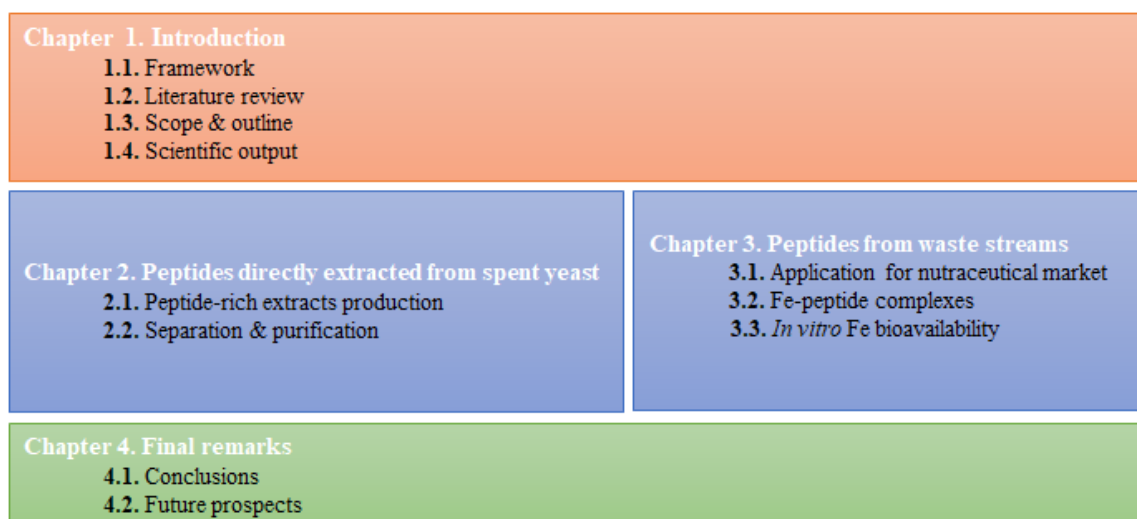


Figure 6. Outline of the present thesis by general segments.

On a more detailed level, the scheme of thesis is represented in **Figure 7**.

The **Chapter 1** comprises a revision of the literature regarding the peptides from spent yeast, such as the processes for their extraction, isolation and purification, their characterization techniques and their bioactive properties that fit into nutraceutical market.

The **Chapter 2** includes the production of peptide-rich extracts directly from spent yeast, where several different extraction methodologies were applied (**Chapter 2.1**) and the best process was selected for the following purification steps, characterizing the final fractions in terms of bioactivities for nutraceutical sector (**Chapter 2.2**).

The **Chapter 3** encompasses the production of peptide-rich extracts from waste streams of β -glucan and mannan extraction processes (yeast cell wall components) by 1 kDa ultrafiltration. From this point, their bioactivities for nutraceutical market were evaluated (**Chapter 3.1**), as well as their Fe-chelating capacity, being optimized a process for Fe-peptide complexes production (**Chapter 3.2**). Finally, the bioavailability of Fe-peptide complexes was compared with Fe salt and a Fe-bisglycinate benchmark through the sequential phases: evaluation of bioaccessible Fe after *in vitro* simulation of human gastrointestinal tract (GIT) and Fe uptake by human colorectal adenocarcinoma (Caco-2) monolayer (**Chapter 3.3**).

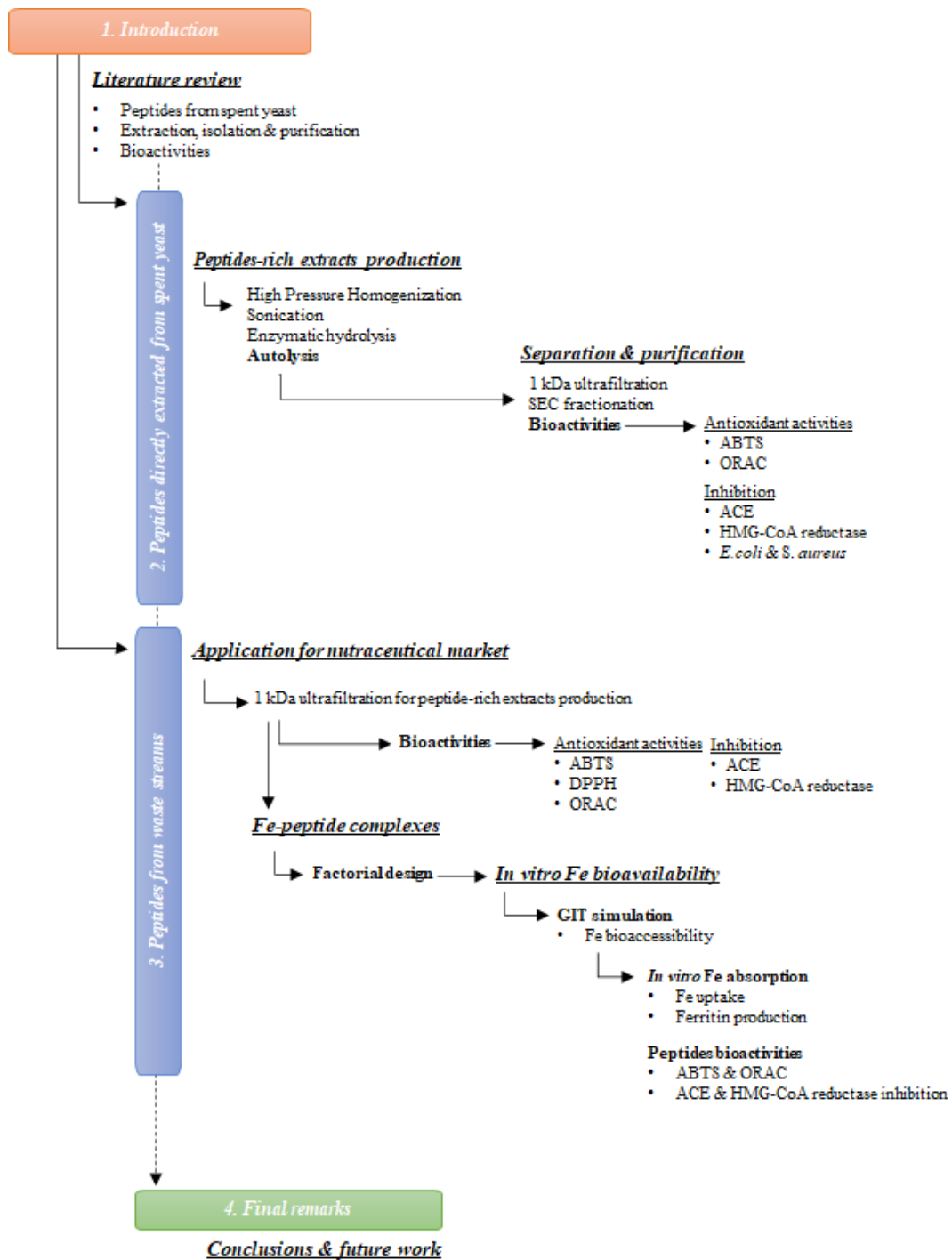


Figure 7. Detailed scheme of the thesis.

1.4. Scientific output

Most of the information presented in this thesis has already undergone peer review, through publication or submission in international journals, and/or presentation in national and international conferences, as elaborated in the following section:

Chapter 1

Publications

Oliveira, A. S., Ferreira, C., Pereira, J. O., Pintado, M. E., & Carvalho, A. P. (2022). Valorisation of protein-rich extracts from spent brewer's yeast (*Saccharomyces cerevisiae*): an overview. *Biomass Conversion and Biorefinery*, 1-23. <https://doi.org/10.1007/s13399-022-02636-5>

Oliveira, A. S., Ferreira, C., Pereira, J. O., Pintado, M. E., & Carvalho, A. P. (2022). Spent brewer's yeast (*Saccharomyces cerevisiae*) as a potential source of bioactive peptides: An overview. *International Journal of Biological Macromolecules*, 208, 1116–1126. <https://doi.org/10.1016/j.ijbiomac.2022.03.094>

Chapter 2

Publications

Oliveira, A. S., Odila Pereira, J., Ferreira, C., Faustino, M., Durão, J., Pereira, A. M., Oliveira, C. M., Pintado, M. E., & Carvalho, A. P. (2022). Spent Yeast Valorization for Food Applications: Effect of Different Extraction Methodologies. *Foods*, 11(24), 4002. <https://doi.org/10.3390/foods11244002>

Oliveira, A. S., Pereira, A. M., Ferreira, C. M. H., Pereira, J. O., Amorim, M., Faustino, M., Durão, J., Pintado, M. E. & Carvalho, A.P. Purification of bioactive peptides from spent yeast autolysates. *Submitted to International Journal of Biological Macromolecules (22th June 2023)*

Oral communication in national conference

Oliveira, A. S., Odila Pereira, J., Ferreira, C., Faustino, M., Durão, J., Pereira, A. M., Oliveira, C. M., Pintado, M. E., & Carvalho, A. P. (2022) Study on peptides extraction methodologies from spent yeast: a sustainable approach. *INSURE.Hub*, 17th November, Porto, Portugal

Chapter 3

Publications

Oliveira, A. S., Pereira, J. O., Ferreira, C., Faustino, M., Durão, J., Pintado, M. E., & Carvalho, A. P. (2022). Peptide-rich extracts from spent yeast waste streams as a source of bioactive compounds for the nutraceutical market. *Innovative Food Science & Emerging Technologies*, 81, 103148. <https://doi.org/10.1016/j.ifset.2022.103148>

Costa, E. M., **Oliveira, A. S.**, Silva, S., Ribeiro, A. B., Pereira, C. F., Ferreira, C., Casanova, F., Pereira, J. O., Freixo, R., Pintado, M. E., Carvalho, A. P., & Ramos, Ó. L. (2023). Spent Yeast Waste Streams as a Sustainable Source of Bioactive Peptides for Skin Applications. *International Journal of Molecular Sciences*, 24(3), 2253. *Mol. Sci.* 2023, 24, 2253. <https://doi.org/10.3390/ijms24032253>. (*Oliveira, A.S. contributed for the antioxidant capacity study of peptide fractions*)

Oliveira, A. S., Ferreira, C. M. H., Pereira, J. O., Sousa, S., Faustino, M., Durão, J., Pereira A. M. P., Pintado, M. E. & Carvalho, A. P. (2023) Production of iron-peptide complexes from spent yeast for nutraceutical industry. *Food and Bioproducts Processing*, <https://doi.org/10.1016/j.fbp.2023.06.006>.

Oliveira, A. S., Ferreira, C. M. H., Pereira, J. O., Silva, S., Costa, E.M., Pereira, A. M. P., Faustino, M., Durão, J., Pintado, M. E. & Carvalho, A. P. Iron-peptide complexes from spent yeast: evaluation of iron absorption using a Caco-2 monolayer. *Submitted to Food Bioscience* (8th June 2023).

Poster in national & international conferences

Oliveira, A. S., Ferreira, C., Pereira, J. O., Pintado, M. E., & Carvalho, A. P. (2021). Peptide rich extracts from spent yeast waste streams as a source of bioactive compounds for nutraceutical market. *XV Encontro Químico dos Alimentos*, 5th-8th September, Madeira, Portugal

Oliveira, A. S., Carvalho, N., Ferreira, C., Pereira, J. O., Pintado, M. E., Madureira, A.R., & Carvalho, A. P. (2021). Peptide-rich extracts from spent yeast as potential microbiota modulators. *Microbiotech21*, 23th-26th November, Lisboa, Portugal

Oliveira, A. S., Ferreira, C., Pereira, J. O., Pintado, M. E., & Carvalho, A. P. (2022) Iron complexation using spent yeast peptides for human supplementation. *5th Food Structure and Functionality Symposium*, 18th-21th September, Cork, Ireland

Oliveira, A. S., Ferreira, C., Pereira, J. O., Silva, S., Costa, E. M., Pintado, M. E., & Carvalho, A. P. (2022) Iron-peptide complexes from spent yeast: evaluation of iron absorption using Caco-2 model. *1st International Congress on Food, Nutrition & Public Health*, 17th November, Lisboa, Portugal

Chapter 2

Peptides directly extracted from spent yeast

2.1. Peptide-rich extracts production

2.2. Separation & purification

2.1. Peptide-rich extracts production*

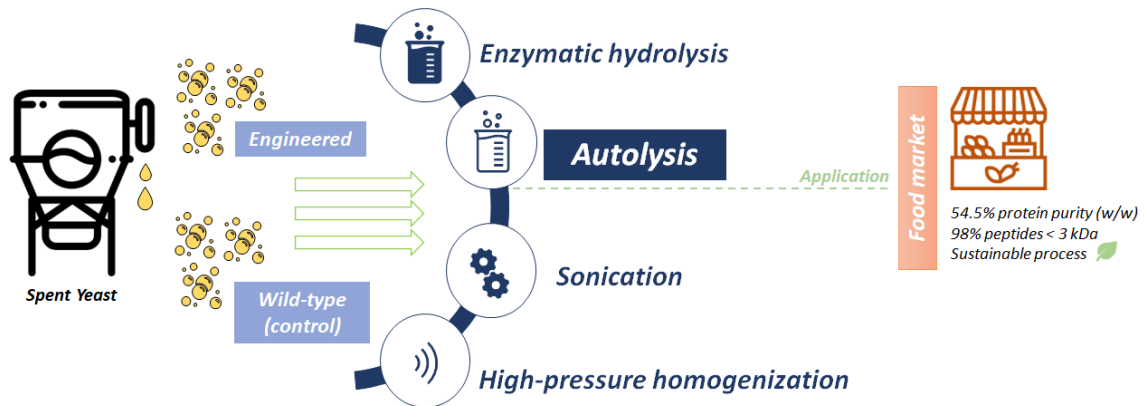


Figure 8. Schematic overview of Section 2.1, illustrating the extraction methods used for both engineered and wild-type yeast strains. Adapted from the graphical abstract of Oliveira, Odila Pereira et al. (2022)

2.1.1. Introduction

The new engineered *S. cerevisiae* strains used in synthetic biology, are genetically modified with the aim of improving or enabling the production capacity of specific molecules. Although the alterations on their genes related to structural components are widely described, only a few publications are focused on perturbation of the cell wall in metabolic engineering (Ramos-Viana et al., 2022). For that reason, one can only question oneself regarding the effects of changes on the yeast morphology, and what effects those changes might have on extraction processes. In one hand, cell wall structural changes might influence the capacity and yield of physical extraction methods, making the cell wall stronger or weaker to these methods, since protein release is directly dependent on its efficient breakage. On the other hand, cytosol enzymatic composition changes may interfere with chemical and enzymatic methods by increasing, for example, the resistance against the action of a particular enzyme that might be used to disrupt the cell during extraction (A. S. Oliveira, Ferreira, et al., 2022b). To the best of our knowledge, there is no studies concerning any possible correlations between engineered yeast alterations and protein extraction so far.

Concerning the increase of worldwide protein demand and the amount of spent yeast generated by brewing and synthetic biology industries, the aim of the present work is to

* Oliveira, A.S., Pereira, J. O, Ferreira, C., Faustino, M., Durão, J., Pereira, A.M., Oliveira, C.M., Pintado, M.E. & Carvalho, A.P. (2022) Spent Yeast Valorization for Food Applications: Effect of Different Extraction Methodologies. *Foods* 11, 4002. <https://doi.org/10.3390/foods11244002>

produce peptide-rich extracts from engineered and non-engineered spent yeast, by applying potentially scalable and sustainable processes at the industrial scale. This will in turn represent more viable options for mass exploration of spent yeast in food and nutraceutical industries using economic and sustainable approaches. Regarding extraction methods on *S. cerevisiae*, thorough reviews have already been conducted on the different physical, chemical and enzymatic methods generally used for protein extraction on spent brewer's yeast (A. S. Oliveira, Ferreira, et al., 2022b). From the described methods generally used for spent brewer's yeast protein extraction, physical methodologies (HPH and sonication), autolysis and enzymatic hydrolysis (enzymatic methods) have been selected, thus covering the majority of the processes used.

Considering the above-mentioned objectives, two steps were idealized. On a first step, the effectiveness of these methods in extracting protein and peptides from spent yeast was evaluated, using a range of parameters such as protein content of extracts produced and their MW distribution. Secondly, the processes protein recovery and sustainable metrics were calculated in order to study the application of extraction process at an industrial level. These parameters were also used to assess the possible differences that distinct engineered strains may or may not induce on the extraction processes (**Figure 8**).

2.1.2. Materials and methods

2.1.2.1. Yeast Strains

Spent yeast of two different *S. cerevisiae* strains, namely “ESY1” and “ESY2”, engineered by Amyris, Inc. to produce β -farnesene, were used in this study. A non-engineered spent brewer's yeast (*Saccharomyces*) kindly supplied by Super Bock Group was used as control (“CSY”). Samples were transported under refrigerated conditions and processed immediately after collection.

2.1.2.2. Yeast pre-treatment

After collection, spent yeast was immediately subjected to two washing processes to remove residual components of fermentation process ($11949 \times g$, 10 min, 4 °C). The supernatant was discarded, and the washed yeast pellet was distributed for the different extraction methods. A sample of spent yeast and washed yeast pellet was collected to DW and protein content determination.

2.1.2.3. Extraction methods

Two physical and two enzymatic methodologies, previously described in literature, were used for protein and peptides extraction from *S. cerevisiae* (A. S. Oliveira, Ferreira, et al., 2022b). The cell suspension for all methods were prepared according to wet yeast weight. A brief description of each methodology is subsequently provided.

High-pressure homogenization

HPH was conducted based on Ekpeni et al. (2016) with some modifications. A cell suspension of 200 mL at 39% (w/v) was prepared in deionized water. Five continuous passages were performed in GEA Lab Homogenizer PandaPLUS 2000 (GEA Group AG, Düsseldorf, Germany), with pressure varying from 600 to 1000 bar during the process since the yeast cell suspension viscosity was increasing. The samples were collected in an ice bath to avoid overheating. At the end of HPH, the cell suspension was centrifuged ($15777 \times g$, 10 min, 4 °C).

Sonication

The protocol of sonication was adapted from Liu et al. (2013) using a JP Selecta CY-500 Ultrasonic Homogenizer (500 W, 20 kHz) coupled with a cylindrical titanium alloy probe tip (\varnothing 10 mm) (Barcelona, Spain). A total volume of 200 mL of 1% cell suspension (w/v) in deionized water was irradiated at 60% amplitude for 30 min in an ice bath (pulse durations of 60 s on and 15 s off). At the end of sonication, the cell suspension was centrifuged ($15777 \times g$, 10 min, 4 °C).

Autolysis

One of Jacob, Hutzler, et al. (2019) methodologies was used to autolyze yeast with some modifications. The washed yeast pellet was dissolved in deionized water (proportion of 1:1 (w/v)) and the autolysis was performed during 16 h at 50 °C with continuous stirring (120 rpm) using a New Brunswick™ Innova® 40/40R Benchtop Orbital Shaker (Eppendorf, Hamburg, Germany). After 16 h, the intrinsic enzymes were inactivated at 95 °C during 5 min. At the end, the cell suspension was centrifuged ($4696 \times g$, 10 min, 4 °C).

Enzymatic Hydrolysis

Enzymatic hydrolysis was carried out using Chae et al. (2001) method. A 20% cell suspension (w/v) was prepared in phosphate buffer 100 mM pH 6.5 (Sodium phosphate monobasic, Sigma-Aldrich, Inc., St. Louis, USA) in order to maintain the optimum pH for enzymes activity. Enzymatic cocktails were added to the sample: 2.0% of Flavourzyme[®], protease from *Aspergillus oryzae* 500 LAPU/g, and 0.6% Protamex[®], protease from *Bacillus* sp. 1.5 AU-N/g (Sigma-Aldrich, Inc., St. Louis, USA). Their amount was calculated according to protein content of spent yeast. The hydrolysis was conducted at 50 °C for 12 h with continuous stirring (120 rpm) using a New Brunswick™ Innova[®] 40/40R Benchtop Orbital Shaker (Eppendorf, Hamburg, Germany). After 12 h, the enzymes were inactivated at 95 °C for 5 min. At the end, the cell suspension was centrifuged (4696 × g, 10 min, 4 °C).

At the end of each extraction process, supernatants rich in protein and peptides were collected and freeze-dried (Freeze-dryer Alpha 2-4 LSCbasic, Martin Christ, Osterode am Harz, Germany).

Sustainable metrics

As a further criterion of evaluation of the extraction processes employed, different metrics of green chemistry and sustainability were calculated for each process assessed. The used metrics were calculated as described by Sheldon et al. (2018). Specifically, the Process Mass Intensity (PMI), Water Intensity (WI) and Energy Intensity Score (EIS) were calculated by:

$$PMI = \frac{\text{total mass in process}}{\text{mass of final product}}$$

$$WI = \frac{\text{mass of water in process}}{\text{mass of final product}}$$

$$EIS = \frac{\text{energy consumption per batch}}{\text{mass of final product}}$$

2.1.2.4. Yeast extract characterization

Protein

Protein content of extracts was determined according to Dumas et al. (1831) by using a Dumatec™ 8000 (Foss, Hilleroed, Denmark). Approximately 50 mg of sample was weighed for aluminium crucible and the analysis was performed at He₂ and O₂ flow rates of 195 mL/min and 300 mL/min, respectively, at 1100 mbar. The protein content was determined from the total N₂ content, multiplied by the conversion factor of 5.5, because of the high content of non-protein nitrogen in yeast (Marson, de Castro, Machado, et al., 2020). A calibration curve from 10 mg to 150 mg of ethylenediaminetetraacetic acid (EDTA) calibration standard (Foss, Hilleroed, Denmark) was used for protein calculation.

Dry weight

DW was determined at 105 °C for 24 h according to standard procedures of the Association of Official Analytical Chemists (AOAC) (Association of Official Analysis Chemists, 2005).

MW distribution

The protein and peptide MW distribution of yeast extracts was analysed in a ultra-high-performance liquid chromatography system (LC-ESI) from Bruker Elute series, coupled to an ultrahigh-resolution quadrupole–quadrupole time-of-flight (UHR–QqTOF) mass spectrometer (Impact II; Bruker Daltonik GmbH, Bremen, Germany) with an Intensity Solo 2 C18 (100 × 2.1 mm, 2.2 μm, Bruker Daltonik GmbH, Bremen, Germany) (BRHSC18022100) was used to analyse the protein and peptide MW distribution of yeast extracts at MS positive mode (150 to 2200 m/z) (C. M. Oliveira et al., 2022). Water with 0.1% of formic acid (A) and acetonitrile with 0.1% of formic acid (B) were used as mobile phases at 0.250 mL/min flow rate in gradient mode. ESI-L Low Concentration Tuning Mix (Agilent Technologies Inc., CA, USA) was used for post-acquisition internal mass calibration at each analysis.

Amino acids

The amino acids quantification was assessed as described by Long et al. (2017) by ortho-phthalaldehyde (OPA)-derivatization using a Chromolith® Performance RP18 (4.6 × 100

mm) column (Merck KGaA, Darmstadt, Germany) for separation by RP-HPLC coupled to a high-resolution fluorescence detector (Agilent Technologies, Inc., California, USA). Before HPLC analysis of total amino acids, an acid hydrolysis (20 h, 115 °C) was performed at 10 mg of extract in 3 mL HCl 6 M under anoxic conditions. Then, pH was adjusted to 3.2 and the solution diluted to a final volume of 10 mL (L. Wang et al., 2016). The derivatization of 20 µL of extract was done in automatic liquid multisampler and 10 µL was injected.

Analysis was done in triplicate and the amino acids quantified according to calibration curves of pure standards (Sigma-Aldrich, Inc., St. Louis, USA) from 1 to 30 mg/L, using norvaline (Sigma-Aldrich, Inc., St. Louis, USA) as internal standard.

Neutral sugars

Neutral sugars derivatized to their alditol acetates were analysed by gas chromatography-flame ionization (GC-FID) detection as described by Pinto et al. (2015) in a 7890B GC System with a DB-225 capillary column (30 m length, 0.25 mm diameter, 0.15 µm thickness) (Agilent Technologies, Inc., California, USA). Before the derivatization reaction, the extracts were hydrolysed using 72% H₂SO₄ (Honeywell, North Carolina, USA) (3 h, room temperature) followed 1 M H₂SO₄ (2.5 h, 100 °C) (Selvendran et al., 1979). The released monosaccharides were converted to their respective alditol acetates using the protocol of Blakeney et al. (Blakeney et al., 1983). Two microliters of sample were injected into the GC-FID and the analysis was performed at split mode with a ratio of 1:60 (200 °C). The initial oven temperature was set for 200 °C and kept for 2 min, then elevated at the rate of 40 °C/min to 220 °C (7 min hold) followed by increase to 230 °C at 20 °C/min (5 min hold) with the total time of analysis being 15 min. The carrier gas was N₂ at a constant flow of 1 mL/min. The equipment was coupled to a H₂ generator (30 mL/min), being also used compressed air at 400 mL/min during the analysis.

Minerals

An optical emission spectrometer Model Optima 7000 DV TM Inductively coupled plasma - optical emission spectrometry (ICP-OES) (Dual View, PerkinElmer Life and Analytical Sciences, Shelton, CT, USA) with radial configuration was used for minerals analysis following the procedure of Chatelain et al. (2014). A calibration curve of a commercial mix standards for ICP analysis (Inorganic Ventures, Christiansburg, USA) (Mo, Zn, Cd, P, Pb, Ni, Co, Mn, Fe, Mg, Ca, Cu, Al, Na and K) from 0.05 to 10 mg/L was applied

for quantification. A microwave digestion was performed before ICP analysis in a speedwave XPERT (Berghof Products + Instruments GmbH, Eningen, Germany) using 250 mg of sample with 6 mL of Suprapur[®] HNO₃ and 1 mL of 35% H₂O₂ (Merck KGaA, Darmstadt, Germany).

Statistical analysis

Statistical analysis was performed using the Real Statistics Resource Pack software (Release 7.2) and the results expressed as average ± standard deviation from assay replicates. Two different fermentation reactors were collected for each spent yeast and each extraction method was performed in triplicate. Procedures of extracts characterization were assessed in triplicate.

Normality of data was tested using the Shapiro-Wilk's test and the comparison between different extraction methods and/or yeasts were performed using the one-way analysis of variance (ANOVA) followed by Tukey's multiple comparisons test, after evaluating the homogeneity of variances using the Levene Test for Equality of Variances.

2.1.3. Results and Discussion

2.1.3.1. Peptide rich-extracts characterization

Protein content (% w/w)

All the extraction methodologies applied to engineered and non-engineered spent yeasts allowed for the production of extracts that can be labelled as “rich in protein” (European Commission, 2012) since a range of protein content from 25.3% to 64.8% (w/w) was observed (**Table 10**). These results are in accordance to protein content obtained by Ganeva et al. (1999), Podpora et al. (2016) and Ferreira et al. (2022) in yeasts. Indeed, the initial protein amount of the raw strains already showed high values from a nutritional point of view (32.9% to 43.0%), which highlights the potential use of engineered spent yeast for mass exploration in food and nutraceutical industries, in a similar mode as what occurs with the non-engineered yeasts. However, the increase of protein content in the final product is still a challenge and, for that reason, different processes have been optimized (A. S. Oliveira, Ferreira, et al., 2022b).

Table 10. Protein content (% w/w) of raw yeast and extracts obtained from each extraction process applied to the different yeast strains (CSY, ESY1 and ESY2).

	CSY	ESY1	ESY2
Raw yeast	43.0 ± 1.1	38.4 ± 2.3	32.9 ± 0.4
Autolysis	64.8 ± 2.4	54.5 ± 1.0	48.3 ± 1.0
Enzymatic hydrolysis	34.6 ± 2.6	30.8 ± 0.4	25.3 ± 0.7
HPH	51.2 ± 3.3	45.6 ± 1.7	44.5 ± 1.8
Sonication	50.2 ± 14.6	50.1 ± 4.3	46.3 ± 0.9

Results are expressed as average ± standard deviation ($n=3$).

An increase of protein content in extracts was observed in relation to raw yeast, after applying the extraction methodologies with exception of enzymatic hydrolysis process (**Table 10; Table S1 and Table S2**).

Enzymatic hydrolysis is based on the application of exogenous enzymes to break yeast cell wall at specific sites to release their protein and peptides. In general, it has been explored in food and nutraceutical industries for production of yeast hydrolysates, using commercial proteolytic enzymes, which are responsible for the composition of peptides produced (A. S. Oliveira, Ferreira, et al., 2022b). For this reason, several studies have been performed in order to assess the best hydrolysis conditions for the maximum enzyme efficiency, such as enzyme dosage, pH, time, and temperature, to be applied at a specific yeast (M. Amorim, Pinheiro, et al., 2019; Chae et al., 2001; Xie et al., 2017). In the present study, hydrolysis conditions optimized by Chae et al. (2001) were used, since they obtained a higher protein yield using *S. cerevisiae* in comparison with other studies (A. S. Oliveira, Ferreira, et al., 2022b). However, these conditions were not optimized for the specific strains hereby used, being that the potential explanation for observing a decrease of protein content in extracts in comparison with raw yeasts. For all yeasts, autolysis, sonication and HPH were the best processes for rich protein extracts production (**Table 10; Table S1 and Table S2**). Autolysis is more advantageous than enzymatic hydrolysis and physical methods as it is only based on action of yeast own enzymes, when cell death phase is initiated, which leads to degradation of cell components and consequently protein and peptides release (A. S. Oliveira, Ferreira, et al., 2022b). Unlike sonication energy related consumption, operational and economical limitations, HPH is widely accepted at industrial scale. However, HPH equipment requires regular and costly maintenance since they easily get clogged.

Regarding the comparison between the strains, no tendencies were observed since the differences of extracts' protein content seemed to be considerably more affected by extraction method than the type of strain used (**Table 10; Table S1 and Table S2**).

Molecular weight distribution

MW distribution of protein and peptides is a standard analysis for the evaluation of spent yeast extraction methods, since different methodologies result in the release of molecules with different sizes, according to their operation mode and extension (A. S. Oliveira, Ferreira, et al., 2022b). Different MW profiles were obtained between yeast strains and extraction processes, as shown in **Figure 9**.

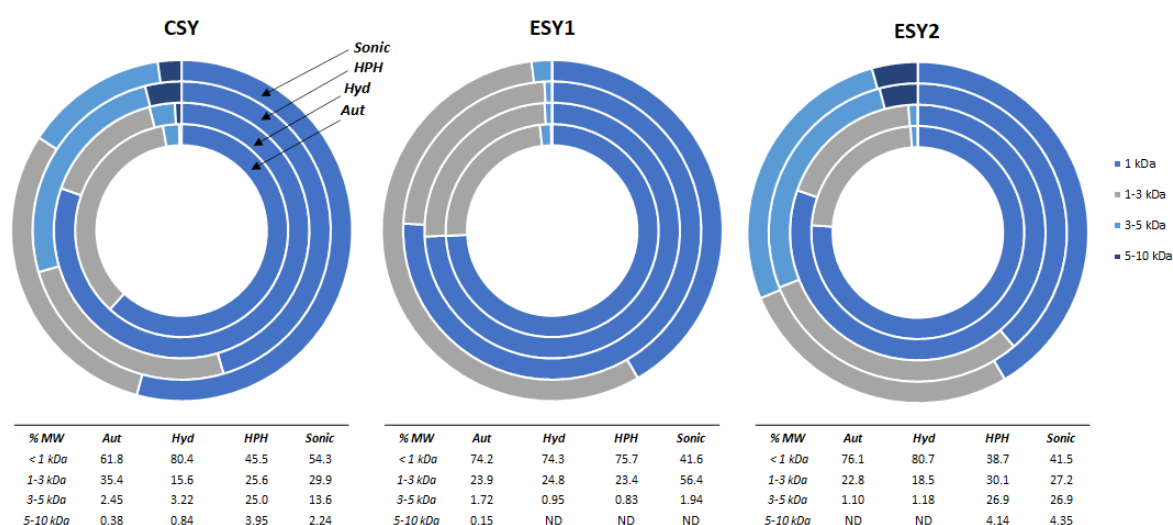


Figure 9. Peptides MW distribution (%) in peptide-rich extracts obtained from each extraction process (Aut – autolysis, Hyd – enzymatic hydrolysis, Sonic – sonication) applied to the different yeast strains (CSY, ESY1 and ESY2). ND – not detected (below low detection limit).

In fact, MW has an important role on peptides bioactivity, since those with small size (3 to 20 amino acids) are described as more specific in their biological functions and choice of biological targets (A. S. Oliveira, Ferreira, et al., 2022a). However, some peptides with a size of 1-3 kDa were also described by their antioxidant and ACE inhibitory activities (M. Amorim, Marques, et al., 2019; Mirzaei et al., 2015). Indeed, a percentage from 15.6 to 56.4% of 1-3 kDa peptides was also observed in this study, suggesting these potential bioactivities of our extracts. On the other hand, lower percentages of peptides about 3-5 kDa were found, followed by residual amounts of 5-10 kDa peptides.

Concerning peptides < 1 kDa of different strains, no alterations were observed between strains, with exception of ESY1 HPH (75.7%) that stands out from CSY (45.5%) and ESY2 (38.7%). The other potential bioactivity fraction (1-3 kDa), the ESY1 sonication (56.4%) pointed out in relation to CSY (29.9%) and ESY2 (27.2%). However, as showed before for

protein content results, no differences were noticed between genetically modified and control strains (**Figure 9**).

Looking at global results of three yeasts, enzymatic methods seemed to allow the high percentage of bioactive peptides under 3 kDa (CSY: ~ 97%, ESY1: ~ 99%, ESY2: ~ 99%). Indeed, autolysis process has been generally described for releasing oligopeptides (2-3 kDa) followed by di-, tri-, and tetra-peptides (< 600 Da), but the size of released peptides is always dependent on controlling the autolysis extension, since peptides of different MW can be obtained on the same process because of their degradation during lysis process (Podpora et al., 2015). Our results are similar to those obtained by Jacob, Hutzler, et al. (2019), as they observed an increase of peptides < 4 kDa and free amino acids at enzymatic protocols in comparison with bead milling and ultrasound.

2.1.3.2. Extraction methodology evaluation

Several physical, chemical, and enzymatic methodologies are available for extracting protein and peptides from spent yeast and a combination of methods is a common practice at industrial level (A. S. Oliveira, Ferreira, et al., 2022b). However, the selection of the most appropriate method is directly related with the intended application of the final product for maximum protein recovery and quality (Marson, de Castro, Belleville, et al., 2020). Protein isolation and purification protocols are often coupled to these extractions in order to fulfil a need of a specific economic sector (A. S. Oliveira, Ferreira, et al., 2022b). However, food and nutraceutical industries have been facing the challenge of establishing a viable process at economic and sustainable levels, since several technologies are difficult to be efficient and reproducible, as well as low cost and scaled-up. In this segment, the protein recovery of each process applied at different yeast strains and the respective sustainable metrics were evaluated.

Protein recovery

From all processes, the percentage of protein recovery was calculated based on the protein amount of raw yeast in relation to protein of produced extracts. As observed in **Figure 10**, a protein recovery from 18.5% to 64.9% was obtained. Indeed, several variables may influence protein recovery values, such as temperature, processed volumes, cell suspension concentration, electric field strength and treatment duration. Determining the

optimal process for protein recovery can be challenging due to the complexity of these variables (A. S. Oliveira, Ferreira, et al., 2022b).

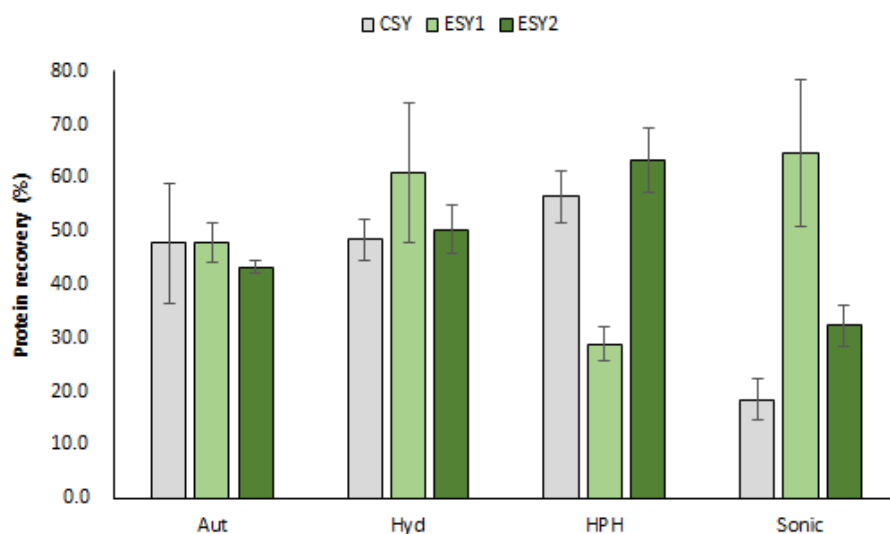


Figure 10. Protein recovery (%) of each extraction process (Aut – autolysis, Hyd – enzymatic hydrolysis, Sonic – sonication) applied to the different yeast strains (CSY, ESY1 and ESY2).

ESY1 sonication showed the highest protein recovery ($64.9 \pm 13.9\%$) from all processes. On the other hand, a statistically significant low protein recovery was verified for the other engineered yeast (ESY2: $32.4 \pm 3.8\%$) in comparison with ESY1 on the same extraction methodology, despite both were higher than control yeast ($18.5 \pm 3.8\%$) (**Figure 10; Table S3 and Table S4**). Indeed, this result corroborates the abovementioned hypothesis that the extraction method may have more influence at protein obtained than the type of yeast strain used. A similar result was obtained for other processes applied, since there were statistically significant ($p < 0.05$) differences between ESY1 and ESY2 at HPH ($28.9 \pm 3.3\%$ and $63.5 \pm 6.0\%$, respectively), confirming the abovementioned assumption (**Figure 10; Table S3 and Table S4**). Regarding the comparison between extraction processes inside each strain, a trend was also not found, since enzymatic processes and HPH allowed the highest protein recovery for CSY and ESY2, in the opposite of ESY1 which was the sonication together with enzymatic methodologies. Therefore, it was not possible to select the best method for spent yeast protein extraction based on protein recovery because of the lack of reproducibility between yeast strains.

Sustainable metrics

Since spent yeast is used for the production of potential animal protein alternatives, such as protein rich extracts, in a circular economy approach of fermentation industrial processes (A. S. Oliveira et al., 2022), it seems important the establishment of a more sustainable and greener process for this production at food and nutraceutical sectors. For this reason, sustainable metrics were calculated for each extraction process performed, in order to compare their “greenness” (**Table 11**).

Table 11. Sustainable metrics (PMI, WI and EIS) of each extraction process applied to the different yeast strains (CSY, ESY1 and ESY2).

		CSY	ESY1	ESY2
Autolysis	PMI	22	27	26
	WI	11	13	13
	EIS	5764	6891	6601
Hydrolysis	PMI	35	36	35
	WI	29	30	28
	EIS	2250	2330	2217
HPH	PMI	27	66	29
	WI	19	48	21
	EIS	44.2	110	47.2
Sonication	PMI	1904	919	1509
	WI	1882	909	1492
	EIS	2353	1137	1865

From the metrics of all processes, there seem to be no differences between the three yeast strains. On the other hand, concerning the processes, autolysis showed low values of PMI and WI, followed by HPH, enzymatic hydrolysis, and sonication, which means autolysis requires the lowest amount of raw yeast for production of protein-rich extracts using the lowest water quantity in process as well. In fact, autolysis has been described as an environmentally sustainable methodology for the recovery of intracellular compounds (Halim et al., 2019). On the other hand, evaluating the EIS, all the processes showed extremely high metrics, an output related to the use of laboratory scale equipment, which does not allow to make a correct assessment in terms of energy consumption. However, from the four extractions, HPH seems to have the lowest energy consumption.

2.1.3.3. Choice of peptide-rich extract for future purification process

After the characterization of peptide-rich extracts produced in terms of protein content and MW, and evaluation of protein recovery and sustainability of processes tested, the extract obtained from yeast strain ESY1 by autolysis was chosen for future work related with isolation and purification of engineered spent yeast peptides. Such choice was based on protein content: $54.5 \pm 1.0\%$ for ESY1 versus $48.3 \pm 1.0\%$ for ESY2 (**Table 10**). Furthermore, there were no observed tendencies in the differences between engineered and wild strains, such as extracts' protein content, MW distribution and protein recovery, which enhance the potential of use of these genetically modified strains for food applications. In fact, results suggest that some of the differences observed in extracts nutritional performance could be more related with the extraction process *per se* instead of the type of yeast strain used for the process. Regarding the extraction process, autolysis revealed to be a highly efficient, sustainable and scalable process. On the one hand, it allowed a high protein content of final extracts on engineered strains (**Table 10**) with a large percentage of peptides under 3 kDa (~98%) (**Figure 9**), which may be potentially bioactive as extensively described in literature (A. S. Oliveira, Ferreira, et al., 2022a). In addition, this process allowed for the lowest amount of biomass required for extract production, with the smallest water consumption (**Table 11**), which important steps to establish a green and sustainable process in food and nutritional sectors. However, a deep evaluation of autolysis energy consumption needs to be performed at industrial level.

Beyond the protein-related parameters evaluated, a more complete nutritional characterization of ESY1 autolysis extract is represented in **Table 12** regarding its potential application in food and nutraceutical sectors.

Table 12. Protein content (% w/w), sugars (% w/w) and minerals (ng/g extract) of peptide-rich extract obtained from autolysis of ESY1.

Protein (%)	Sugars (%)	Minerals (ng/g)				
		P	Mg	Ca	K	Total
54.5 ± 1.0	14.8 ± 0.7	14.2 ± 1.0	4.34 ± 0.37	1.55 ± 0.13	16.5 ± 0.5	36.9 ± 1.9

Results are expressed in average \pm standard deviation ($n=3$). ND – Not detected (below low detection limit).

The protein content of ESY1 autolysate showed to be higher than those obtained by Bertolo et al. (2019) ($39.3 \pm 0.9\%$) and Jacob, Striegel, et al. (2019) ($42.4 \pm 3.0\%$). On the

other hand, several studies described high protein percentages in autolysates, but they have used purification processes coupled with the extraction, in order to increase the content of protein in the final product (M. Amorim et al., 2016; A. S. Oliveira et al., 2022), which raises the interest of future work related to peptide purification processes. Likewise, the amount of sugars and minerals obtained is concordant with the range reviewed by Marson, de Castro, Belleville, et al. (2020). Furthermore, the total and individual amount of EAA exceeded the FAO/WHO recommendations (**Table 13**) (with exception of Met) which highlights their potential use in food and nutraceutical industries. Indeed, these organizations have been describing spent brewer's yeast as a potential source of EAA (Puligundla et al., 2020) which was corroborated by the present study. The obtained results align with the range of amino acids of the autolysates obtained by Podpora et. (2015) and Jacob, Hutzler, et al. (2019).

Table 13. EAA (mg/g protein) of peptide-rich extract obtained from autolysis of ESY1.

	EAA	FAO/WHO reference ^c
Cys	6.94 ± 0.41	6.0
His	47.1 ± 5.0	15.0
Thr	60.4 ± 2.4	11.0
Arg	59.1 ± 3.9	NM
Val	72.8 ± 4.4	15.0
Met	8.97 ± 1.89	16.0
Phe	43.7 ± 2.6	21.0 ^b
Tyr ^a	41.3 ± 3.6	
Ile	56.9 ± 3.2	15.0
Leu	78.1 ± 4.8	21.0
Lys	69.9 ± 2.5	18.0
Total	545 ± 35	138

Results are expressed in average ± standard deviation ($n=3$). ^a Non-essential, ^b Phe + Tyr. ^c World Health Organization (2007). NM – not mentioned. Arg - Arginine, Ile - Isoleucine, Leu - Leucine

2.1.4. Conclusions

The present study showed that engineered modified spent yeast have the same performance in terms of peptide-rich extracts production than non-engineered type, being an alternative to animal protein sources for food and nutraceutical industries. Indeed, the nutritional analysis of extracts obtained showed their potential to be applied at a healthy and balanced diet. Furthermore, using the substantial quantity of spent yeast generated by fermentation industries represents a significant step towards establishing circular economy in industry. When aiming for a sustainable and environmentally friendly approach to

ingredient production, autolysis was chosen as the extraction methodology due to its interesting sustainable metrics in terms of biomass and water consumption, as well as high protein content obtained, as well as low MW peptides. However, it is crucial to assess the energy consumption and corresponding economic considerations at an industrial level in order to evaluate the actual effective environmental friendliness and sustainability of the process. On the next section (*Section 2.2. Separation & purification*), the isolation of peptides fractions from ESY1 autolysate will be performed together with the evaluation of its potential bioactivities.

2.1.5. Supplemental material

Table S1. P-values of comparison of protein content (% w/w) between different yeast strains.

	Autolysis	Hydrolysis	HPH	Sonic
CSY vs. ESY1	2.57E-07	3.94E-03	4.19E-03	1.00
CSY vs. ESY2	3.43E-09	2.15E-06	2.53E-03	7.98E-01
ESY1 vs. ESY2	2.06E-04	4.48E-04	7.71E-01	8.10E-01

$n(\text{CSY and ESY1})=6, n(\text{ESY2})=4$

Table S2. P-values of comparison of protein content (% w/w) between different extraction methodologies.

	CSY	ESY1	ESY2
Hydrolysis vs. autolysis	6.65E-06	8.11E-13	4.44E-12
Hydrolysis vs. raw yeast	6.57E-01	7.28E-03	2.96E-05
Hydrolysis vs. HPH	7.85E-03	5.74E-09	4.30E-11
Hydrolysis vs. sonication	1.31E-02	4.22E-011	1.48E-11
Autolysis vs. raw yeast	1.45E-02	4.88E-07	7.93E-09
Autolysis vs. HPH	3.67E-02	2.13E-05	3.37E-03
Autolysis vs. sonication	2.25E-02	3.44E-02	1.60E-01
Raw yeast vs. HPH	6.69E-01	1.06E-02	2.42E-07
Raw yeast vs. sonication	7.62E-01	5.36E-05	4.34E-08
HPH vs. sonication	9.99E-01	2.78E-02	2.38E-01

$n(\text{CSY and ESY1})=6, n(\text{ESY2})=4$

Table S3. *P*-values of comparison of protein recovery (%) between different yeast strains.

	Autolysis	Hydrolysis	HPH	Sonic
CSY vs. ESY1	1.00	6.47E-02	3.50E-07	2.23E-06
CSY vs. ESY2	6.32E-01	9.34E-01	9.14E-02	8.07E-02
ESY1 vs. ESY2	6.18E-01	1.83E-01	9.48E-08	2.88E-04

n(CSY and ESY1)=6, *n*(ESY2)=4

Table S4. *P*-values of comparison of protein recovery (%) between different extraction methodologies.

	CSY	ESY1	ESY2
Hydrolysis vs. autolysis	9.98E-01	1.32E-01	1.47E-01
Hydrolysis vs. HPH	1.86E-01	8.55E-05	4.85E-03
Hydrolysis vs. sonication	1.09E-06	9.13E-01	3.47E-04
Autolysis vs. HPH	1.39E-01	1.52E-02	1.23E-04
Autolysis vs. sonication	1.51E-06	3.65E-02	1.64E-02
HPH vs. sonication	2.35E-08	2.06E-05	1.45E-06

n(CSY and ESY1)=6, *n*(ESY2)=4

2.2. Separation & purification*

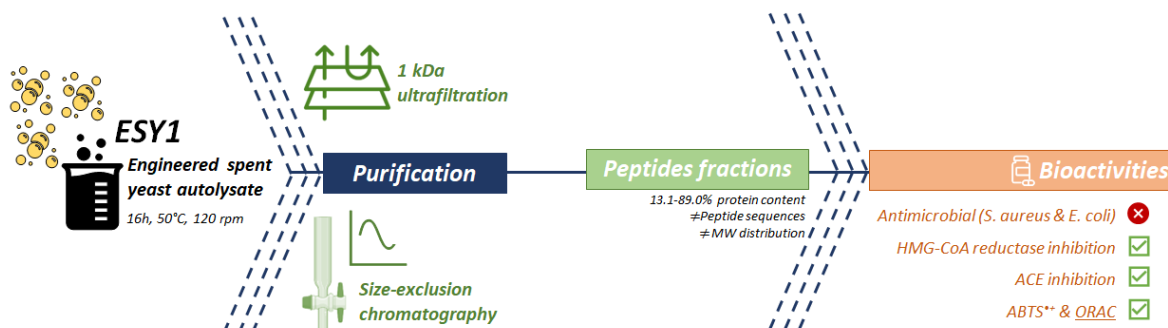


Figure 11. Schematic overview of Section 2.2, outlining the purification techniques employed for autolysate ESY1, such as ultrafiltration and SEC. Adapted from the graphical abstract of article in preparation*

2.2.1. Introduction

In the last decades, the interest for yeast ingredients has been growing in several economic sectors, due to their established biologically relevant properties, with several extraction and purification processes for their production have been developed over time (Marson, de Castro, Belleville, et al., 2020). Bioactive peptides are one example of these molecules, with demonstrated antimicrobial, antihypertensive and antioxidant properties, among others, especially in agri-food and cosmetic sectors (A. S. Oliveira, Ferreira, et al., 2022a). However, in the production of these bioactive peptides, the application of physical, chemical or enzymatic extraction processes to the yeast, which cleave and release proteins from the cell envelope, may not always be enough to obtain a specific bioactive peptide. For that reason, several isolation and purification processes have been implemented in conjunction with extraction to decrease yeast cell debris and other contaminants that can influence the final biological properties fraction (A. S. Oliveira, Ferreira, et al., 2022b).

Membrane filtration technology has been widely used for the separation and concentration of spent yeast protein and bioactive peptides, since it can be operated under gentle conditions, allowing cell debris removal with low energy consumption and without compromising molecular structures, and consequently, their biological activities (Vollet

* Oliveira, A.S, Pereira, A. M., Ferreira, C. M. H., Pereira, J. O., Amorim, M., Faustino, M., Durão, J., Pintado, M. E. & Carvalho, A.P. *Purification of bioactive peptides from spent yeast autolysates*. In preparation to submission in *International Journal of Biological Macromolecules*.

Marson et al., 2020). Depending on the protein, peptide MW, and the intended application, different membrane filtration cut-offs and materials can be used in order to obtain the desired product (D. Liu et al., 2010). Furthermore, this technology has been widely used in food industry for processing new ingredients and foods due to its green characteristics (Dhineshkumar & Ramasamy, 2017). On the other hand, chromatographic separation has become one of the most effective and widely used technique for the purification of bioactive peptides, regarding pharmaceutical research. In fact, bioactive peptides from spent yeast have been isolated by gel filtration (Gddoa Al-sahlany et al., 2020; Mirzaei et al., 2015) that is considered a fast and reproducible protocol. Gel filtration, such as SEC, separation depends on molecules size and shape since it is based on sieving properties of the stationary phase matrix (A. S. Oliveira, Ferreira, et al., 2022b). However, the cost of SEC apparatus is substantially higher than membrane filtration. One must, however, bear in mind that the final process cost and selectivity are inversely related, meaning that a value-added ingredient needs to be produced towards an overall cost-effective process (A. S. Oliveira, Ferreira, et al., 2022b).

Meanwhile, the nutraceutical sector has been working on yeast bioactive peptides mainly because of their antihypertensive (M. Amorim, Marques, et al., 2019) and antioxidant (H. Guo et al., 2020) features that has been used for the management of cardiovascular diseases development (Mirzaei et al., 2015). Antidiabetic potential of yeast extracts has also been reported (Hu et al., 2014) as well as anti-stress effects (H. S. Lee et al., 2009), *in vitro* immunostimulation (Williams et al., 2016) and *in vivo* influence in bone growth (H. S. Lee et al., 2011).

Similarly to what happens in brewing industry, *S. cerevisiae* strains have been engineered in order to produce commercial target ingredients in large scale through their fermentation processes (A. S. Oliveira et al., 2022), where significant amounts of spent yeast have been generated, which must be valued in a circular economy approach.

Considering the bioactive potential of spent yeast peptides and their significant amount generated by industry, as by-products in industrial waste, the aim of the present study was the application of purification processes to a peptide-rich extract from engineered spent yeast autolysate “ESY1”, previously produced (*Section 2.1. Peptide-rich extracts production*) for the obtention of bioactive peptides-rich fractions with targeted biological properties for dietary supplementation. After literature review (A. S. Oliveira, Ferreira, et al., 2022b), two purification methodologies were chosen: ultrafiltration and gel filtration, using SEC. The purified peptide-rich fractions were then characterized and assessed for their potential

bioactive properties, namely antimicrobial, anticholesterolemic, antihypertensive and antioxidant properties (**Figure 11**). To the best of our knowledge, the present study assessed the effect of peptides from spent yeast in targeting cholesterol levels through HMG-CoA reductase inhibition for the first time.

2.2.2. Material and methods

2.2.2.1. Peptide-rich autolysate “ESY1”

The peptide-rich autolysate “ESY1” used in the present study was studied in *Section 2.1. Peptide-rich extracts production*. Their yeast strain origin, production process and extract choice were also explained on this section (*Section 2.1.2. Material and methods*).

2.2.2.2. Purification of bioactive peptides

Ultrafiltration

As illustrated in **Figure 12**, peptide-rich extract was resuspended in deionized water (10 g/L) and the solution underwent in an Amicon[®] stirred cell model (Merck KGaA, Darmstadt, Germany) using a 1 kDa cut-off Ultracel[®] regenerated cellulose membrane (Merck KGaA, Darmstadt, Germany). Thereafter, the retentate was diafiltrated with 3 volumes of deionized water, resulting in two purified fractions with different peptide MW: “ESY1 > 1 kDa” and “ESY1 < 1 kDa”. At the end, samples were freeze-dried for further analysis.

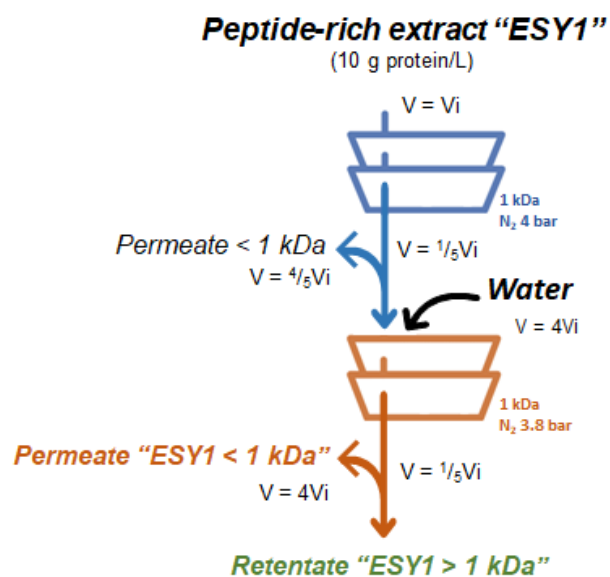


Figure 12. Diagram of ultrafiltration process for production of peptide-rich fractions with different MW: "ESY1 > 1 kDa" and "ESY1 < 1 kDa".

Size-exclusion chromatography

Size exclusion chromatography, using a Hiprep™ 26/10 Desalting column (GE Healthcare) was performed in an ÄKTA Pure™ 25 M (Cytiva, USA) purification system, and monitored by ultra-violet absorption at 280 nm using a UV detector. Lyophilized peptide-rich extract was resuspended in ultrapure water to a final concentration of 9 g/L and filtered through a 0.45 µm filter (Chromafil® PET-45/25, Macherey-Nagel, Germany) before being loaded into a pre-equilibrated column (injection volumes of 2 mL). Ultrapure water, at a flow rate of 5 mL/min, was used as elution buffer and fractions of 5 mL were collected.

2.2.2.3. Peptides chemical characterization

Protein determination

Dumas

Protein content of ultrafiltration fractions "ESY1 > 1 kDa" and "ESY1 < 1 kDa" was performed using the Dumas method (1831) described at *Section 2.1.2.4. Protein*.

Bicinchoninic acid & dry weight

Protein concentration of SEC fractions was determined using the Pierce™ BCA protein assay kit (Thermo Fisher Scientific Inc., Massachusetts, USA), according to the manufacturer's instructions. Bicinchoninic acid (BCA) interacts with Cu¹⁺ resulting from the reduction of Cu²⁺ ions from the copper sulphate by peptide bonds in alkaline pH, forming a purple-coloured complex with a strong linear absorbance at a wavelength of 562 nm with increasing protein concentrations (Smith et al., 1985). Protein content of the fractions was calculated after DW determination (described at *Section 2.1.2.4 Dry weight*).

Molecular weight distribution

The MW of peptides in SEC and ultrafiltration fractions was evaluated using a HPLC system (Agilent Technologies Inc., Santa Clara, CA, USA) with an AdvanceBio SEC 130A 2.7 µm (7.8 × 300 mm) column (Agilent Technologies Inc., Santa Clara, CA, USA) based on Tian et al. (2020) methodology with some modifications. The elution was carried out using 150 mM sodium phosphate buffer (Sigma-Aldrich, Inc., St. Louis, MO, USA) at 1 mL/min flow rate. The elution was monitored at 280 nm and conalbumin (75 kDa), ovoalbumin (43 kDa), carbonic anhydrase (29 kDa), ribonuclease A (13.7 kDa), aprotinin (6.5 kDa), Lys peptide (775 Da) and Trp (204 Da) were used as standards for the calibration curve.

Proteomics

A nanoLC-MS/MS, namely Ultimate 3000 liquid chromatography system coupled to a Q-Exactive Hybrid Quadrupole-Orbitrap mass spectrometer (Thermo Scientific, Bremen, Germany), was used for peptides identification as described by Osório et al. (2021). Samples were loaded onto a trapping cartridge (Acclaim PepMap C18 100 Å, 5 mm × 300 µm i.d., 160454, Thermo Scientific, Bremen, Germany) and after 3 min loading, the trap column was switched in-line to a 50 cm × 75 µm inner diameter EASY- Spray column (ES803, PepMap RSLC, C18, 2 µm, Thermo Scientific, Bremen, Germany). Data acquisition was controlled by Xcalibur 4.0 and Tune 2.9 software (Thermo Scientific, Bremen, Germany).

Peptide sequences were obtained using the Proteome Discoverer 2.5.0.400 software (Thermo Scientific, Bremen, Germany), as described by Osório et al. (2021), using *S. cerevisiae* protein sequence database instead. After identifying the peptide sequences, we conducted an *in silico* search of these sequences against databases that contain information

on known peptide activities. The databases used in our analysis included the Database of Antimicrobial Activity and Structure of Peptides (DBAASP) (Pirtskhalava et al., 2021), the Data repository of antimicrobial peptides (DRAMP) (Shi et al., 2022), the Collection of Anti-Microbial Peptides (CAMP) (Gawde et al., 2023), the Antimicrobial Peptide Database (APD) (G. Wang et al., 2016) and the BIOPEP-UWM™ (Minkiewicz et al., 2019). Unique matches and partial matches were both considered.

2.2.2.4. Peptides bioactivity

Antimicrobial

Time-growth inhibition curves of *E. coli* (DSM1576) and *S. aureus* (DSM799) (Deutsche Sammlung von Mikroorganismen und Zellkulturen, Braunschweig, Germany) were performed to assess the potential antimicrobial activity. According to the reported values of antimicrobial peptides in literature (A. S. Oliveira, Ferreira, et al., 2022a), all samples were prepared at 0.5% (w/v) in Mueller Hinton (MH) growth medium (Biokar Diagnostic, Beauvais, France) and sterilized using 0.22 µm filters (Millipore, Billerica, MA, USA). Both bacterial strains were used as monocultures and grown in Tryptic Soy Agar (TSA; Biokar Diagnostic, Beauvais, France) before the assay, with 3 g/L of yeast extract (Sigma-Aldrich, Munich, Germany) at 37 °C for 24 h under aerobic conditions. One colony was then picked, transferred to a tube with 10 mL of MH and grown at the same abovementioned conditions. On the day of experiment, bacteria inoculums were adjusted to an optical density (OD) at 625 nm of 0.08-1 (corresponding to a cell density of 1×10^8 cells/mL), followed by a 10-times dilution in MH to obtain the working inoculums. For the bacterial growth inhibition assay, 980 µL of each sample were inoculated with 20 µL of the working bacterial inoculums. After mixing, 200 µL of the suspensions were pipetted to a 96-well microtiter plate (Nunc, Darmstadt, Germany), and the OD at 625 nm was assessed during 24 h at 37 °C, with 1 h intervals, using a microplate reader (Epoch, Vermont, USA). Inoculated MH medium was used as a negative control and inoculated MH medium with 0.5% (w/v) ampicillin, a concentration known to inhibit *E. coli* and *S. aureus* growth (Proma et al., 2020) was used as positive control. Blanks of the samples were performed to correct sample colour OD interference.

ACE inhibition assay

The method of Amorim et al. (2019) was exploited for ACE inhibition assay using o-Abs-Gly-p-nitro-Phe-OH trifluoroacetate salt (Bachem, Bubendorf, Switzerland) as substrate and 42 mU/mL of ACE (peptidyl-dipeptidase A from rabbit lung) (Sigma- Aldrich, St Louis, USA). The calculation of ACE inhibition (%) was performed according to:

$$ACE\ inhibition = \frac{F_{control} - F_{sample}}{F_{control}} \times 100$$

where $F_{control}$ and F_{sample} are the fluorescence of control (maximum ACE activity) and sample, respectively. The calculation of IC₅₀ values (concentration needed to inhibit 50% of ACE activity) for all samples was performed by non-linear fitting of the data, using a four-parameter logistic regression model. The assay was performed in triplicate.

Antioxidant

Scavenging activity using ABTS

The ABTS^{•+} scavenging activity was assessed by the method described by Gonçalves et al. (2019) with some modifications for a 96-well plate scale. The ABTS^{•+} was generated by reaction of ABTS and potassium persulphate after incubation at room temperature in the dark for 16 h. Then, ABTS^{•+} stock solution was filtered with a 0.45 µm syringe filter and daily diluted to prepare a working solution with an absorbance of 0.70 ± 0.02 at 734 nm. A standard curve of Trolox (50 – 560 µM) was also prepared daily. A polystyrene 96-well microplate (Thermo Fisher Scientific, MA, USA) was used for the reaction where 15 µL of sample, Trolox or solvent was added to 200 µL ABTS^{•+} working solution. The incubation was carried out at room temperature in a microplate reader during 5 min and the absorbance at 734 nm was read upon completion. The ABTS^{•+} scavenging activity percentage was calculated by:

$$ABTS^{•+}\ scavenging\ activity = \frac{A_{control} - A_{sample}}{A_{control}} \times 100$$

where A_{control} and A_{sample} are the absorbances of control and sample, respectively. The assay was performed in triplicate. The Trolox standard curve was used to express TE antioxidant activity of extracts ($\mu\text{mol/g}$ sample). The assay was performed in triplicate.

Oxygen radical absorbance capacity

The procedure of Coscueta et al. (2019) was used for oxygen radical absorbance capacity (ORAC) assay. Trolox standard curve (10 to 80 μM) allows the calculation of TE antioxidant activity of samples ($\mu\text{mol/g}$ sample), after assessing the area under curve (AUC) for each sample. The assay was performed in triplicate.

HMG-CoA reductase inhibition assay

HMG-CoA Reductase Activity Assay Kit (colorimetric) (Abcam, Cambridge, United Kingdom) was used for assessing the HMG-CoA reductase inhibition according to the manufacturer's guidelines. The method measured the decrease of absorbance at 340 nm in a microplate reader, during 15 min, which resulted from the consumption of nicotinamide adenine dinucleotide phosphate (NADPH) by the enzyme. Two time points within the linear range, and with a minimum of 2 min apart, of absorbance were used for calculations of the HMG-CoA reductase activity (U/mg protein) and the HMG-CoA reductase inhibition (%), as recommended by the manufacturer. Atorvastatin was used as a reference drug inhibitor and Pravastatin as a commercial inhibitor (control). The assay was performed in triplicate in two independent plates.

2.2.2.5. Statistical analysis

The statistical analysis was performed using the Real Statistics Resource Pack software (Release 7.2) the results expressed as average \pm standard deviation from assay replicates. Outliers were excluded using the interquartile range with multiplier of 2.2 and data normality was checked using the Shapiro-Wilk test. Protein and bioactivities results were subjected to one-way ANOVA followed by Tukey's post hoc test.

2.2.3. Results and Discussion

2.2.3.1. Protein content (% w/w)

Purification of peptide-rich extract by SEC allowed the separation of four peptide fractions as observed in the chromatogram (**Figure 13**) that were collected and assessed for their protein content. Differently, only two purified fractions, “ESY1 > 1 kDa” and “ESY1 < 1 kDa”, were obtained from ultrafiltration purification and quantified for their protein content by Dumas. Protein content in a variety of samples can be rapidly determine by the Dumas, an analytical method for the quantification of nitrogen, that is in accordance with international standards such as AOAC (Association of Official Analysis Chemists, 2005; Dumas, 1831). However, due to quantity restrictions, protein content in SEC fractions was determined by the combination of BCA and dry weight determinations instead.

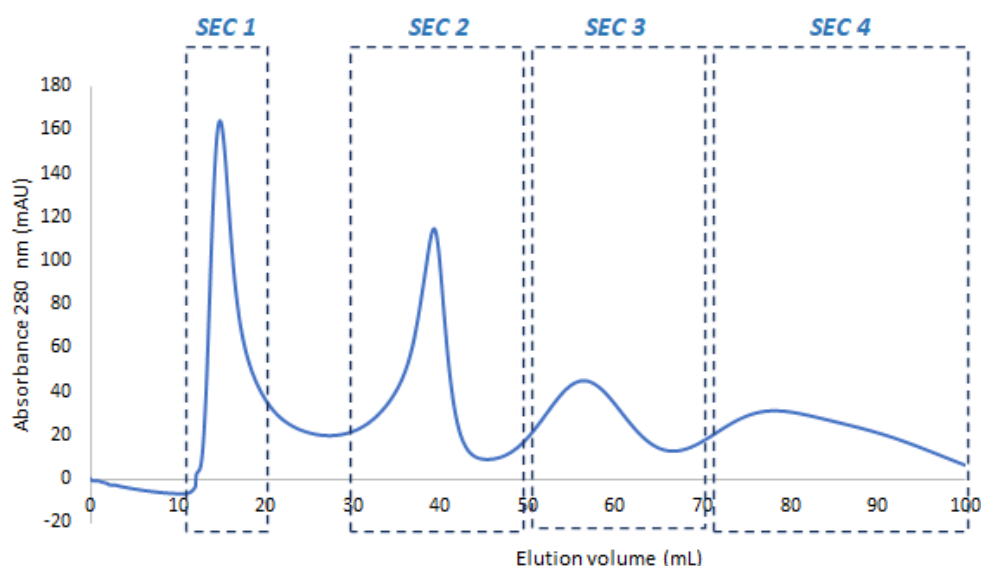


Figure 13. Elution profile of the SEC purification of peptide-rich extract “ESY1”. Four different peptide fractions, corresponding to the four peaks observed, were collected (SEC 1 to 4).

Protein content of the different fractions obtained by ultrafiltration and SEC, as well as protein content of ESY1 (*Section 2.1. Peptide-rich extracts production*) can be seen in **Table 14**. Results show that protein content significant increased ($p < 0.05$) in ESY1 < 1 kDa ($61.7 \pm 0.6\%$) when compared to ESY1 > 1 kDa ($22.5 \pm 0.1\%$). The protein content here reported for ESY1 < 1 kDa is in according to nutritional protein fractions obtained by Amorim et al. (2016), using a 10 kDa and 3 kDa ultrafiltration on spent yeast hydrolysates. Indeed, a high protein amount was obtained in the present study than Amorim, Pinheiro, et al. (2019), after yeast autolysis, hydrolysis and 3 kDa ultrafiltration, since their extracts with ACE inhibitory

activity did not exceed 40%. Furthermore, Jung et al. (2011) demonstrated strong antioxidant activity of a high CHP content yeast hydrolysate (64.9% of protein) while using a 10 kDa ultrafiltration process. Protein content also significantly improves ($p < 0.05$) in SEC 4 ($89.0 \pm 0.8\%$) when compared to SEC 1 ($20.2 \pm 3.4\%$), SEC 2 ($13.1 \pm 4.3\%$) and SEC 3 ($43.6 \pm 3.1\%$). These results are somewhat expected, since during both filtration processes, molecules are separated based on their sizes. Thus, in the ultrafiltration process, smaller molecules like minor proteins, peptides and amino acids, will pass through the 1 kDa cut-off membrane towards fraction, producing the cleaner ESY1 < 1 kDa fraction, while other larger molecules than proteins that are present in the extract will be retained in fraction ESY1 > 1 kDa, thus decreasing protein content in this fraction. Similarly, during gel filtration by SEC, these molecules with higher MW will be eluted first, while molecules with smaller MW will be trapped within the porous matrix, being eluted later, in fractions where the amount. Furthermore, the protein content determined for the SEC 2 fraction, reveals that the higher number of other molecules are in that fraction.

Table 14. Protein content (% w/w) of original ESY1 extract and fractions obtained from ultrafiltration (ESY1 >1 kDa and ESY1 < 1 kDa) and SEC (1 to 4).

		Protein (%)
Original ESY1^a		54.5 ± 1.0
Ultrafiltration^a	ESY1 > 1 kDa	22.5 ± 0.1
	ESY1 < 1 kDa	61.7 ± 0.6
SEC fractions^b	SEC 1	20.2 ± 3.4
	SEC 2	13.1 ± 4.3
	SEC 3	43.6 ± 3.1
	SEC 4	89.0 ± 0.8

Results are expressed as average ± standard deviation ($n=3$). ^a Dumas (1831), ^b BCA. p -values can be consulted in **Table S5**.

When comparing both purification approaches, it is possible to conclude that SEC produced the fraction with the highest ($p < 0.05$) protein amount (SEC 4; $89.0 \pm 0.8\%$), supporting reports of being one of the widely techniques for isolation of antimicrobial, antihypertensive and antidementia peptides from *S. cerevisiae* (A. S. Oliveira, Ferreira, et al., 2022a). However, costs associated to chromatography equipment are substantially higher than those associated with the ultrafiltration methodology, indicating that SEC needs to produce a value-added ingredient in order to justify their use. Indeed, this is the reason

why chromatographic techniques are more frequently applied in purification of pharmaceutical proteins and peptides (Pratap et al., 2017). Nevertheless, some authors have already reported their use to produce yeast peptides with important biological properties, such as antihypertensive (Kanauchi et al., 2005; J. Kim et al., 2004; Kohama et al., 1990; Mirzaei et al., 2015; Ni, Li, Guo, et al., 2012; Ni, Li, Liu, et al., 2012), antimicrobial (Branco et al., 2014, 2017; Caldeira et al., 2019; Gddoa Al-sahlany et al., 2020) and antioxidant (Mirzaei et al., 2015). In contrast, the use of ultrafiltration with filter membranes offers several advantages for concentrating proteins and peptides. One significant advantage is its low energy consumption. Additionally, it provides a gentle treatment of molecules, preserving their integrity and functionality. These reasons contribute to the widespread adoption of ultrafiltration in food processing industry (Mohammad et al., 2012; Vollet Marson et al., 2020; Zeko-Pivač et al., 2023) or to the production of peptides with important bioactivities for nutraceutical supplementation, including antihypertensive (M. Amorim, Marques, et al., 2019; Hu et al., 2014; J. Kim et al., 2004; Mirzaei et al., 2015; Ni, Li, Guo, et al., 2012; A. S. Oliveira et al., 2022), antimicrobial (Albergaria et al., 2010; Branco et al., 2014; Caldeira et al., 2019; Comitini et al., 2005; Gddoa Al-sahlany et al., 2020), antioxidant (M. Amorim, Marques, et al., 2019; H. Guo et al., 2020; Hu et al., 2014; Jung et al., 2011; Mirzaei et al., 2015; A. S. Oliveira et al., 2022) and, more recently, anticholesterolemic (A. S. Oliveira et al., 2022). Furthermore, in this work, the ultrafiltration fractions obtained can be classified as “rich in protein” according to the European Commission (European Commission, 2012). This designation highlights their potential as ingredients for nutraceutical market, as already reported before (*Section 2.1. Peptide-rich extracts production*). All things considered, both techniques seem to be interesting processes to be included in protein-rich extracts production, but their choice requires a cost-effectiveness evaluation directly related to the economic sector to be applied.

2.2.3.2. Molecular weight distribution

ESY1 showed the highest representative MW population of peptides under 1 kDa (74.5%), followed by 1-3 kDa (23.9%), and small percentages of 3-5 kDa (1.72%) and 5-10 kDa (0.15%) (*Section 2.1. Peptide-rich extracts production*). For this reason, a 1 kDa cut-off membrane filtration was chosen for peptides separation. However, these results are very different from other works reporting MW of 5 to 35 kDa in spent yeast autolysates. Indeed,

peptides under 3 kDa were only obtained after including enzymatic hydrolysis in process (M. Amorim, Pinheiro, et al., 2019; Marson et al., 2022; Xie et al., 2017).

Protein and peptides MW distribution of the ultrafiltration and SEC fractions was assessed by HPLC-SEC. Unfortunately, the MW of ESY1, and respective ultrafiltration fractions, could not be determined by HPLC-SEC, since a good chromatographic resolution was not obtained with our column, probably related with their complex matrix. For that reason, it was assumed that ESY1 ultrafiltration fractions own MW associated with cut-off membrane separation, that is, peptides above 1 kDa in ESY1 > 1 kDa and peptides under 1 kDa in ESY1 < 1 kDa. Results regarding the protein and peptides MW distribution in SEC fractions (**Table 15**) show that the most representative population in SEC 1 had a MW around 3 kDa (75.4%), while the most representative in fraction SEC 2 had approximately 1 kDa (45.9%). Peptides below 300 Da characterized fraction SEC 3 (91.0%) and amino acids composed the majority of fraction 4 (92.6% under 200 Da) (**Table 15**). Comparing the MW distribution of all samples, SEC 2 and SEC 3 seemed to be similar with the original ESY1, being mostly constituted by ≤ 1 kDa peptides, and promising bioactive fractions.

Table 15. Protein and peptides MW distribution in SEC fractions represented as percentage of chromatogram total area (% total area).

SEC fractions	MW (kDa)	% total area
SEC 1	121	10.6
	3.16	75.4
	0.41	8.32
	0.21	5.67
SEC 2	108	9.38
	53.4	4.49
	1.37	45.9
	0.37	21.2
SEC 3	0.20	19.0
	0.96	3.31
	0.59	5.64
	0.36	51.3
SEC 4	0.20	39.7
	0.56	2.00
	0.39	5.41
	<0.2	92.6

After analysis of protein content and MW determinations, it possible to hypothesise that fractions ESY1 < 1 kDa and SEC 4 are the ones with the most promising for bioactive properties, as it has been reported that peptides containing 3 to 20 amino acids are highly specific in their biological functions and in choosing biological and metabolic targets (A. S. Oliveira, Ferreira, et al., 2022a).

2.2.3.3. Proteomics analysis

After proteomics analysis, several peptide sequences were identified in ESY1 and respective fractions obtained by ultrafiltration and SEC, from approximately 600 to 5000 Da (Table S6). As expected, the original extract “ESY1” had the highest number of peptide sequences identified, along with fraction ESY1 > 1 kDa (6343). These were followed by SEC 1 (1803) and SEC 4 (599), while both less than 300 peptides were identified in SEC 2 and SEC 3 (Table 16). The main intend of this analysis was to identify potential bioactivities related to the peptide sequences found in the samples by matching those sequences with bioactive peptides reported in different peptide bioactivity databases (PBD, Section 2.2.2.3. Proteomics for details). After conducting a thorough search in the data found in each of the PBD, sequences of our peptides present in all our fractions were found within the sequences of peptides listed in the PBD, with antibacterial, antimicrobial and antifungal activities reported (Table 16). However, it is important to note that only partial matches were identified during our analysis. Specifically, our peptide sequence was found as a component within a larger peptide sequence in the PBD, and an exact match was not found.

Table 16. Peptide sequences identified in original ESY1 extract, and fractions obtained from ultrafiltration (ESY1 > 1 kDa and ESY1 < 1 kDa) and SEC (1 to 4), together with their bioactivities reported in PBD.

		Total sequences number	Number of matched sequences in PBD*	MW range (Da) of matched sequences in PBD*	PBD* reported bioactivities
Original	ESY1	6343	42	648-1857	
	ESY1 > 1 kDa	6343	31	816-1720	
Ultrafiltration	ESY1 < 1 kDa	212	3	890-2153	Antibacterial,
	SEC 1	1803	17	816-1780	antimicrobial and
SEC	SEC 2	246	2	947-1448	antifungal
	SEC 3	291	4	831-1448	
	SEC 4	599	10	831-1530	

*PBD: BAASP, DRAMP, CAMP, APD and BIOPEP-UWM™.

Several authors already described antimicrobial activities of yeast peptides (Branco et al., 2014, 2017; Caldeira et al., 2019; Gddoa Al-sahlany et al., 2020), and therefore these results are not surprising. However, considering the partial matches observed, it is plausible to argue that there is untapped potential to enhance the antimicrobial activity of these extracts. One potential approach is to reduce autolysis time, thereby minimizing peptide breakdown and achieving a closer match to those peptides described in the PBD. Nonetheless, the antimicrobial potential is still present and, for that reason, the effect upon the growth curves for two important food-related pathogen agents, exposed to our samples, was addressed and detailed in the next section.

2.2.3.4. Bioactivities

Antimicrobial

To evaluate the potential antimicrobial activity of the different peptide fractions collected after ultrafiltration and SEC, a growth inhibition assay was carried out, and results of the fractions impact on *E. coli* and *S. aureus* growth can be seen in **Figure 14**. Contrary to what was expected from the PBD results, none of the peptide fractions promoted bacterial growth inhibition. As a matter of fact, all fractions (except SEC 1 against *S. aureus*) seem to be promote bacterial growth.

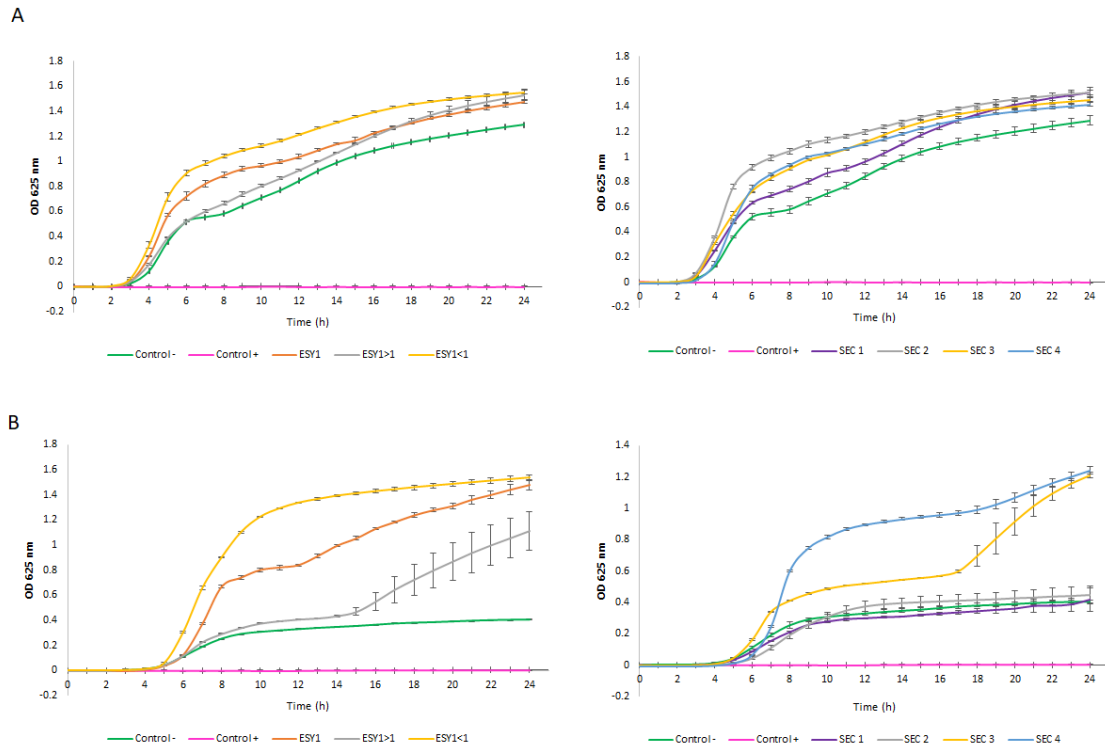


Figure 14. Growth curves for *E. coli* (A) and *S. aureus* (B) exposed to original *ESY1* extract and fractions obtained from ultrafiltration (*ESY1* > 1 kDa and *ESY1* < 1 kDa; on the left) and SEC (1 to 4; on the right).

Antimicrobial peptides are usually amphipathic and cationic short peptides, whose activity strongly depends on their amino acid sequence, size and charge (Jenssen et al., 2006; Powers & Hancock, 2003). Although their mechanism is not clear yet, the best described mode of action for antimicrobial peptides regards the electrostatic interaction between the cationic peptides and the negatively charged components present on the pathogen membrane bilayers, allowing them to accumulate on the membranes and form pores by ‘barrel-stave’, ‘carpet’ or ‘toroidal pore’ mechanisms. (Mookherjee et al., 2020; A. S. Oliveira, Ferreira, et al., 2022a). For these reasons, the lack of antimicrobial activity, when compared with the peptide sequences in the PBD, might be due to the fact that the peptides identified in the different fractions have an inferior number of amino acids with a positive net charge, such as Lys, arginine (Arg) or tryptophan (Trp), know to play an important role in the antimicrobial activity of these peptides (Chan et al., 2006; Powers & Hancock, 2003). On the other hand, it is possible that the promotion of bacterial growth in these fractions is attributed to residual sugars. As previously reported, peptide-rich fractions derived from spent yeast contain certain amounts of sugar, potentially including glucose, which could contribute to bacterial proliferation (A. S. Oliveira et al., 2022). Nevertheless, it would be interesting to investigate the potential antimicrobial properties of these peptide fractions against other pathogenic agents in the future. Since different microorganisms have distinct

membrane components, their interactions with the peptides in each fraction could vary, leading to diverse outcomes. Exploring such variations could provide valuable insights into the broader antimicrobial potential of these peptide fractions.

Anticholesterolemic, antihypertensive and antioxidant activities

Even though the peptide fractions did not display any antimicrobial activity, other important bioactivities for nutraceutical market, such as antihypertensive, antioxidant and anticholesterolemic activities, were assessed.

HMG-CoA reductase is a catalyst in the conversion of HMG-CoA to mevalonate, an important intermediate in the cholesterol biosynthesis (DeBose-Boyd, 2008). HMG-CoA reductase inhibitors such as statins have been, thus, widely used in the treatment of hypercholesterolemia. In this work, the original extract and the different peptide fraction collected after both purification steps were assessed for their anticholesterolemic properties. As expected, after the addition of the ultrafiltration and SEC for purification of the extract autolysate, a significant higher HMG-CoA reductase inhibition ($p < 0.05$) was observed for all the fractions obtained, when compared with the original ESY1, thus increasing from 40.3 to 70.8-77.7%, depending on the fractions (**Table 17, Table S7**). Regarding literature, the current results are according to Aparecida et al. (2015) since it was demonstrated 45% of HMG-CoA inhibition in *Amaranthus cruentus* protein hydrolysate < 3 kDa which comprised the amino acid sequences GGV, IVG/LVG and VGVI/VGVL. Also Ashraf et al. (2020) showed 60 to 80% of this enzyme inhibition in peptides <3 kDa from faba and adzuki bean (Ashraf et al., 2020). However, these results do not seem to be related with protein content or predominant MW of fractions since no tendency was observed in this sense.

Table 17. IC50 values (mg/mL) obtained in ACE-inhibition assay, ABTS⁺ and ORAC activities (μmol TE/g sample), and HMG-CoA reductase inhibition (%) of original ESY1 extract and fractions obtained from ultrafiltration (ESY1 > 1 kDa and ESY1 < 1 kDa) and SEC (1 to 4).

		HMG-CoA reductase inhibition* (%)	ACE – IC50 (mg/mL)	ABTS ⁺ (μmol TE/g sample)	ORAC (μmol TE/g sample)
Original	ESY1	40.3 ± 2.0	1.69 ± 0.16	157 ± 60	626 ± 22
Ultrafiltration	ESY1 < 1	74.0 ± 4.6	1.80 ± 0.12	255 ± 56	708 ± 109
	ESY1 > 1	70.8 ± 2.4	2.59 ± 0.10	181 ± 44	237 ± 85
SEC	SEC 1	77.5 ± 0.3	3.21 ± 0.33	90.5 ± 16.9	2036 ± 277
	SEC 2	75.9 ± 0.3	2.28 ± 0.15	77.4 ± 5.1	2608 ± 330
	SEC 3	77.7 ± 1.8	2.47 ± 0.09	173 ± 51	43610 ± 3532
	SEC 4	71.3 ± 1.2	1.43 ± 0.08	300 ± 17	41091 ± 1021

Results are expressed as average ± standard deviation (n=3). *For Caco-2 biocompatible concentrations (A. S. Oliveira et al., 2022).

ACE is a zinc metallopeptidase that catalyses the conversion of angiotensin I to angiotensin II, a strong vasoconstrictor with direct effect on the raising of blood pressure (Zhao, 2008). For this reason, molecules with ACE inhibition activity can help in the management of hypertension. The peptide-rich extract and the different fractions were evaluated for their antihypertensive activity using an ACE inhibition assay and by calculating their IC50 (Table 17, Table S7).

Original ESY1 and fractions SEC 4 and ESY1 < 1 kDa, showed the highest activity, corresponding to the lowest IC50 values, followed by SEC 2, SEC 3 and ESY1 > 1 kDa, and, finally, SEC 1 ($p < 0.05$). While the higher ACE inhibitions of fractions ESY1 < 1 kDa and SEC 4 are in accordance with their low MW distribution and protein content/purity, the high ACE inhibition value obtained for original ESY1 indicates the contribution not only of all proteins and peptides, but also of some other components of the extract. SEC 1 was characterized with the highest MW distribution (~3 kDa) which can justify its lowest bioactivity. Indeed, small peptides (~ 2 to 20 amino acids) have been hypothesised have ACE inhibition activity by binding to the hydrophobic C-terminal tripeptide of the enzyme substrate, preventing ACE-substrate binding, and, consequently, the conversion of angiotensin I to the angiotensin II (J. Kim et al., 2004). Also Amorim, Pinheiro, et al. (2019) showed high antihypertensive activity in yeast hydrolysate permeates when compared with the respective retentate fractions which are according with the present result results of ESY1 > 1 kDa (2.59 mg/mL) and ESY1 < 1 kDa (1.80 mg/mL) (Table 17, Table S7).

Oxidative stress, caused by high intracellular levels of ROS has been frequently associated with aging and aging-related diseases and antioxidant molecules can delay the

oxidation by scavenging ROS through different reactions, thus reducing ROS to less reactive forms (Shields et al., 2021). Aromatic amino acids present in the peptide sequences have been presumed to be capable to quench the free radicals through a direct electron transfer mechanism, while the pyrrolidine ring of proline residues may interact with secondary structure of peptides, thus increasing their flexibility and ability to quench singlet oxygen (M. Amorim, Marques, et al., 2019). The potential antioxidant activity of the original extract and the peptide fractions was determined using two scavenging-based assays: ABTS^{•+} and ORAC. While the ABTS^{•+} assay measures the relative ability of antioxidants to reduction of cation radical ABTS^{•+} into ABTS[•] as compared with a Trolox, a water-soluble analogous of vitamin E and a known antioxidant, the ORAC assay is based on generation of the radical peroxy (ROO[•]), a radical with biological importance (Prior et al., 2003).

In the ABTS^{•+} assay, fractions SEC 4 and ESY1 < 1 kDa showed the highest activity, followed by ESY1, ESY1 > 1 kDa and SEC 3. SEC 1 and SEC 2 demonstrated to have the lowest activity ($p < 0.05$) (**Table 17, Table S7**).

As discussed above for ACE-inhibition, antioxidant activity of spent yeast peptide fractions has been related with their MW since Guo et al. (2020) showed stronger activity effect for hydrolysates under 1 kDa than under 3 kDa. In fact, a similar tendency can be observed in our study, since SEC 4 is predominant characterized by < 0.2 Da population and ESY1 < 1 kDa with peptides under 1 kDa, but the same MW-activity assumption cannot be made for other samples tested. Comparing the present results with literature, Podpora et al. (2016) obtained higher ABTS^{•+} scavenging activity (4615 to 5069 $\mu\text{M TE/g extract}$) for protein hydrolysates, containing large amounts of free amino acids and peptides from 703 to 1740 Da, than the current investigation. However, the authors related these results with the presence of phenolic compounds, which were not evaluated in the present study.

On the other hand, the SEC fractions demonstrated the highest ORAC values, especially SEC 3 and SEC 4, followed by original ESY1 and ultrafiltration fractions ($p < 0.05$) (**Table 17, Table S7**).

The results of SEC 4 are according to Marson et al. (2020) since they obtained a range of 85 000 to 500 000 $\mu\text{mol TE/g extract}$ in spent yeast hydrolysates after 3 and 10 kDa ultrafiltration. A possible MW relationship can be linked to these results since SEC 4 and 3, with lowest MW that SEC1 and 2, presented the highest activity.

When comparing the results obtained by the two antioxidant assays, it is possible to see some differences between them. When working with peptide-rich extract, or even peptide fractions, data interpretation can be tricky due to their complex nature and composition.

Moreover, different assays have been used to evaluate antioxidant properties and the results obtained in those assays are frequently different among them, as all methodologies their advantages and limitations (Schaich et al., 2015). Nevertheless, it is clear that both ultrafiltration and SEC originate some fraction with higher biological activities than the original peptide-rich extract.

2.2.4. Conclusion

The present work reports the production of peptide fractions derived from a spent yeast extract autolysate. The fractions were obtained using 1 kDa ultrafiltration or gel filtration, using SEC. These processes allowed to generation of fractions with distinct characteristics, mainly in terms of protein content, MW distribution and peptide sequences. While the original extract autolysate and respective ultrafiltration and SEC fractions did not show any antimicrobial effect, interesting results regarding their antihypertensive, anticholesterolemic and antioxidant properties were observed. These results suggest that these fractions hold promise as potential candidates for dietary supplementation in the form of a single product. All purified peptide fractions showed higher HMG-CoA reductase inhibition values than the original extract. These results demonstrate these processes as promising candidates for the development of new anticholesterolemic ingredients using yeast autolysates. The peptide fractions with the highest protein content/purity (ESY1 < 1 kDa and SEC 4) revealed potential for the formulation of antihypertensive ingredients, as these were the ones with the higher ACE inhibition values. Regarding the antioxidant activity, significantly superior ORAC values were observed in fractions SEC 4 and SEC 3.

In addition, results presented in this study suggests that the addition of a purification step in the production of bioactive peptides from spent yeast autolysates can be advantageous for generating ingredients with specific targeted bioactivities for the nutraceutical market. These purification processes enable the isolation and concentration of bioactive peptides, enhancing their potential application in the development of functional food and dietary supplements. These findings emphasize the importance of implementing purification strategies in order to optimize the production of bioactive peptide ingredients for the nutraceutical industry.

2.2.5. Supplementary material

Table S5. *P-values of comparison of protein content (% w/w) between ESY1 and fractions obtained from ultrafiltration and SEC.*

	<i>p-value</i>
SEC 1 vs. SEC 2	1.91E-01
SEC 1 vs. SEC 3	9.13E-05
SEC 1 vs. SEC 4	3.23E-08
SEC 1 vs. ESY1	5.05E-05
SEC 1 vs. ESY1 > 1 kDa	9.59E-01
SEC 1 vs. ESY1 < 1 kDa	2.38E-06
SEC 2 vs. SEC 3	1.27E-05
SEC 2 vs. SEC 4	1.36E-08
SEC 2 vs. ESY1	9.15E-06
SEC 2 vs. ESY1 > 1 kDa	5.83E-02
SEC 2 vs. ESY1 < 1 kDa	7.35E-07
SEC 3 vs. SEC 4	6.14E-07
SEC 3 vs. ESY1	5.30E-01
SEC 3 vs. ESY1 > 1 kDa	1.95E-04
SEC 3 vs. ESY1 < 1 kDa	6.05E-04
SEC 4 vs. ESY1	2.62E-06
SEC 4 vs. ESY1 > 1 kDa	4.54E-08
SEC 4 vs. ESY1 < 1 kDa	5.81E-05
ESY1 vs. ESY1 > 1 kDa	9.61E-05
ESY1 vs. ESY1 < 1 kDa	6.98E-03
ESY1>1 vs. ESY1 < 1 kDa	3.69E-06

n=3

Table S6. *Peptides identification on original ESY1 and respective ultrafiltration (ESY1 > 1 kDa and ESY1 < 1 kDa) and SEC (1 to 4) fractions.*

File can be downloaded from: <https://figshare.com/s/834803a54e2728ab12d6>

Table S7. *P-values of comparison of HMG-CoA reductase and ACE inhibition assays, together with antioxidant activities (ABTS and ORAC), between ESY1 and fractions obtained from ultrafiltration and SEC.*

	HMG-CoA	ACE	ABTS⁺	ORAC
ESY1 vs. ESY1 > 1 kDa	1.24E-06	9.74E-01	8.14E-01	9.99E-01
ESY1 vs. ESY1 < 1 kDa	5.26E-07	1.79E-04	7.87E-06	1.00E+00
ESY1 vs. SEC 1	1.07E-07	3.94E-07	5.05E-03	6.62E-01
ESY1 vs. SEC 2	1.51E-07	8.76E-03	1.28E-03	2.91E-01
ESY1 vs. SEC 3	2.16E-07	7.55E-04	9.71E-01	1.15E-14
ESY1 vs. SEC 4	1.07E-06	5.25E-01	2.04E-09	1.15E-14
ESY1 > 1 kDa vs. ESY1 < 1 kDa	6.90E-01	7.31E-04	1.33E-03	9.97E-01
ESY1 > 1 kDa vs. SEC 1	5.19E-02	1.06E-06	3.79E-05	3.03E-01
ESY1 > 1 kDa vs. SEC 2	1.66E-01	4.12E-02	1.13E-05	8.57E-02
ESY1 > 1 kDa vs. SEC 3	6.90E-02	3.35E-03	9.99E-01	1.15E-14
ESY1 > 1 kDa vs. SEC 4	1.00E+00	1.62E-01	4.26E-07	1.15E-14
ESY1 < 1 kDa vs. SEC 1	5.06E-01	6.45E-03	8.64E-13	6.37E-01
ESY1 < 1 kDa vs. SEC 2	9.13E-01	3.27E-01	8.69E-13	2.49E-01
ESY1 < 1 kDa vs. SEC 3	5.32E-01	9.71E-01	2.46E-04	1.15E-14
ESY1 < 1 kDa vs. SEC 4	8.22E-01	1.10E-05	2.11E-01	1.15E-14
SEC 1 vs. SEC 2	9.57E-01	1.37E-04	9.92E-01	9.86E-01
SEC 1 vs. SEC 3	1.00E+00	1.37E-03	2.26E-04	1.15E-14
SEC 1 vs. SEC 4	7.77E-02	5.42E-08	1.74E-14	1.15E-14
SEC 2 vs. SEC 3	9.50E-01	8.01E-01	6.17E-05	1.15E-14
SEC 2 vs. SEC 4	2.43E-01	3.32E-04	1.79E-14	1.15E-14
SEC 3 vs. SEC 4	9.96E-02	3.82E-05	6.88E-08	1.74E-01

n=3

Chapter 3

Peptides from waste streams

3.1. Application for nutraceutical market

3.2. Fe-peptide complexes

3.3. In vitro Fe bioavailability

3.1. Application for nutraceutical market^{*†}

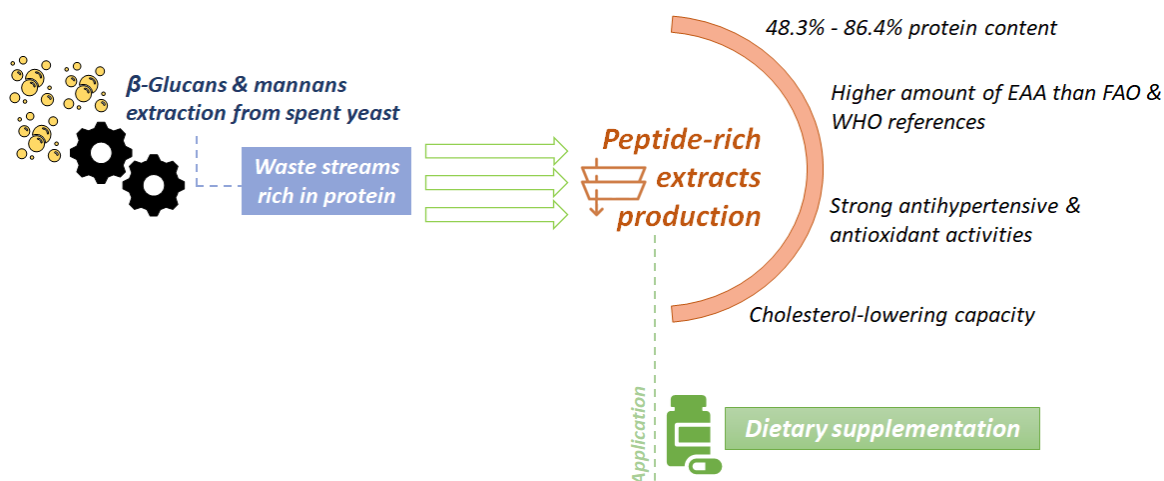


Figure 15. Schematic overview of this Section 3.1, illustrating the process of generating peptide-rich extracts through 1 kDa ultrafiltration using β -glucans and mannans waste streams extraction from spent yeast. Adapted from the graphical abstract of Oliveira et al. (2022).

3.1.1. Introduction

Over the years, several extraction methods of mannans and β -glucan from spent yeast have been described (Freimund et al., 2003; X. Y. Liu et al., 2008; X. Tian et al., 2019), since these molecules present numerous promising bioactivities, such as prebiotic and bacterial pathogen inhibition for mannans (Faustino et al., 2021), and mainly immunopharmacological properties for β -glucan (Avramia & Amariei, 2021). As a matter of fact, engineered spent yeast has been the target of such processes as well (Faustino et al., 2022) since synthetic biology industry has been generating large amounts of unused spent yeast in the last years.

Generally, these extraction processes start with yeast cell lysis, followed by separation of the released target compounds from the remaining unwanted cell components. These unwanted waste streams are usually proteins rich, since they represent one of the main yeast

* Oliveira, A. S., Pereira, J. O., Ferreira, C., Faustino, M., Durão, J., Pintado, M. E., & Carvalho, A. P. (2022). Peptide-rich extracts from spent yeast waste streams as a source of bioactive compounds for the nutraceutical market. *Innovative Food Science & Emerging Technologies*, 81, 103148. <https://doi.org/10.1016/j.ifset.2022.103148>

† Costa, E. M., Oliveira, A. S., Silva, S., Ribeiro, A. B., Pereira, C. F., Ferreira, C., Casanova, F., Pereira, J. O., Freixo, R., Pintado, M. E., Carvalho, A. P. & Ramos, O. L. (2023). Spent Yeast Waste Streams as a Sustainable Source of Bioactive Peptides for Skin Applications. *International Journal of Molecular Sciences*, 24, 2253. <https://doi.org/10.3390/ijms24032253>

components (about 45% to 60% of DW) (Vieira et al., 2019). For this reason, waste streams of mannans and β -glucan extraction processes can be further processed to recover proteins and peptides in a circular economy-based approach.

As studied on *Section 2.2. Separation & purification*, membrane filtration technology has demonstrated to be the most cost-effective process for producing peptide-rich extracts from spent yeast autolysates, while concentrating the protein content and obtaining fractions with different MW. In fact, we observed strong antioxidant and antihypertensive activities, with particular significance of fractions with peptides under 1 kDa. Furthermore, for the first time, the inhibition of HMG-CoA reductase by spent yeast peptides was demonstrated, thereby elevating their potential anti-cholesterolemic properties.

Due to the rising trend in production of ingredients from spent yeast, the consequently generated protein rich waste streams can be valued in a circular economy approach, as well as the presence of several important bioactive properties of spent yeast peptide-rich extracts for nutraceutical market (*Section 2.2. Separation & purification*), the aim of the present study was: (i) to assess the feasibility of obtaining peptide-rich extracts from spent yeast waste streams obtained during β -glucans and mannans extraction processes, using membrane filtration, and (ii) to evaluate the potential of those peptide-rich extracts to be used as dietary supplements, by measuring their antihypertensive, antioxidant and anti-cholesterolemic potential (**Figure 15**).

3.1.2. Material and methods

3.1.2.1. Yeast strain

Spent yeast of *S. cerevisiae* strains, engineered by Amyris, Inc. to produce β -farnesene, was used in this study.

3.1.2.2. Peptide-rich extracts production

Peptide-rich extracts were obtained from waste streams of β -glucan (Gpep) and mannan (Mpep) extraction processes from spent yeast (Faustino et al., 2022, 2023; Freimund et al., 2003; X. Y. Liu et al., 2008; X. Tian et al., 2019). Liquid stream (supernatants) underwent 1 kDa cut-off ultrafiltration as described in *Section 2.2.2.2. Ultrafiltration* in order to get peptide rich fractions with different MW: Gpep > 1 kDa, Gpep < 1 kDa, Mpep > 1 kDa and Mpep < 1 kDa (**Figure 16**).

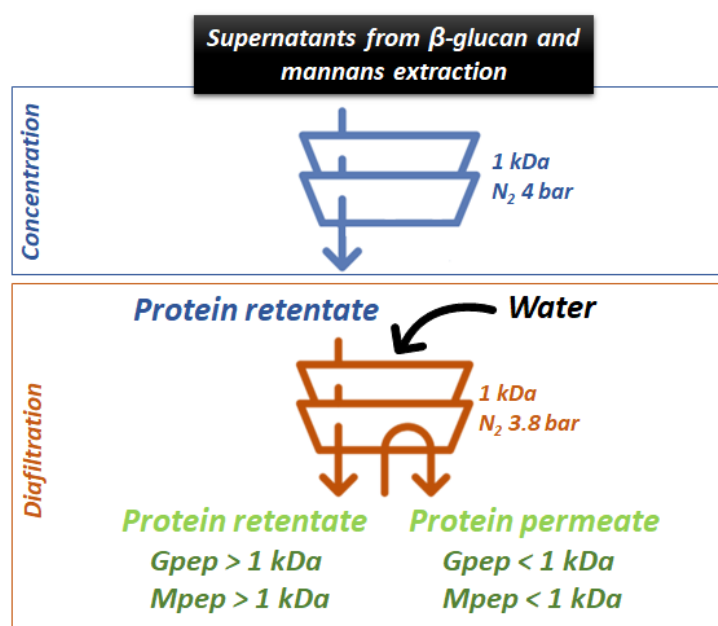


Figure 16. Diagram for ultrafiltration process of waste streams of β -glucan and mannans extraction processes from spent yeast to obtain peptide-rich extracts.

3.1.2.3. Peptide-rich extracts characterization

Protein

Protein content of fractions was determined by Pierce™ BCA protein assay kit as described in *Section 2.2.2.3. BCA*.

Dry weight

DW analysis was performed according to AOAC standard procedures described on *Section 2.1.2.4. Dry weight*.

Amino acids

Total amino acids analysis was performed as described at *Section 2.1.2.4. Amino acids*.

Neutral sugars

Neutral sugars quantification was assessed by their derivatization to their alditol acetates and GC-FID analysis as reported in *Section 2.1.2.4. Neutral sugars*.

Minerals

Minerals determination was performed by ICP-OES, after microwave digestion, as explained on *Section 2.1.2.4. Minerals*.

Molecular weight distribution

A preliminary MW peptide evaluation of original Gpep and Mpep supernatants (non-treated waste streams) was performed by FPLC to select the cut-off of ultrafiltration membrane. A two-column set composed by a Superdex[®] 200 Increase 10/300 GL and a Superdex[®] peptide 10/300 GL columns (Cytiva, USA) coupled to an ÄKTA Pure 25 purification (Cytiva, USA) was exploited and a 0.05 M phosphate buffer pH 7.0, containing 0.15 M sodium chloride and 0.2 g/L of sodium azide, was used as mobile phase at a flow rate of 0.5 mL/min. The elution was monitored at 280 nm and thyroglobulin (669 kDa), aldolase (158 kDa), conalbumin (75 kDa), ovoalbumin (43 kDa), carbonic anhydrase (29 kDa), ribonuclease A (13.7 kDa), whey peptide (1.2 kDa) and Trp (180 Da) were used as standards for calibration curve.

The evaluation of MW peptides distribution in Gpep and Mpep fractions was performed as abovementioned at *Section 2.1.2.4. MW distribution*.

In vitro cytotoxicity assessment

Caco-2 cell culture

Caco-2 cells were provided from American Type Culture Collection (HTB-37, VA, USA) and grown at 37 °C in a humidified atmosphere of 95% air and 5% CO₂ using high glucose (4.5 g/L) Dulbecco's Modified Eagle's Medium (DMEM) supplemented with 10% (v/v) heat-inactivated fetal bovine serum (Thermo Fisher Scientific, MA, USA), 1% (v/v) penicillin–streptomycin–fungizone (Lonza, Verviers, Belgium), and 1% (v/v) of non-EAA 100× (Sigma-Aldrich, St. Louis, USA). Cells were used between passages 26 and 29.

Cytotoxicity assay

Cytotoxicity evaluation was performed according to the International Organization for Standardization (ISO) 10993-5:2009 standard (International Organization for

Standardization, 2009). The cells were seeded at 1×10^4 cells/well in a 96-well microplate and after overnight incubation at 37 °C, they were treated with different concentrations of Gpep and Mpep fractions (from 0.8 to 5 mg/mL) prepared in fresh culture medium. Dimethyl sulfoxide (Sigma-Aldrich, St. Louis, USA) at 10% (v/v) in culture media was used as a cell-death control and plain culture media was used as a growth control. After 24 h-exposure, the PrestoBlue[®] reagent (Invitrogen, Massachusetts, USA) was added to each well and incubated for 2 h. Fluorescence was recorded (excitation 570 nm; emission 610 nm) after incubation using a microplate reader. All assays were performed in quadruplicate.

Biological activities

ACE inhibition assay

The ACE inhibition assay was performed according to the method described on *Section 2.2.2.4. ACE inhibition assay*. The assay was performed in triplicate.

Antioxidant capacity

Scavenging activity using ABTS

The ABTS^{•+} scavenging activity was assessed by the method described in *Section 2.2.2.4. Scavenging activity using ABTS*. The assay was performed in triplicate and the antioxidant activity of extracts results were expressed as $\mu\text{mol TE/g extract}$.

Scavenging activity using DPPH[•]

DPPH[•] scavenging activity was carried out according to Prior, Wu, and Schaich (2005) with some modifications for a 96-well microplate scale. A 600 μM stock solution of DPPH[•] was prepared in methanol (stored in the dark at -20 °C) and diluted prior to use to 60 μM by adjusting the absorbance to 0.600 ± 0.100 at 515 nm (working solution). A standard curve of Trolox (7.5 – 240 μM) was also daily prepared. A polystyrene 96-well microplate was used from mixture reaction where 25 μL of sample, Trolox or solvent was added to 175 μL DPPH[•] working solution. The incubation was carried out at 25 °C in a microplate reader during 30 min and the absorbance at 515 nm was read in the end. The DPPH[•] scavenging activity percentage was calculated using:

$$DPPH^{\bullet} \text{ scavenging activity} = \frac{A_{\text{control}} - A_{\text{sample}}}{A_{\text{control}}} \times 100$$

where A_{control} and A_{sample} are the absorbances of control and sample, respectively. The assay was performed in triplicate. The Trolox standard curve was used to express TE antioxidant activity of extracts ($\mu\text{mol/g}$ extract).

Oxygen radical absorbance capacity

ORAC assay was assessed as described in *Section 2.2.2.4. ORAC*. The assay was performed in triplicate and the antioxidant activity of extracts results were expressed as $\mu\text{mol TE/g}$ extract.

HMG-CoA reductase inhibition assay

HMG-CoA Reductase Activity Assay Kit was performed according to the manufacturer's guidelines, being the protocol described in *Section 2.2.2.4. HMG-CoA reductase inhibition assay*. The assay was performed in triplicate in two independent plates.

3.1.2.4. Statistical analysis

Results were expressed as average \pm standard deviation from assay replicates. Statistical analysis was performed using the Real Statistics Resource Pack software (Release 7.2). Normality of data was tested using the Shapiro-Wilk's test and the comparison between different peptide-rich fractions were performed using the one-way ANOVA followed by Tukey's multiple comparisons test.

3.1.3. Results and discussion

3.1.3.1. Nutritional analysis

The supernatants of β -glucan (Gpep) and mannan (Mpep) processes were collected in order to produce peptide-rich extracts in a circular economy-based approach. To select the ultrafiltration membrane MW cut-off, a preliminary MW evaluation was performed by FPLC. Most peptides obtained are distributed in a range around 1000 Da (**Figure 17**) which

are in close agreement with the MW distribution observed for ESY1 spent yeast autolysate produced earlier in *Section 2.1. Peptide-rich extracts production*.

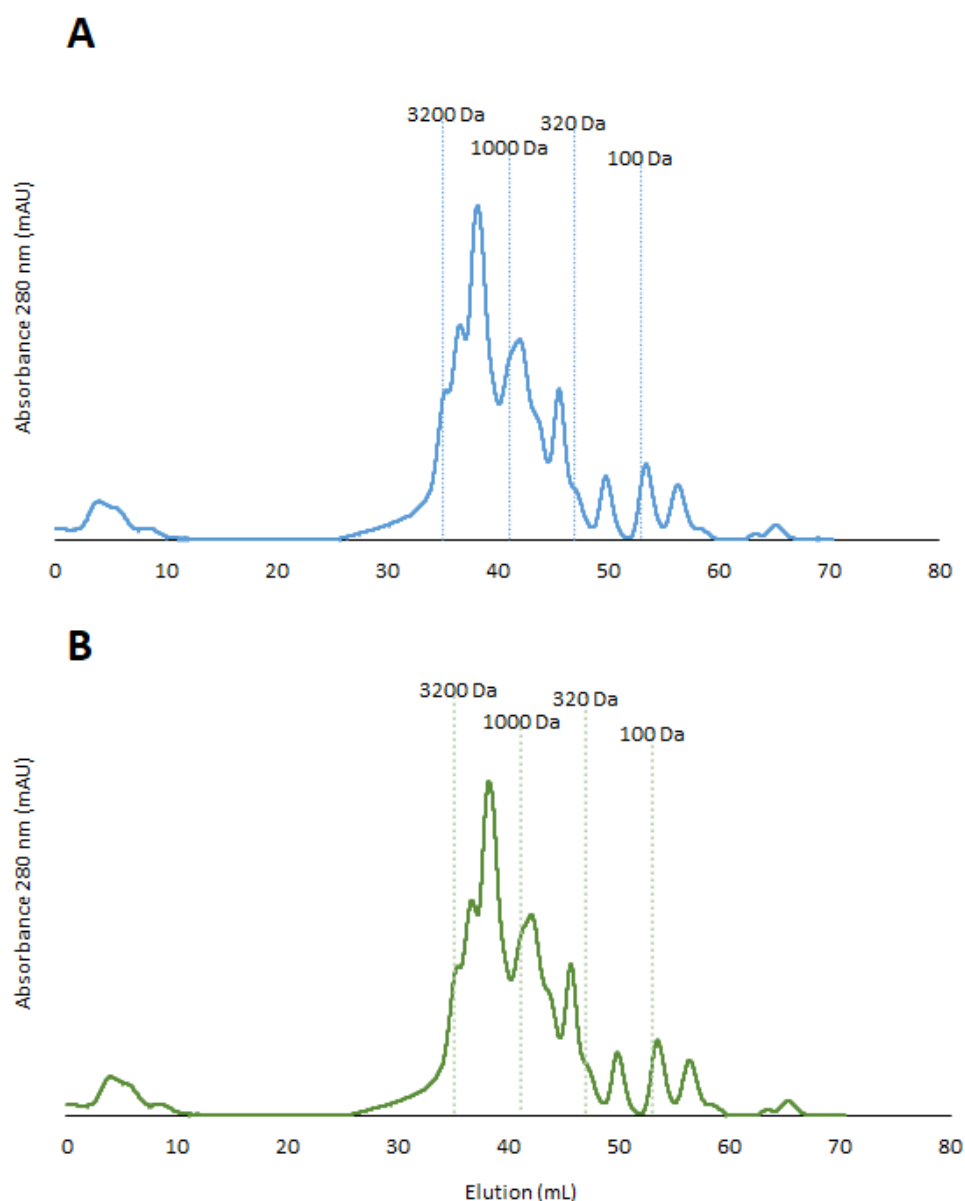


Figure 17. FPLC profiles of the (A) *Gpep* and (B) *Mpep* original supernatants (non-treated waste streams).

As demonstrated in *Section 2.2. Separation & purification*, ultrafiltration seemed to be the most cost-effective method for peptide-rich extracts production for application in dietary supplementation and, for that reason, it was applied to the present supernatants. A diafiltration process was executed in order to purify the final extracts. At the end of membrane filtration, samples were freeze-dried.

A high range of protein content was observed in final peptide-rich extracts (48% to 86%) (**Table 18**) in relation to fractions produced from engineered spent yeast autolysate (ESY1)

(Section 2.2. Separation & purification) (23% to 62%) which means that peptide-rich extracts obtained from spent waste streams processes may also have nutritional potential to be applied to nutraceutical market, favouring the circular economy approach. However, no significant differences were observed between protein amount of different Gpep and Mpep fractions ($p > 0.05$).

Table 18. Protein concentration (% w/w), sugars (% w/w) and minerals (ng/g extract) of peptide-rich extracts.

	Protein (%)	Sugars (%)	Minerals (ng/g)					Total
			P	Mg	Ca	Na	K	
<i>Gpep > 1 kDa</i>	67.2 ± 16.0	28.2 ± 7.9	4.20 ± 0.03	1.52 ± 0.01	2.31 ± 0.02	ND	3.32 ± 0.02	11.4 ± 0.1
<i>Gpep < 1 kDa</i>	67.6 ± 25.6	4.34 ± 1.73	13.8 ± 1.3	8.20 ± 0.50	7.91 ± 0.34	0.673 ± 0.101	37.0 ± 3.2	67.5 ± 5.5
<i>Mpep > 1 kDa</i>	86.4 ± 8.7	7.44 ± 0.22	5.22 ± 0.01	1.04 ± 0.01	0.100 ± 0.010	7.63 ± 0.01	13.0 ± 0.0	27.0 ± 0.0
<i>Mpep < 1 kDa</i>	48.3 ± 15.9	3.32 ± 1.06	9.39 ± 0.01	2.07 ± 0.01	0.189 ± 0.010	41.8 ± 0.01	64.7 ± 0.0	118 ± 0.0

Results are expressed in average ± standard deviation ($n=2$). ND – Not detected (below low detection limit).

Concerning this topic, other important nutritional parameters for nutraceutical application were also assessed and listed in **Table 18**, such as sugars and minerals content. As expected, a small sugar content was determined in all peptide extracts (3-7%) (except *Gpep > 1 kDa*) since we are working on waste streams from polysaccharides extraction. The extract with higher sugar content (*Gpep > 1 kDa* in relation to *Gpep* and *Mpep < 1 kDa*) ($p < 0.05$) (**Table S8**) may contain some oligosaccharides, since β -glucan and mannans extraction processes are distinct, and probably generate different sizes of saccharides.

Comparing with spent yeast from previous studies, Amorim et al. (2016) obtained higher sugar concentrations in 3 kDa hydrolysates (27% to 48%) than the present study. However, these differences may be related with spent yeast source since our raw material is not the original spent yeast (as used by Amorim et al. (2016)), but waste streams from polysaccharides (β -glucan and mannans) extraction processes. Since these molecules are the target polysaccharides within their corresponding extraction processes, their waste streams will be favouring protein content over sugars. Other authors have applied multi-step sequential membrane filtration technology with different cut-off membranes to spent yeast hydrolysates. With a 15-8-1 kDa process, Marson et al. (2022) obtained a 8 kDa retentate with 68.6% of protein purity, as high as observed in our *Gpep* fractions, although the respective sugar amount was lower (5.7%). On the other hand, the 1 kDa retentate and

permeate showed only 25.8% and 18.5% of protein content, respectively, which are lower values from those found in the present study. With a 50-8-1 kDa ultrafiltration, the 1 kDa fractions presented protein content values ranging from 31.7 to 46.2%, which are close to Mpep < 1 kDa results. In fact, a sequential filtration process seems to be a good choice for protein purification in spent yeast hydrolysates since in all ultrafiltration steps undesirable compounds for food industry were retained, such as sugars, but the protein yield of the process can be compromised. In comparison, and given our more cleaner starting matrix, the use of a single filtration step seems more efficient for obtaining high purity protein extracts.

Concerning mineral concentrations (**Table 18**), fractions < 1 kDa presented the highest concentrations (67-118 ng/g) ($p < 0.05$) (**Table S8**) in particular Mpep < 1 kDa with an excess of Na and K, which can be related with the addition of saline solutions in some of the extraction steps (Freimund et al., 2003). A similar result was found by Amorim et al. (2016), since the permeate fractions presented a higher total amount of minerals than the retentates, namely in Na and K. These authors suggest their use for an alternative to common salt or as mineral enhancer in food, given that the higher content in K compared to Na can prevent cardiovascular diseases and high blood pressure.

Regarding the literature references about spent yeast as potential source of EAA within FAO and WHO recommendations (Marson, de Castro, Belleville, et al., 2020), their profile was analysed in the present study and reported in **Table 19**. Worth noting that although Trp is an EAA, the applied analytical method was not suitable for its quantification.

Table 19. EAA content (mg/g protein) of peptide-rich extracts.

	<i>Gpep</i> > 1 kDa	<i>Gpep</i> < 1 kDa	<i>Mpep</i> > 1 kDa	<i>Mpep</i> < 1 kDa	FAO/WHO reference ^a
Asp	76.8 ± 32.6	44.3 ± 20.8	105 ± 35	18.8 ± 1.5	-
Glu	76.2 ± 21.7	77.0 ± 6.7	111 ± 29.4	58.4 ± 2.4	-
Cys	6.87 ± 2.04	3.89 ± 0.31	4.80 ± 1.14	1.67 ± 1.26	-
Ser	52.1 ± 30.5	29.5 ± 17.8	66.0 ± 36.9	9.17 ± 1.16	-
His*	22.8 ± 12.2	19.3 ± 12.7	25.8 ± 11.9	10.6 ± 8.0	15.0
Gly	32.3 ± 3.26	24.3 ± 4.2	41.9 ± 7.7	9.03 ± 1.74	-
Thr*	35.2 ± 9.3	27.4 ± 5.2	49.2 ± 11.1	15.5 ± 8.8	11.0
Arg*	28.1 ± 6.0	18.7 ± 2.6	35.4 ± 8.6	14.2 ± 7.5	NM
Ala	29.4 ± 9.3	29.4 ± 7.5	52.3 ± 18.1	15.7 ± 15.2	-
Tyr	15.0 ± 3.8	15.7 ± 5.8	29.0 ± 6.7	23.0 ± 24.8	21.0 ^b
Phe*	14.5 ± 5.3	20.6 ± 6.7	32.1 ± 12.4	9.37 ± 0.53	
Val*	34.2 ± 10.9	44.1 ± 11.7	64.2 ± 24.2	21.6 ± 1.8	15.0
Ile*	24.5 ± 8.4	30.6 ± 6.1	44.2 ± 15.1	12.6 ± 1.8	15.0
Leu*	29.4 ± 8.3	40.7 ± 6.7	57.8 ± 13.0	17.1 ± 3.0	21.0
Lys*	46.3 ± 9.8	35.3 ± 8.4	59.0 ± 16.4	17.7 ± 5.6	18.0
Sum	524 ± 173	461 ± 123	778 ± 248	254 ± 85	-
Sum EAA	235 ± 70	239 ± 60	368 ± 113	119 ± 37	136

Results are expressed in average ± standard deviation (*n*=2). * EAA, ^a World Health Organization (2007), ^b Phe + Tyr. NM – Not mentioned, Asp – Aspartic acid, Arg – Arginine.

The total content of EAA of *Gpep* > 1 kDa, *Gpep* < 1 kDa and *Mpep* > 1 kDa exceeded that of FAO/WHO recommendations (World Health Organization, 2007), as well as the individual EAA in all fractions (except His, leucine (Leu) and Lys in *Mpep* < 1 kDa) which profiles the obtained peptide-rich extracts in the present study good candidates for dietary supplementation and functional foods.

Regarding the non-EAA (**Table 19**), the high amount of Glu (58.4 to 111 mg/g protein) increases the potential application of these extracts in the food market, since Glu is linked to strong flavour-enhancing properties. In fact, monosodium glutamate, a salt form of Glu is one of the well-known flavour ingredients used by food industry since it provides the typical “umami” flavour. Recently, its use has become a strategy for common salt substituent in foods as well (Maluly et al., 2017). For athletic performance, alanine supplementation has become a common practice among competitive athletes since its mechanism is involved in delaying the fatigue during high-intensity exercise (Hoffman et al., 2018).

The amino acids profile depends on the method and conditions of protein extraction applied to yeast (Jacob, Hutzler, et al., 2019; Podpora et al., 2015, 2016) and several authors

have suggested their application in food market since the higher EAA content than those recommended by FAO/WHO (Caballero-Córdoba & Sgarbieri, 2000; Jacob, Hutzler, et al., 2019; Podpora et al., 2015, 2016; Vieira et al., 2016) and the amount of promising amino acids to be applied in flavour enhancing (M. Amorim et al., 2016; Podpora et al., 2016).

On the other hand, the discover of aspartic acid and Glu, Cys, His and Lys in Gpép and Mpép extracts (**Table 19**) shows a potential use of these extracts for Fe-binding and to produce Fe-peptide chelates as demonstrated by Hoz et al. (2014). These amino acids have functional groups capable of establishing coordinated covalent bonds and their considerable free amounts in fractions < 1 kDa can make them Fe-delivery components to produce food supplements targeted for anti-anaemic market.

3.1.3.2. Molecular weight profile

As explained on *Section 2.2. Separation & purification*, it was not possible to determine the MW distribution of ESY1 ultrafiltration fractions by SEC because of absence of chromatographic resolution with the column used. For this reason, LC-ESI-qTOF/MS method was used for Gpép and Mpép MW analysis.

As expected, the fractions of Gpép and Mpép < 1 kDa had approximately 88% and 85% of peptides under 1000 Da, respectively, with about 50% of these being under 500 Da. On other hand, the Gpép and Mpép fractions > 1 kDa presented 39% and 63% of peptides above 1 kDa (**Figure 18**).

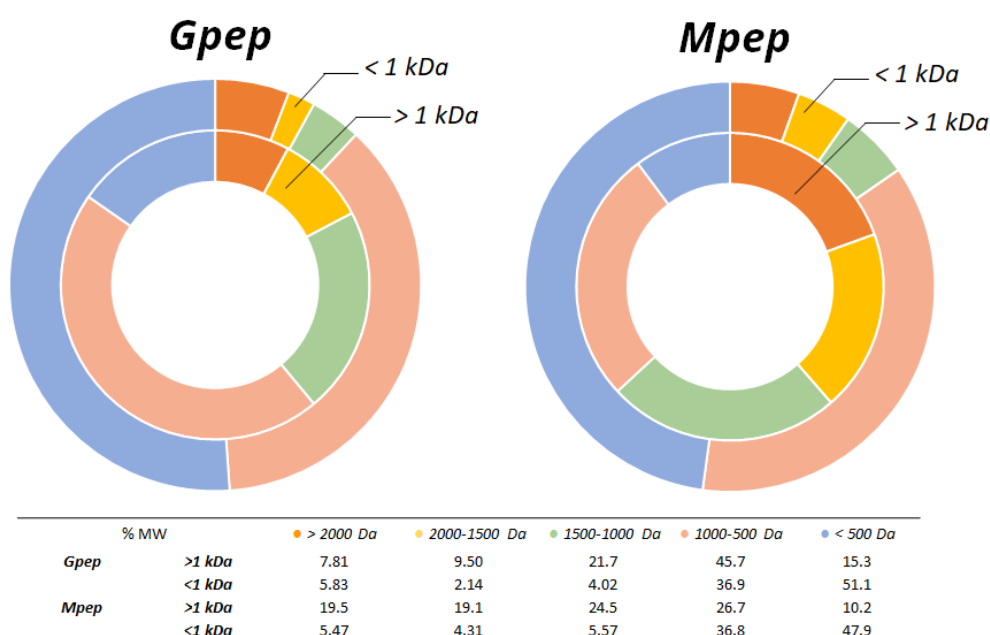


Figure 18. Peptides MW distribution (%) in peptide-rich extracts under and above 1 kDa.

The unexpected large percentage of peptides under 1 kDa observed in Gpep > 1 kDa fraction (61%) may be related with the limited selectivity of ultrafiltration cut-off membranes due to fouling phenomena and critical flux, since they are directly related with transference phenomenon and protein interactions, which have been described as the main challenges of membrane filtration processes (Vollet Marson et al., 2020). Huang et al. (2012) maximized the protein yield from spent yeast using a 5 kDa PES ultrafiltration, applying a Box-Behnken design. The authors found that the optimal conditions operation (2.7% of yeast concentration, pH 5.0 and 14.0 psi of pressure) allowed a 95.0% of protein yield which underlines the importance of investigating these parameters to ensure a high-performance ultrafiltration process. In line with the present results, by performing a 5 kDa ultrafiltration after enzymatic hydrolysis, Hu et al. (2014) obtained a yeast peptide hydrolysate with 80.4% peptides < 1 kDa, followed by 18.3% of 1-3 kDa and some residues between 3-5 kDa. By applying a sequential filtration membrane process using 50-8-1 and 15-8-1 kDa to spent yeast hydrolysates, Marson et al. (2022) observed a gradual change of peptides MW: 50% of peptides < 1 kDa on the first retentates (50 and 15 kDa), followed by 65% on the second (8 kDa) and 80% on the last (1 kDa), finishing with 90% < 1 kDa on the final permeate. The first retentates had a maximum of 19% of peptides with higher MW (> 7 kDa).

3.1.3.3. *In vitro* cytotoxicity assessment

Considering the application of the present peptide-rich extracts in nutraceutical market, Caco-2 cell line was used to evaluate their cytotoxic effect with the objective of finding a non-cytotoxic concentration for performing the following bioactivities assays. In fact, Caco-2 cell line is the most widely used *in vitro* model for studies of permeability, transport and absorption of substances since they are derived from human colorectal adenocarcinoma and present high morphological and physiological similarity to the human enterocyte, thus being representative of the human intestinal barrier, and, to a lesser extent, to the human intestine (Osakwe, 2016).

Caco-2 were treated over a period of 24 h with increased concentrations of the peptide-rich extracts obtained from 0.8 to 5 mg/mL. As described in ISO 10993-5:2009 (International Organization for Standardization, 2009), an ingredient may have a cytotoxic potential if cell viability is reduced more than 30% of the non-treated cells. PrestoBlue[®] was used as a cell viability indicator since when added to living cells it is metabolically reduced,

becoming highly fluorescent. The number of viable cells, or metabolically active, correlates to the fluorescence intensity measured (Invitrogen, 2010).

The Caco-2 metabolism was inhibited more than 30% as of 2.5 mg/mL of Gpep extracts which means that equal and above concentrations cannot be used in following biological assays due to potential cytotoxic (**Figure 19**).

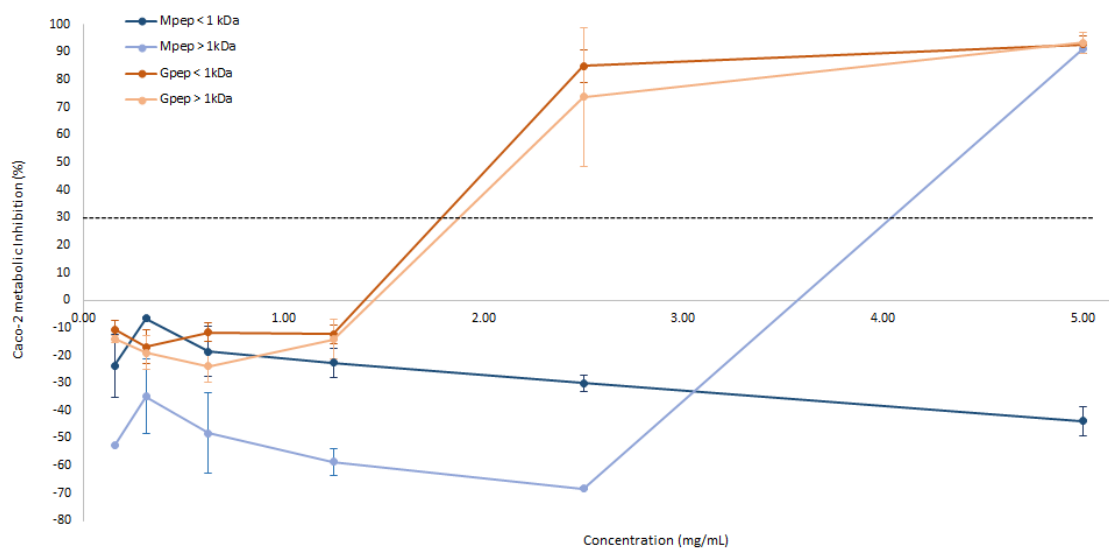


Figure 19. Caco-2 metabolic inhibition after 24 h-exposure to peptide-rich extracts (0.8-5 mg/mL) (n=4).

On the other hand, Mpep < 1 kDa and > 1 kDa had a completely different behaviour from each other since all the tested concentrations of Mpep < 1 kDa did not inhibit cell metabolism, whereas Mpep > 1 kDa decreased Caco-2 metabolism at concentrations higher than 5 mg/mL. The differences observed may be associated to peptides structure and characteristics such as charge, amino acids profile and sequence. Besides, other unknown components may also be present in peptide-rich extracts. Regarding these results, the peptide-rich extracts concentrations chosen for the bioactivities were: Gpep > 1 kDa and < 1 kDa - 1.25 mg/mL, and Mpep > 1 kDa - 2.50 mg/mL and Mpep < 1 kDa - 5.00 mg/mL since they appeared not to change cells viability more than 30% as mentioned in ISO 10993-5:2009 (International Organization for Standardization, 2009).

Mirzaei et al. (2019) found that the fractions 3-5 kDa (0.5 and 1 mg/mL) and < 3 kDa (0.5-2 mg/mL) did not decrease significantly the Caco-2 cell viability at 24 h exposure. In fact, they reported non-cytotoxic concentrations below 2 mg/mL which agrees with the current study, which observed Mpep < 1 kDa being non-cytotoxic below 5 mg/mL.

However, these differences are strongly dependent on the methods used for production of yeast protein and the resulting nature of the extract obtained.

3.1.3.4. Biological activity

Anti-cholesterolemic, antihypertensive and antioxidant activities

The potential effect of Gpep and Mpep fractions on cholesterol-lowering was assessed by HMG-CoA reductase inhibition assay (**Table 20**).

Table 20. IC50 values (mg/mL) at ACE-inhibition assay, HMG-CoA reductase inhibition (%), and ABTS⁺, ORAC and DPPH[•] (μmol TE/g extract) activities of peptide-rich extracts.

		HMG-CoA reductase inhibition (%) *	ACE-IC50 (mg/mL)	ABTS⁺ (μmol TE/g extract)	ORAC (μmol TE/g extract)	DPPH[•] (μmol TE/g extract)
Gpep	> 1 kDa	71.3 ± 7.7	1.54 ± 0.04	337 ± 123	654 ± 64	110 ± 26
	< 1 kDa	69.8 ± 3.8	0.99 ± 0.04	450 ± 115	1041 ± 50	114 ± 31
Mpep	> 1 kDa	63.6 ± 5.6	1.43 ± 0.07	416 ± 166	663 ± 75	125 ± 39
	< 1 kDa	62.0 ± 4.2	1.72 ± 0.11	492 ± 109	926 ± 62	133 ± 32

Results are expressed in average ± standard deviation (n=3). *For Caco-2 biocompatible concentrations.

All peptide fractions inhibited HMG-CoA activity from 62.0% to 71.3% (**Table 20**) but no significant differences were found between fractions under and above 1 kDa and between the type of waste stream used (Gpep vs. Mpep) (p > 0.05). However, these results are according to the previous data of *Section 2.2. Separation & purification* since we already obtained HMG-CoA inhibition of 70.8% to 74.0% for ESY1 and 1 kDa ultrafiltration fractions. In fact, the ultrafiltration process allowed for an increase in the bioactivity in relation to original autolysate (40.3%) but also no differences were observed between fractions (*Section 2.2. Separation & purification*).

Regarding the high cholesterol levels, which may be linked with lipid metabolic disorders, other studies have previously explored the anti-obesity effect of yeast hydrolysates, but the effect on cholesterol pathway was not studied (Jung et al., 2014; J. H. Kim et al., 2012; Park et al., 2013). Further studies on the subject are needed to draw further conclusions since our studies were the first to demonstrate HMG-CoA reductase inhibition related with spent yeast peptides.

The potential antihypertensive properties of produced peptide-rich extracts were evaluated using the ACE-inhibitory assay and the results were shown in **Table 20**. The peptide rich-extracts have IC₅₀ values ranging from 0.99 to 1.72 mg/mL for ACE-inhibition, with the greatest antihypertensive effect found in Gpep < 1 kDa (0.99 mg/mL), followed by Mpep > 1 kDa and Gpep >1 kDa, and, at least, Mpep < 1 kDa ($p < 0.05$) (**Table S9**). The lower peptide MW of Gpep < 1 kDa (36.9% 1000-500 Da, 51.1% < 500 Da), in comparison with fractions > 1 kDa, can be associated with the antihypertensive activity, as described by Amorim et al. (2016). However, the same hypothesis cannot be applied to Mpep < 1 kDa (36.8% 1000-500 Da, 47.9% < 500 Da) which has the lowest antihypertensive activity. In this case, the lower ACE-inhibition can be attributed to the lower amount of protein ($48.3 \pm 15.9\%$) and amino acids (254 ± 85 mg/g protein), in comparison with the other three fractions (**Table 18**). As explained on the discussion of *Section 2.2. Separation & purification*, some authors have pointed out that high amounts of hydrophobic amino acids can be related with ACE-inhibition activity by a structure–activity relationship but there is not enough evidence so far that corroborates this hypothesis (A. S. Oliveira, Ferreira, et al., 2022a). In comparison with our previous results (*Section 2.2. Separation & purification*), ESY1 < 1 kDa presented similar IC₅₀ values (1.80 mg/mL) to those of the current study, with this fraction having a higher activity than ESY1 > 1 kDa (2.59 mg/mL). However, no MW-activity relationship was established since the original ESY1 autolysate presented a similar outcome than respective fraction < 1 kDa.

Indeed, the absence of peptide MW association with bioactivity was also observed for ABTS and DPPH• (**Table 20**) since no significant differences were found between Gpep and Mpep fractions ($p > 0.05$). However, all samples demonstrated the ability to reduce the cationic radical ABTS^{•+} with concentrations of TE ranging from 337 to 492 μmol/g extract and to reduce DPPH• in a range of 110 to 133 μmol TE/g extract. Comparing ABTS and DPPH• methods, DPPH• provided lower values of TE than ABTS^{•+}, as already described in literature, since DPPH• is much more stable than ABTS^{•+} (Mareček et al., 2017). A similar result was found by Guo et al. (2020) since they obtained a strong ABTS^{•+} scavenging ability from all yeast protein hydrolysates while at the same time no observed capacity of DPPH• scavenge was observed with the same extracts. Although the high reactivity of ABTS^{•+} can be advantageous, since it can react with a wider range of antioxidants, the instability of ABTS^{•+} solution can lead to biased results, and thus is important the support results with other assays, like DPPH• and/or ORAC. Regarding the ultrafiltration fractions of ESY1 (*Section 2.2. Separation & purification*), high ABTS^{•+} scavenging activity was obtained in

the present study (181 to 255 $\mu\text{mol TE/g}$ extract) which corroborates the potential of peptide fractions from waste streams to be applied as dietary supplement as well. Furthermore, DPPH[•] scavenging activity obtained in the current investigation was stronger than those found by Marson, de Castro, Machado et al. (2020) in 35 kDa spent yeast hydrolysates.

On the other hand, ORAC activity showed statistically significant differences ($p < 0.05$) between different MW fractions, with both < 1 kDa fractions, showing a higher activity than the 1 kDa fractions (**Table 20** and **Table S9**), as demonstrated in ESY1 ultrafiltration fractions (708 and 237 $\mu\text{mol TE/g}$ extract for ESY1 < 1 kDa and > 1 kDa, respectively) (*Section 2.2. Separation & purification*). As explained on *Section 2.2. Separation & purification*, these differences are explained by the *in vitro* antioxidant assays follow distinct redox mechanisms and ORAC is the most similar assay to physiological conditions with the generation of radical peroxy.

Regarding the importance of the combined effects in one single product as functional ingredient for food industry, several authors studied the antioxidant properties of spent yeast peptides together with ACE and/or α -glucosidase inhibition and immunostimulant activities (M. Amorim, Marques, et al., 2019; Hassan, 2011; Jung et al., 2011; Mirzaei et al., 2015; Vieira et al., 2017). Currently, the antioxidant activity has been linked to the amendment of chronic disorders, such as hypertension, diabetes, aging, cancer, and neurodegenerative disorders (M. Amorim, Marques, et al., 2019). In the present study, regarding HMG-CoA reductase and ACE inhibitions, together with antioxidant results, and the similar performance to peptide-rich fractions directly extracted from spent yeast (ESY1 > 1 and < 1 kDa), these Gpep and Mpep fractions from waste streams showed to be good bioactive ingredients to be potentially incorporated in functional food and commercialized at nutraceutical market.

3.1.4. Conclusion

The present study has demonstrated the possibility to produce peptide-rich extracts from waste streams from spent yeast β -glucans and mannans extraction processes, using 1 kDa ultrafiltration technology. The results have shown that yeast extracts with high protein content and EAA, comprising about 1 kDa MW peptides, were capable of strong ACE and HMG-CoA reductase inhibition, ABTS^{•+} and DPPH[•] reduction, and peroxy radicals' protection effect (ORAC), indicating their antihypertensive, anti-cholesterolemic and antioxidant capacities. In this way, the peptide-rich extracts produced in this study have

demonstrated their potential for incorporation into formulations aimed at commercialization in the nutraceutical market for human supplementation. Additionally, their high amount of Glu also makes them promising ingredients to be applied as flavour enhancers.

3.1.5. Supplementary material

Table S8. *P-values of comparison of nutritional analysis between different Gpep and Mpep peptide-rich fractions: sugars (%) and minerals (ng/g extract).*

	<i>Sugars</i>	<i>Minerals</i>
Gpep > 1 kDa vs. < 1 kDa	4.75E-02	4.71E-04
Gpep > 1 kDa vs. Mpep > 1 kDa	7.35E-02	5.24E-02
Gpep > 1 kDa vs. Mpep < 1 kDa	4.15E-02	4.70E-05
Gpep < 1 kDa vs. Mpep > 1 kDa	9.45E-01	1.68E-03
Gpep < 1 kDa vs. Mpep < 1 kDa	9.98E-01	7.13E-04
Mpep > 1 kDa vs. < 1 kDa	8.87E-01	7.52E-05

n=2

Table S9. *P-values of comparison of ACE inhibition (IC50 - mg/mL) and ORAC (μmol TE/g extract) assays between different Gpep and Mpep peptide-rich fractions.*

	<i>ACE</i>	<i>ORAC</i>
Gpep > 1 kDa vs. < 1 kDa	4.80E-03	3.26E-04
Gpep > 1 kDa vs. Mpep > 1 kDa	3.12E-01	9.98E-01
Gpep > 1 kDa vs. Mpep < 1 kDa	7.33E-01	3.39E-03
Gpep < 1 kDa vs. Mpep > 1 kDa	1.43E-02	3.88E-04
Gpep < 1 kDa vs. Mpep < 1 kDa	2.99E-03	1.98E-01
Mpep > 1 kDa vs. < 1 kDa	1.15E-01	4.23E-03

n=3

3.2. Fe-peptide complexes*

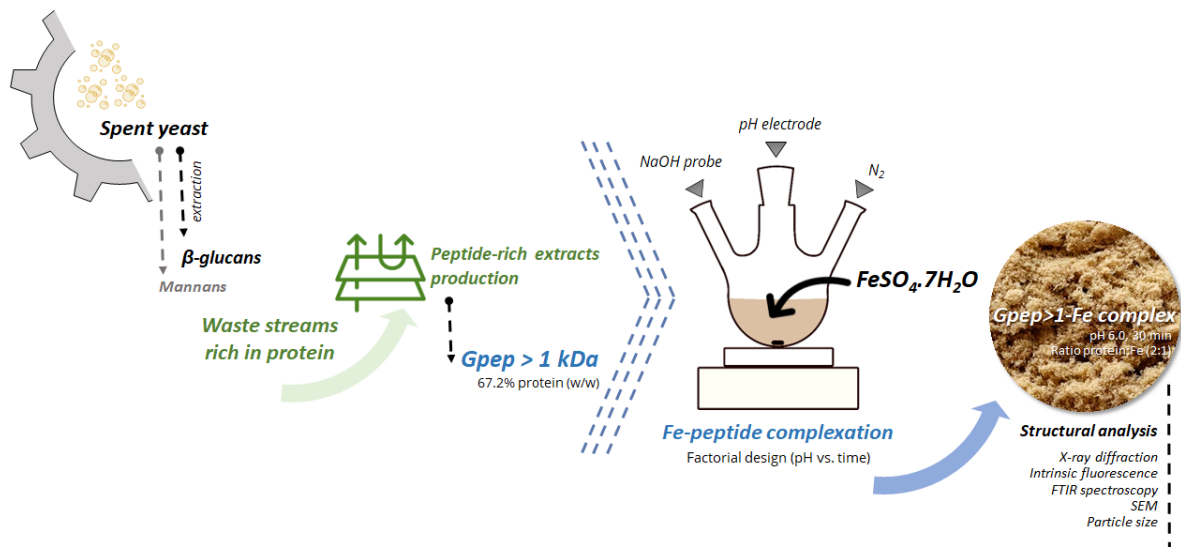


Figure 20. Schematic overview of Section 3.2, showcasing the process of generating peptide-Fe complexes derived from spent yeast peptide-rich extracts. Adapted from the graphical abstract of submitted article*.

3.2.1. Introduction

Fe is an important micronutrient in human nutrition, as it is involved in many biochemical processes in human metabolism such as oxygen transport, electron transfer reactions, gene regulation, and cell growth and differentiation (Waldvogel-Abramowski et al., 2014).

Given its importance in human metabolism, health problems may arise if not enough Fe is consumed ingested. In fact, Fe deficiency is a major concern and one of the most widespread micronutrient deficiencies globally (Y. Zhang et al., 2021). According to the WHO about 1.62 billion people suffered from anaemia, a form of Fe deficiency in blood cells, with greater prevalence in developing countries (World Health Organization, 2008). More recent numbers report that 30% of women aged between 15 and 49 years and 40% of children under 5 years suffered from anaemia in 2019 (World Health Organization, 2021), while other estimates place the global age-standardized point prevalence of anaemia at around 23% (Safiri et al., 2021).

Although adults lose low amounts of Fe daily, 1 mg to 2 mg for man and woman, respectively (Collins & Anderson, 2012; Eckert et al., 2016), adequate quantities of Fe must be ingested in order to maintain Fe homeostasis. This is especially important considering

* Oliveira, A. S, Ferreira, C. M. H., Pereira, J. O., Sousa, S., Faustino, M., Durão, J., Pereira A. M. P., Pintado, M. E. & Carvalho, A. P. Production of iron-peptide complexes from spent yeast for nutraceutical industry. Submitted to *Food and Bioproducts Processing* (16th January 2023)

that only 5% to 18% of Fe naturally present in food is absorbed by the human body during the gastrointestinal digestion (Eckert et al., 2016). Factors such as living standards, food choices and food quality may also impact the levels of Fe absorbed by an individual; for example, plant-based Fe sources are less bioavailable than animal-based ones (Athira et al., 2021).

Fe supplementation in the diet is an effective way to address the problem of its deficiency, particular in cases where Fe bioavailability in diet is low. Elemental Fe and certain common Fe salts, such as Fe sulphate, carbonate, citrate, and fumarate, are commonly used in food fortification (Fairweather-Tait & Teucher, 2002). However, these salts have some drawbacks. First, these forms of Fe have low bioavailability (Athira et al., 2021; Y. Zhang et al., 2021), and the consequently high amounts of Fe required to rectify Fe deficiency can cause health issues such as production of ROS species (Caetano-Silva et al., 2015), Fenton reactions, gastrointestinal irritation, vomiting, lethargy, grey cyanosis, pneumonitis, convulsions, coma and even death in extreme cases (Jeppsen & Borzelleca, 1999). Secondly, these simple salt forms can interact with food components, causing perceived changes in food properties such as flavour, colour or texture (Shubham et al., 2020).

One potential solution to these problems is the use of Fe-peptide complexes. These complexes are described as being more bioaccessible, bioavailable and safe than the aforementioned Fe salts (W. Wu et al., 2020). Their increased bioaccessibility is due to the competition of peptides with other organic molecules, such as phytates, tannins, oxalates and polyphenols, which can precipitate Fe at physiological pH (Anderson et al., 2018; Eckert et al., 2016; Lazarte et al., 2015; S.-H. Lee & Song, 2009; W. Wu et al., 2020). Some reported results also show that organic forms of Fe have greater absorption rates than inorganic forms, although they are still limited by their carrier capacity (L. Y. Zhang et al., 2017). Finally, safety is also cited as a reason for the preference of Fe-peptide complexes over other forms of Fe supplementation (Caetano-Silva et al., 2020; W. Wu et al., 2020).

Several sources of peptides have been tested recently, including whey protein (Athira et al., 2021; Caetano-Silva et al., 2015, 2017; O'Loughlin et al., 2015), mung beans (Budseekoad et al., 2018; Y. Zhang et al., 2021), Antarctic krill (T. Wang et al., 2020), maitake (*Grifola frondosa*) (Yuan et al., 2019), casein digest (Smialowska et al., 2017), Pacific cod skin (W. Wu et al., 2017), sea cucumber (*Stichopus japonicus*) ovum hydrolysates (Sun et al., 2017), Alaska pollock skin (*Gadus chalcogrammus*) (Chen et al., 2017; L. Guo et al., 2013, 2015), sugar cane (de la Hoz et al., 2014), anchovy (H. Wu et al.,

2012), and chickpea (Torres-Fuentes et al., 2012), among others. A common reason for choosing a particular peptide source is to valorise protein-rich sub- and by-products from other processes, thus promoting circular economy.

Motivated by the desire to create new, healthy, effective, and safe Fe-peptide complexes for the nutraceutical industry of Fe supplementation, and by the need to further process and add value to these by-products, the viability of peptide-rich extracts produced by 1 kDa ultrafiltration on *Section 3.1. Application for nutraceutical market* as sources for Fe-peptide complexes and chelating agents were studied. Variables such as pH, time, protein-to-Fe ratio and oxidative conditions were also studied and evaluated. Finally, the physicochemical characterization of Fe-peptide complexes was performed to understand the complexation behaviour and final product properties (**Figure 20**).

3.2.2. Material and methods

3.2.2.1. Peptide-rich fraction production

Peptide fractions used in this study were produced following 1 kDa ultrafiltration of *Section 3.1. Application for nutraceutical market*. As demonstrated at **Figure 21**, a total of three different MW peptide fractions for each waste stream were obtained: retentate “Gpep > 1 kDa” and permeates “Gpep < 1 kDa FS” (first ultrafiltration permeate fraction) and “Gpep < 1 kDa DF” (diafiltration permeate fraction) from β -glucan, and retentate “Mpep > 1 kDa” and permeates “Mpep < 1 kDa FS” and “Mpep < 1 kDa DF” from mannans.

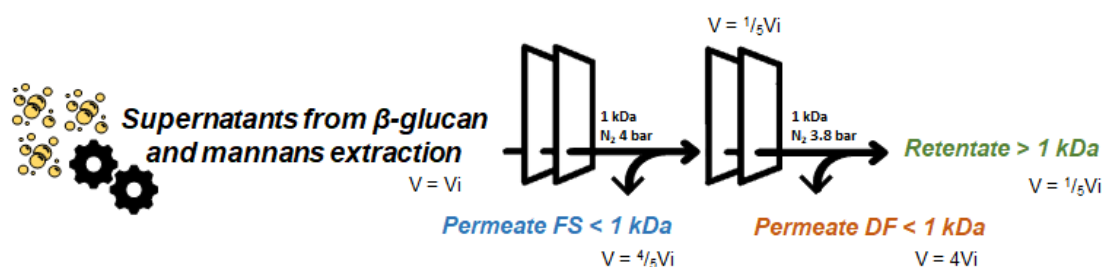


Figure 21. Diagram for ultrafiltration of protein-rich supernatants from yeast β -glucan and mannan extraction processes to obtain peptide fractions.

3.2.2.2. Chemical characterization of peptide-rich fractions

Protein

Protein content of fractions was determined by Pierce™ BCA protein assay kit as described in *Section 2.2.2.3. BCA*.

Dry weight

DW analysis was performed according to AOAC standard procedures described on *Section 2.1.2.4. Dry weight*.

3.2.2.3. Fe-peptides complexation

Fraction initial screening - reaction without N₂

An initial complexation screening was performed using the protocol of Caetano-Silva et al. (2015) with some modifications. Each peptide-rich fraction was prepared at 0.2% protein (w/w) in deionized water and 0.1% of Fe (w/w) (FeSO₄·7H₂O; Sigma-Aldrich, Inc., St. Louis, USA) was added to the solution under stirring, corresponding to protein:Fe ratio of 2:1. The solution was stirred for one hour with the pH monitored and adjusted periodically to 7.0. In the end, the solution was centrifuged (12000 × g, 5 min) and the supernatant was filtered (ø = 0.45 µm; Chromafil® polyester (PET)-45/25, Macherey-Nagel, Germany). The soluble Fe from the resulting solution was measured by ICP-OES. Each extract was tested in triplicate and the results expressed as a percentage of the total added Fe (% of initial), are presented as an average of $n=3$.

Complex formation – anoxic conditions

Experimental setup

A schematic of the experimental setup used for the complexation reaction in the presence of a N₂ atmosphere is displayed in **Figure 22A**.

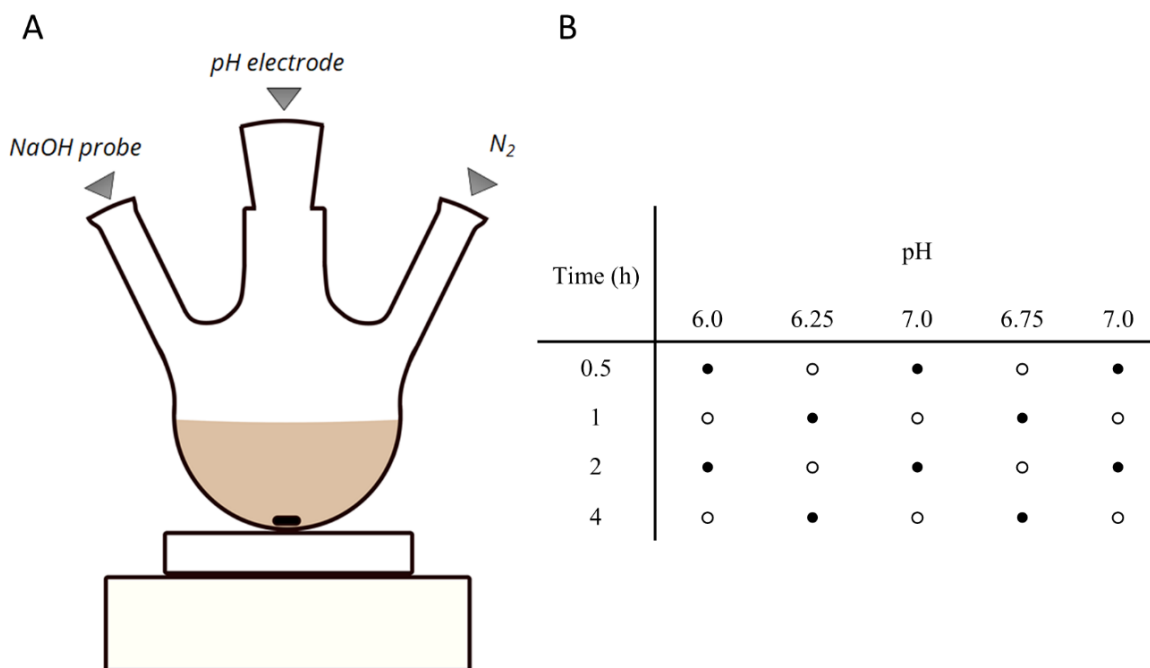


Figure 22. *A: Experimental design of the complexation reaction setup using N_2 , pH control and NaOH probe. B: Conditions of pH and time on the complexation reaction efficiency assays. ●: combination tested; ○: combination not tested.*

A three necked 500 mL flask was used for the purpose. When not in use, the flask necks would be closed using the appropriate stoppers. The middle neck was used to insert a pH electrode for live control, and one of the side necks was used to insert the NaOH probe of Automatic Potentiometric Titrator AT-710 system (Kyoto Electronics Manufacturing Co. Ltd, Japan) to adjust pH during reaction. The second side neck was used to insert a N_2 line. The flask was placed in a magnetic stirrer and a magnetic bar was inserted in the flask to stir the solution during the reaction.

Reaction protocol

A peptide-rich solution was prepared to a protein concentration of 0.02% (w/w) and placed in the reaction flask. N_2 was purged for 10 min and 0.01% of Fe (w/w) was added while the solution was continuously stirred and purged for more 10 min. Finally, the pH of the solution was slowly increased to pH 7.0. For the next 30 min, the solution was kept under N_2 purge and the pH was monitored and adjusted to 7.0 accordingly. At the end of reaction, the solution was collected in a flask under a N_2 atmosphere and stored at room temperature overnight. In the next day, the pH of solution was adjusted back to pH 7.0, followed by centrifugation ($12000 \times g$, 5 min) and filtration for some precipitate remotion ($\phi = 0.45 \mu\text{m}$).

The soluble Fe from the resulting solution was measured by ICP-OES. Each reaction was performed in triplicate and the results expressed as a percentage of the total added Fe (% of initial), are presented as an average of $n=3$. Blank experiments were also carried out, where the same conditions were tested, in duplicate, in the absence of peptide extracts.

Factorial design and statistical analysis

To find the optimal complexation conditions, a two-factor factorial design was used. The effect of pH was studied at five different levels (6.00, 6.25, 6.50, 6.75 and 7.00) while time was varied at four levels (0.5, 1.0, 2.0 and 4 h). As to reduce the number of conditions, only 50% of the total possible combinations were performed, as shown in **Figure 22B**. Each combination was performed in triplicate. Experiments were conducted in a randomized order.

To model the response of % of complexed Fe to the tested factors, the following second-order polynomial model was chosen as described by:

$$Y = b_0 + b_1X_1 + b_2X_2 + b_3X_1X_2 + b_4X_1^2 + b_5X_2^2 + \epsilon$$

Where Y is the percentage of the initial Fe in solution after complexation reaction, b_i represent the different coefficients of each factor, X_i represent pH and time factors and ϵ the random experimental error.

The model was fitted using the using the Real Statistics Resource Pack software (Release 7.2) with multivariate regression as the optimization and fitting method. To analyse extreme data points of the regression fit and determine their validity, the Cook's D method was applied. Data points with a value greater than 0.2 were considered for removal from the regression, and the regression was conducted a second time.

Fe determination

Fe determination was performed by ICP-OES, after microwave digestion, as explained on *Section 2.1.2.4. Minerals*.

3.2.2.4. Complex characterization

X-ray diffraction

The diffraction of X-rays (XRD) was analysed using an X-ray diffractometer (Rigaku MiniFlex 600, Tokyo, Japan). Freeze dried samples were packed in a sample plate and measured using the following conditions: Cu α radiation, operated at 40 kV and 15 mA, with 2θ range from 3° to 80° , a scanning speed of 3° min^{-1} , and a step of 0.01° .

Intrinsic fluorescence

The intrinsic fluorescence emission spectra were recorded using a microplate reader (Synergy H1, Biotek Instruments, Winooski, USA). A wavelength of 280 nm was used for excitation of samples and emission wavelengths from 300 to 400 nm were recorded in of 5 nm increments. Samples were measured in triplicate and the results were expressed as an average.

Fourier-transform infrared spectroscopy

A diamond crystal of attenuated total reflectance (ATR) assembly Perkin-Elmer Frontier Fourier-transform infrared (FTIR) spectrometer coupled with a Universal ATR Sampling Accessory (Massachusetts, USA) was used to obtain infrared spectra. Samples were measured in a wave number range between 4000 and 550 cm^{-1} with a resolution of 1 cm^{-1} .

Scanning Electron Microscopy

The samples morphology was evaluated using a Phenom XL G2 (Thermo Fischer Scientific, The Netherlands) scanning electron microscope (SEM). Sample powders were placed over double-sided adhesive carbon tape (NEM tape; Nisshin, Japan), which covered the observation pins, and were coated with gold/palladium on a sputter coater (Polaron, Germany). An acceleration voltage of 5 kV in high-vacuum mode was used and all images are representative of the morphology of each sample.

Particle size

The particle size distribution was assessed using a Malvern Mastersizer 3000 - Laser Diffraction (Malvern Instruments Ltd., UK) with a refractive index of 1.40 and absorption

of 0.01 parameters selected. Ethanol absolute was used as dispersant. According to the laser diffraction through the particles of material, a scattering pattern was generated and then used to calculate the particle size via Mie theory.

3.2.3. Results and Discussion

3.2.3.1. Protein content

The supernatants of yeast β -glucan and mannan extractions were submitted to 1 kDa ultrafiltration and diafiltrated and the protein concentration of the peptide-rich fractions was determined thereafter. A protein content ranging 23.0 to 86.4% (w/w) was found, as shown in **Table 21**.

Table 21. Protein concentration (% w/w) of peptide-rich fractions.

	Gpep			Mpep		
	> 1 kDa	FS < 1 kDa	DF < 1 kDa	> 1 kDa	FS < 1 kDa	DF < 1 kDa
Protein (%)	67.2 ± 16.0	23.0 ± 1.3	67.6 ± 25.6	86.4 ± 8.7	44.8 ± 5.8	48.3 ± 15.9

Results are expressed in average ± standard deviation ($n=4$).

Several authors have used membrane filtration to produce peptide fractions with low MW, since these are described as better ligands for mineral binding (Caetano-Silva et al., 2018; de la Hoz et al., 2014; O’Loughlin et al., 2015; Yuan et al., 2019). The high selectivity and efficiency together with low energy consumption makes it quite appealing to food industry (Marson, de Castro, Belleville, et al., 2020). In fact, for ideal Fe complexation, peptides should be ranging in size from 300 to 1500 Da (Caetano-Silva et al., 2020). Therefore, the size of peptides is a key factor for complexation. As a result, the first step of this study was to evaluate of complexation capacity of different MW fractions produced. The peptide rich solutions for the following complex reactions were prepared according to the protein concentrations listed above (**Table 21**)

3.2.3.2. Fraction complexation capacity screening

The values of soluble Fe (II) found at the end of the one hour reaction, as measured by ICP-OES, are found in **Figure 23A**.

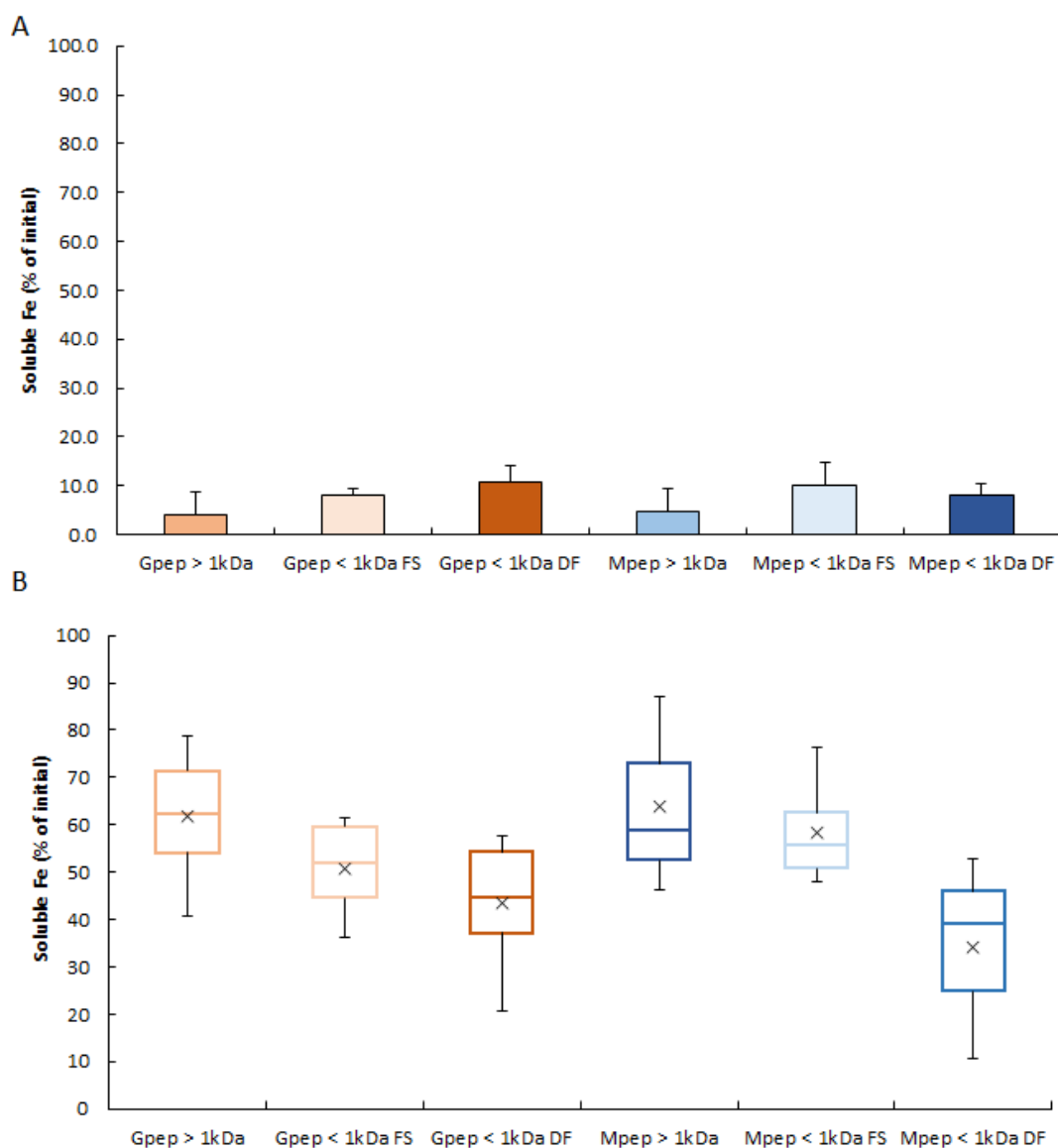


Figure 23. A: Soluble Fe (% of initial) after complexation reaction with no N₂ atmosphere (n=2). B: Soluble Fe (% of initial) after complexation reaction with solution purge and N₂ atmosphere (n=6).

Almost all reactions resulted in less than 10% of the initial Fe remaining in solution, with exception of Gpep <1 kDa DF and Mpep <1 kDa DF, with 10.7% and 10.0% respectively. The lowest amount of Fe in solution was found at the concentrated fractions (> 1 kDa) of both by-products, with 3.92% and 4.68% for Gpep and Mpep, respectively.

During the complexation reaction under normal conditions, the pH was very unstable for at least the first 30 min, consistently decreasing as it was adjusted to 7.0. At the same time, the formation of a precipitate was observed as NaOH was added to the solutions to adjust the pH to the required value. There are two factors that may be responsible for the decrease in pH. One possibility is that ferrous Fe (II) may be at its solubility limit and precipitate out as Fe(OH)₂ (Monhemius, 1977), depleting hydroxide from solution and thereby reducing

pH. The constant stirring of the solution in open air may also contribute to the oxidation of ferrous Fe (II) into Fe (III), which is even more insoluble at neutral pH (Monhemius, 1977). On the other hand, it is possible that protons may be released by peptides and/or proteins as a result of the complexation and consequent change in pKa of some acid/base moieties (Onufriev & Alexov, 2013). However, the formation of a thick brown precipitate seems to support the first hypothesis. The amount of soluble Fe found at the end of the reaction (**Figure 23A**) also supports the previously discussed assumptions. Overall, the amount of Fe present in the solution is low, ranging from about 4% to 10.5%. Despite this range, statistical analysis reveals no differences between different fractions.

Comparing these results with literature, they are somewhat low since Sun et al. (2017) have found values ranging from 15% to 90% of the added Fe in their samples. However, proteins of this study were extracted from other matrix, such as sea cucumber ovum hydrolysates. On the other hand, our values are in the same range as those found by Wu et al. (2017) using peptides from Pacific cod skin gelatine for complexation. Other sort of optimization was performed by Caetano et al. (2017) which allowed soluble Fe yields between 40% and 90% when using different Fe: protein ratios and working with whey protein hydrolysates. Also in this study, the authors tested different ultrafiltration fractions (filtrate and retentate) as well the original hydrolysate and, contrary to our study, found differences in complexation behaviour between different fractions (Caetano-Silva et al., 2017). Similarly, O'Loughlin et al. (2015) studied the complexation capacity of two whey protein hydrolysates that were subjected to an ultrafiltration cascade. The two fractions studied (30 kDa retentate and 1 kDa permeate) have shown slightly different behaviours, with a decrease in Fe solubility when reaching pH 7. Nonetheless, more than 80% of Fe remained soluble (O'Loughlin et al., 2015).

Once Fe oxidation was observed during the reactions under normal conditions, together with the low complexation yield, new conditions were tested, including the use of an anoxic environment. In these reactions, N₂ was used to purge the reaction solution and the environment of the reaction was sealed under a N₂ atmosphere. Under these conditions a different behaviour was observed. Precipitation still occurred, but to a lesser degree and with a different colour than in the first case (greenish instead of ochre). Also, pH variation was observed but to a lesser degree, being the solution much more stable than in the previous experiment. Overall, an improvement was observed, with larger amounts of soluble Fe still found, with values averaging from 39% (M_{pep} < 1 kDa) to 64% (M_{pep} > 1 kDa). This is in

stark contrast to the previous results obtained under normal atmosphere conditions (**Figure 23B**).

Interestingly, the permeate fractions (FS and DF) had less soluble Fe compared to the concentrate fractions which had the largest. In fact, it is possible to observe a trend in the data suggesting that the lower the size of peptides in solution, the less Fe is maintained in solution. However, this trend and differences between steps of filtration within the same by-product are not statistically significant ($p > 0.05$).

In comparison with literature previously discussed, this data set is more comparable to that of Sun et al (2017). However, lower percentages of soluble Fe than O'Loughlin et al (2015) or Caetano et al. (2015, 2017) were still obtained, which may be related with two main complexation factors: interference of time (reaction and precipitation kinetics) and pH (protonation and complexation equilibria), as reviewed by Caetano et al (2020). These two factors were explored in more detail in the next experimental set.

3.2.3.3. Complex formation conditions optimization

An analysis in the literature reveals that different conditions for conducting Fe-peptide complexation have been explored. Zhou et al. (2012) used seven different pH levels in the 5.0-8.0 pH range while Smialowska et al. (2017) tested three different pH from 2.75 to 6.7. While some works use a single pH value, the authors differ on the pH chosen. For example, the following values have been used: pH 5.0 (W. Wu et al., 2020; Yuan et al., 2019), pH 6.0 (T. Wang et al., 2020) or pH 7.0 (Caetano-Silva et al., 2015, 2017; Sun et al., 2017). However, most works focus on a 5-8 range, though a pH higher than 7.0 may not be desirable since a formation of precipitate was observed at the first screening assay. On the other hand, a lower pH may compromise complexation, as fewer moieties will be deprotonated and available for complexation. For this reason, a pH ranging from 6.0 to 7.0 was chosen for our optimization study. Also, from the experience obtained in the previous experiments, the solution pH continuously decreases over time, even past one hour. In fact, in a test experiment (data not shown) that was conducted over the period of four hours, pH was still not fully stable. The observation that 24 hours later the pH has decreased raises the question of what the ideal time for the complexation reaction is, and if it is pH dependent. Therefore, different times were also tested, ranging from 0.5 h to 4 h. Gpеп > 1 kDa was the peptide fraction chosen for this optimization since "> 1 kDa" samples presented a high soluble Fe

in the screening study and Gpep > 1 kDa had higher median values of soluble Fe found in the screening study.

The results of soluble Fe at the end of the complexation reaction for each set of conditions tested can be found in **Table 22**.

Table 22. Soluble Fe (% of initial) found for each condition tested in the experimental factorial design.

pH	Time (h)	Complexed Fe (% of initial)
6.00	0.5	88.0 ± 3.1
6.00	2.0	86.4 ± 1.5
6.25	1.0	83.5 ± 6.7
6.25	4.0	65.8 ± 8.6
6.50	0.5	55.1 ± 8.6
6.50	2.0	73.3 ± 9.5
6.75	1.0	71.2 ± 5.5
6.75	4.0	41.7 ± 13.4
7.00	0.5	53.4 ± 6.3
7.00	2.0	36.2 ± 11.4

Results are expressed as average ± standard deviation ($n=3$).

The highest average value, 88.0%, was found at pH 6.0 and 0.5 h of reaction, followed by other low pH and low time reaction conditions. In fact, if the average values are plotted just considering pH or time alone (**Figure 24**), a trend of decreasing soluble Fe as pH increases can be observed, where at pH 7.0 values are similar to those found in the previous experiment.

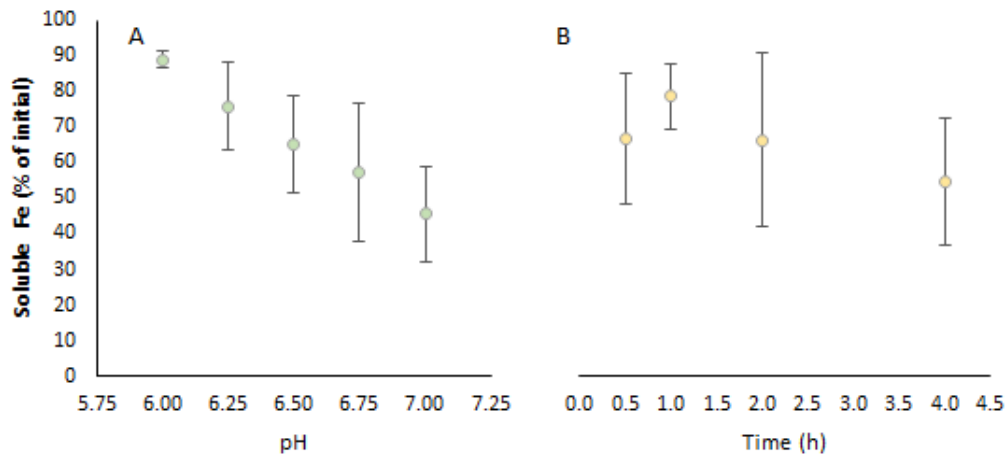


Figure 24. Soluble Fe in complexation reactions tested at experimental factorial design, as percentage of initially added, in function of pH (A) and in function of time (B) (n=3).

Regarding time (t), there is no clear trend, but the highest values are found for 1 h. However, time does not seem to have a large impact on the final solubility of Fe as pH has.

The fitting of our model using a multivariate regression analysis to the obtained data returns the following:

$$Fe_{\text{complexed}}(\%) = 32.27\text{pH} + 64.35t - 8.49\text{pH} \cdot t - 4.61\text{pH}^2 - 3.25t^2 + 50.04$$

With $R^2 = 0.794$ and $p < 0.0001$.

The corresponding response surface of the proposed model can be seen in **Figure 25** and the residuals of the multivariate regression in **Figure S1**.

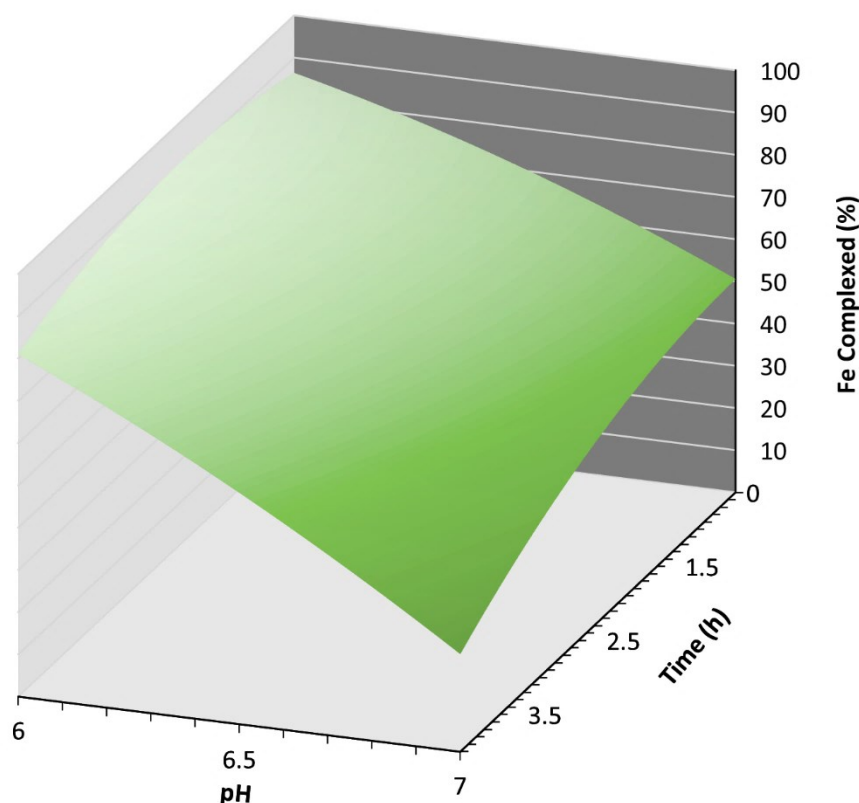


Figure 25. Response surface depicting soluble Fe (as % of initial added) versus time and pH. Model obtained from applying multivariate regression to complexation data, according to formula described in the main text.

The results presented in **Figure 25** show the trend already observed in **Figure 24**. Within the tested intervals of pH and time, the model predicts pH as the most important factor affecting the outcome of the complexation reaction. Using a pH as high as 7.0 is not advantageous, as most Fe (II) will either precipitate or oxidate and readily precipitate, while pH 6 is more ideal, with the model predicting values around 80% to 90% complexed, in contrast to pH 7.0 with values around 20% to 55%.

Regarding time, its influence seems pH related. At lower pHs, the time influence is not very noticeable, as seen in **Figure 25**, at pH 6.0, a 10 percent points difference from best to worst yields can be observed, with the greater difference at pH 7, where a 35 percent points difference is observed. The ideal time for complexation also changes slightly over pH, from 2 h at pH 6.0 to 1 h at pH 7.0. The observed changes may be linked to how precipitation kinetics and equilibria are affected by pH. At higher pH (7.0), the stability of Fe-peptide complexes decreases, leading to release of free Fe and peptides. The free Fe ions tend to precipitate more easily at this pH, due to more favourable conditions for precipitation to occur. Moreover, lower pH levels tend to increase the stability of the Fe-peptide complexes as noted by Ahile et al. (2020).

However, since the difference in yield between 0.5 h and 1 h reaction time at pH 6.0 was found to be minimal, the extra resources required for a longer reaction time (energy and N₂) were deemed unjustifiable for the small increase in yield observed. Consequently, a reaction time of 0.5 h and pH 6.0 were chosen as optimal conditions for complexation reactions of Fe (II) with Gpep > 1 kDa FD fraction.

3.2.3.4. Complex characterization

X-ray diffraction

A powerful method for assessing the structural changes in peptides following complexation with metal ions is XRD analysis (Walters et al., 2018). As demonstrated by several studies, XRD can provide valuable information on conformational changes in peptides following complexation with metals such as Fe (Jin et al., 2011; Malison et al., 2021; L. Wang et al., 2018). Generally, peptide samples exhibit weak or no crystalline reflections, but instead a broad band at around 2θ 20°, which is characteristic of an amorphous sample. The presence of metal ions can result in changes on this spectrum, such as the appearance of sharp reflection bands, which are indicative of structural changes in the peptide (Walters et al., 2018).

The X-ray diffraction patterns of Gpep > 1 kDa, Gpep>1kDa-Fe and Fe hydroxides are depicted in **Figure 26**.

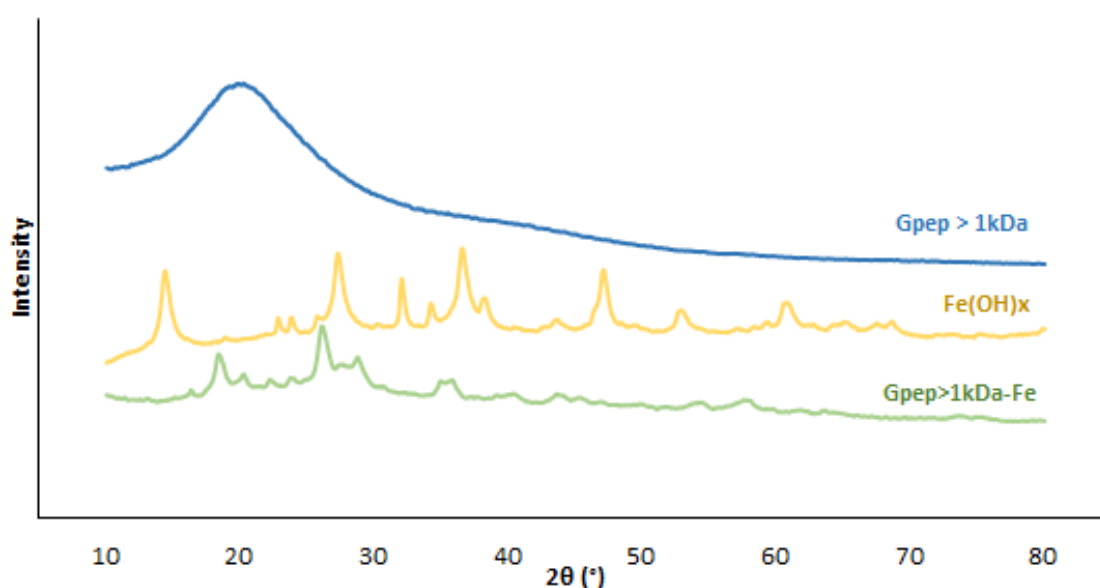


Figure 26. XRD patterns of Gpep > 1 kDa, Gpep>1kDa-Fe complex and Fe hydroxides (Fe(OH)_x) from 3° to 80°.

Fe precipitates from the reaction without Gpep > 1 kDa (blanks) were used as control for Fe hydroxides. The Gpep > 1 kDa presents a major broad band centred around 2θ 20° , as expected. On the other hand, with the addition of Fe, Gpep>1kDa-Fe exhibits two strong crystal diffraction peaks, as well as some other small diffraction peaks. The two major peaks are found at 2θ 18.5° and 26° . The analysis of Fe precipitates spectrum reveals that these have a different pattern of crystallization than that of Gpep>1kDa-Fe, as evidenced by the increased number of reflections. There are four main peaks at 2θ 14.5° , 27.4° , 36.7° and 47.2° , which both differ in quantity as well as in angle of reflexion. Similar results were found by Yang et al. (2019), where the Fe complexes created by the authors had a different XRD pattern compared to the original materials used, or by Zhu et al. (2018), although in the latter the signal difference was low due to the low crystallization level of the matrix.

Intrinsic fluorescence

The averaged spectra obtained for the three replicates of Gpep>1kDa-Fe complexes, as well as for Gpep > 1 kDa, can be seen in **Figure 27**.

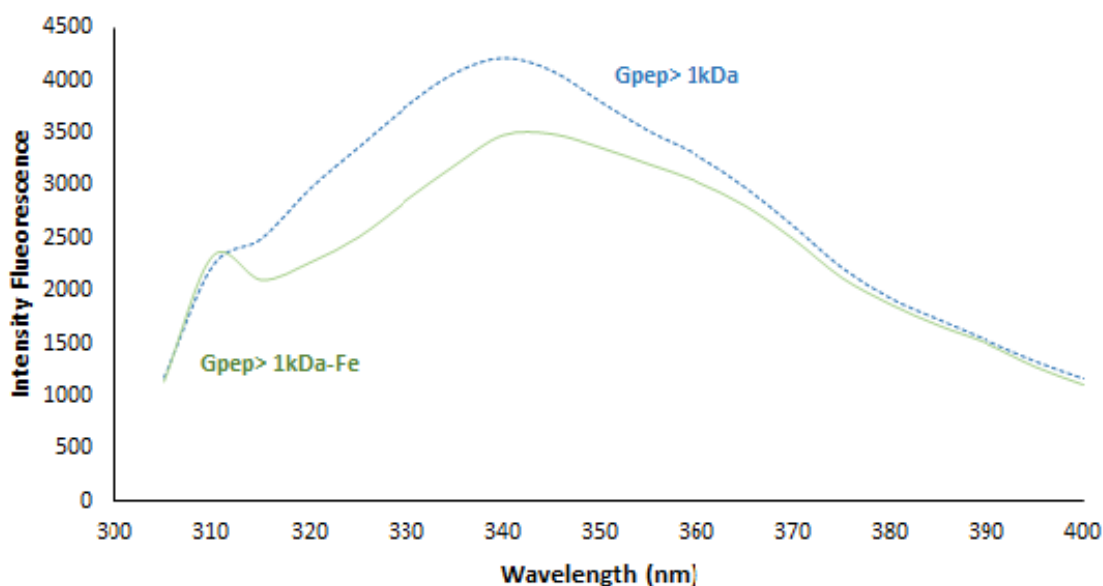


Figure 27. Fluorescence emission spectra of Gpep > 1 kDa and Gpep>1kDa-Fe complexes ($n=3$). Excitation wavelength = 280 nm; emission wavelength = 300 to 400 nm.

It is possible to observe a decrease in the fluorescence band at 340 nm, caused by the addition of FeSO_4 to Gpep > 1 kDa. This is likely due to the quenching of Trp residues in the peptide by Fe ions as noted by Wu et al. (2012). Furthermore, a red-shift in peak intensity from 340 nm to 345 nm is observed, this is also attributed to the quenching of Trp residues

in the peptide by the Fe ions and is consistent with previous reports. For example Wu et al. (2012) have demonstrated that the addition of FeSO₄ to anchovy muscle protein resulted in a decrease in fluorescence between 310 nm and 400 nm, after excitation at 295 nm, while at the same time, registering a red-shift in the emission spectra. Similarly, β -lactoglobulin hydrolysates also showed a decrease in fluorescence intensity at the same wavelength when Fe salts were added, with a simultaneous red-shift in emission spectra (Zhou et al., 2012). On the other hand, Lin et al. (2021) did not register a red-shift in emission spectra, unlike other studies, while observing the reduction of intensity on fluorescence. These changes may be attributed to the conformational changes of peptides caused by complexation, which results in less exposure of Trp to solvent, resulting in an emission behaviour change (Walters et al., 2018).

FTIR spectroscopy

The study of new complexes with FTIR is common practice, given its easiness and simplicity of use. The information provided is also valuable since there are several functional groups that can take part in the complexation with Fe (II). Shifts in amides I, II and III, as well as in carboxyl (-COOH), hydroxyl (-OH), sulfhydryl (-SH), and methyl (-CH₃) groups, usually part of peptide side chains, all may provide useful information regarding structural and chemical changes resulting from complexation (Walters et al., 2018). These changes, such as the appearance of new bands at specific wavenumbers, demonstrate the formation of covalent bonds between the peptide and the metal ions and a strong binding of the two entities. Therefore, the analysis of the comparison of FTIR spectra from un-complexed fraction and complexed fraction may be of help to evaluate how the peptides have complexed Fe (II).

The ATR-FTIR spectra for Gpep > 1 kDa, Gpep>1kDa-Fe complex and Fe hydroxides are presented in **Figure 28**.

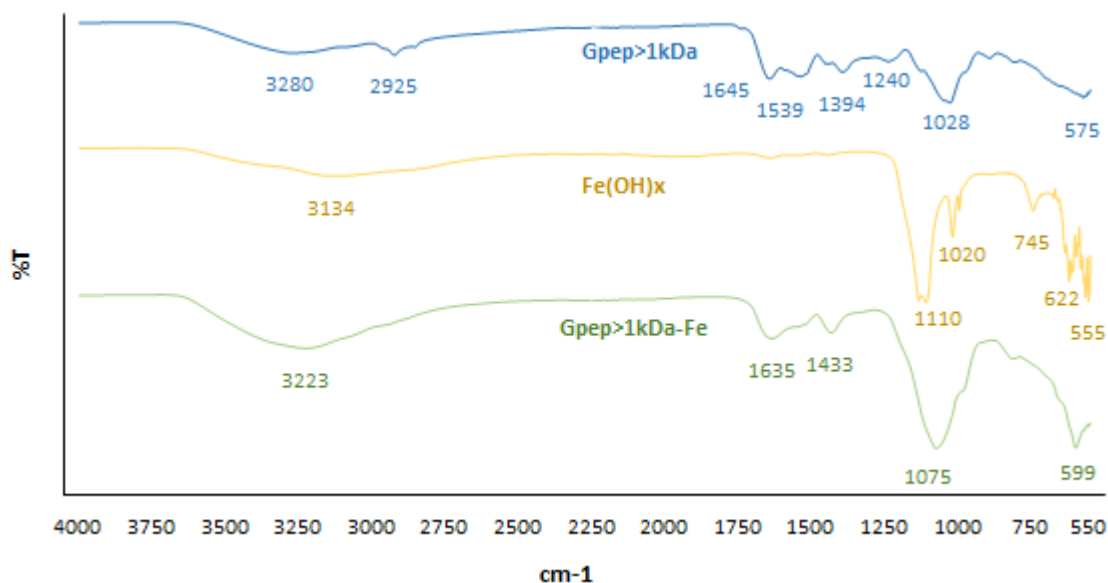


Figure 28. FTIR spectra of *Gpep* > 1 kDa, *Gpep*>1kDa-Fe complex and Fe hydroxides (Fe(OH)_x) in the region from 4000 to 550 cm^{-1} and identification of the main peaks observed.

The first major difference is the presence of two very intense and sharp bands in the *Gpep*>1kDa-Fe complex spectrum at 1075 and 599 cm^{-1} , whereas they are considerably smaller in the *Gpep* > 1 kDa spectrum. These bands are likely due to the presence of sulphate ions, as result of the added Fe sulphate salt for the complex formation (Coates, 2006). The influence of different counter ions in infrared (IR) spectra has been previously described (Caetano-Silva et al., 2017), and the presence of this strong band makes it difficult to analyse the spectra in this region. Bands in the region of 500 cm^{-1} and 1100 cm^{-1} have been associated with the stretching vibration of N-Fe and C-O-Fe bounds, respectively (Caetano-Silva et al., 2017; G. Huang et al., 2011; W. Wu et al., 2017; Zhou et al., 2012). For example, Caetano et al. (2017) related a shift in the ν_s C-O bands from 1110–1039 to 1117 cm^{-1} to the formation of Fe-O-C bonds, while bands at 1430 and 1620 cm^{-1} were related to symmetric and asymmetric (respectively) stretching vibration of Fe-COO bonds (Caetano-Silva et al., 2017). On the other hand, Zhou et al. (2012) described the appearance of strong bands at wavelengths of 1086, 1181, and 1253 cm^{-1} which the authors attribute to the coordination of the C-O-Fe bond in the peptide-Fe complex, while relating the shift at 3408 to 3375 cm^{-1} to complexation at amine groups in the peptide (Zhou et al., 2012). Observations in this range would be of practical importance, as they allow us to better understand the chemical interactions between the peptide and Fe ions but are obscured by the presence of the bands associated with sulphate ions.

Nonetheless, a number of band shifts were observed, providing insight into the specific interactions between the peptide and Fe ions. One of the most significant shifts observed

was the shift of the band at 1433, from the original 1394 cm^{-1} which can be attributed to carboxyl groups. This shift has been previously associated with a COO-Fe (Caetano-Silva et al., 2017). Additionally, changes were also observed in the Amide I and Amide II bands of Gpep > 1 kDa, found at 1645 and 1539 cm^{-1} respectively. The Amide I band shifted from 1645 to 1635 cm^{-1} , which may suggest the formation of COO-Fe bounds (Caetano-Silva et al., 2017). The Amide II band also reduced in intensity. This intensity reduction may be attributed to the interaction of the amide II groups with the metal ions, as previously reported (Alhazmi, 2019).

A broad band at 3280 cm^{-1} was observed at the original substrate, which can be attributed to Amine A (W. Wu et al., 2017). However, in the complex FTIR spectrum, this band has shifted to 3223 cm^{-1} as a result of the complexation reaction, which strongly supports the claim that peptides have successfully complexed with Fe.

Comparison with the FTIR spectra of Fe precipitates (without peptide supernatant), most likely Fe hydroxides, showed little similarity in the position of the main bands between Fe precipitates and Fe complexes spectra. A broad band can be observed at 3134 cm^{-1} , most likely related to the O-H of the hydroxides in the precipitate, dissimilar to the 3223 cm^{-1} band on the complex. The presence of sharp peaks at 1110, 1020, 745, 622 and 555 cm^{-1} in the Fe(OH)_x spectrum, which are not present in the complexes spectrum, further confirms the difference between the two.

Scanning electron microscopy

The morphological properties of Gpep > 1 and its Fe complexes were analysed using SEM and the results are presented in **Figure 29**.

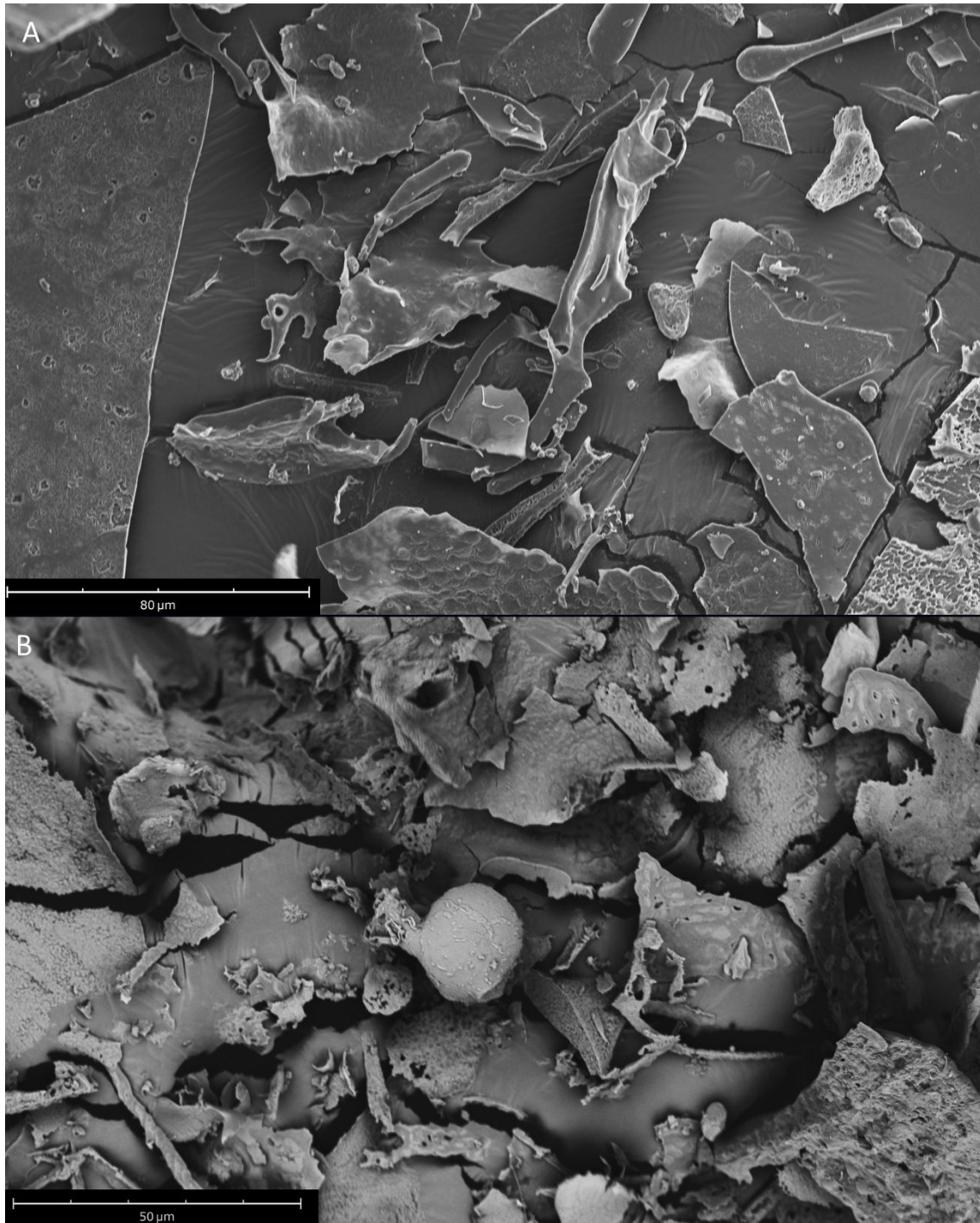


Figure 29. SEM microscopic morphology of *Gpep* > 1 kDa freeze-dried samples (A) versus freeze-dried Fe-peptide complexes formed with *Gpep* > 1 kDa (B).

Both samples are mostly characterized by rough shape particles with different sizes, which is a common feature when freeze-drying is used as a drying method (Liapis & Bruttini, 2020). However, notable differences were observed in the shape and structure of the particles. *Gpep* > 1 sample was composed of irregular flat plate-shaped flakes, which is characteristic of amorphous material. In contrast, *Gpep*>1-Fe complexes showed some small spherical particles with uneven surface in a compact and fragmented foundation. This

observation is consistent with previous studies, which have shown that Fe binding can change the original flat peptide plates and result in the formation of spherical structures (Ferreira et al., 2022; S. Lin et al., 2021; T. Wang et al., 2020).

Particle size

The particle size distribution of Gpep > 1kDa and Gpep>1kDa-Fe complexes were analyzed and the results are shown in **Table 23**. As particle size is a critical parameter that can affect the flow properties of powders, it is important to understand how the complexation with Fe ions affects the size of the particles. As shown in the table, the median particle size (Dv50) of Gpep>1kDa-Fe complex was < 11.1 μm , while Gpep > 1 kDa presented particles < 39.1 μm . Similarly, at 90% distribution (Dv90) the Gpep>1kDa-Fe complexes had particle sizes of 39.2 μm , while Gpep > 1 kDa was found to have particle sizes of < 83.2 μm . These results suggest that the complexation of Gpep > 1 kDa with Fe²⁺ ions leads to a reduction in the particle size, which can be attributed to structural folding and molecular structure rearrangement, which some authors called the “bridging role” between Fe²⁺ and peptides’ carboxyl group (Li et al., 2019). The reduction of particle size after complexation can also be confirmed by morphological analysis of Gpep > 1 kDa and Gpep>1kDa-Fe complexes (**Figure 29**), is already been described by other authors (Ferreira et al., 2022; T. Wang et al., 2020).

Table 23. Particle size distribution parameters of peptide fraction Gpep > 1 kDa and Gpep>1kDa-Fe complexes.

		Gpep > 1 kDa	Gpep>1kDa -Fe complexes
Particle size parameters (μm)	Dv10	9.12 \pm 0.04	0.749 \pm 0.001
	Dv50	39.2 \pm 0.1	11.1 \pm 0.1
	Dv90	83.2 \pm 0.3	39.2 \pm 0.1

Results are expressed as average \pm standard deviation ($n=3$). Dv10 - 10th percentile of the cumulative volume distribution, Dv50 - 50th percentile of the cumulative volume distribution, Dv90 - 90th percentile of the cumulative volume distribution.

3.2.4. Conclusion

In summary, this study has demonstrated the potential of waste streams from β -glucan and mannan production processes as a source for eco-friendly Fe-peptide complexes. Through a multifactor factorial experimental design, the optimal conditions for producing these complexes were determined. From a pure mathematical standpoint, the best conditions were pH 6.0 and 1 h of reaction. However, when evaluating reagent consumption and the

final yields, a time of 0.5 h is deemed more reasonable. The presence and quality of the complexes was also evaluated by structural and chemical characterization methods. Thus, a new eco-friendly, waste reducing alternative Fe-complex has been formulated and characterized. These findings suggest that these complexes are promising options for Fe supplementation and merit further studies regarding biocompatibility and bioavailability need to be conducted in order to assess the feasibility of the use of such complexes as Fe supplementation. Additionally, this research also presents a valuable approach to valorising industrial waste streams and reduces the environmental impact by repurposing them in a sustainable way.

3.2.5. Supplementary material

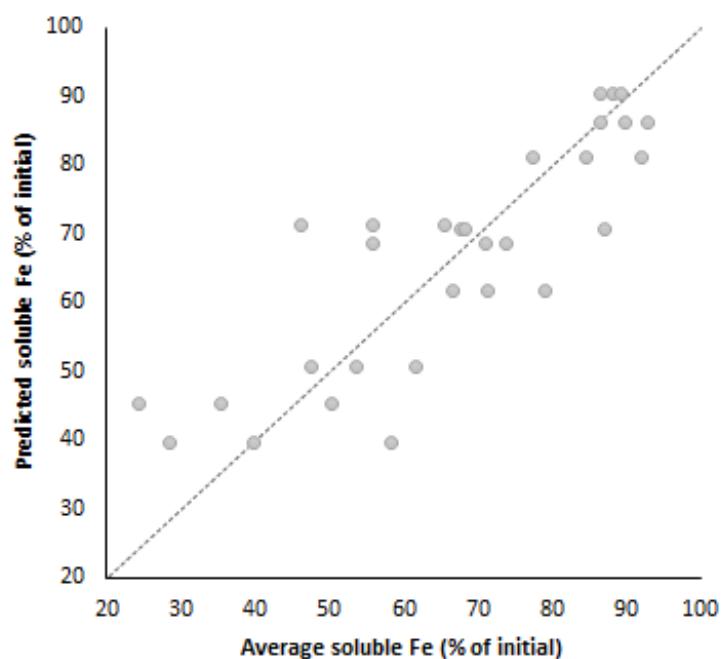


Figure S1. Residual distribution of the fitted model versus the experimental data.

3.3. *In vitro* Fe bioavailability*

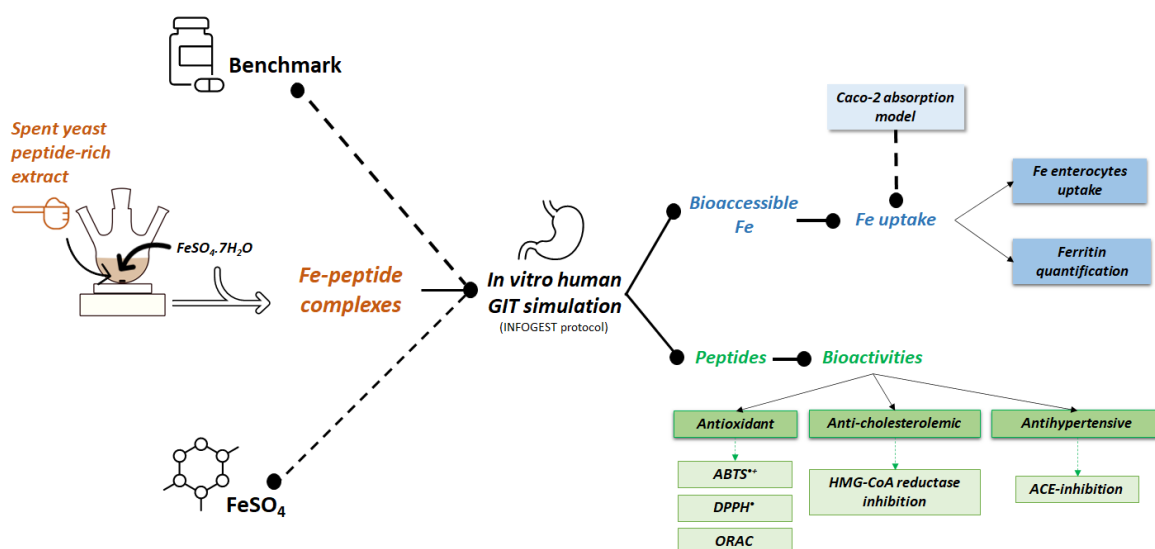


Figure 30. Schematic overview of Section 3.3, demonstrating the *in vitro* absorption performance of Fe-peptide complexes, Fe salt and benchmark. Adapted from the graphical abstract of submitted article*.

3.3.1. Introduction

Dietary intake of Fe includes two forms which are differently absorbed by the human body: heme and non-heme Fe (elemental Fe). Both are mostly absorbed in the first portion of the intestine, namely in the duodenum and proximal jejunum, by differentiated enterocytes geared for vectorial transport of Fe and other nutrients. In fact, Fe movement may be divided into three main steps: 1) Fe entrance in the enterocyte; 2) movement of Fe inside the cell to the basal layer and 3) export of Fe from the enterocyte through the basal layer into circulation (Collins & Anderson, 2012). Heme Fe is present mainly in meat, poultry and fish, being ready to be absorbed by the folate transporter present in duodenal enterocytes. On the other hand, elemental Fe's absorption, found in plant foods in two valence states (Fe^{2+} or Fe^{3+}), may be affected by different factors related to GIT: enzymes, pH and interactions with other food components (phytates, oxalates and polyphenols) (Anderson et al., 2018; Collins & Anderson, 2012; Shubham et al., 2020). To be absorbed by the duodenal enterocytes, elemental Fe needs to be reduced to its ferrous form (Fe^{2+}) by reducing agents and/or enzymes, such as duodenal cytochrome *b*, so it can be later

* Oliveira, A. S, Ferreira, C. M. H., Pereira, J. O., Silva, S., Costa, E.M., Pereira, A. M. P., Faustino, M., Durão, J., Pintado, M. E. & Carvalho, A. P. Iron-peptide complexes from spent yeast: evaluation of iron absorption using a Caco-2 monolayer. Submitted to *Food Bioscience* (8th June 2023)

transported by the divalent metal transporter 1 (DMT1) into the duodenal cytoplasm. Both valence Fe states (Fe^{2+} and Fe^{3+}) are present in the apical layer of the enterocyte where the Fe pathway starts (Anderson et al., 2018; Collins & Anderson, 2012; W. Wu et al., 2020). Besides the challenge of non-heme Fe absorption, the amount of bioavailable dietary Fe is considered low (5-18%) (Eckert et al., 2016), thus contributing to human Fe deficiency, which is the major cause of one of the most prevalent nutritional diseases worldwide - anaemia (W. Wu et al., 2017).

As demonstrated in *Section 3.2. Fe-peptide complexes*, Fe-peptide complexes may be considered as an alternative to conventional salt-based Fe supplementation, since spent yeast peptides were capable of binding Fe, improving its uptake and transport in duodenal enterocytes by the increase of its solubility.

Once Fe-peptide complexes pass intact through the GIT and Fe is released from them at the duodenum, minerals and peptides may follow their usual route for absorption in different pathways. Bioactive peptides may enter the cells through specific peptide transporters present in the intestinal epithelium, such as peptide transporter 1 (PepT1) for di- and tripeptides, endocytosis of the cell membrane for oligopeptides, and paracellular passive diffusion for both (Caetano-Silva et al., 2020; Wada & Lönnerdal, 2014; Y. Zhang et al., 2021). Therefore, it is possible that peptides keep their structural integrity, remaining bioactive for action in the human body. Nevertheless, some authors even defend the possibility of some Fe amount may be absorbed by the same peptide route, since it is not well-known in what manner Fe is absorbed when is bound with organic molecules (Caetano-Silva et al., 2020).

This study aimed to evaluate the performance of Fe-peptide complexes produced from spent yeast during *in vitro* GIT digestion, by calculating the amount of bioaccessible Fe at the end of intestinal phase, together with protein amount and peptides MW profile. Following an *in vitro* GIT simulation, Caco-2 cells were exposed to the digested samples to evaluate the Fe uptake and ferritin (FER) production in enterocytes, so as to understand the potential of complexes to increase Fe bioavailability. Finally, several bioactive properties of the remaining digested peptides were measured, namely antioxidant, antihypertensive and anti-cholesterolemic, to combine a promising Fe-delivery ingredient with peptides' biological value in a single product. A Fe-bisglycinate benchmark and an inorganic Fe salt were added to the study, enabling a comparative performance of our complexes versus alternatives of Fe supplementation (**Figure 30**).

3.3.2. Material and methods

3.3.2.1. Production of peptide fraction

Waste streams resulting from β -glucan extraction from engineered spent yeast (*S. cerevisiae*) were used to produce a peptide rich-fraction through 1 kDa ultrafiltration, as detailed in *Section 3.1.2.2. Peptide-rich extracts production.*

3.3.2.2. Synthesis of Fe-peptide complexes

Fe-peptide complexes were synthesised as explained in *Section 3.2.2.3. Complex formation – anoxic conditions*, using the chosen conditions from the factorial design (protein:Fe ratio of 2:1 (w/w), pH 6.0, 30 min, anoxic conditions). The soluble Fe in the complexes was evaluated by ICP-OES, as described in *Section 2.1.2.4. Minerals.*

3.3.2.3. *In vitro* simulation of human gastrointestinal tract

In order to assess the gastrointestinal performance of Fe-peptide complexes in comparison with different alternatives for Fe supplementation, “Gentle iron” (Fe bisglycinate 20 mg) benchmark (Solgar, Leonia, NJ, USA) and an inorganic Fe salt in the form of ferrous sulphate ($\text{FeSO}_4 \cdot 7\text{H}_2\text{O}$; Sigma-Aldrich, Inc., St. Louis, USA) were used in this study. The three different Fe formulations were submitted to an *in vitro* simulation of human GIT, as adapted from Brodkorb et al. (2019) (International Network on Food Digestion and Health (INFOGEST) protocol). The amount of Fe was standardized among all formulations according to the recommended daily doses of “Gentle iron” for adults: 1 capsule *per* day, which is equivalent to 20 mg of Fe. Therefore, Fe-peptide complexes and Fe salt were weighted and placed into acid-resistant hydroxypropyl methylcellulose (HPMC) capsules (Qualicaps, Whitsett, NC, USA) up to a total Fe concentration of 200 mg/L in INFOGEST protocol. Likewise, according to the information provided by the manufacturer, the benchmark was also encapsulated in HPMC, using bulking and anti-caking agents in formulation of Fe-bisglycinate. An *in vitro* GIT simulation with empty capsules (without any Fe content) was also performed to be used as negative control. Since Fe-peptide complexes are administered in capsule format, the oral phase was skipped, and the digestion was started at the gastric level. At the end of intestinal phase, samples were

heated for 10 min at 80 °C for enzymatic inactivation and then stored at -20 °C until further analysis.

Regarding the study of the bioactivities of the peptides comprised in the complexes and the benchmark, new samples without Fe content were also digested using the GIT protocol: a) “Gpep>1”: peptide extract used for complex production in the same amount presented in Fe-peptide complexes capsules, and b) “Gly”: glycine, in the same amount presented in “Gentle iron” capsules. A GIT simulation without sample was also performed to be used as negative control (“GIT blank”).

3.3.2.4. Fe uptake using a Caco-2 monolayer

Cell culture

The cell culture conditions of human colon carcinoma cells were described in *Section 3.1.2.3. Caco-2 cell culture.*

Cell viability

The cell viability protocol was outlined in *Section 3.1.2.3. Cytotoxicity assay.* GIT samples were filtrated ($\varnothing = 0.45 \mu\text{m}$) to eliminate insoluble material resulting from GIT, so that Caco-2 cells were only exposed to soluble sample fractions. Cells were exposed to decreasing concentrations and different Fe concentrations were observed between the initial samples (**Table 24, dilution 0**) since they correspond to bioaccessible Fe fractions at the end of GIT (**Table 25**). Bioaccessible Fe concentrations and the corresponding successive dilutions in fresh medium are presented in **Table 24**.

Table 24. Bioaccessible Fe concentration (mg/L) of GIT samples and successive dilutions performed for PrestoBlue® assay.

Dilution	<i>GIT control</i>	<i>Fe-peptide complex</i>	<i>Fe salt</i>	<i>Benchmark</i>
5	NA	0.154	0.218	3.08
4	NA	0.308	0.436	6.17
3	NA	0.616	0.873	12.3
2	NA	1.23	1.75	24.7
1	NA	2.47	3.49	49.4
0	NA	4.74	6.98	98.7

NA – Not applicable.

Fe uptake

Caco-2 cells were seeded at 1.5×10^5 cells/mL in cell culture inserts with $0.4 \mu\text{m}$ transparent PET membranes (Corning, NY, USA) placed within 6-well microplates. At each well, 2 mL of cell suspension were added to the apical chamber, whereas 2.5 mL of medium were inserted into the basal chamber. The content of apical and basal chambers was replaced with fresh medium every 2 d until usage (2 mL and 2.5 mL, respectively). Cell culture was kept for 14 more days for differentiation (Lea, 2015).

After 14 days, cells were washed with warm phosphate-buffered saline (PBS) buffer and exposed to GIT samples in apical chamber, with a soluble Fe concentration adjusted to $50 \mu\text{M}$ (A. Sharma et al., 2017; Shilpashree et al., 2020), as this concentration did not show alterations in Caco-2 viability. Before the dilution in fresh medium, the initial GIT samples were filtered (using sterile syringe filters, $\varnothing = 0.22 \mu\text{m}$ (Sartorius, Gottingen, Germany)) to obtain only the soluble Fe fraction, since this is the bioaccessible amount to be potentially absorbed by enterocytes. A volume of 2.5 mL of fresh medium was added to the basal chamber and after 2 h of exposure, the solutions from apical and basal chambers were collected for determination of Fe transport across the Caco-2 monolayers by ICP-OES. Fresh medium was added to both chambers, after washing the cells with warm PBS, that were then returned to the incubator for an additional 22 h period to allow FER synthesis. Afterwards, the content of both compartments was collected for Fe analysis, since the amount of Fe uptake by enterocytes during the exposure time (2 h) might be expelled to the medium until the end of period incubation (24 h). Additionally, to a GIT negative control (GIT sample without Fe content), a plain media control (unexposed cells) was also used in the assay. The enterocytes Fe uptake by enterocytes was calculated by:

$$Fe \text{ uptake ratio} = \frac{\frac{[Fe]_i - [Fe]_{2h}}{[Protein]}}{[Fe]_i}$$

where $[Fe]_i$ is the Fe concentration in the initial samples, $[Fe]_{2h}$ is the Fe concentration of collected samples after 2 h exposure, and $[Protein]$ is the cell well protein concentration. Results are expressed as ng Fe/ng initial Fe. mg protein. The assay was performed in sextuplicate.

Ferritin production

After incubation, cells were washed with cold PBS and scraped with 3 mL of cold 0.5 M EDTA-PBS solution (pH 8.0), the solution was collected, and the process repeated with 1 mL. Samples were then centrifuged ($685 \times g$, 20 min, 4 °C) and the supernatants were discarded. The cell pellets were resuspended in 300 μ L of ice-cold lysis buffer (0.5M EDTA-PBS with 1% v/v Triton X-100 (Sigma-Aldrich, St. Louis, USA)) and incubated on ice for 1 h. Cell lysates were centrifuged again ($18516 \times g$, 30 min, 4 °C) and the supernatants were collected. Cell protein content was evaluated by the Bradford method (Bradford, 1976) using BSA (bovine serum albumin) (Thermo Fisher Scientific Inc., Massachusetts, USA) for calibration.

The FER synthesis by Caco-2 was evaluated in the cell lysates using the Human FER enzyme-linked immunosorbent assay (ELISA) Kit (RAB0197; Sigma-Aldrich, St. Louis, USA) according to manufacturer's instructions. The amount of FER synthesized by the cells was determined by:

$$FER \text{ synthesis} = \frac{[FER_p]}{[Protein]}$$

where $[FER_p]$ is the FER produced amount, after 24 h since the initial exposure, and $[Protein]$ is the cell protein content, and results were expressed in ng FER/mg protein. The assay was performed in sextuplicate.

3.3.2.5. Chemical characterization of GIT samples

Protein content

Protein quantification of samples, before and after GIT protocol, and GIT negative control, was carried out by Dumas (1831) described at *Section 2.1.2.4. Protein*. The multiplication factor for estimation of total nitrogen was 6.25 (AOAC, 2005).

Protein and peptides molecular weight

The protein and peptide MW distribution of Fe-peptide complexes, before and after GIT protocol, and negative GIT control, was performed by LC-ESI-qTOF/MS according to the procedure described in *Section 2.1.2.4. MW distribution*.

Before LC-ESI-qTOF/MS analysis, peptides were concentrated and the Fe was eliminated, using solid-phase extraction (SPE) Lichrolut EN cartridges (40-120 μm , 500 mg, 6 mL) (Merck KGaA, Darmstadt, Germany). These were first preconditioned with acetonitrile and water before loading 15 mL of sample (2.5 g protein/mL). Peptides were eluted with 5 mL of acetonitrile and then injected.

Fe determination

The determination of Fe in Fe-peptide complex, benchmark and Fe salt, before and after GIT and Caco-2 cell exposure, was performed by ICP-OES using the methodology described in *Section 2.1.2.4. Minerals*.

3.3.2.6. Biological activity of GIT samples

ACE inhibition assay

The ACE inhibition assay was performed according to the protocol described in *Section 2.2.2.4. ACE inhibition assay*. The assay was performed in triplicate.

Antioxidant capacity

Scavenging activity using ABTS

The ABTS^{•+} scavenging activity was assessed by the method described in *Section 2.2.2.4. Scavenging activity using ABTS*. The Trolox standard curve was used to express TE antioxidant activity of samples ($\mu\text{mol/g}$ protein). The assay was performed in triplicate.

Scavenging activity using DPPH[•]

The DPPH[•] scavenging activity was assessed by the method described in *Section 3.1.2.3. Scavenging activity using DPPH[•]*. The Trolox standard curve was used to express TE antioxidant activity of samples ($\mu\text{mol/g}$ protein). The assay was performed in triplicate.

Oxygen radical absorbance capacity

ORAC assay was assessed as described in *Section 2.2.2.4. ORAC*. The Trolox standard curve was used to express TE antioxidant activity of samples ($\mu\text{mol/g}$ protein). The assay was performed in triplicate.

HMG-CoA reductase inhibition assay

HMG-CoA Reductase Activity Assay Kit was used for assessing the HMG-CoA reductase inhibition according to the description in *Section 2.2.2.4. HMG-CoA reductase inhibition assay*. The assay was performed in triplicate in two independent plates.

3.3.2.7. Statistical analysis

The statistical analysis was performed using the Real Statistics Resource Pack software (Release 7.2). Outliers were excluded using the interquartile range method with multiplier of 2.2 and data normality was checked using the Shapiro-Wilk test. Fe and FER results from different groups of Caco-2 uptake assay were subjected to one way ANOVA followed by Tukey's post hoc test.

3.3.3. Results and Discussion

3.3.3.1. *In vitro* simulation of gastrointestinal tract

Fe bioaccessible (%)

The soluble Fe content of samples subjected to simulated *in vitro* GIT were analysed at the end of the intestinal phase, since this fraction corresponds to its bioaccessible fraction which can potentially be absorbed by the duodenal enterocytes (**Table 25**).

Table 25. Final soluble Fe concentration (mg/L) in samples after *in vitro* GIT simulation and its percentage (%) in comparison with initial protocol concentration (200 mg/L).

	<i>GIT control</i>	<i>Fe-peptide complex</i>	<i>Fe salt</i>	<i>Benchmark</i>
<i>Soluble (mg/L)</i>	0.741 \pm 0.138	4.74 \pm 0.31	6.98 \pm 0.30	98.7 \pm 1.1
<i>% of initial content</i>	NA	2.37 \pm 0.15	3.49 \pm 0.15	49.3 \pm 0.6

Results are expressed at average \pm standard deviation ($n=2$). NA- non applicable.

This fraction was obtained by filtrating the suspended solid particles from the digested samples ($\phi = 0.45 \mu\text{m}$) obtained during GIT protocol. Since initial GIT samples were prepared to obtain a Fe concentration of 200 mg/L, it was observed that benchmark showed the highest percentage of bioaccessible Fe ($49.3 \pm 0.6\%$ from the initial), followed by Fe-peptide complex ($2.37 \pm 0.15\%$) and Fe salt ($3.49 \pm 0.15\%$), with no significant differences between them. Despite the expectations, a negligible concentration of soluble Fe was observed in GIT control (**Table 24**) which can be related with impurities of enzymatic solution reagents used in GIT protocol since pepsin, pancreatin and bile are powder extracts derived from porcine (Sigma-Aldrich, Inc., St. Louis, USA).

Since all samples were submitted to GIT simulation in acid resistant HPMC capsules, the behaviour of Fe salt followed the expected pattern, where on intestine environment, the Fe salt was released from the capsule and the soluble Fe may precipitate, making it unavailable to be absorbed. This result were consistent with those of Wang et al. (2011), which obtained a percentage of Fe-release above 5% at pH 7.0 for FeSO_4 . Otherwise, the small amount of bioaccessible Fe in the peptide complex sample was not expected, since the binding should have protected the mineral from becoming insoluble under intestinal conditions, as occurred with the benchmark, where almost 50% of Fe was bioaccessible (**Table 25**). The reported benchmark results for ferrous bisglycinate are consistent with those from previous studies, which showed an absorption rate of approximately 40% (S. Lin et al., 2021). These data suggests that HPMC capsules used for preparation of Fe salt and complexes for GIT protocol seem not to be the most suitable material. In fact, it has been shown that HPMC is capable of absorbing Fe^{3+} in a pH range of 3.0 to 7.0 from 100 to 1000 ppm (Sözüğeçer & Bayramgil, 2013). For this reason, it is therefore possible that Fe^{2+} may also be absorbed into the HPMC solid debris. This potential HPMC adsorption of Fe was not observed for benchmark, possibly due to differences in the capsule's characteristics, although both are reported having the same base material. The use of bulking agents on the benchmark formulation may also have protected Fe from becoming insoluble during the GIT protocol, being responsible for its high bioaccessible fraction in relation to complexes.

On the other hand, another possible explanation for the low amount of bioaccessible Fe in our complex may be related with peptide degradation during intestinal GIT phase, when the capsule content is released. In fact, complexation reaction increases Fe solubility and bioavailability, if the peptides chosen for the reaction are digestion-resistant to protect Fe through the chemical changes along GIT (Caetano-Silva et al., 2020). Although the stomach's low pH will increase Fe solubility, since its reduced form (Fe^{2+}) is promoted, the

protonation of Fe-binding sites will weaken the metal-peptide bounds, which may lead to Fe release from peptides before they arrive at the duodenum to be absorbed (Caetano-Silva et al., 2020). For this reason, and limiting the potential mineral interaction with food components, acid-resistant capsules were used in the present study as reported by other authors (Bryszewska, 2019; Filiponi et al., 2019).

At intestinal pH, the Fe-peptide bounds are favoured because of the deprotonation of peptides amino acids residues' carboxyl groups, increasing complex stability. However, if peptides used were less efficient in binding Fe at this phase, some non-complexed Fe could precipitate, since free Fe solubility decrease at duodenum alkaline pH, making it unavailable to be absorbed. Indeed, similar preliminary results were previously observed, when increasing the pH of complex production from 6.0 to 7.0 lead to a decrease in soluble Fe from 88.0% to 53.4% (*Section 3.2. Fe-peptide complexes*). For this reason, the Fe released from peptides at this stage may be bound to other molecules of GIT solutions (Caetano-Silva et al., 2018), turning insoluble and thus not bioaccessible. Indeed, the strength of Fe-peptide bound is the key: it must be strong enough to prevent Fe release before duodenum, preventing its complexation with other diet components, but, at the same time, weak enough to allow the Fe release to be transported by carriers in the apical site of enterocytes (Caetano-Silva et al., 2020).

Protein profile

In an attempt to evaluate the protein profile of Fe-peptides complexes, before and after digestion, analysis of peptides MW and protein content (%) were performed.

Before GIT, the percentage of peptides < 1500 Da rounded about 85% (**Figure 31**), which is of particular relevance, as peptides with MW between 300 and 1500 Da are described to hold higher affinity for binding with Fe (W. Wu et al., 2020).

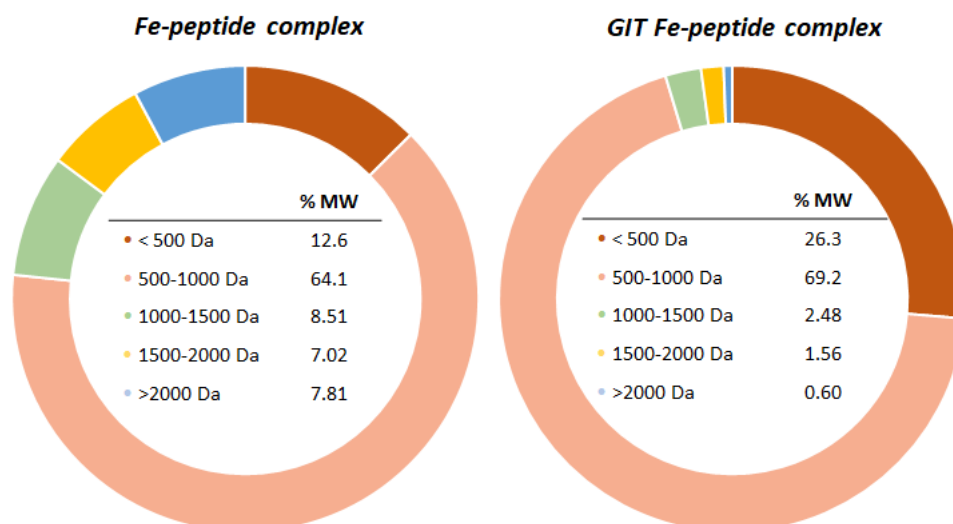


Figure 31. Peptides MW distribution (%) in Fe-peptide complex before (left) and after (right) in vitro GIT simulation.

After GIT, this percentage increased to 98%, as expected, due to the degradation of the peptides under GIT's different conditions. The decrease of complexed peptides size during simulated GIT was already reported by Lin et al. (2021). For this reason, it would be important to explore how this degradation may affect the binding Fe-peptides, as well as study other peptide features as structure, amino acid composition and steric effects, in order to understand how the binding strength of Fe-peptides in complexes production can be improved to make Fe from complexes at the end of intestinal phase more bioaccessible to be absorbed (Gómez-Grimaldos et al., 2020). However, these analyses were not performed in this work since Fe-peptide complexes were prepared using a peptide-rich extract originating from a yeast by-product that, despite containing 67.2% of protein (w/w), was also composed of other components, such as sugars and residual minerals (A. S. Oliveira et al., 2022). These components hinder the possible evaluation of the peptide sequence and, consequently, the study of the complexes' binding mechanism. In fact, in a similar study, Athira et al. (2021) were not successful in reaching a conclusion about the binding mechanism and how this may influence the Fe bioaccessibility at different chemical environments during GIT, as they identified too many amino acid sequences in the used whey protein hydrolysates. On the other hand, some authors included chromatographic processes for peptides or complexes purification, thus making the identification of amino acid sequences and their potential sites for mineral binding easier (Caetano-Silva et al., 2015; W. Wu et al., 2017). However, the inclusion of this additional step would drastically

increase the complex production cost, making it not cost-effective (A. S. Oliveira, Ferreira, et al., 2022b), and, for that reason, it was not considered in the present study.

Regarding the protein content, the initial amount on Fe-peptide complex ($20.8 \pm 0.9\%$; w/w) was enhanced to $45.5 \pm 2.0\%$ after digestion. However, it must be pointed out that the main contributor for this increase was the enzymatic cocktail used in GIT protocol, since the final protein content of other samples subjected to the same digestion procedure have similar results (GIT control: $45.3 \pm 0.2\%$, Fe salt: $44.2 \pm 0.9\%$ and benchmark: $43.6 \pm 1.3\%$). Indeed, the same tendency was observed in benchmark, since the protein percentage increased from $17.7 \pm 0.7\%$ to $43.6 \pm 1.3\%$ with GIT.

3.3.3.2. Fe uptake study

After the determination of bioaccessible Fe following the GIT simulation, the evaluation of the amount that enters in duodenal enterocytes (bioavailable Fe) is fundamental, because the condition “higher bioaccessibility, higher bioavailability” is not always observed (Caetano-Silva et al., 2020). For this reason, an *in vitro* model using a Caco-2 monolayer was exploited to evaluate Fe uptake of the Fe-peptide complexes, “Gentle iron” benchmark and Fe salt samples, together with negative GIT control (without any Fe content). Caco-2 cells have been described as the reference *in vitro* model, since this cell line spontaneously differentiates, acquiring similar characteristics to mature enterocytes, thus acting as the intestinal mucosa barrier and simulating the absorption conditions in humans. Moreover, this cell line has been shown to be suitable for food Fe bioavailability studies (Gómez-Grimaldos et al., 2020) since it occurs via DMT1 that is expressed in the apical side of these enterocytes.

Cell viability

Before the uptake assay, Caco-2 were exposed to filtered GIT samples for 24 h, according to ISO 10993-5:2009 protocol (International Organization for Standardization, 2009), to understand the effect of GIT matrix on cells and to select a non-cytotoxic concentration for the Fe uptake protocol. The toxicity of Fe^{2+} is related to the excessive production of free radicals, which influence cell membrane stability, leading to the initiation of lipid peroxidation and DNA damage. However, some authors have described a toxicity decrease when Fe^{2+} is bound to the peptides (Eckert et al., 2016).

Regarding Fe concentrations (**Table 24**), Caco-2 metabolism was inhibited by more than 30% (30.1% to 68.4%) only when exposed to direct GIT samples (dilution 0), which means that these concentrations are cytotoxic and cannot be used in the subsequent assay. Despite the fact that all diluted samples displayed no cytotoxic effects against Caco-2, Fe concentration was adjusted to 50 μ M for the uptake assay, as suggested by other authors (A. Sharma et al., 2017; Shilpashree et al., 2020), which is equivalent to 2.8 mg/L of Fe. The GIT control sample was also diluted for uptake assay, used as control of GIT matrix, based on dilution of Fe-peptide complexes. The non-cytotoxic profile of the diluted samples (**Table 24**, dilution 1 to 5) are in agreement to Wang et al. (2014) since they did not observe a significant decrease of Caco-2 viability from 10 to 50 mg/L Fe of digested lactoglobulin hydrolysate-Fe complexes.

Fe uptake and ferritin production

After 14 days of cells differentiation to allow for a monolayer formation and cell polarization, Fe uptake by Caco-2 was performed and the Fe was measured on initial exposure solutions (GIT samples diluted for 50 μ M in fresh medium), and on solutions from apical and basal chambers after Caco-2 exposure (2 h and 24 h) by ICP-OES. However, after Fe analysis of initial samples, it was observed that Fe concentrations were not corresponding to the theoretical concentration of 50 μ M prepared (2.8 mg/L) (**Table 26**).

Table 26. Fe concentration (mg/L) on initial samples of Caco-2 exposure (GIT samples theoretically diluted for 50 μ M in fresh medium).

	<i>Fe-peptide complexes</i>	<i>Control GIT</i>	<i>Fe salt</i>	<i>Benchmark</i>
Initial Caco-2 exposure	0.750	< LOD	0.863	2.51

<LOD – below limit of detection

These variations may be related to the formation of some precipitates during samples' freezing, since they were preserved at -20 °C after GIT until being used for Fe uptake protocol. The calculation of Fe uptake rate by enterocytes was performed by the difference of Fe concentration at initial samples, and apical after 2 h exposure, being normalized by initial exposure Fe for final calculation, to compare the results between the different samples. Indeed, the inclusion of this normalization step is essential for an accurate calculation since the exposure of enterocytes to higher Fe concentrations in some samples may influence the expression of genes involved in cellular Fe metabolism, which may subsequently promote or decrease Fe uptake (Kalgaonkar & Lönnnerdal, 2009). The ratio of

Fe:protein (ng Fe/ng initial Fe.mg protein) was also used as an index of Fe uptake as a measure of normalization for the number of cells exposed.

The results of Fe uptake of Fe-peptide complexes, Fe salt and benchmark are presented in **Figure 32**.

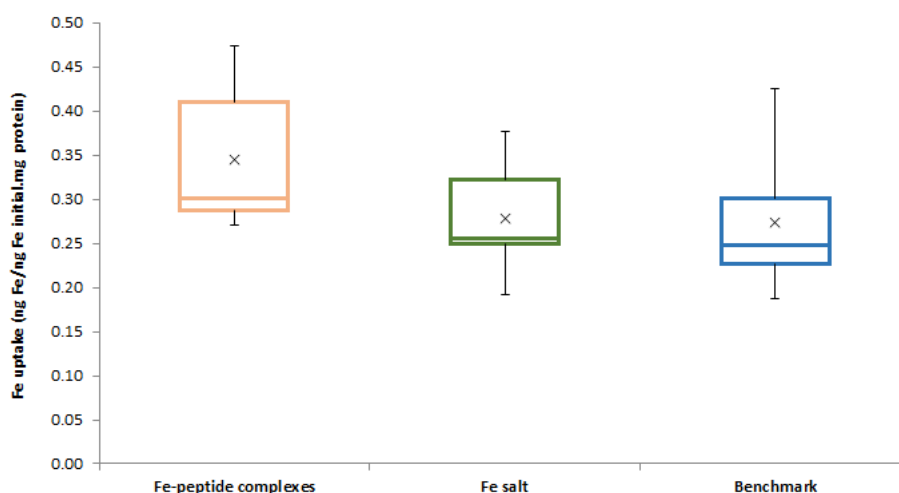


Figure 32. Fe uptake by Caco-2 cells exposed to Fe-peptide complexes, Fe salt and benchmark. All samples were compared by Tukey's test ($n=6$).

On average, our Fe peptide complexes recorded higher ratios of Fe uptake than those recorded for Fe salt and benchmark. However, no statistically significant differences were found in Caco-2 Fe uptake between all samples ($p > 0.05$).

As expected, no Fe was detected in cell culture medium collected from Caco-2 control ($< \text{LOD}$). Fe was also not detected at basal samples ($< \text{LOD}$), meaning that it was stored in the enterocytes, and was not excreted for the extracellular medium. The same result was observed in fresh medium collected after 24 h exposure at apical and basal solutions, confirming this assumption.

Additionally, the FER produced in enterocytes was also quantified, since Caco-2 can synthesize this protein in response to high intracellular Fe levels (Shilpashree et al., 2020). Indeed, it was observed an increase of FER levels in cells exposed to the different Fe-containing samples (3.26 to 3.33 ng/mg protein) regarding cells exposed to GIT control (2.88 ± 0.08 ng/mg protein), evidencing that Fe enters the enterocytes and suggesting its transport by cell membrane and subsequent retention (A. Sharma et al., 2017), thus confirming our results for Fe uptake by Caco-2 (**Figure 32**). These results are presented as FER produced in relation to GIT control cells in **Figure 33**.

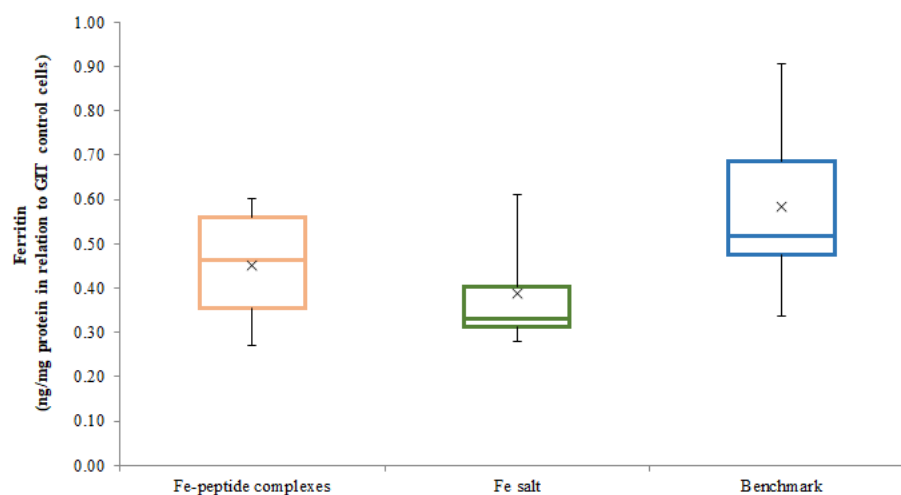


Figure 33. FER produced by Caco-2 cells exposed to Fe-peptide complexes, Fe salt and benchmark in relation to cells exposed to GIT control. All samples were compared by Tukey's test ($n=6$).

However, no statistically significant alterations were found between Fe-peptide complexes, Fe salt and benchmark ($p > 0.05$) as shown by Fe uptake (**Figure 32**). Since FER production in Caco-2 is possibly related to Fe bioavailability, a correlation of FER levels and Fe uptake was explored using Pearson's method. However, no significant relation was found ($p > 0.05$).

Looking at the obtained results, it is possible to affirm that our Fe-peptide complexes led to an increase of Fe uptake and FER production. However, this increase appears trivial when compared to other studies that reported a significant Fe uptake and increase of FER synthesis by Caco-2 cells when exposed to digested Fe-peptide complexes, using natural peptides from different sources as ligands (Caetano-Silva et al., 2018; Chen et al., 2017; Eckert et al., 2016; Filiponi et al., 2019; García-Nebot et al., 2013; A. Sharma et al., 2017; Shilpashree et al., 2020; X. Wang et al., 2014). A possible explanation for this difference may concern the different digestion protocols used. In fact, the abovementioned authors use comparatively simple digestions procedures, with demineralized digestive enzymes (pepsin and pancreatin-bile solutions) with the appropriate pH values readjusted. Differently, in this work, digestion of the samples was attained using the INFOGEST protocol (Brodkorb et al., 2019), recently developed by this international research network to better mimic the human physiological conditions and the complex digestion process that undergoes in the human digestive tract. This international standardized methodology requires, however, an elaborated GIT matrix comprising, among other elements, several electrolytes that may be affecting the different cellular mechanisms, such as their metabolism (e.g., adenosine triphosphate (ATP) cell

content and cell barrier integrity), by hyperosmotic stress (Grauso et al., 2019), thus compromising the cells stimulation for Fe uptake and consequently FER synthesis. Furthermore, bile salts used in the GIT matrix, which are likely to still be present in samples, have been reported to hold emulsifying properties (Garner et al., 1991; Neves et al., 2019), that can provoke cell membrane lysis. Nevertheless, as far as our knowledge extents, this has been the first time that the INFOGEST protocol was used for the digestion of Fe-peptide complexes. Furthermore, as per our current knowledge, this has also been the first time that peptides from engineered spent yeast waste streams were used to evaluate Fe *in vitro* absorption from complexes, using a circular economy approach. Finally, different *in vitro* methodologies already described in literature, from GIT (Brodkorb et al., 2019) to Caco-2 exposure to Fe complexes (Caetano-Silva et al., 2018; Remondetto et al., 2004; A. Sharma et al., 2017; Shilpashree et al., 2020) have been combined and adapted in this work to develop alternative methodologies to understand the performance of our ingredient regarding other Fe supplementation alternatives.

The mechanism of Fe-peptide complexes' entry in the enterocyte is still unclear since it is not consensual how Fe is absorbed when bound to organic molecules. Some authors pointed out the DMT1 carrier as the main responsible, since it is expressed at apical site of enterocytes in human body, but other studies described the expression of other transporters which appear to function independently of DMT1 (Aly et al., 2016). On the other hand, the peptides' carrier PepT1, also expressed in the intestinal epithelium, may also be involved in Fe absorption since low MW peptides are bound to this mineral (Caetano-Silva et al., 2020).

FER synthesis has also been used to evaluate Fe uptake by enterocytes as an indirect measure since cells synthesize this protein in response to increasing intracellular Fe levels. This intracellular protein has the ability to store Fe, releasing this mineral in a controlled environment when needed (Brissot & Loréal, 2016). However, the regulation of Fe absorption *in vivo* involves the communication of epithelium with other organs, such as liver via hepcidin production, which points out a limitation of using only Caco-2 cell line as *in vitro* model of Fe absorption (Scheers et al., 2014). For this reason, in spite of the Fe uptake and FER synthesis enhancement observed by our Fe-peptide complexes at Caco-2, it might be interesting to reproduce this study using co-culture models including hepatocytes (e.g. HepG2) for a closer physiological approach. Another co-cultured model that would better translate the complexity of the intestinal interface would consider a membrane seeded using a mucus-producing intestinal cell line (HT-29-MTX), since Laparra et al. (2009) observed

that mucin production can tightly regulate Fe absorption by modulating the expression of DMT1.

Given their performance, our Fe-peptide complexes, seem to be a promising alternative for Fe dietary supplementation, since they had a similar behaviour to Fe salt and to the benchmark regarding the Fe uptake levels and FER synthesis (**Figure 32 and Figure 33**). In fact, complexes can be considered a better choice than Fe salt for supplementation, since the latter have the disadvantage of Fe-binding with absorption inhibitors during GIT, such as phytates and phenolics, that are usually present in a normal diet (Chen et al., 2017).

It was also demonstrated that high Fe bioaccessibility was not directly related to its high bioavailability, as the benchmark showed the highest value of soluble Fe after GIT (**Table 25**) but similar values of Fe uptake and FER production were observed when comparing to Fe-peptide complexes and Fe salt (**Figure 32 and Figure 33**). This hypothesis was already pointed out by other authors (Caetano-Silva et al., 2020) and is further corroborated in the present study.

3.3.3.3. Biological activity of GIT samples

ABTS^{•+} and FRAP activities of whey protein Fe-complexes have been reported to decrease after Fe complexation, regarding the original whey peptides, by Athira et al. (2021) thus, suggesting the influence of Fe on redox mechanisms of the methods used for bioactivity evaluation. For this reason, and assuming that Fe released from peptides at the end of GIT follows its pathway thus being absorbed into the blood, the remaining peptides of Fe-peptide complexes might remain bioaccessible in the human body and be absorbed as well. Regarding the “Gentle iron” benchmark (Fe bisglycinate) the same assumption was taken, which would result in a substantial amount of free glycine bioaccessible at the end of GIT to be transported into the bloodstream. Following this assumption for both samples, and considering the importance of bioactive peptides in several physiological functions in the human body (A. S. Oliveira et al., 2022), new samples without Fe content were digested using the GIT protocol and their potential bioactivities for nutraceutical market were assessed. The results for antioxidant capacity, antihypertensive activity (ACE) and anti-cholesterolemic activity (HMG-CoA reductase inhibition) are shown in **Table 27**.

Table 27. Antioxidant activity (ABTS⁺, DPPH[•] and ORAC), expressed as $\mu\text{mol TE/g}$ of protein, and inhibition percentage (%) of ACE and HMG-CoA reductase of GIT samples: blank, Gpep > 1 kDa and Gly.

	ABTS ⁺	ORAC	DPPH [•]	HMG-CoA*	ACE*
	$\mu\text{mol TE/g protein}$			% inhibition	
GIT blank	220 ± 42	200 ± 8		22.2 ± 7.9	40.3 ± 0.5
Gpep > 1 kDa	238 ± 63	761 ± 22	< LOQ	33.3 ± 3.9	40.8 ± 1.9
Gly	231 ± 51	357 ± 11		36.1 ± 0.0	33.2 ± 1.1

Results are expressed in average \pm standard deviation ($n=3$). < LOQ – Below limit of quantification, *For Caco-2 biocompatible extract concentration reported at Oliveira et al. (2022)

Regarding the antioxidant properties, all samples showed ability to reduce ABTS⁺ but no significant differences were observed between GIT blank and samples (**Table S10**), which may suggest that Gpep > 1 kDa and Gly do not present scavenging ABTS⁺ activity. Likewise, it was not demonstrated scavenging DPPH[•] activity of GIT blank or samples since the values found were below the method detection limit (**Table 27**). In fact, ABTS⁺ is a more reactive radical than DPPH[•] which may lead to biased results, and thus is important to support its results with other assays (Mareček et al., 2017). On the other hand, Gpep > 1 presented the highest ORAC activity ($761 \pm 22 \mu\text{mol TE/g protein}$), followed by Gly ($357 \pm 11 \mu\text{mol TE/g protein}$) and blank ($200 \pm 8 \mu\text{mol TE/g protein}$) ($p < 0.05$) (**Table S10**). The values obtained for Gpep > 1 kDa are in accordance to Xiao et al. (2022) and Conway et al. (2013), which studied antioxidant properties of chicken, buttermilk and whey protein hydrolysates. In fact, yeast peptides were already described for their antioxidant properties demonstrated by ORAC (M. Amorim, Marques, et al., 2019; Costa et al., 2023). Nevertheless, glycine and its derivatives were also reported by their high scavenging activity (Kitts, 2021; Shen et al., 2019; Suh et al., 2003) which is according to their described human body protective effect against oxidative damage since this non-EAA is used for glutathione synthesis (Díaz-Flores et al., 2013; Pérez-Torres et al., 2016).

Indeed, the differences observed on the three scavenging activity assays may be related to their different mechanisms of oxidative chain reactions, producing different free radicals. Phenomena of redox mechanisms are involved in ABTS⁺ and DPPH[•] assays but the former involves the reduction of cation-radical ABTS⁺ into ABTS^{•+} by electron transference of an antioxidant, while DPPH[•] is reduced by hydrogen atom donation of an antioxidant (A. S. Oliveira et al., 2022). On the other hand, ORAC assay is also based on hydrogen transference but its biologically more relevant than other scavenging assays because the radical generated, peroxy, is also found in physiological conditions (Prior et al., 2003).

On the other hand, Gpep > 1 kDa did not show a higher inhibition of ACE and HMG-CoA reductase than the blank, which indicates that no antihypertensive and anti-cholesterolemic effects were found after GIT. In fact, in order to maintain their bioactive properties, peptides need to resist GIT degradation to reach the blood stream in an active form (Coscueta et al., 2019). However, in the present study, this may not be the main reason for the lack of these bioactive properties since only a small amount of peptides remains after GIT, being samples mainly composed by the protein content of GIT enzymatic matrix, which indicates that it may not be correct to relate the decrease of bioactivity to digested yeast peptides. Indeed, peptide rich-fractions from spent yeast (> 1 kDa) already demonstrated HMG-CoA inhibition at 1.5 and 2.5 mg/mL (60-70%) and a IC50 of 1.5 mg/mL at ACE-inhibition assay (A. S. Oliveira et al., 2022), which suggests that the absence of effect may be influenced by the low peptides concentration.

3.3.4. Conclusion

Fe-peptide complexes produced from spent yeast peptide-rich extracts showed potential as promising alternatives for Fe dietary supplementation. After *in vitro* GIT digestion, the resulting bioaccessible Fe amount was absorbed by the duodenal enterocytes, resulting in the promotion of FER synthesis. Moreover, Fe complexes had a similar performance to Fe salt and a benchmark of Fe-bisglycinate, without having Fe salt's disadvantages of binding with food compounds during GIT and causing health problems, such as gastrointestinal irritations. Additionally, peptides from the complexes demonstrated antioxidant properties which may be important to protect Fe from oxidation during the different GIT environments and is a valuable bonus to the Fe supplementation. Further *in vivo* studies of Fe-peptide complexes should be conducted, since several compounds produced by other organs other than the intestine are involved in the Fe absorption mechanism.

3.3.5. Supplementary material

Table S10. P-values of comparison of antioxidant activity (ABTS^{•+} and ORAC) and inhibition percentage (%) of ACE and HMG-CoA reductase between GIT samples: blank, Gpep > 1 kDa and Gly.

	ABTS ^{•+}	ORAC	HMG-CoA	ACE
GIT blank vs. Gpep > 1 kDa	6.61E-01	2.92E-08	2.19E-01	8.89E-01
GIT blank vs. Gly	8.66E-01	3.60E-05	1.38E-01	1.32E-03
Gpep > 1 kDa vs. Gly	9.31E-01	1.88E-07	8.55E-01	9.16E-04

n=3

Chapter 4

Final remarks

- 4.1. Conclusions*
- 4.2. Future work*

4.1. Conclusions

The present thesis showcases the potential of using engineered spent yeast from synthetic biology industry aiming to contribute towards several of the United Nations Sustainable Development Goals. It also aims to enhance human nutrition, optimize food resources, and promote sustainability through the establishment of circular economy principles. Furthermore, considering the recent growing amount of spent yeast generated by this industry, as well as its high protein content, the creation of added value products aimed at the nutraceutical markets, similar in characteristics to the ones obtained from the accepted wild brewers spent yeast, was an important goal of the present work.

Taking this into account, this work started off by first applying several extraction methodologies of protein and peptides from yeast, already extensively described in the literature, to produce peptide-rich extracts from two different strains of engineered spent yeast (**Chapter 2.1**). Their protein-related nutritional performance was then evaluated and compared with the peptide rich-extracts produced from a non-engineered spent yeast strain, together with the assessment of the applied processes in terms of protein recovery and sustainability. It was concluded that the engineered spent yeast peptide-rich extracts had a similar performance to the wild type, with a protein content ranging from 25.3% to 54.5%, and 68.7% to 99.0% of peptides < 3 kDa, being an alternative to animal protein sources for application in a healthy and balanced diet. Regarding the sustainability topic, after calculation of biomass and water consumption metrics, autolysis showed to be the most sustainable approach for extract production, though other green metrics, such as energy consumption and economic balance, need to be deeply explored in order to establish this process at an industrial level. Therefore, taking into account sustainability and protein recovery from all processes, together with protein content of final extract and their low MW peptides, the ESY1 autolysate extract was chosen for the subsequent peptides purification study, aiming to explore their potential bioactivities (**Chapter 2.2**). Two extremely distinct methods in terms of cost-effectiveness separation and purification (ultrafiltration and SEC) were used for the production of bioactive peptides from ESY1. The effects of the obtained fractions were evaluated regarding antimicrobial, antihypertensive and antioxidant potential, and compared with the original ESY1 autolysate. Two ultrafiltration and four SEC fractions were produced, with peptides thus separated by MW, and the protein concentrated in some

fractions with the removal of some undesirable yeast extraction remaining compounds and debris.

All fractions showed high ACE inhibition (IC₅₀: 1.80 to 3.21 mg/mL), together with ABTS^{•+} scavenging activity (77.4 to 300 μmol TE/g) and ORAC (237 to 43610 μmol TE/g), thus revealing several promising properties for the formulation of one single product with distinct biological activities for the nutraceutical market. Indeed, all fractions are mostly constituted by peptides with similar MW (≤ 1 kDa) which aligns with the observed similarity in bioactivity outcomes. However, HMG-CoA reductase inhibition observed for the fractions (~ 70%) was stronger than that of the original ESY1 (~40%), which may indicate the need to include a purification step to enhance the cholesterol-lowering properties. To the best of our knowledge, the HMG-CoA reductase inhibition by spent yeast peptides was demonstrated for the first time in the present thesis. For this reason, and concerning the ultrafiltration and SEC cost-effectiveness, ultrafiltration seems to be the most suitable method for peptide-rich extracts production targeting the nutraceutical market.

Beyond the use of engineered spent yeast, the present thesis also adapted the previously applied methodologies to the rich-in protein waste streams arising from mannans and β-glucans extraction from spent yeast, in order to comply with the circular economy concepts (**Chapter 3.1**). Indeed, ultrafiltration allowed the production of extracts with interesting characteristics from a nutritional point of view, including high protein (67.2% to 86.4%) and EAA (119 to 368 mg/g protein) contents, above the FAO/WHO EAA references. Regarding their bioactivities, the extracts inhibit ACE (IC₅₀: 0.99 to 1.72 mg/mL) and HMG-CoA reductase (62.0% to 71.3%), reduce ABTS^{•+} (337 to 492 μmol TE/g) and DPPH[•] (110 to 133 μmol TE/g), and protect from peroxy radicals' production (654 to 1041 μmol TE/g). Indeed, these extracts presented similar nutritional and bioactive performances than peptide-rich fractions directly extracted from spent yeast, thus they are also potentially interesting ingredients for the nutraceutical industry. Regarding different fractions performance on both studies, we hypothesized about peptides MW and hydrophobic amino acids, but these assumptions were not always corroborated. In fact, synergic, antagonism or additive effects may occur since we are working with extracts and not with pure ingredients, hampering the explanation for the bioactivities observed.

Considering the presence of some amino acids on the waste streams peptide-rich extracts that are known for the formation of coordinated covalent bonds with Fe, such as Asp, Glu, Cys, Ser, His, Lys and Arg, the optimization of Fe-peptide complexes formulation was performed in an attempt to produce dietary supplements targeted for the anti-anaemic market

without the side effects described for Fe salts, and also as a sustainable competitor for the Fe-bisglycinate already present in the market (**Chapter 3.2**). During the screening of the different fractions, the use of nitrogen revealed to be an essential condition for obtaining a significant degree of complexed Fe, and fractions > 1 kDa presented high soluble Fe amount. For that reason, Gpep > 1 kDa was chosen for condition optimization using a factorial design. Results showed that the optimal conditions for complexation were pH 6.0, during 30 min, using a Fe:protein ratio of 2:1, which allowed to obtain 88.0% of complexed Fe. The binding of Fe to peptides' extract was confirmed by comparative analysis of complexes and Gpep > 1 kDa samples through XRD, fluorescence, FTIR, SEM and particle size analysis. The obtained results revealed the potential of waste streams peptide-rich extracts to be used as Fe supplementation in the form of Fe peptide complexes. To assess the feasibility of such claim, Fe-peptide complexes were subjected to *in vitro* GIT simulation, using the recommended Fe supplementation dose for human (20 mg/day), followed by an *in vitro* study of Fe uptake from complexes by enterocytes, the responsible cells for Fe uptake and transport to the bloodstream (**Chapter 3.3**). A Fe-bisglycinate benchmark and an Fe salt were added to the study in order to evaluate the performance of our complexes regarding commercially available Fe supplementation alternatives. After GIT, Fe-complexes and Fe salt showed similar Fe bioaccessible values (2% to 3%), contrasting with benchmark (49%), which may be mainly related with Fe protection promoted by the bulking and other agents only present in the commercial formulation. However, an identical profile of Fe uptake and FER production in Caco-2 cells was observed for the three samples, which makes Fe-peptide complexes a promising alternative for Fe dietary supplementation, without having Fe salt's disadvantages of binding with food compounds during GIT and causing health problems, such as gastrointestinal irritations. Additionally, the remaining GIT peptides demonstrated to have antioxidant properties, which may contribute to Fe protection during GIT, contributing with a, additional valuable bioactive property to the anti-anaemic product.

Overall, engineered spent yeast and the resulting waste streams from the production of mannans and β -glucans have the potential to be valorised into several protein-based products and to be marketed in the nutraceutical market, owing to their similar nutritional and biological performances when compared to non-engineered strains and benchmarks. Furthermore, this approach contributes for the implementation of circular economy, sustainable food resources alternatives and additional commercial alternatives of Fe-delivery supplements.

4.2. Future work

Overall, the present thesis showed the potential of using engineered spent yeast to produce compounds with suitable nutritional and bioactive characteristics for application as dietary supplements in nutraceutical market. However, the proposed products may contain some residual genetic yeast material that has been modified and which was not evaluated. For this reason, an extensive scientific risk assessment should be performed, regarding Food and Drug Administration (FDA) and European Food Safety Authority (EFSA) genetically modified organisms' (GMO) regulations, to understand their eventual market limitations before commercialization. In fact, there is a massive discussion about the safety of GMO products, highlighting the importance of this sort of studies, since alternatives to natural food sources need to emerge because of the exponential growth of world's population.

Another relatable problem is the nucleic acids content in our peptide-rich extracts, since one of the challenges from yeast food supplements targeted for human consumption is their presence and removal, mainly RNA. High intake of nucleic acids may result in health issues, such as uric acid increase (resulting in "gout"). However, some of the described processes for their reduction involved treatments using strong chemical and/or enzymatic treatments. For these reasons, the evaluation of their content should be performed, and it would be interesting the development of a new and more gentle removal process without compromising the product final features.

Also on this line, several protein and peptide purification methods can be applied to peptide-rich extracts in order to remove some undesirable components, and to concentrate and/or isolate desired peptides. Despite the present study applies two of the most used purification techniques with very distinct cost-effectiveness characteristics, namely ultrafiltration and gel filtration techniques (**Chapter 2.2.**), other processes can be applied (**Chapter 1.2.**) and some preliminary experiments were already conducted using polyelectrolytes and ion-exchange resins. From both, ion-exchange resins showed to be a more scalable potential method to explore, but several variables need to be deeply studied and optimized for their use, such as resin type, protein concentration and time, among others. In fact, working with yeast isolated peptides in near future will be really helpful based on future prediction of some potential biological properties conducted *in silico* bases on the amino acid sequences identified from our extracts. Furthermore, the mechanism by which ACE and HMG-CoA reductase are inhibited, as well as antioxidant activity, may be

elucidated by this approach as well (**Chapter 2.2. and 3.1.**). Taking into account the positive impact of the peptide-rich extracts on hypertension and cholesterol, and aiming to combine several nutraceutical properties in one single product (**Chapter 2.2. and 3.1.**), the study of other pathways regarding metabolic disorders would be interesting to evaluate, as for example the cases of α -glucosidase or dipeptidyl peptidase-4 (DPP4), that are related with stimulation of insulin production.

In addition to the bioactivities related with nutraceutical sector, the valorisation of our peptides in other economic sectors, as cosmetics, would be interesting to investigate. Indeed, a preliminary study was already performed, and Costa et al. (2023) demonstrated the positive effect of Gpep and Mpep fractions upon the production of metabolites relevant for skin health, such as pro-collagen I α I, hyaluronic acid, fibronectin, cytokeratin-14, elastin and aquaporin-9. From all, the overall best performance was of an average promotion of 41.3% over the six metabolites at keratinocytes and fibroblasts cell lines regarding the Gpep > 1 kDa at 100 μ g/mL. However, the investment on peptides purification methods should be extensively studied for this application.

Regarding the production of yeast Fe-peptide complexes and the low bioaccessible fraction obtained (**Chapter 3.3.**), a preliminary formulation was developed in an attempt to protect Fe from the different GIT environments, since the use of gastrointestinal resistant capsules seemed not to be enough. Similar to the used in the Fe-bisglycinate benchmark composition, 0.5% of magnesium stearate was also added as anti-caking agent to our Fe-complexes, and no alterations in relation to original complexes were observed in terms of structural and physical properties (FTIR spectre and particle size). However, the *in vitro* GIT simulation followed by enterocytes Fe uptake of such formulation should have been assessed, to understand their biological effect on Fe bioavailability. Furthermore, the bulking agents of benchmark could also have been added to our product or other type of formulations could be explored, such as microencapsulated preparations. Nevertheless, the real effect of our Fe-peptide complexes and Fe-bisglycinate benchmark is being evaluated on an *in vivo* study, currently ongoing. At the present, the two ingredients are being orally and daily administrated to Wistar rats with anaemia for 4 weeks (5 mg Fe/kg) and some biomarkers related with Fe metabolism will soon be evaluated.

References

- Agrawal, P. B., & Pandit, A. B. (2003). Isolation of α -glucosidase from *Saccharomyces cerevisiae*: cell disruption and adsorption. *Biochemical Engineering Journal*, 15(1), 37–45. [https://doi.org/10.1016/S1369-703X\(02\)00178-X](https://doi.org/10.1016/S1369-703X(02)00178-X)
- Ahile, U. J., Wuana, R. A., Itodo, A. U., Sha'Ato, R., & Dantas, R. F. (2020). Stability of iron chelates during photo-Fenton process: The role of pH, hydroxyl radical attack and temperature. *Journal of Water Process Engineering*, 36, 101320. <https://doi.org/10.1016/j.jwpe.2020.101320>
- Akardere, E., Özer, B., Çelem, E. B., & Önal, S. (2010). Three-phase partitioning of invertase from Baker's yeast. *Separation and Purification Technology*, 72(3), 335–339. <https://doi.org/10.1016/j.seppur.2010.02.025>
- Akhtar, Y., & Isman, M. B. (2018). Insects as an Alternative Protein Source. In *Proteins in Food Processing* (pp. 263–288). Elsevier. <https://doi.org/10.1016/B978-0-08-100722-8.00011-5>
- Albergaria, H., Francisco, D., Gori, K., Arneborg, N., & Girio, F. (2010). *Saccharomyces cerevisiae* CCMI 885 secretes peptides that inhibit the growth of some non-Saccharomyces wine-related strains. *Applied Microbiology and Biotechnology*, 86(3), 965–972. <https://doi.org/10.1007/s00253-009-2409-6>
- Alhazmi, H. (2019). FT-IR Spectroscopy for the Identification of Binding Sites and Measurements of the Binding Interactions of Important Metal Ions with Bovine Serum Albumin. *Scientia Pharmaceutica*, 87(1), 5. <https://doi.org/10.3390/scipharm87010005>
- Aly, E., López-Nicolás, R., Darwish, A. A., Frontela-Saseta, C., & Ros-Berruezo, G. (2016). Supplementation of infant formulas with recombinant human lactoferrin and/or galactooligosaccharides increases iron bioaccessibility as measured by ferritin formed in Caco-2 cell model. *Food Research International*, 89, 1048–1055. <https://doi.org/10.1016/j.foodres.2016.08.030>
- Amorim, M. M., Pereira, J. O., Monteiro, K. M., Ruiz, A. L., Carvalho, J. E., Pinheiro, H., & Pintado, M. (2016). Antiulcer and antiproliferative properties of spent brewer's yeast peptide extracts for incorporation into foods. *Food and Function*, 7(5), 2331–2337. <https://doi.org/10.1039/c6fo00030d>

- Amorim, M., Marques, C., Pereira, J. O., Guardão, L., Martins, M. J., Osório, H., Moura, D., Calhau, C., Pinheiro, H., & Pintado, M. (2019). Antihypertensive effect of spent brewer yeast peptide. *Process Biochemistry*, *76*, 213–218. <https://doi.org/10.1016/j.procbio.2018.10.004>
- Amorim, M., Pereira, J. O., Gomes, D., Pereira, C. D., Pinheiro, H., & Pintado, M. M. M. (2016). Nutritional ingredients from spent brewer's yeast obtained by hydrolysis and selective membrane filtration integrated in a pilot process. *Journal of Food Engineering*, *185*, 42–47. <https://doi.org/10.1016/j.jfoodeng.2016.03.032>
- Amorim, M., Pinheiro, H., & Pintado, M. (2019). Valorization of spent brewer's yeast: Optimization of hydrolysis process towards the generation of stable ACE-inhibitory peptides. *LWT - Food Science and Technology*, *111*, 77–84. <https://doi.org/10.1016/j.lwt.2019.05.011>
- Anderson, G. J., Lu, Y., Frazer, D. M., & Collins, J. F. (2018). Intestinal Iron Absorption. In *Reference Module in Biomedical Sciences* (2nd ed., pp. 1–11). Elsevier. <https://doi.org/10.1016/B978-0-12-801238-3.65641-6>
- Apar, D. K., & Özbek, B. (2008). Protein releasing kinetics of bakers' yeast cells by ultrasound. *Chemical and Biochemical Engineering Quarterly*, *22*(1), 113–118.
- Ashraf, J., Awais, M., Liu, L., Khan, M. I., Tong, L., Ma, Y., Wang, L., Zhou, X., & Zhou, S. (2020). Effect of thermal processing on cholesterol synthesis, solubilisation into micelles and antioxidant activities using peptides of *Vigna angularis* and *Vicia faba*. *LWT-Food Science and Technology*, *129*, 109504. <https://doi.org/10.1016/j.lwt.2020.109504>
- Ason, K. (2019). *Effective use of yeast and yeast extract residue*. <https://patents.google.com/patent/US10196430B2>
- Association of Official Analysis Chemists. (2005). Official Methods of Analysis of AOAC International. In *Association of Official Analysis Chemists International*.
- Athira, S., Mann, B., Sharma, R., Pothuraju, R., & Bajaj, R. K. (2021). Preparation and characterization of iron-chelating peptides from whey protein: An alternative approach for chemical iron fortification. *Food Research International*, *141*, 110133. <https://doi.org/10.1016/j.foodres.2021.110133>
- Avramia, I., & Amariei, S. (2021). Spent Brewer's yeast as a source of insoluble β -glucans. *International Journal of Molecular Sciences*, *22*(2), 1–26. <https://doi.org/10.3390/ijms22020825>
- Balasundaram, B., & Harrison, S. T. L. (2008). Influence of the extent of disruption of

- Bakers' yeast on protein adsorption in expanded beds. *Journal of Biotechnology*, 133(3), 360–369. <https://doi.org/10.1016/j.jbiotec.2007.07.724>
- Bertolo, A. P., Biz, A. P., Kempka, A. P., Rigo, E., & Cavaleiro, D. (2019). Yeast (*Saccharomyces cerevisiae*): evaluation of cellular disruption processes, chemical composition, functional properties and digestibility. *Journal of Food Science and Technology*, 56(8), 3697–3706. <https://doi.org/10.1007/s13197-019-03833-3>
- Blakeney, A. B., Harris, P. J., Henry, R. J., & Stone, B. A. (1983). A simple and rapid preparation of alditol acetates for monosaccharide analysis. *Carbohydrate Research*, 113(2), 291–299. [https://doi.org/10.1016/0008-6215\(83\)88244-5](https://doi.org/10.1016/0008-6215(83)88244-5)
- Bombe, K. (2019). *Specialty Yeast Market by Type (Yeast Extract, Yeast Autolysate, Yeast Beta - Glucan), Application (Bakery Production, Flavoring, Biofuels), Species (Saccharomyces Cerevisiae, Kluyveromyces), and Industry – Global Forecast to 2025*. https://www.meticulousresearch.com/product/specialty-yeast-market-5032/?utm_source=Globnewswire.com&utm_medium=PressRelease&utm_campaign=Paid
- Bradford, M. M. (1976). A rapid and sensitive method for the quantitation of microgram quantities of protein utilizing the principle of protein-dye binding. *Analytical Biochemistry*, 72(1–2), 248–254. [https://doi.org/10.1016/0003-2697\(76\)90527-3](https://doi.org/10.1016/0003-2697(76)90527-3)
- Branco, P., Francisco, D., Chambon, C., Hébraud, M., Arneborg, N., Almeida, M. G., Caldeira, J., & Albergaria, H. (2014). Identification of novel GAPDH-derived antimicrobial peptides secreted by *Saccharomyces cerevisiae* and involved in wine microbial interactions. *Applied Microbiology and Biotechnology*, 98(2), 843–853. <https://doi.org/10.1007/s00253-013-5411-y>
- Branco, P., Francisco, D., Monteiro, M., Almeida, M. G., Caldeira, J., Arneborg, N., Prista, C., & Albergaria, H. (2017). Antimicrobial properties and death-inducing mechanisms of saccharomycin, a biocide secreted by *Saccharomyces cerevisiae*. *Applied Microbiology and Biotechnology*, 101(1), 159–171. <https://doi.org/10.1007/s00253-016-7755-6>
- Brissot, P., & Loréal, O. (2016). Iron metabolism and related genetic diseases: A cleared land, keeping mysteries. *Journal of Hepatology*, 64(2), 505–515. <https://doi.org/10.1016/j.jhep.2015.11.009>
- Brodkorb, A., Egger, L., Alming, M., Alvito, P., Assunção, R., Ballance, S., Bohn, T., Bourlieu-Lacanal, C., Boutrou, R., Carrière, F., Clemente, A., Corredig, M., Dupont, D., Dufour, C., Edwards, C., Golding, M., Karakaya, S., Kirkhus, B., Le Feunteun, S.,

- ... Recio, I. (2019). INFOGEST static *in vitro* simulation of gastrointestinal food digestion. *Nature Protocols*, *14*(4), 991–1014. <https://doi.org/10.1038/s41596-018-0119-1>
- Brogden, K. A. (2005). Antimicrobial peptides: Pore formers or metabolic inhibitors in bacteria? *Nature Reviews Microbiology*. <https://doi.org/10.1038/nrmicro1098>
- Bryszewska, M. (2019). Comparison Study of Iron Bioaccessibility from Dietary Supplements and Microencapsulated Preparations. *Nutrients*, *11*(2), 273. <https://doi.org/10.3390/nu11020273>
- Budseekoad, S., Yupanqui, C. T., Sirinupong, N., Alashi, A. M., Aluko, R. E., & Youravong, W. (2018). Structural and functional characterization of calcium and iron-binding peptides from mung bean protein hydrolysate. *Journal of Functional Foods*, *49*, 333–341. <https://doi.org/10.1016/j.jff.2018.07.041>
- Butylina, S., Shataeva, L. K., & Nyström, M. (2007). Separation of nucleoprotein complexes with antioxidant activity from yeast *Saccharomyces cerevisiae*. *Separation and Purification Technology*, *53*(1), 64–70. <https://doi.org/10.1016/j.seppur.2006.06.014>
- Bystryak, S., Santockyte, R., & Peshkovsky, A. S. (2015). Cell disruption of *S. cerevisiae* by scalable high-intensity ultrasound. *Biochemical Engineering Journal*, *99*, 99–106. <https://doi.org/10.1016/j.bej.2015.03.014>
- Bzducha-Wróbel, A., Błażej, S., Kawarska, A., Stasiak-Różańska, L., Gientka, I., & Majewska, E. (2014). Evaluation of the Efficiency of Different Disruption Methods on Yeast Cell Wall Preparation for β -Glucan Isolation. *Molecules*, *19*(12), 20941–20961. <https://doi.org/10.3390/molecules191220941>
- Caballero-Córdoba, G. M., & Sgarbieri, V. C. (2000). Nutritional and toxicological evaluation of yeast (*Saccharomyces cerevisiae*) biomass and a yeast protein concentrate. *Journal of the Science of Food and Agriculture*, *80*(3), 341–351. [https://doi.org/10.1002/1097-0010\(200002\)80:3<341::AID-JSFA533>3.3.CO;2-D](https://doi.org/10.1002/1097-0010(200002)80:3<341::AID-JSFA533>3.3.CO;2-D)
- Caetano-Silva, M. E., Alves, R. C., Lucena, G. N., Frem, R. C. G., Bertoldo-Pacheco, M. T., Lima-Pallone, J. A., & Netto, F. M. (2017). Synthesis of whey peptide-iron complexes: Influence of using different iron precursor compounds. *Food Research International*, *101*, 73–81. <https://doi.org/10.1016/j.foodres.2017.08.056>
- Caetano-Silva, M. E., Bertoldo-Pacheco, M. T., Paes-Leme, A. F., & Netto, F. M. (2015). Iron-binding peptides from whey protein hydrolysates: Evaluation, isolation and sequencing by LC-MS/MS. *Food Research International*, *71*, 132–139. <https://doi.org/10.1016/j.foodres.2015.01.008>

- Caetano-Silva, M. E., Cilla, A., Bertoldo-Pacheco, M. T., Netto, F. M., & Alegría, A. (2018). Evaluation of *in vitro* iron bioavailability in free form and as whey peptide-iron complexes. *Journal of Food Composition and Analysis*, 68(October 2016), 95–100. <https://doi.org/10.1016/j.jfca.2017.03.010>
- Caetano-Silva, M. E., Netto, F. M., Bertoldo-Pacheco, M. T., Alegría, A., & Cilla, A. (2020). Peptide-metal complexes: obtention and role in increasing bioavailability and decreasing the pro-oxidant effect of minerals. *Critical Reviews in Food Science and Nutrition*, 0(0), 1–20. <https://doi.org/10.1080/10408398.2020.1761770>
- Caldeira, J., Almeida, G., Macedo, A. L., Silva, J. P. M., & Albergaria, H. (2019). Saccharomycin, a biocide from *S. cerevisiae* that kill-off other yeasts. *Annals of Medicine*, 51, 94–95. <https://doi.org/10.1080/07853890.2018.1562694>
- Celus, I., Brijs, K., & Delcour, J. A. (2007). Enzymatic hydrolysis of brewers' spent grain proteins and technofunctional properties of the resulting hydrolysates. *Journal of Agricultural and Food Chemistry*, 55(21), 8703–8710. <https://doi.org/10.1021/jf071793c>
- Chae, H. J., Joo, H., & In, M. (2001). Utilization of brewer's yeast cells for the production of food-grade yeast extract. Part 1: effects of different enzymatic treatments on solid and protein recovery and flavor characteristics. *Bioresource Technology*, 76(3), 253–258. [https://doi.org/10.1016/S0960-8524\(00\)00102-4](https://doi.org/10.1016/S0960-8524(00)00102-4)
- Chan, D. I., Prenner, E. J., & Vogel, H. J. (2006). Tryptophan- and arginine-rich antimicrobial peptides: Structures and mechanisms of action. *Biochimica et Biophysica Acta (BBA) - Biomembranes*, 1758(9), 1184–1202. <https://doi.org/10.1016/j.bbamem.2006.04.006>
- Chatelain, P. G., Pintado, M. E., & Vasconcelos, M. W. (2014). Evaluation of chitoooligosaccharide application on mineral accumulation and plant growth in *Phaseolus vulgaris*. *Plant Science*, 215–216, 134–140. <https://doi.org/10.1016/j.plantsci.2013.11.009>
- Chauhan, V., & Kanwar, S. S. (2019). Bioactive peptides: Synthesis, functions and biotechnological applications. In *Biotechnological Production of Bioactive Compounds*. Elsevier B.V. <https://doi.org/10.1016/B978-0-444-64323-0.00004-7>
- Chen, Q., Guo, L., Du, F., Chen, T., Hou, H., & Li, B. (2017). The chelating peptide (GPAGPHGPPG) derived from Alaska pollock skin enhances calcium, zinc and iron transport in Caco-2 cells. *International Journal of Food Science & Technology*, 52(5), 1283–1290. <https://doi.org/10.1111/ijfs.13396>

- Clark, E. D. B. (2001). Protein refolding for industrial processes. *Current Opinion in Biotechnology*, 12(2), 202–207. [https://doi.org/10.1016/S0958-1669\(00\)00200-7](https://doi.org/10.1016/S0958-1669(00)00200-7)
- Coates, J. (2006). Interpretation of Infrared Spectra, A Practical Approach. In *Encyclopedia of Analytical Chemistry* (pp. 1–23). John Wiley & Sons, Ltd. <https://doi.org/10.1002/9780470027318.a5606>
- Collins, J. F., & Anderson, G. J. (2012). Molecular Mechanisms of Intestinal Iron Transport. In *Physiology of the Gastrointestinal Tract* (First Edit, Vol. 2, pp. 1921–1947). Elsevier. <https://doi.org/10.1016/B978-0-12-382026-6.00071-3>
- Comitini, F., Ferretti, R., Clementi, F., Mannazzu, I., & Ciani, M. (2005). Interactions between *Saccharomyces cerevisiae* and malolactic bacteria: Preliminary characterization of a yeast proteinaceous compound(s) active against *Oenococcus oeni*. *Journal of Applied Microbiology*, 99(1), 105–111. <https://doi.org/10.1111/j.1365-2672.2005.02579.x>
- Contreras, M. del M., Lama-Muñoz, A., Manuel Gutiérrez-Pérez, J., Espinola, F., Moya, M., & Castro, E. (2019). Protein extraction from agri-food residues for integration in biorefinery: Potential techniques and current status. *Bioresource Technology*, 280(February), 459–477. <https://doi.org/10.1016/j.biortech.2019.02.040>
- Conway, J. (2021). *Beer production worldwide from 1998 to 2020*. <https://www.statista.com/statistics/270275/worldwide-beer-production/>
- Conway, V., Gauthier, S. F., & Pouliot, Y. (2013). Antioxidant activities of buttermilk proteins, whey proteins, and their enzymatic hydrolysates. *Journal of Agricultural and Food Chemistry*, 61(2), 364–372. <https://doi.org/10.1021/jf304309g>
- Coscuela, E. R., Campos, D. A., Osório, H., Nerli, B. B., & Pintado, M. (2019). Enzymatic soy protein hydrolysis: A tool for biofunctional food ingredient production. *Food Chemistry: X*, 1, 100006. <https://doi.org/10.1016/j.fochx.2019.100006>
- Costa, E. M., Oliveira, A. S., Silva, S., Ribeiro, A. B., Pereira, C. F., Ferreira, C., Casanova, F., Pereira, J. O., Freixo, R., Pintado, M. E., Carvalho, A. P., & Ramos, Ó. L. (2023). Spent Yeast Waste Streams as a Sustainable Source of Bioactive Peptides for Skin Applications. *International Journal of Molecular Sciences*, 24(3), 2253. <https://doi.org/10.3390/ijms24032253>
- Currie, J. A., Dunnill, P., & Lilly, M. D. (1972). Release of protein from Bakers' yeast (*Saccharomyces cerevisiae*) by disruption in an industrial agitator mill. *Biotechnology and Bioengineering*, 14(5), 725–736. <https://doi.org/10.1002/bit.260140504>
- de la Hoz, L., Nunes da Silva, V. S., Morgano, M. A., & Pacheco, M. T. B. (2014). Small

- peptides from enzymatic whey hydrolyzates increase dialyzable iron. *International Dairy Journal*, 38(2), 145–147. <https://doi.org/10.1016/j.idairyj.2013.12.009>
- DeBose-Boyd, R. A. (2008). Feedback regulation of cholesterol synthesis: sterol-accelerated ubiquitination and degradation of HMG CoA reductase. *Cell Research*, 18(6), 609–621. <https://doi.org/10.1038/cr.2008.61>
- Dhakal, R., Bajpai, V. K., & Baek, K.-H. (2012). Production of gaba (γ – Aminobutyric acid) by microorganisms: a review. *Brazilian Journal of Microbiology*, 43(4), 1230–1241. <https://doi.org/10.1590/S1517-83822012000400001>
- Dhineshkumar, V., & Ramasamy, D. (2017). Review on Membrane Technology Applications in Food and Dairy Processing. *Journal of Applied Biotechnology & Bioengineering*, 3(5), 399–407. <https://doi.org/10.15406/jabb.2017.03.00077>
- Díaz-Flores, M., Cruz, M., Duran-Reyes, G., Munguia-Miranda, C., Loza-Rodríguez, H., Pulido-Casas, E., Torres-Ramírez, N., Gaja-Rodríguez, O., Kumate, J., Baiza-Gutman, L. A., & Hernández-Saavedra, D. (2013). Oral supplementation with glycine reduces oxidative stress in patients with metabolic syndrome, improving their systolic blood pressure. *Canadian Journal of Physiology and Pharmacology*, 91(10), 855–860. <https://doi.org/10.1139/cjpp-2012-0341>
- Dick, K. J., Molan, P. C., & Eschenbruch, R. (1992). The isolation from *Saccharomyces cerevisiae* of two antibacterial cationic proteins that inhibit malolactic bacteria. *Vitis*, 31(2), 105–116.
- Dumas, J. B. A. (1831). Procédes de l’analyse organique. *Annales de Chimie et de Physique*, 198–205.
- Eckert, E., Lu, L., Unsworth, L. D., Chen, L., Xie, J., & Xu, R. (2016). Biophysical and in vitro absorption studies of iron chelating peptide from barley proteins. *Journal of Functional Foods*, 25, 291–301. <https://doi.org/10.1016/j.jff.2016.06.011>
- Ekpeni, L. E. N., Benyounis, K. Y., Nkem-Ekpeni, F. F., Stokes, J., & Olabi, A. G. (2015). Underlying factors to consider in improving energy yield from biomass source through yeast use on high-pressure homogenizer (hph). *Energy*, 81, 74–83. <https://doi.org/10.1016/j.energy.2014.11.038>
- Ekpeni, L. E. N., Benyounis, K. Y., Stokes, J., & Olabi, A. G. (2016). Improving and optimizing protein concentration yield from homogenized baker’s yeast at different ratios of buffer solution. *International Journal of Hydrogen Energy*, 41(37), 16415–16427. <https://doi.org/10.1016/j.ijhydene.2016.05.243>
- European Commission. (2012). *Nutrition claims*. <https://food.ec.europa.eu/safety/labelling->

and-nutrition/nutrition-and-health-claims/nutrition-claims_en

- Fairweather-Tait, S. J., & Teucher, B. (2002). Iron and calcium bioavailability of fortified foods and dietary supplements. *Nutrition Reviews*, *60*(11), 360–367. <https://doi.org/10.1301/00296640260385801>
- Farra, C. D. (2015). *Cosmetic and/or pharmaceutical composition comprising a yeast peptide hydrolysate and use of the yeast peptide hydrolysate as an active agent for strengthening hair*. <https://patents.google.com/patent/US8933036B2/en>
- Faustino, M., Durão, J., Pereira, C. F., Oliveira, A. S., Pereira, J. O., Pereira, A. M., Ferreira, C., Pintado, M. E., & Carvalho, A. P. (2022). Comparative Analysis of Mannans Extraction Processes from Spent Yeast *Saccharomyces cerevisiae*. *Foods*, *11*(23), 3753. <https://doi.org/10.3390/foods11233753>
- Faustino, M., Durão, J., Pereira, C. F., Pintado, M. E., & Carvalho, A. P. (2021). Mannans and mannan oligosaccharides (MOS) from *Saccharomyces cerevisiae* – A sustainable source of functional ingredients. *Carbohydrate Polymers*, *272*(April). <https://doi.org/10.1016/j.carbpol.2021.118467>
- Faustino, M., Pereira, C. F., Durão, J., Sofia Oliveira, A., Odila Pereira, J., Ferreira, C., Pintado, M. E., & Carvalho, A. P. (2023). Effect of drying technology in *Saccharomyces cerevisiae* mannans: structural, physicochemical, and functional properties. *Food Chemistry*, 135545. <https://doi.org/10.1016/j.foodchem.2023.135545>
- Feldmann, H. (2012). Yeast Cell Architecture and Functions. In *Yeast: Molecular and Cell Biology* (Second Edi, pp. 5–24). Wiley-VCH Verlag GmbH & Co. KGaA. <https://doi.org/10.1002/9783527659180.ch2>
- Ferreira, C., Pereira, C. F., Oliveira, A. S., Faustino, M., Pereira, A. M., Durão, J., Pereira, J. O., Pintado, M. E., & Carvalho, A. P. (2022). A Step for the Valorization of Spent Yeast through Production of Iron – Peptide Complexes — A Process Optimization Study. *Processes*, *10*(8), 1–13. <https://doi.org/10.3390/pr10081464>
- Filiponi, M. P., Gaigher, B., Caetano-Silva, M. E., Alvim, I. D., & Pacheco, M. T. B. (2019). Microencapsulation performance of Fe-peptide complexes and stability monitoring. *Food Research International*, *125*(November 2018), 108505. <https://doi.org/10.1016/j.foodres.2019.108505>
- Fleet, G. H. (2007). Yeasts in foods and beverages: impact on product quality and safety. *Current Opinion in Biotechnology*, *18*(2), 170–175. <https://doi.org/10.1016/j.copbio.2007.01.010>
- Food Agricultural Organization of the United Nations. (2019). *Food balance sheets: Protein*

- supply quantity (g/capita/day)*. <http://www.fao.org/faostat/en/#data/FBS>
- Food and Agriculture Organization of the United Nations. (2018). *The future of food and agriculture – Alternative pathways to 2050*. <http://www.fao.org/global-perspectives-studies/resources/detail/en/c/1157082/>
- Freimund, S., Sauter, M., Käppeli, O., & Dutler, H. (2003). A new non-degrading isolation process for 1,3-β-D-glucan of high purity from baker's yeast *Saccharomyces cerevisiae*. *Carbohydrate Polymers*, *54*(2), 159–171. [https://doi.org/10.1016/S0144-8617\(03\)00162-0](https://doi.org/10.1016/S0144-8617(03)00162-0)
- Ganeva, V., & Galutzov, B. (1999). Electropulsation as an alternative method for protein extraction from yeast. *FEMS Microbiology Letters*, *174*(2), 279–284. <https://doi.org/10.1111/j.1574-6968.1999.tb13580.x>
- Ganeva, V., Galutzov, B., & Teissié, J. (2003). High yield electroextraction of proteins from yeast by a flow process. *Analytical Biochemistry*, *315*(1), 77–84. [https://doi.org/10.1016/S0003-2697\(02\)00699-1](https://doi.org/10.1016/S0003-2697(02)00699-1)
- García-Nebot, M. J., Barberá, R., & Alegría, A. (2013). Iron and zinc bioavailability in Caco-2 cells: Influence of caseinophosphopeptides. *Food Chemistry*, *138*(2–3), 1298–1303. <https://doi.org/10.1016/j.foodchem.2012.10.113>
- Garner, C. M., Mills, C. O., Elias, E., & Neuberger, J. M. (1991). The effect of bile salts on human vascular endothelial cells. *BBA - Molecular Cell Research*, *1091*(1), 41–45. [https://doi.org/10.1016/0167-4889\(91\)90219-N](https://doi.org/10.1016/0167-4889(91)90219-N)
- Gaspar, L. M., Machado, A., Coutinho, R., Sousa, S., Santos, R., Xavier, A., Figueiredo, M., Teixeira, M. de F., Centeno, F., & Simões, J. (2019). Development of potential yeast protein extracts for red wine clarification and stabilization. *Frontiers in Microbiology*, *10*, 1–13. <https://doi.org/10.3389/fmicb.2019.02310>
- Gaver, D., & Huyghebaert, A. (1991). Optimization of yeast cell disruption with a newly designed bead mill. *Enzyme and Microbial Technology*, *13*(8), 665–671. [https://doi.org/10.1016/0141-0229\(91\)90082-L](https://doi.org/10.1016/0141-0229(91)90082-L)
- Gawde, U., Chakraborty, S., Wagh, F. H., Barai, R. S., Khanderkar, A., Indraguru, R., Shirsat, T., & Idicula-Thomas, S. (2023). CAMPR4: a database of natural and synthetic antimicrobial peptides. *Nucleic Acids Research*, *51*, D377–D383. <https://doi.org/10.1093/nar/gkac933>
- Gddoa Al-sahlany, S. T., Altemimi, A. B., Abd Al-Manhel, A. J., Niamah, A. K., Lakhssassi, N., & Ibrahim, S. A. (2020). Purification of Bioactive Peptide with Antimicrobial Properties Produced by *Saccharomyces cerevisiae*. *Foods*, *9*(3), 1–11.

<https://doi.org/10.3390/foods9030324>

- Ge, L., Wang, X. T., Tan, S. N., Tsai, H. H., Yong, J. W. H., & Hua, L. (2010). A novel method of protein extraction from yeast using ionic liquid solution. *Talanta*, *81*(4–5), 1861–1864. <https://doi.org/10.1016/j.talanta.2010.02.034>
- Goetz, H., Kuschel, M., Wulff, T., Sauber, C., Miller, C., Fisher, S., & Woodward, C. (2004). Comparison of selected analytical techniques for protein sizing, quantitation and molecular weight determination. *Journal of Biochemical and Biophysical Methods*, *60*(3), 281–293. <https://doi.org/10.1016/j.jbbm.2004.01.007>
- Gómez-Grimaldos, N. A., Gómez-Sampedro, L. J., Zapata-Montoya, J. E., López-García, G., Cilla, A., & Alegría-Torán, A. (2020). Bovine plasma hydrolysates' iron chelating capacity and its potentiating effect on ferritin synthesis in Caco-2 cells. *Food and Function*, *11*(12), 10907–10912. <https://doi.org/10.1039/d0fo02502j>
- Gonçalves, G. A., Corrêa, R. C. G., Barros, L., Dias, M. I., Calhella, R. C., Correa, V. G., Bracht, A., Peralta, R. M., & Ferreira, I. C. F. R. (2019). Effects of *in vitro* gastrointestinal digestion and colonic fermentation on a rosemary (*Rosmarinus officinalis L*) extract rich in rosmarinic acid. *Food Chemistry*, *271*, 393–400. <https://doi.org/10.1016/j.foodchem.2018.07.132>
- Grand View Research. (2022). *Synthetic Biology Market Size, Share & Trends Analysis Report By Product (Enzymes, Cloning Technologies Kits), By Technology (PCR, NGS), By Application (Non-healthcare, Healthcare), By End-use, And Segment Forecasts, 2023 - 2030*. <https://www.grandviewresearch.com/industry-analysis/synthetic-biology-market>
- Grauso, M., Lan, A., Andriamihaja, M., Bouillaud, F., & Blachier, F. (2019). Hyperosmolar environment and intestinal epithelial cells: impact on mitochondrial oxygen consumption, proliferation, and barrier function *in vitro*. *Scientific Reports*, *9*(1), 1–14. <https://doi.org/10.1038/s41598-019-47851-9>
- Grönberg, A. (2018). Ion exchange chromatography. In *Biopharmaceutical Processing: Development, Design, and Implementation of Manufacturing Processes* (pp. 379–399). Elsevier. <https://doi.org/10.1016/B978-0-08-100623-8.00018-9>
- Guo, H., Guo, S., & Liu, H. (2020). Antioxidant activity and inhibition of ultraviolet radiation-induced skin damage of Selenium-rich peptide fraction from selenium-rich yeast protein hydrolysate. *Bioorganic Chemistry*, *105*(October), 104431. <https://doi.org/10.1016/j.bioorg.2020.104431>
- Guo, L., Harnedy, P. A., O'Keeffe, M. B., Zhang, L., Li, B., Hou, H., & FitzGerald, R. J.

- (2015). Fractionation and identification of Alaska pollock skin collagen-derived mineral chelating peptides. *Food Chemistry*, *173*, 536–542. <https://doi.org/10.1016/j.foodchem.2014.10.055>
- Guo, L., Hou, H., Li, B., Zhang, Z., Wang, S., & Zhao, X. (2013). Preparation, isolation and identification of iron-chelating peptides derived from Alaska pollock skin. *Process Biochemistry*, *48*(5–6), 988–993. <https://doi.org/10.1016/j.procbio.2013.04.013>
- Halim, R., Hill, D. R. A., Hanssen, E., Webley, P. A., Blackburn, S., Grossman, A. R., Posten, C., & Martin, G. J. O. (2019). Towards sustainable microalgal biomass processing: anaerobic induction of autolytic cell-wall self-ingestion in lipid-rich *Nannochloropsis* slurries. *Green Chemistry*, *21*(11), 2967–2982. <https://doi.org/10.1039/C8GC03186J>
- Hassan, H. M. M. (2011). Antioxidant and Immunostimulating Activities of Yeast (*Saccharomyces cerevisiae*) Autolysates. *World Applied Sciences Journal*, *15*(8), 1110–1119.
- Hayes, M. (2018). Food Proteins and Bioactive Peptides: New and Novel Sources, Characterisation Strategies and Applications. *Foods*, *7*(3), 38. <https://doi.org/10.3390/foods7030038>
- Hedenskog, G., & Mogren, H. (1973). Some methods for processing of single-cell protein. *Biotechnology and Bioengineering*, *15*(1), 129–142. <https://doi.org/10.1002/bit.260150110>
- Hedhammar, M., Karlström, A. E., & Hober, S. (2006). *Chromatographic methods for protein purification*, Royal Institute of Technology, Stockholm, Sweden. Stockholm: Royal Institute of Technology.
- Henchion, M., Hayes, M., Mullen, A., Fenelon, M., & Tiwari, B. (2017). Future Protein Supply and Demand: Strategies and Factors Influencing a Sustainable Equilibrium. *Foods*, *6*(7), 53. <https://doi.org/10.3390/foods6070053>
- Hobson, J. (1991). *A co-hydrolytic process for the production of novel extracts from yeast and non-yeast proteins* (Patent No. WO1991016447A1). <https://patents.google.com/patent/WO1991016447A1/en>
- Hoffman, J. R., Varanoske, A., & Stout, J. R. (2018). Effects of β -Alanine Supplementation on Carnosine Elevation and Physiological Performance. *Advances in Food and Nutrition Research*, *84*, 183–206. <https://doi.org/10.1016/BS.AFNR.2017.12.003>
- Hu, S., Wang, X., Guo, S., Li, L., & Hou, Y. (2014). Preparation and Properties of Bioactive Peptides from Yeast Protein. *Focusing on Modern Food Industry*, *3*(0), 52.

<https://doi.org/10.14355/fmfi.2014.03.007>

- Huang, G., Ren, Z., & Jiang, J. (2011). Separation of Iron-Binding Peptides from Shrimp Processing By-products Hydrolysates. *Food and Bioprocess Technology*, 4(8), 1527–1532. <https://doi.org/10.1007/s11947-010-0416-3>
- Huang, K., Gao, J. yong, Ma, S., & Lu, J. jiong. (2012). Optimising separation process of protein and polysaccharide from spent brewer's yeast by ultrafiltration. *International Journal of Food Science and Technology*, 47(6), 1259–1264. <https://doi.org/10.1111/j.1365-2621.2012.02967.x>
- Huang, Y. -T, & Kinsella, J. E. (1986). Phosphorylation of yeast protein: Reduction of ribonucleic acid and isolation of yeast protein concentrate. *Biotechnology and Bioengineering*, 28(11), 1690–1698. <https://doi.org/10.1002/bit.260281112>
- Huang, Y., Wang, J., Hou, Y., & Hu, S. Q. (2020). Production of yeast hydrolysates by *Bacillus subtilis* derived enzymes and antihypertensive activity in spontaneously hypertensive rats. *Food Biotechnology*, 34(3), 262–281. <https://doi.org/10.1080/08905436.2020.1791174>
- Iida, Y., Tuziuti, T., Yasui, K., Kozuka, T., & Towata, A. (2008). Protein release from yeast cells as an evaluation method of physical effects in ultrasonic field. *Ultrasonics Sonochemistry*, 15(6), 995–1000. <https://doi.org/10.1016/j.ultsonch.2008.02.013>
- Indumathi, P., & Mehta, A. (2016). A novel anticoagulant peptide from the Nori hydrolysate. *Journal of Functional Foods*, 20, 606–617. <https://doi.org/10.1016/j.jff.2015.11.016>
- International Organization for Standardization. (2009). Biological evaluation of medical devices in Tests for *in vitro* cytotoxicity. *International Organization for Standardization: Geneva*, 34.
- Invitrogen. (2010). *PrestoBlue cell viability reagent protocol*. Product Information Sheet by Life Technologies. https://tools.thermofisher.com/content/sfs/manuals/PrestoBlue_Reagent_PIS_15Oct10.pdf
- Jacob, F. F., Hutzler, M., & Methner, F. J. (2019). Comparison of various industrially applicable disruption methods to produce yeast extract using spent yeast from top-fermenting beer production: influence on amino acid and protein content. *European Food Research and Technology*, 245(1), 95–109. <https://doi.org/10.1007/s00217-018-3143-z>
- Jacob, F. F., Striegel, L., Rychlik, M., Hutzler, M., & Methner, F.-J. (2019). Yeast extract production using spent yeast from beer manufacture: influence of industrially

- applicable disruption methods on selected substance groups with biotechnological relevance. *European Food Research and Technology*, 245(6), 1169–1182. <https://doi.org/10.1007/s00217-019-03237-9>
- Jaeger, A., Arendt, E. K., Zannini, E., & Sahin, A. W. (2020). Brewer's Spent Yeast (BSY), an Underutilized Brewing By-Product. *Fermentation*, 6(4), 123. <https://doi.org/10.3390/fermentation6040123>
- James, C. J., Coakley, W. T., & Hughes, D. E. (1972). Kinetics of protein release from yeast sonicated in batch and flow systems at 20 kHz. *Biotechnology and Bioengineering*, 14(1), 33–42. <https://doi.org/10.1002/bit.260140105>
- Jamshad, M., & Darby, R. A. J. (2012). Disruption of Yeast Cells to Isolate Recombinant Proteins. In *Methods in Molecular Biology* (pp. 237–246). https://doi.org/10.1007/978-1-61779-770-5_20
- Jenssen, H., Hamill, P., & Hancock, R. E. W. (2006). Peptide Antimicrobial Agents. *Clinical Microbiology Reviews*, 19(3), 491–511. <https://doi.org/10.1128/CMR.00056-05>
- Jeppsen, R. ., & Borzelleca, J. . (1999). Safety Evaluation of Ferrous Bisglycinate Chelate. *Food and Chemical Toxicology*, 37(7), 723–731. [https://doi.org/10.1016/S0278-6915\(99\)00052-6](https://doi.org/10.1016/S0278-6915(99)00052-6)
- Jin, Y. G., Fu, W. W., & Ma, M. H. (2011). Preparation and structure characterization of soluble bone collagen peptide chelating calcium. *African Journal of Biotechnology*, 10(50), 10204–10211. <https://doi.org/10.5897/ajb10.1923>
- Jolly, R. (1978). *Modified protein*. <https://patents.google.com/patent/US4107334A>
- Jones, S. W., Karpol, A., Friedman, S., Maru, B. T., & Tracy, B. P. (2020). Recent advances in single cell protein use as a feed ingredient in aquaculture. *Current Opinion in Biotechnology*, 61(2), 189–197. <https://doi.org/10.1016/j.copbio.2019.12.026>
- Josic, D., & Kovac, S. (2010). Reversed-phase high performance liquid chromatography of proteins. *Current Protocols in Protein Science*, 2010, 1–22. <https://doi.org/10.1002/0471140864.ps0807s61>
- Jung, E. Y., Cho, M. K., Hong, Y. H., Kim, J. H., Park, Y., Chang, U. J., & Suh, H. J. (2014). Yeast hydrolysate can reduce body weight and abdominal fat accumulation in obese adults. *Nutrition*, 30(1), 25–32. <https://doi.org/10.1016/j.nut.2013.02.009>
- Jung, E. Y., Lee, H. S., Choi, J. W., Ra, K. S., Kim, M. R., & Suh, H. J. (2011). Glucose Tolerance and Antioxidant Activity of Spent Brewer's Yeast Hydrolysate with a High Content of Cyclo-His-Pro (CHP). *Journal of Food Science*, 76(2), 272–278. <https://doi.org/10.1111/j.1750-3841.2010.01997.x>

- Kadam, S. U., Tiwari, B. K., Álvarez, C., & O'Donnell, C. P. (2015). Ultrasound applications for the extraction, identification and delivery of food proteins and bioactive peptides. *Trends in Food Science & Technology*, *46*(1), 60–67. <https://doi.org/10.1016/j.tifs.2015.07.012>
- Kalgaonkar, S., & Lönnerdal, B. (2009). Receptor-mediated uptake of ferritin-bound iron by human intestinal Caco-2 cells. *The Journal of Nutritional Biochemistry*, *20*(4), 304–311. <https://doi.org/10.1016/j.jnutbio.2008.04.003>
- Kaltashov, I. A., Bobst, C. E., Pawlowski, J., & Wang, G. (2020). Mass spectrometry-based methods in characterization of the higher order structure of protein therapeutics. *Journal of Pharmaceutical and Biomedical Analysis*, *184*, 113169. <https://doi.org/10.1016/j.jpba.2020.113169>
- Kanauchi, O., Igarashi, K., Ogata, R., Mitsuyama, K., & Andoh, A. (2005). A Yeast Extract High in Bioactive Peptides has a Blood-Pressure Lowering Effect in Hypertensive Model. *Current Medicinal Chemistry*, *12*(26), 3085–3090. <https://doi.org/10.2174/092986705774933461>
- Kim, J., Dae-Hyoung, L., Jong-Soo, L., Chung, K., & Jeong, S. (2004). Characterization of antihypertensive angiotensin I-converting enzyme inhibitor from *Saccharomyces cerevisiae*. *Journal of Microbiology and Biotechnology*, *14*(6), 1318–1323.
- Kim, J. H., Jung, E. Y., Hong, Y. H., Bae, S. H., Kim, J. M., Noh, D. O., Nozaki, T., Inoue, T., & Suh, H. J. (2012). Short communication: Pet foods with yeast hydrolysate can reduce body weight and increase girth in beagle dogs. *Canadian Journal of Animal Science*, *92*(2), 207–210. <https://doi.org/10.4141/CJAS2011-123>
- Kim, K. M., Chang, U. J., Kang, D. H., Kim, J. M., Choi, Y. M., & Suh, H. J. (2004). Yeast hydrolysate reduces body fat of dietary obese rats. *Phytotherapy Research*, *18*(11), 950–953. <https://doi.org/10.1002/ptr.1582>
- Kim, S. K. (2016). Marine glycobiology: Principles and applications. In *Marine Glycobiology: Principles and Applications* (First ed.). CRC Press.
- Kinsella, J. E., & Damodaran, S. (1984). Dissociation of Yeast Nucleoprotein Complexes by Chemical Phosphorylation. *Journal of Agricultural and Food Chemistry*, *32*(5), 1030–1032. <https://doi.org/10.1021/jf00125a021>
- Kitts, D. D. (2021). Antioxidant and functional activities of mrps derived from different sugar–amino acid combinations and reaction conditions. *Antioxidants*, *10*(11). <https://doi.org/10.3390/antiox10111840>
- Klimek-Ochab, M., Brzezińska-Rodak, M., Zymańczyk-Duda, E., Lejczak, B., & Kafarski,

- P. (2011). Comparative study of fungal cell disruption-scope and limitations of the methods. *Folia Microbiologica*, 56(5), 469–475. <https://doi.org/10.1007/s12223-011-0069-2>
- Klis, F. M., Mol, P., Hellingwerf, K., & Brul, S. (2002). Dynamics of cell wall structure in *Saccharomyces cerevisiae*. *FEMS Microbiology Reviews*, 26(3), 239–256. <https://doi.org/10.1111/j.1574-6976.2002.tb00613.x>
- Kohama, Y., Nagase, Y., Oka, H., Nakagawa, T., Teramoto, T., Murayama, N., Tsujibo, H., Inamori, Y., & Mimura, T. (1990). Production of angiotensin-converting enzyme inhibitors from baker's yeast glyceraldehyde-3-phosphate dehydrogenase. *Journal of Pharmacobio-Dynamics*, 13(12), 766–771. <https://doi.org/10.1248/bpb1978.13.766>
- Kortes, J. (2020). *Process flavours with low acrylamide*. <https://patents.google.com/patent/EP3357345B1/en>
- Koubaa, M., Imatoukene, N., Drévillon, L., & Vorobiev, E. (2020). Current insights in yeast cell disruption technologies for oil recovery: A review. *Chemical Engineering and Processing - Process Intensification*, 150(September 2019), 107868. <https://doi.org/10.1016/j.cep.2020.107868>
- Kuhad, R. C., Singh, A., Tripathi, K. K., Saxena, R. K., & Eriksson, K.-E. L. (1997). Microorganisms as an Alternative Source of Protein. *Nutrition Reviews*, 55(3), 65–75. <https://academic.oup.com/nutritionreviews/article-lookup/doi/10.1111/j.1753-4887.1997.tb01599.x>
- Kurcz, A., Błażej, S., Kot, A. M., Bzducha-Wróbel, A., & Kieliszek, M. (2018). Application of Industrial Wastes for the Production of Microbial Single-Cell Protein by Fodder Yeast *Candida utilis*. *Waste and Biomass Valorization*, 9(1), 57–64. <https://doi.org/10.1007/s12649-016-9782-z>
- Kushnirov, V. V. (2000). Rapid and reliable protein extraction from yeast. *Yeast*, 16(9), 857–860. [https://doi.org/10.1002/1097-0061\(20000630\)16:9<857::AID-YEA561>3.0.CO;2-B](https://doi.org/10.1002/1097-0061(20000630)16:9<857::AID-YEA561>3.0.CO;2-B)
- Laparra, J. M., Glahn, R. P., & Miller, D. D. (2009). Different responses of Fe transporters in Caco-2/HT29-MTX cocultures than in independent Caco-2 cell cultures. *Cell Biology International*, 33(9), 971–977. <https://doi.org/10.1016/j.cellbi.2009.06.001>
- Lazarte, C. E., Carlsson, N. G., Almgren, A., Sandberg, A. S., & Granfeldt, Y. (2015). Phytate, zinc, iron and calcium content of common Bolivian food, and implications for mineral bioavailability. *Journal of Food Composition and Analysis*, 39, 111–119. <https://doi.org/10.1016/j.jfca.2014.11.015>

- Lea, T. (2015). Caco-2 Cell Line. In *The Impact of Food Bioactives on Health* (pp. 103–111). Springer International Publishing. https://doi.org/10.1007/978-3-319-16104-4_26
- Lee, D. H., Lee, D. H., & Lee, J. S. (2007). Characterization of a new antimentia β -secretase inhibitory peptide from *Saccharomyces cerevisiae*. *Enzyme and Microbial Technology*, *42*(1), 83–88. <https://doi.org/10.1016/j.enzmictec.2007.08.003>
- Lee, H. S., Jung, E. Y., Bae, S. H., Kwon, K. H., Kim, J. M., & Suh, H. J. (2011). Stimulation of osteoblastic differentiation and mineralization in MC3T3-E1 cells by yeast hydrolysate. *Phytotherapy Research*, *25*(5), 716–723. <https://doi.org/10.1002/ptr.3328>
- Lee, H. S., Jung, E. Y., & Suh, H. J. (2009). Chemical composition and anti-stress effects of yeast hydrolysate. *Journal of Medicinal Food*, *12*(6), 1281–1285. <https://doi.org/10.1089/jmf.2009.0098>
- Lee, S.-H., & Song, K. Bin. (2009). Purification of an iron-binding nona-peptide from hydrolysates of porcine blood plasma protein. *Process Biochemistry*, *44*(3), 378–381. <https://doi.org/10.1016/j.procbio.2008.12.001>
- Li, B., He, H., Shi, W., & Hou, T. (2019). Effect of duck egg white peptide-ferrous chelate on iron bioavailability in vivo and structure characterization. *Journal of the Science of Food and Agriculture*, *99*(4), 1834–1841. <https://doi.org/10.1002/jsfa.9377>
- Liapis, A., & Bruttini, R. (2020). Freeze drying. In *Handbook of industrial drying* (pp. 309–343).
- Lin, H. M., Chan, E. C., Chen, C., & Chen, L. F. (1991). Disintegration of yeast cells by pressurized carbon dioxide. *Biotechnology Progress*, *7*(3), 201–204. <https://doi.org/10.1021/bp00009a001>
- Lin, H. M., Yang, Z., & Chen, L. F. (1992). An improved method for disruption of microbial cells with pressurized carbon dioxide. *Biotechnology Progress*, *8*(2), 165–166. <https://doi.org/10.1021/bp00014a012>
- Lin, S., Hu, X., Li, L., Yang, X., Chen, S., Wu, Y., & Yang, S. (2021). Preparation, purification and identification of iron-chelating peptides derived from tilapia (*Oreochromis niloticus*) skin collagen and characterization of the peptide-iron complexes. *Lwt*, *149*(231), 111796. <https://doi.org/10.1016/j.lwt.2021.111796>
- Lindblom, M. (1977). Properties of intracellular ribonuclease utilized for RNA reduction in disintegrated cells of *Saccharomyces cerevisiae*. *Biotechnology and Bioengineering*, *19*(2), 199–210. <https://doi.org/10.1002/bit.260190204>
- Liu, D., Ding, L., Sun, J., Boussetta, N., & Vorobiev, E. (2016). Yeast cell disruption

- strategies for recovery of intracellular bio-active compounds — A review. *Innovative Food Science and Emerging Technologies*, 36, 181–192. <https://doi.org/10.1016/j.ifset.2016.06.017>
- Liu, D., Lebovka, N. I., & Vorobiev, E. (2013). Impact of Electric Pulse Treatment on Selective Extraction of Intracellular Compounds from *Saccharomyces cerevisiae* Yeasts. *Food and Bioprocess Technology*, 6(2), 576–584. <https://doi.org/10.1007/s11947-011-0703-7>
- Liu, D., Savoie, R., Vorobiev, E., & Lanoisellé, J. L. (2010). Effect of disruption methods on the dead-end microfiltration behavior of yeast suspension. *Separation Science and Technology*, 45(8), 1042–1050. <https://doi.org/10.1080/01496391003727890>
- Liu, D., Zeng, X.-A. A., Sun, D.-W. W., & Han, Z. (2013). Disruption and protein release by ultrasonication of yeast cells. *Innovative Food Science & Emerging Technologies*, 18, 132–137. <https://doi.org/10.1016/j.ifset.2013.02.006>
- Liu, X. Y., Wang, Q., Cui, S. W., & Liu, H. Z. (2008). A new isolation method of β -d-glucans from spent yeast *Saccharomyces cerevisiae*. *Food Hydrocolloids*, 22(2), 239–247. <https://doi.org/10.1016/j.foodhyd.2006.11.008>
- Long, W. (2017). Automated amino acid analysis using an Agilent Poroshell HPH-C18 column. *Application Note, Agilent Technologies, Inc., Publicatio*, 1–10.
- Lonvaud-Funel, A. (2000). Lactic acid bacteria in the quality improvement and depreciation of wine. *Antonie van Leeuwenhoek*, 76(1–4), 317–331. <http://www.ncbi.nlm.nih.gov/pubmed/10532386>
- Lothe, R. R., Purohit, S. S., Shaikh, S. S., Malshe, V. C., & Pandit, A. B. (1999). *Purification of α -glucosidase and invertase from bakers' yeast on modified polymeric supports*. 293–306. <https://doi.org/10.1023/A:1008126628635>
- Lowry, O. H., Rosebrough, N. J., Farr, A. L., & Randall, R. J. (1951). Protein measurement with the Folin phenol reagent. *The Journal of Biological Chemistry*. [https://doi.org/10.1016/0922-338X\(96\)89160-4](https://doi.org/10.1016/0922-338X(96)89160-4)
- Mæhre, H. K., Dalheim, L., Edvinsen, G. K., Elvevoll, E. O., & Jensen, I. J. (2018). Protein determination—method matters. *Foods*, 7(1). <https://doi.org/10.3390/foods7010005>
- Malison, A., Arpanutud, P., & Keeratipibul, S. (2021). Chicken foot broth byproduct: A new source for highly effective peptide-calcium chelate. *Food Chemistry*, 345(November 2020), 128713. <https://doi.org/10.1016/j.foodchem.2020.128713>
- Maluly, H. D. B., Arisseto-Bragotto, A. P., & Reyes, F. G. R. (2017). Monosodium glutamate as a tool to reduce sodium in foodstuffs: Technological and safety aspects.

- Food Science and Nutrition*, 5(6), 1039–1048. <https://doi.org/10.1002/fsn3.499>
- Mareček, V., Míkyška, A., Hampel, D., Čejka, P., Neuwirthová, J., Malachová, A., & Cerkal, R. (2017). ABTS and DPPH methods as a tool for studying antioxidant capacity of spring barley and malt. *Journal of Cereal Science*, 73, 40–45. <https://doi.org/10.1016/j.jcs.2016.11.004>
- Marson, G. V., de Castro, R. J. S., Belleville, M.-P., & Hubinger, M. D. (2020). Spent brewer's yeast as a source of high added value molecules: a systematic review on its characteristics, processing and potential applications. *World Journal of Microbiology and Biotechnology*, 36(7), 95. <https://doi.org/10.1007/s11274-020-02866-7>
- Marson, G. V., de Castro, R. J. S., Machado, M. T. da C., da Silva Zandonadi, F., Barros, H. D. de F. Q., Maróstica Júnior, M. R., Sussulini, A., & Hubinger, M. D. (2020). Proteolytic enzymes positively modulated the physicochemical and antioxidant properties of spent yeast protein hydrolysates. *Process Biochemistry*, 91(November 2019), 34–45. <https://doi.org/10.1016/j.procbio.2019.11.030>
- Marson, G. V., Lacour, S., Hubinger, M. D., & Belleville, M. P. (2022). Serial fractionation of spent brewer's yeast protein hydrolysate by ultrafiltration: A peptide-rich product with low RNA content. *Journal of Food Engineering*, 312(July 2021), 110737. <https://doi.org/10.1016/j.jfoodeng.2021.110737>
- Meadows, A. L., Hawkins, K. M., Tsegaye, Y., Antipov, E., Kim, Y., Raetz, L., Dahl, R. H., Tai, A., Mahatdejkul-Meadows, T., Xu, L., Zhao, L., Dasika, M. S., Murarka, A., Lenihan, J., Eng, D., Leng, J. S., Liu, C.-L., Wenger, J. W., Jiang, H., ... Tsong, A. E. (2016). Rewriting yeast central carbon metabolism for industrial isoprenoid production. *Nature*, 537(7622), 694–697. <https://doi.org/10.1038/nature19769>
- Middelberg, A. P. J. (1995). Process-scale disruption of microorganisms. *Biotechnology Advances*, 13(3), 491–551. [https://doi.org/10.1016/0734-9750\(95\)02007-P](https://doi.org/10.1016/0734-9750(95)02007-P)
- Minkiewicz, I., Iwaniak, & Darewicz. (2019). BIOPEP-UWM Database of Bioactive Peptides: Current Opportunities. *International Journal of Molecular Sciences*, 20(23), 5978. <https://doi.org/10.3390/ijms20235978>
- Mirzaei, M., Mirdamadi, S., Ehsani, M. R., & Aminlari, M. (2018). Production of antioxidant and ACE-inhibitory peptides from *Kluyveromyces marxianus* protein hydrolysates: Purification and molecular docking. *Journal of Food and Drug Analysis*, 26(2), 696–705. <https://doi.org/10.1016/j.jfda.2017.07.008>
- Mirzaei, M., Mirdamadi, S., Ehsani, M. R., Aminlari, M., & Hosseini, E. (2015). Purification and identification of antioxidant and ACE-inhibitory peptide from *Saccharomyces*

- cerevisiae protein hydrolysate. *Journal of Functional Foods*, 19, 259–268. <https://doi.org/10.1016/j.jff.2015.09.031>
- Mirzaei, M., Mirdamadi, S., & Safavi, M. (2019). Antioxidant activity and protective effects of *Saccharomyces cerevisiae* peptide fractions against - H₂O₂ - induced oxidative stress in Caco - 2 cells. *Journal of Food Measurement and Characterization*, 13(4), 2654–2662. <https://doi.org/10.1007/s11694-019-00186-5>
- Mirzaei, M., Shavandi, A., Mirdamadi, S., Soleymanzadeh, N., Motahari, P., Mirdamadi, N., Moser, M., Subra, G., Alimoradi, H., & Goriely, S. (2021). Bioactive peptides from yeast: A comparative review on production methods, bioactivity, structure-function relationship, and stability. *Trends in Food Science & Technology*, 118, 297–315. <https://doi.org/https://doi.org/10.1016/j.tifs.2021.10.008>
- Mohammad, A. W., Ng, C. Y., Lim, Y. P., & Ng, G. H. (2012). Ultrafiltration in food processing industry: review on application, membrane fouling, and fouling control. *Food and Bioprocess Technology*, 5(4), 1143–1156. <https://doi.org/10.1007/s11947-012-0806-9>
- Monhemius, A. J. (1977). Precipitation Diagrams for Metal Hydroxides, Sulphides, Arsenates and Phosphates. *Transactions of the Institution of Mining and Metallurgy, Section C: Mineral Processing and Extractive Metallurgy*, 86.
- Mookherjee, N., Anderson, M. A., Haagsman, H. P., & Davidson, D. J. (2020). Antimicrobial host defence peptides: functions and clinical potential. *Nature Reviews Drug Discovery*, 19(5), 311–332. <https://doi.org/10.1038/s41573-019-0058-8>
- Mukherjee, M., Nandi, A., Chandra, K., Saikia, S. K., Jana, C. K., & Das, N. (2020). Protein extraction from *Saccharomyces cerevisiae* at different growth phases. *Journal of Microbiological Methods*, 172, 105906. <https://doi.org/10.1016/j.mimet.2020.105906>
- Nandy, S. K., & Srivastava, R. K. (2018). A review on sustainable yeast biotechnological processes and applications. *Microbiological Research*, 207, 83–90. <https://doi.org/10.1016/j.micres.2017.11.013>
- Nasseri, A. T., Rasoul-Ami, S., Morowvat, M. H., & Ghasemi, Y. (2011). Single Cell Protein: Production and Process. *American Journal of Food Technology*, 6(2), 103–116. <https://doi.org/10.3923/ajft.2011.103.116>
- Nehete, J., Narkhede, M., Bhambar, R., Gawali, S., Narkhede, M., & Gawali, S. (2013). Natural proteins: Sources, isolation, characterization and applications. *Pharmacognosy Reviews*, 7(14), 107. <https://doi.org/10.4103/0973-7847.120508>
- Neves, M. C., Filipe, H. A. L., Reis, R. L., Ramalho, J. P. P., Coreta-Gomes, F., Moreno,

- M. J., & Loura, L. M. S. (2019). Interaction of bile salts with lipid bilayers: An atomistic molecular dynamics study. *Frontiers in Physiology*, 10(APR), 1–11. <https://doi.org/10.3389/fphys.2019.00393>
- Ni, H., Li, L., Guo, S.-S., Li, H.-H., Jiang, R., & Hu, S.-Q. (2012). Isolation and identification of an angiotensin-I converting enzyme inhibitory peptide from yeast (*Saccharomyces cerevisiae*). *Current Analytical Chemistry*, 8(1), 180–185. <https://doi.org/10.2174/157341112798472224>
- Ni, H., Li, L., Liu, G., & Hu, S. (2012). Inhibition Mechanism and Model of an Angiotensin I-Converting Enzyme (ACE)-Inhibitory Hexapeptide from Yeast (*Saccharomyces cerevisiae*). *PLoS ONE*, 7(5), 1–7. <https://doi.org/10.1371/journal.pone.0037077>
- O'Loughlin, I. B., Kelly, P. M., Murray, B. A., FitzGerald, R. J., & Brodtkorb, A. (2015). Molecular Characterization of Whey Protein Hydrolysate Fractions with Ferrous Chelating and Enhanced Iron Solubility Capabilities. *Journal of Agricultural and Food Chemistry*, 63(10), 2708–2714. <https://doi.org/10.1021/jf505817a>
- Ohshima, T., Sato, M., & Saito, M. (1995). Selective release of intracellular protein using pulsed electric field. *Journal of Electrostatics*, 35(1), 103–112. [https://doi.org/10.1016/0304-3886\(95\)00014-2](https://doi.org/10.1016/0304-3886(95)00014-2)
- Okolie, C. L., Akanbi, T. O., Mason, B., Udenigwe, C. C., & Aryee, A. N. A. (2019). Influence of conventional and recent extraction technologies on physicochemical properties of bioactive macromolecules from natural sources: A review. *Food Research International*, 116, 827–839. <https://doi.org/10.1016/j.foodres.2018.09.018>
- Oliveira, A. M., & Oliva Neto, P. de. (2011). Improvement in RNA extraction from *S. cerevisiae* by optimization in the autolysis and NH₃ hydrolysis. *Brazilian Archives of Biology and Technology*, 54(5), 1007–1018. <https://doi.org/10.1590/S1516-89132011000500019>
- Oliveira, A. S., Ferreira, C., Pereira, J. O., Pintado, M. E., & Carvalho, A. P. (2022a). Spent brewer's yeast (*Saccharomyces cerevisiae*) as a potential source of bioactive peptides: An overview. *International Journal of Biological Macromolecules*, 208, 1116–1126. <https://doi.org/https://doi.org/10.1016/j.ijbiomac.2022.03.094>
- Oliveira, A. S., Ferreira, C., Pereira, J. O., Pintado, M. E., & Carvalho, A. P. (2022b). Valorisation of protein-rich extracts from spent brewer's yeast (*Saccharomyces cerevisiae*): an overview. *Biomass Conversion and Biorefinery*, 0123456789. <https://doi.org/10.1007/s13399-022-02636-5>
- Oliveira, A. S., Odila Pereira, J., Ferreira, C., Faustino, M., Durão, J., Pereira, A. M.,

- Oliveira, C. M., Pintado, M. E., & Carvalho, A. P. (2022). Spent Yeast Valorization for Food Applications: Effect of Different Extraction Methodologies. *Foods*, *11*(24), 4002. <https://doi.org/10.3390/foods11244002>
- Oliveira, A. S., Pereira, J. O., Ferreira, C., Faustino, M., Durão, J., Pintado, M. E., & Carvalho, A. P. (2022). Peptide-rich extracts from spent yeast waste streams as a source of bioactive compounds for the nutraceutical market. *Innovative Food Science & Emerging Technologies*, *81*, 103148. <https://doi.org/10.1016/j.ifset.2022.103148>
- Oliveira, C. M., Horta, B., Leal, T., Pintado, M., & Oliveira, C. S. S. (2022). Valorization of Spent Sugarcane Fermentation Broth as a Source of Phenolic Compounds. *Processes*, *10*(7), 1339. <https://doi.org/10.3390/pr10071339>
- Onufriev, A. V., & Alexov, E. (2013). Protonation and pK changes in protein–ligand binding. *Quarterly Reviews of Biophysics*, *46*(2), 181–209. <https://doi.org/10.1017/S0033583513000024>
- Orlean, P. (2012). Architecture and biosynthesis of the *Saccharomyces cerevisiae* cell wall. *Genetics*, *192*(3), 775–818. <https://doi.org/10.1534/genetics.112.144485>
- Osakwe, O. (2016). Preclinical In Vitro Studies: Development and Applicability. In *Social Aspects of Drug Discovery, Development and Commercialization* (pp. 129–148). Elsevier. <https://doi.org/10.1016/B978-0-12-802220-7.00006-5>
- Osório, H., Silva, C., Ferreira, M., Gullo, I., Máximo, V., Barros, R., Mendonça, F., Oliveira, C., & Carneiro, F. (2021). Proteomics analysis of gastric cancer patients with diabetes mellitus. *Journal of Clinical Medicine*, *10*(3), 1–14. <https://doi.org/10.3390/jcm10030407>
- Parapouli, M., Vasileiadi, A., Afendra, A.-S., & Hatziloukas, E. (2020). *Saccharomyces cerevisiae* and its industrial applications. *AIMS Microbiology*, *6*(1), 1–32. <https://doi.org/10.3934/microbiol.2020001>
- Park, Y., Kim, J. H., Lee, H. S., Jung, E. Y., Lee, H., Noh, D. O., & Suh, H. J. (2013). Thermal stability of yeast hydrolysate as a novel anti-obesity material. *Food Chemistry*, *136*(2), 316–321. <https://doi.org/10.1016/j.foodchem.2012.08.047>
- Payen, C., & Thompson, D. (2019). The renaissance of yeasts as microbial factories in the modern age of biomanufacturing. *Yeast*, *36*(12), 685–700. <https://doi.org/10.1002/yea.3439>
- Pereira, P. R., Freitas, C. S., & Paschoalin, V. M. F. (2021). *Saccharomyces cerevisiae* biomass as a source of next-generation food preservatives: Evaluating potential proteins as a source of antimicrobial peptides. *Comprehensive Reviews in Food Science*

- and Food Safety*, 20(5), 4450–4479. <https://doi.org/10.1111/1541-4337.12798>
- Pérez-Torres, I., Zuniga-Munoz, A., & Guarner-Lans, V. (2016). Beneficial Effects of the Amino Acid Glycine. *Mini-Reviews in Medicinal Chemistry*, 17(1), 15–32. <https://doi.org/10.2174/1389557516666160609081602>
- Pinto, M., Coelho, E., Nunes, A., Brandão, T., & Coimbra, M. A. (2015). Valuation of brewers spent yeast polysaccharides: A structural characterization approach. *Carbohydrate Polymers*, 116, 215–222. <https://doi.org/10.1016/j.carbpol.2014.03.010>
- Pirtskhalava, M., Amstrong, A. A., Grigolava, M., Chubinidze, M., Alimbarashvili, E., Vishnepolsky, B., Gabrielian, A., Rosenthal, A., Hurt, D. E., & Tartakovsky, M. (2021). DBAASP v3: database of antimicrobial/cytotoxic activity and structure of peptides as a resource for development of new therapeutics. *Nucleic Acids Research*, 49(D1), D288–D297. <https://doi.org/10.1093/nar/gkaa991>
- Podpora, B., Swiderski, F., Sadowska, A., Piotrowska, A., & Rakowska, R. (2015). Spent Brewer's Yeast Autolysates as a New and Valuable Component of Functional Food and Dietary Supplements. *Journal of Food Processing & Technology*, 6(12). <https://doi.org/10.4172/2157-7110.1000526>
- Podpora, B., Swiderski, F., Sadowska, A., Rakowska, R., & Wasiak-Zys, G. (2016). Spent brewer's yeast extracts as a new component of functional food. *Czech Journal of Food Sciences*, 34(6), 554–563. <https://doi.org/10.17221/419/2015-CJFS>
- Powers, J.-P. S., & Hancock, R. E. . (2003). The relationship between peptide structure and antibacterial activity. *Peptides*, 24(11), 1681–1691. <https://doi.org/10.1016/j.peptides.2003.08.023>
- Pratap, G., Jadaun, S., Dixit, S., Saklani, V., Mendiratta, S., Jain, R., & Singh, S. (2017). *HPLC for Peptides and Proteins : Principles , Methods and Applications*. 8(1), 1–6. <https://doi.org/10.5530/phm.2017.8.1>
- Prior, R. L., Hoang, H., Gu, L., Wu, X., Bacchiocca, M., Howard, L., Hampsch-Woodill, M., Huang, D., Ou, B., & Jacob, R. (2003). Assays for hydrophilic and lipophilic antioxidant capacity (oxygen radical absorbance capacity (ORACFL)) of plasma and other biological and food samples. *Journal of Agricultural and Food Chemistry*, 51(11), 3273–3279. <https://doi.org/10.1021/jf0262256>
- Prior, R. L., Wu, X., & Schaich, K. (2005). Standardized Methods for the Determination of Antioxidant Capacity and Phenolics in Foods and Dietary Supplements. *Journal of Agricultural and Food Chemistry*, 53(10), 4290–4302. <https://doi.org/10.1021/jf0502698>

- Proma, F. H., Shourav, M. K., & Choi, J. (2020). Post-antibiotic effect of ampicillin and levofloxacin to escherichia coli and staphylococcus aureus based on microscopic imaging analysis. *Antibiotics*, *9*(8), 1–13. <https://doi.org/10.3390/antibiotics9080458>
- Puligundla, P., Mok, C., & Park, S. (2020). Advances in the valorization of spent brewer's yeast. *Innovative Food Science & Emerging Technologies*, *62*, 102350. <https://doi.org/10.1016/j.ifset.2020.102350>
- Rai, A. K., Pandey, A., & Sahoo, D. (2019). Biotechnological potential of yeasts in functional food industry. *Trends in Food Science & Technology*, *83*, 129–137. <https://doi.org/10.1016/j.tifs.2018.11.016>
- Rakowska, R., Sadowska, A., Dybkowska, E., & Świdorski, F. (2017). Spent yeast as natural source of functional food additives. *Roczniki Panstwowego Zakladu Higieny*, *68*(2), 115–121. <http://www.ncbi.nlm.nih.gov/pubmed/28646828>
- Ramos-Viana, V., Møller-Hansen, I., Kempen, P., & Borodina, I. (2022). Modulation of the cell wall protein Ecm33p in yeast *Saccharomyces cerevisiae* improves the production of small metabolites. *FEMS Yeast Research*, *August*, 1–11. <https://doi.org/10.1093/femsyr/foac037>
- Remondetto, G. E., Beyssac, E., & Subirade, M. (2004). Iron Availability from Whey Protein Hydrogels: An *in vitro* Study. *Journal of Agricultural and Food Chemistry*, *52*(26), 8137–8143. <https://doi.org/10.1021/jf040286h>
- Ritala, A., Häkkinen, S. T., Toivari, M., & Wiebe, M. G. (2017). Single Cell Protein—State-of-the-Art, Industrial Landscape and Patents 2001–2016. *Frontiers in Microbiology*, *8*(OCT). <https://doi.org/10.3389/fmicb.2017.02009>
- Rudravaram, R., Chandel, A. K., Rao, L. V., Hui, Y. Z., & Ravindra, P. (2009). Bio (Single Cell) Protein: Issues of Production, Toxins and Commercialisation Status. In *Agricultural Wastes* (pp. 129–153). http://agrifs.ir/sites/default/files/Agricultural_Wastes_0.pdf
- Ryan, D. J., Spraggins, J. M., & Caprioli, R. M. (2019). Protein identification strategies in MALDI imaging mass spectrometry: a brief review. *Current Opinion in Chemical Biology*, *48*, 64–72. <https://doi.org/10.1016/j.cbpa.2018.10.023>
- Sá, A. G. A., Moreno, Y. M. F., & Carciofi, B. A. M. (2020). Plant proteins as high-quality nutritional source for human diet. *Trends in Food Science & Technology*, *97*, 170–184. <https://doi.org/10.1016/j.tifs.2020.01.011>
- Safiri, S., Kolahi, A. A., Noori, M., Nejadghaderi, S. A., Karamzad, N., Bragazzi, N. L., Sullman, M. J. M., Abdollahi, M., Collins, G. S., Kaufman, J. S., & Grieger, J. A.

- (2021). Burden of anemia and its underlying causes in 204 countries and territories, 1990–2019: results from the Global Burden of Disease Study 2019. *Journal of Hematology and Oncology*, *14*(1), 185. <https://doi.org/10.1186/s13045-021-01202-2>
- San Martin, D., Ibaruri, J., Iñarra, B., Luengo, N., Ferrer, J., Alvarez-Ossorio, C., Bald, C., Gutierrez, M., & Zufia, J. (2021). Valorisation of Brewer's Spent Yeasts' Hydrolysates as High-Value Bioactive Molecules. *Sustainability*, *13*(12), 6520. <https://doi.org/10.3390/su13126520>
- Sánchez, A., & Vázquez, A. (2017). Bioactive peptides: A review. *Food Quality and Safety*, *1*(1), 29–46. <https://doi.org/10.1093/fqs/fyx006>
- Schaich, K. M., Tian, X., & Xie, J. (2015). Hurdles and pitfalls in measuring antioxidant efficacy: A critical evaluation of ABTS, DPPH, and ORAC assays. *Journal of Functional Foods*, *14*, 111–125. <https://doi.org/10.1016/j.jff.2015.01.043>
- Scheers, N. M., Almgren, A. B., & Sandberg, A.-S. (2014). Proposing a Caco-2/HepG2 cell model for *in vitro* iron absorption studies. *The Journal of Nutritional Biochemistry*, *25*(7), 710–715. <https://doi.org/10.1016/j.jnutbio.2014.02.013>
- Selvendran, R. R., March, J. F., & Ring, S. G. (1979). Determination of aldoses and uronic acid content of vegetable fiber. *Analytical Biochemistry*, *96*(2), 282–292. [https://doi.org/10.1016/0003-2697\(79\)90583-9](https://doi.org/10.1016/0003-2697(79)90583-9)
- Sharma, A., Shilpa Shree, B. G., Arora, S., & Kapila, S. (2017). Preparation of lactose-iron complex and its cyto-toxicity, in-vitro digestion and bioaccessibility in Caco-2 cell model system. *Food Bioscience*, *20*, 125–130. <https://doi.org/10.1016/j.fbio.2017.10.001>
- Sharma, S., Singh, R., & Rana, S. (2011). Bioactive peptides: A review. *International Journal Bioautomation*, *15*(4), 223–250. <https://doi.org/10.1093/fqs/fyx006>
- Sheldon, R. A. (2018). Metrics of Green Chemistry and Sustainability: Past, Present, and Future. *ACS Sustainable Chemistry & Engineering*, *6*(1), 32–48. <https://doi.org/10.1021/acssuschemeng.7b03505>
- Shen, Y., Tebben, L., Chen, G., & Li, Y. (2019). Effect of amino acids on Maillard reaction product formation and total antioxidant capacity in white pan bread. *International Journal of Food Science and Technology*, *54*(4), 1372–1380. <https://doi.org/10.1111/ijfs.14027>
- Shetty, J. K., & Kinsella, J. E. (1980a). Ready separation of proteins from nucleoprotein complexes by reversible modification of lysine residues. *Biochemical Journal*, *191*(1), 269–272. <https://doi.org/10.1042/bj1910269>

- Shetty, J. K., & Kinsella, J. E. (1980b). Lysinoalanine formation in yeast proteins isolated by alkaline methods. *Journal of Agricultural and Food Chemistry*, 28(4), 798–800. <https://doi.org/10.1021/jf60230a019>
- Shetty, K. J., & Kinsella, J. E. (1979). Preparation of Yeast Protein Isolate With Low Nucleic Acid By Succinylation. *Journal of Food Science*, 44(3), 633–638. <https://doi.org/10.1111/j.1365-2621.1979.tb08464.x>
- Shi, G., Kang, X., Dong, F., Liu, Y., Zhu, N., Hu, Y., Xu, H., Lao, X., & Zheng, H. (2022). DRAMP 3.0: an enhanced comprehensive data repository of antimicrobial peptides. *Nucleic Acids Research*, 50(D1), D488–D496. <https://doi.org/10.1093/nar/gkab651>
- Shields, H. J., Traa, A., & Van Raamsdonk, J. M. (2021). Beneficial and Detrimental Effects of Reactive Oxygen Species on Lifespan: A Comprehensive Review of Comparative and Experimental Studies. *Frontiers in Cell and Developmental Biology*, 9. <https://doi.org/10.3389/fcell.2021.628157>
- Shilpashree, B. G., Arora, S., Kapila, S., & Sharma, V. (2020). Whey protein-iron or zinc complexation decreases pro-oxidant activity of iron and increases iron and zinc bioavailability. *LWT*, 126, 109287. <https://doi.org/10.1016/j.lwt.2020.109287>
- Shubham, K., Anukiruthika, T., Dutta, S., Kashyap, A. V., Moses, J. A., & Anandharamakrishnan, C. (2020). Iron deficiency anemia: A comprehensive review on iron absorption, bioavailability and emerging food fortification approaches. *Trends in Food Science & Technology*, 99, 58–75. <https://doi.org/10.1016/j.tifs.2020.02.021>
- Shynkaryk, M. V., Lebovka, N. I., Lanoisellé, J. L., Nonus, M., Bedel-Clotour, C., & Vorobiev, E. (2009). Electrically-assisted extraction of bio-products using high pressure disruption of yeast cells (*Saccharomyces cerevisiae*). *Journal of Food Engineering*, 92(2), 189–195. <https://doi.org/10.1016/j.jfoodeng.2008.10.041>
- Siddiqi, S. F., Titchener-Hooker, N. J., & Shamlou, P. A. (1997). High pressure disruption of yeast cells: The use of scale down operations for the prediction of protein release and cell debris size distribution. *Biotechnology and Bioengineering*, 55(4), 642–649. [https://doi.org/10.1002/\(SICI\)1097-0290\(19970820\)55:4<642::AID-BIT6>3.0.CO;2-H](https://doi.org/10.1002/(SICI)1097-0290(19970820)55:4<642::AID-BIT6>3.0.CO;2-H)
- Smialowska, A., Matia-Merino, L., & Carr, A. J. (2017). Assessing the iron chelation capacity of goat casein digest isolates. *Journal of Dairy Science*, 100(4), 2553–2563. <https://doi.org/10.3168/jds.2016-12090>
- Smith, P. K., Krohn, R. I., Hermanson, G. T., Mallia, A. K., Gartner, F. H., Provenzano, M. D., Fujimoto, E. K., Goeke, N. M., Olson, B. J., & Klenk, D. C. (1985). Measurement

- of protein using bicinchoninic acid. *Analytical Biochemistry*, 150(1), 76–85.
[https://doi.org/10.1016/0003-2697\(85\)90442-7](https://doi.org/10.1016/0003-2697(85)90442-7)
- Soares, R., Mendonça, S., de Castro, L. Í., Menezes, A., & Arêas, J. (2015). Major Peptides from Amaranth (*Amaranthus cruentus*) Protein Inhibit HMG-CoA Reductase Activity. *International Journal of Molecular Sciences*, 16(2), 4150–4160.
<https://doi.org/10.3390/ijms16024150>
- Sombutyanuchit, P., Suphantharika, M., & Verduyn, C. (2001). Preparation of 5'-GMP-rich yeast extracts from spent brewer's yeast. *World Journal of Microbiology and Biotechnology*, 17(2), 163–168. <https://doi.org/10.1023/A:1016686504154>
- Sözüğeçer, S., & Bayramgil, N. P. (2013). Activity of glucose oxidase immobilized onto Fe³⁺ attached hydroxypropyl methylcellulose films. *Colloids and Surfaces B: Biointerfaces*, 101, 19–25. <https://doi.org/10.1016/j.colsurfb.2012.05.029>
- Stewart, G. G. (2016). *Saccharomyces* species in the production of beer. *Beverages*, 2(4).
<https://doi.org/10.3390/beverages2040034>
- Suh, H., Lee, H., & Jung, J. (2003). Mycosporine Glycine Protects Biological Systems Against Photodynamic Damage by Quenching Singlet Oxygen with a High Efficiency¶. *Photochemistry and Photobiology*, 78(2), 109.
[https://doi.org/10.1562/0031-8655\(2003\)078<0109:mgpbsa>2.0.co;2](https://doi.org/10.1562/0031-8655(2003)078<0109:mgpbsa>2.0.co;2)
- Sui, H., Zhou, J., Ma, G., Niu, Y., Cheng, J., He, L., & Li, X. (2018). Removal of ionic liquids from oil sands processing solution by ion-exchange resin. *Applied Sciences*, 8(9), 1611. <https://doi.org/10.3390/app8091611>
- Sun, N., Cui, P., Jin, Z., Wu, H., Wang, Y., & Lin, S. (2017). Contributions of molecular size, charge distribution, and specific amino acids to the iron-binding capacity of sea cucumber (*Stichopus japonicus*) ovum hydrolysates. *Food Chemistry*, 230, 627–636.
<https://doi.org/10.1016/j.foodchem.2017.03.077>
- Takaloo, Z., Nikkhah, M., Nemati, R., Jalilian, N., & Sajedi, R. H. (2020). Autolysis, plasmolysis and enzymatic hydrolysis of baker's yeast (*Saccharomyces cerevisiae*): a comparative study. *World Journal of Microbiology and Biotechnology*, 36(5), 1–14.
<https://doi.org/10.1007/s11274-020-02840-3>
- Tang, C., Wang, L., Zang, L., Wang, Q., Qi, D., & Dai, Z. (2023). On-demand biomufacturing through synthetic biology approach. *Materials Today Bio*, 18, 100518. <https://doi.org/https://doi.org/10.1016/j.mtbio.2022.100518>
- Tian, R., Feng, J., Huang, G., Tian, B., Zhang, Y., Jiang, L., & Sui, X. (2020). Ultrasound driven conformational and physicochemical changes of soy protein hydrolysates.

<https://doi.org/10.1016/j.ultsonch.2020.105202>

- Tian, X., Yang, P., & Jiang, W. (2019). Effect of Alkali Treatment Combined with High Pressure on Extraction Efficiency of β -d-Glucan from Spent Brewer's Yeast. *Waste and Biomass Valorization*, 10(5), 1131–1140. <https://doi.org/10.1007/s12649-017-0130-8>
- Torres-Fuentes, C., Alaiz, M., & Vioque, J. (2012). Iron-chelating activity of chickpea protein hydrolysate peptides. *Food Chemistry*, 134(3), 1585–1588. <https://doi.org/10.1016/j.foodchem.2012.03.112>
- Vieira, E. F., Carvalho, J., Pinto, E., Cunha, S., Almeida, A. A., & Ferreira, I. M. P. L. V. O. (2016). Nutritive value, antioxidant activity and phenolic compounds profile of brewer's spent yeast extract. *Journal of Food Composition and Analysis*, 52, 44–51. <https://doi.org/10.1016/j.jfca.2016.07.006>
- Vieira, E. F., Cunha, S. C., & Ferreira, I. M. P. L. V. O. (2019). Characterization of a Potential Bioactive Food Ingredient from Inner Cellular Content of Brewer's Spent Yeast. *Waste and Biomass Valorization*, 10(11), 3235–3242. <https://doi.org/10.1007/s12649-018-0368-9>
- Vieira, E. F., Melo, A., & Ferreira, I. M. P. L. V. O. (2017). Autolysis of intracellular content of Brewer's spent yeast to maximize ACE-inhibitory and antioxidant activities. *LWT - Food Science and Technology*, 82, 255–259. <https://doi.org/10.1016/j.lwt.2017.04.046>
- Vollet Marson, G., Belleville, M., Lacour, S., & Dupas Hubinger, M. (2020). Membrane Fractionation of Protein Hydrolysates from By-Products: Recovery of Valuable Compounds from Spent Yeasts. *Membranes*, 11(1), 23. <https://doi.org/10.3390/membranes11010023>
- Wada, Y., & Lönnerdal, B. (2014). Bioactive peptides derived from human milk proteins - mechanisms of action. *Journal of Nutritional Biochemistry*, 25(5), 503–514. <https://doi.org/10.1016/j.jnutbio.2013.10.012>
- Waldvogel-Abramowski, S., Waeber, G., Gassner, C., Buser, A., Frey, B. M., Favrat, B., & Tissot, J.-D. (2014). Physiology of Iron Metabolism. *Transfusion Medicine and Hemotherapy*, 41(3), 213–221. <https://doi.org/10.1159/000362888>
- Walters, M., Esfandi, R., & Tsopmo, A. (2018). Potential of Food Hydrolyzed Proteins and Peptides to Chelate Iron or Calcium and Enhance their Absorption. *Foods*, 7(10), 172. <https://doi.org/10.3390/foods7100172>
- Wang, G., Li, X., & Wang, Z. (2016). APD3: the antimicrobial peptide database as a tool

- for research and education. *Nucleic Acids Research*, 44, D1087–D1093. <https://doi.org/10.1093/nar/gkv1278>
- Wang, J., Li, M., Zheng, F., Niu, C., Liu, C., Li, Q., & Sun, J. (2018). Cell wall polysaccharides: before and after autolysis of brewer's yeast. *World Journal of Microbiology and Biotechnology*, 34(9), 137. <https://doi.org/10.1007/s11274-018-2508-6>
- Wang, L., Ding, Y., Zhang, X., Li, Y., Wang, R., Luo, X., Li, Y., Li, J., & Chen, Z. (2018). Isolation of a novel calcium-binding peptide from wheat germ protein hydrolysates and the prediction for its mechanism of combination. *Food Chemistry*, 239, 416–426. <https://doi.org/10.1016/j.foodchem.2017.06.090>
- Wang, L., Yang, J., Wang, Y., Zhang, J., Gao, Y., Yuan, J., Su, A., & Ju, X. (2016). Study on Antioxidant Activity and Amino Acid Analysis of Rapeseed Protein Hydrolysates. *International Journal of Food Properties*, 19(9), 1899–1911. <https://doi.org/10.1080/10942912.2015.1085397>
- Wang, T., Lin, S., Cui, P., Bao, Z., Liu, K., Jiang, P., Zhu, B., & Sun, N. (2020). Antarctic krill derived peptide as a nanocarrier of iron through the gastrointestinal tract. *Food Bioscience*, 36, 100657. <https://doi.org/10.1016/j.fbio.2020.100657>
- Wang, X., Ai, T., Meng, X. L., Zhou, J., & Mao, X. Y. (2014). *In vitro* iron absorption of α -lactalbumin hydrolysate-iron and β -lactoglobulin hydrolysate-iron complexes. *Journal of Dairy Science*, 97(5), 2559–2566. <https://doi.org/10.3168/jds.2013-7461>
- Wang, X., Li, M., Li, M., Mao, X., Zhou, J., & Ren, F. (2011). Preparation and characteristics of yak casein hydrolysate-iron complex. *International Journal of Food Science and Technology*, 46(8), 1705–1710. <https://doi.org/10.1111/j.1365-2621.2011.02672.x>
- Williams, R., Dias, D. A., Jayasinghe, N., Roessner, U., & Bennett, L. E. (2016). Beta-glucan-depleted, glycopeptide-rich extracts from Brewer's and Baker's yeast (*Saccharomyces cerevisiae*) lower interferon-gamma production by stimulated human blood cells *in vitro*. *Food Chemistry*, 197, 761–768. <https://doi.org/10.1016/j.foodchem.2015.11.015>
- World Health Organization. (2007). Protein and amino acid requirements in human nutrition. Report of a Joint WHO/FAO/UNU Expert Consultation. In *WHO Technical Report Series*.
- World Health Organization. (2008). *Worldwide prevalence of anaemia 1993–2005*. <https://www.who.int/publications/i/item/9789241596657>

- World Health Organization. (2021). *Anaemia in women and children*. https://www.who.int/data/gho/data/themes/topics/anaemia_in_women_and_children, Assessed on 10th June 2021. https://www.who.int/data/gho/data/themes/topics/anaemia_in_women_and_children
- Wu, H., Liu, Z., Zhao, Y., & Zeng, M. (2012). Enzymatic preparation and characterization of iron-chelating peptides from anchovy (*Engraulis japonicus*) muscle protein. *Food Research International*, *48*(2), 435–441. <https://doi.org/10.1016/j.foodres.2012.04.013>
- Wu, T., Yu, X., Hu, A., Zhang, L., Jin, Y., & Abid, M. (2015). Ultrasonic disruption of yeast cells: Underlying mechanism and effects of processing parameters. *Innovative Food Science & Emerging Technologies*, *28*, 59–65. <https://doi.org/10.1016/j.ifset.2015.01.005>
- Wu, W., Li, B., Hou, H., Zhang, H., & Zhao, X. (2017). Identification of iron-chelating peptides from Pacific cod skin gelatin and the possible binding mode. *Journal of Functional Foods*, *35*, 418–427. <https://doi.org/10.1016/j.jff.2017.06.013>
- Wu, W., Yang, Y., Sun, N., Bao, Z., & Lin, S. (2020). Food protein-derived iron-chelating peptides: The binding mode and promotive effects of iron bioavailability. *Food Research International*, *131*(1), 108976. <https://doi.org/10.1016/j.foodres.2020.108976>
- Xiao, C., Toldrá, F., Zhao, M., Zhou, F., Luo, D., Jia, R., & Mora, L. (2022). *In vitro* and *in silico* analysis of potential antioxidant peptides obtained from chicken hydrolysate produced using Alcalase. *Food Research International*, *157*. <https://doi.org/10.1016/j.foodres.2022.111253>
- Xie, J., Cui, C., Ren, J., Zhao, M., Zhao, L., & Wang, W. (2017). High solid concentrations facilitate enzymatic hydrolysis of yeast cells. *Food and Bioprocess Processing*, *103*, 114–121. <https://doi.org/10.1016/j.fbp.2017.03.004>
- Yamada, E. A., & Sgarbieri, V. C. (2005). Yeast (*Saccharomyces cerevisiae*) protein concentrate: Preparation, chemical composition, and nutritional and functional properties. *Journal of Agricultural and Food Chemistry*, *53*(10), 3931–3936. <https://doi.org/10.1021/jf0400821>
- Yang, Y. Z., Li, M. J., Zhou, B. B., Zhang, Q., Li, X. L., Zhang, J. K., & Wei, Q. P. (2019). Synthesis, characterization, and evaluation of bioactivity of novel Fe(II) nano-complexes based on sucrose, glucose, and fructose. *Chemical Papers*, *73*(2), 321–329. <https://doi.org/10.1007/s11696-018-0582-8>
- Yuan, B., Zhao, C., Cheng, C., Huang, D., Cheng, S., Cao, C., & Chen, G. (2019). A peptide-

- Fe(II) complex from *Grifola frondosa* protein hydrolysates and its immunomodulatory activity. *Food Bioscience*, 32, 100459. <https://doi.org/10.1016/j.fbio.2019.100459>
- Zeko-Pivač, A., Habschied, K., Kulisic, B., Barkow, I., & Tišma, M. (2023). Valorization of Spent Brewer's Yeast for the Production of High-Value Products, Materials, and Biofuels and Environmental Application. *Fermentation*, 9(3), 208. <https://doi.org/10.3390/fermentation9030208>
- Zhang, L., Jin, Y., Xie, Y., Wu, X., & Wu, T. (2014). Releasing polysaccharide and protein from yeast cells by ultrasound: Selectivity and effects of processing parameters. *Ultrasonics Sonochemistry*, 21(2), 576–581. <https://doi.org/10.1016/j.ultsonch.2013.10.016>
- Zhang, L. Y., Li, X. F., Liao, X. D., Zhang, L. Y., Lu, L., & Luo, X. G. (2017). Effect of iron source on iron absorption and gene expression of iron transporters in the ligated duodenal loops of broilers. *Journal of Animal Science*, 95(4), 1587. <https://doi.org/10.2527/jas2016.1147>
- Zhang, T., Lei, J., Yang, H., Xu, K., Wang, R., & Zhang, Z. (2011). An improved method for whole protein extraction from yeast *Saccharomyces cerevisiae*. *Yeast*, 28(11), 795–798. <https://doi.org/10.1002/yea.1905>
- Zhang, Y., Ding, X., & Li, M. (2021). Preparation, characterization and *in vitro* stability of iron-chelating peptides from mung beans. *Food Chemistry*, 349(December 2020), 129101. <https://doi.org/10.1016/j.foodchem.2021.129101>
- Zhao, Y. (2008). Structure and Function of Angiotensin Converting Enzyme and Its Inhibitors. *Chinese Journal of Biotechnology*, 24(2), 171–176. [https://doi.org/10.1016/S1872-2075\(08\)60007-2](https://doi.org/10.1016/S1872-2075(08)60007-2)
- Zhou, J., Wang, X., Ai, T., Cheng, X., Guo, H. Y., Teng, G. X., & Mao, X. Y. (2012). Preparation and characterization of β -lactoglobulin hydrolysate-iron complexes. *Journal of Dairy Science*, 95(8), 4230–4236. <https://doi.org/10.3168/jds.2011-5282>
- Zhu, X., Zou, R., Sun, P., Wang, Q., & Wu, J. (2018). A supramolecular peptide polymer from hydrogen-bond and coordination-driven self-assembly. *Polymer Chemistry*, 9(1), 69–76. <https://doi.org/10.1039/C7PY01901G>